IMPERIAL COLLEGE OF SCIENCE TECHNOLOGY
AND MEDICINE
ROYAL SCHOOL OF MINES

DEPARTMENT OF EARTH RESOURCES ENGINEERING

MODELLING AND PREDICTION OF ENVIRONMENTAL NOISE LEVELS NEAR MECHANISED SURFACE MINES AND QUARRIES

by

Khanindra PATHAK

A thesis submitted for the degree of Doctor of Philosophy of the University of London and for Diploma of Imperial College

London, October 1996

Lib.
Loan
Copy

This thesis is dedicated to the
memory of my
Father

ABSTRACT

The surface mining and quarrying operations are often blamed for their degrading impacts on environmental noise over the residential areas closer to the working site. The acoustic environment near a surface mine is directly related to the noise generating activities involving a number of types of mining machinery. The propagation of noise from these sources is affected by the pit geometry, terrain conditions and atmospheric parameters. The sources and the affecting parameters being variable and numerous, there is no simple method for the exact determination of sound pressure levels near these operations. As a result, predicted values of sound pressure levels near mining areas have not been used as an input for mine planning and design. Thus, there is no acoustically designed surface mine or a quarry and alternative operating schemes of such mines are not tested for their noise impact.

The main objective of this research was to develop a method to determine the sound power level of the distributed and randomly excited noise sources within a surface mine so that the environmental noise impact can be predicted based on the distribution and operation schedules of the machinery deployed. Using the concept of Equivalent Acoustic Centre (EAC), a methodology has been developed to determine the sound power levels of the work-zones within a surface mine or a quarry. Three techniques, namely the Experimental Measurement Technique, the Acoustic Database Technique and the Activity Accounting Technique have been developed to build a Source Power Model to evaluate the sound power levels of mining operations and to incorporate them in a noise prediction system.

The noise attenuation due to absorption of the sound energy by the ground surface and by air was studied to develop the attenuation models as components of the surface mining noise prediction system. Existing theories of atmospheric absorption were incorporated to an air attenuation model and integrated to the mining noise prediction system. The effect of pit-walls as a noise barrier was treated as a case of multiple image sources and the pit-wall attenuation model was developed correlating the pit geometry and source-receiver configuration. The source power model was integrated with the attenuation models to provide a practical tool to predict the sound pressure levels at a receiver location. Experiments were designed and conducted at a limestone quarry to determine the necessary field data as well as to validate the use of the noise prediction system. The results showed that the predictive models developed in this research will be useful in mine planning and acoustic design for environmental management.

ACKNOWLEDGEMENTS

There were many without whose help, support and co-operation this research would not have been completed. First and foremost I thank Dr Sevket Durucan, my supervisor for his dynamic guidance, continuous support and motivating inspiration. My thanks to Dr Douglas Owen who baptised me in the field of C++ programming. All my experiments would not have been carried out without the support and help of Mr Brendan O'Reilly of Outokumpu Zinc Tara Mines Ltd and Mr Kevin O'Brien of Industrial and Marine Acoustics Ltd, from the Republic of Ireland. My gratitude goes to Dr Sunao Kunimatsu, Safety Engineering Department of NIRE, Japan who accompanied me during the field experiments. I also thank Dr Takehiro Isei, Director, Safety Engineering Department, NIRE for his valuable suggestions. I thank Prof. Frank Fahy of Southampton University who could kindly spare a day for discussions. I also thank Dr S. K. Sarma of the Department of Civil Engineering, Imperial College for his valuable academic suggestions and encouragement.

I acknowledge my indebtedness to my sponsor the Association of Commonwealth Universities (ACU) who selected me for the Commonwealth Academic Staff Scholarship to carry out this research. I thank Prof. A. K. Ghosh, the former Director of the Indian School of Mines for allowing me to take this opportunity. My thanks go to all my colleagues at the Department of Engineering and Mining and Machinery, Indian School of Mines, Dhanbad for their inspiration and co-operation.

I thank Dr Jonathan Jenkin of the ACU and the Officers of the British Council who have been very helpful and co-operative during my stay in the United Kingdom. I also thank with gratitude the personnel in the Environmental Unit at Tara Mines, the Republic of Ireland.

My sincere thanks go to the present and past members of the Mining and Environment Research Group. I felt fortunate enough from the very first day of joining this group with so many talented colleagues. I express my deep gratitude to Dr Wilson

Mutagwaba, Dr Elena Clarici, Dr Ji Quan Shi, Dr Knud Sinding, Dr Osman Cicek, Mr Serge Martinson, Mr Peter Johnston, Mr Geoff Johnston, Ms Anna Kore, Mr Yakup Unlü, Mr Csaba Sinka, Mr Luigi Vercelli, Ms Amanda Warner, Mr Sameh Ahmed and Mr Mahammad Ali Ebrahimi Farsangi. My sincere thanks go to Dr Pradyut Goswami and Anuradha who helped me during the initial period of the research. I acknowledge the help of Ms Claire Imrie with sincere gratitude and thanks for her smiling acceptance for the tedious job of proof-reading of this thesis.

I also thank Sanjay and Pragati, Joy and Bibhuti, Ajay and Rashmi, Sudeshna and Debdas, Andrew and Masaio, Jogen and Priti, Dr Cida Das and Poli Das and all my neighbours at Nansen Village who have supported me and my family in countless ways during the last three years. I thank Mr and Mrs Weinberg, Mrs Valerie Mandlin and Mrs. Helen Chaplen for their caring encouragement for my work.

I also thank Dr Anil Ranjan Barthakur and Lahari Barthakur who had been continuously encouraging me during this research.

There were the two who have sacrificed a lot. They have supported me most and showed deep love and patience. They remained as my constant encouragement. My gratitude for ever goes to them, my wife Swapna and daughter Jushmita.

AFFIRMATION

The work submitted in this thesis is my own and has not been submitted for any other degree. As a result of this research, the following publications have been presented:

Pathak, K., Durucan, S. and O'Reilly, B; 1995. Modelling and Prediction of Far-Field Noise Levels near Mechanised Quarries and Surface Mines, Proc. Euro Noise 95, An International INCE Symposium, Lyon, France, 21-23 March 1995, Vo. 1, pp. 237-244.

Pathak, K., Durucan, S., O'Reilly, B., Kunimatsu, S., 1996.Impacts of Environmental Noise due to Front End Loader and Dump Truck Operation in a Quarry — A Case Study, Proc. Noise and Planning, the 1996 International Congress on "Acoustics applied to planning: from Technical Technical Standards to Environmental Standards" at Pisa, Italy, pp.209-213.

TABLE OF CONTENTS

Abstract i
Acknowledgement ii
Affirmation iv
List of Figures xi
List of plates xviii
List of Tables xix
List of Acronyms xxii
List of Notations xxiv

CHAPTER 1

INTRODUCTION AND OBJECTIVES 1

1.1 Introduction 1

1.2 Noise from Surface Mining and Quarrying 3

1.3 Research Objectives 5

CHAPTER 2

REVIEW OF ENVIRONMENTAL ACOUSTICS 10

2.1 Introduction 10

2.2 Basic Concepts 13

2.2.1 Acoustic Variables and their Relationships 13
2.2.2 Decibel Scale 19
2.2.3 Sound Power 20
2.2.4 Combined Effects of Sound 22
2.2.5 Frequency Weighting 23
2.2.6 Directional Characteristics of Sound Sources 25
2.2.7 Sound Field 26

2.3 Present Status of Noise Awareness 28

2.4 Summary 31

CHAPTER 3

CURRENT TECHNIQUES OF INDUSTRIAL NOISE ASSESSMENT 33

3.1 Introduction 33

3.2 Noise Measurement 34

3.2.1 Index for Noise Estimation 35
3.2.1.1 Sound Pressure Level 36
3.2.1.2 Equivalent Sound Level 41
3.2.1.3 Percentile Exceeded Sound Level 43
3.2.1.4 Day-Night Sound Level 43
3.2.1.5 Community Noise Equivalent Level 44
3.2.1.6 Day Average Sound Level 44
3.2.1.7 Noise Exposure Level 45
3.2.1.8 Day Average Sound Level 46
3.2.2 Errors in Noise Measurements 46

3.3 Noise Assessment 48

3.4 Industrial Noise Assessment and Prediction 51

3.4.1 Sound Output of Processes and Plants 53
3.4.2 Attenuation of Noise Level 54
3.4.2.1 Attenuation by Spreading 54
3.4.2.2 Influence of Ground Surfaces 56
3.4.2.3 Absorption by Air 59
3.4.2.4 Presence of a Barrier 60
3.4.3 Meteorological Conditions 62
3.4.3.1 Viscosity 63
3.4.3.2 Humidity 63
3.4.3.3 Rain and Fog 64
3.4.3.4 Temperature 65
3.4.3.5 Wind 66
3.4.3.6 Turbulence 69
3.4.4 Presence of Other Sources 70
3.4.5 Other Attenuation 70

3.5 The Calculation of Noise Levels near Industrial Complexes 72

3.5.1 Activity L_{eqA} Method. 73
3.5.2 Plant Sound Power Method 75
3.5.3 Calculation of Leq for Mobile Plant 77
3.5.3.1 Mobile Plants within a Small Area 78
3.5.3.2 Mobile Plants on Regular Routes 79
3.5.3.3 Road Traffic Noise 79

3.6 Summation of Sound Levels 80

3.7 Summary 81

CHAPTER 4

THE DEVELOPMENT OF A SOURCE CHARACTERISATION MODEL FOR SURFACE MINING AND QUARRYING NOISE 83

4.1 Introduction 83

4.2 Theory of Equivalent Acoustic Centre (EAC) 88

4.2.1 Determination of Sound Power Level at the EAC 92

4.3 The Development of Source Characterisation Model 94

4.3.1 Experimental Measurement Technique (EMT) 96

4.3.1.1 The Application of Experimental Measurement Technique to determine the EAC of Tara Mines 99

4.3.2 Acoustic Database Technique (ADT) 106

4.3.3 Activity Accounting Technique (AAT) 108

4.3.3.1 Work Study of Equipment Complex 110

4.3.3.2 Establishment of Noise Signature 110

4.3.3.3 The Assessment of Activity Sound Power Levels 111

4.3.3.4 Experimental Verification of the AAT 113

4.4 **Conclusion** 121

CHAPTER 5

THE DEVELOPMENT OF A GROUND ATTENUATION MODEL 123

5.1 Introduction 123

5.2 Attenuation due to the Ground Surface 125

5.2.1 Acoustic Phenomena over the Ground Surface 127

5.2.2 Reflected Acoustic Waves on an Air-Solid Interface 129

5.2.3 Characteristic Impedance of the Ground 135

5.2.4 Evaluation of the Sound Field over a Ground Surface 138

5.2.5 Excess Attenuation by Ground Absorption 141

5.3 The Development of the Ground Attenuation Model 142

5.4 Experimental Evaluation of Flow Resistivity 147

5.4.1 Experimental Design 148

5.4.2 Analysis of Results and Discussion 152

5.4.2.1 Experiments over Grass Covered Soft Soil 153

5.4.2.2 Experiments over Settled Quicksand 156

5.4.2.3 Experiments over the Road Surface 159

5.4.2.4 Effects of Distance on Ground Absorption 161

5.4.2.5 Effects of Wind Velocity on Ground Attenuation 164

5.5 Conclusion 165

CHAPTER 6

THE DEVELOPMENT OF AN AIR ATTENUATION MODEL 166

6.1 Introduction 166

6.2 Excess Attenuation due to Air 167

6.3 Theory of Molecular Absorption 168

6.4 Evaluation of Air Absorption 173

6.5 Meteorological Effects on Sound Propagation 177

6.5.1 Ray Path Curvature 178

6.5.2 Meteorological Considerations 181

6.5.3 Estimation without Wind Profile Measurements 182

6.5.4 The Sound Propagation Parameter 184

6.6 The Development of the Air Attenuation Model 184

6.7 Conclusion 190

CHAPTER 7

THE DEVELOPMENT OF A PIT-WALL ATTENUATION MODEL 191

7.1 Introduction 191

7.2 The Basic Theory of Barrier Attenuation 194

7.2.1 Wind Effect on Barrier Attenuation 197

7.3 Barrier Attenuation of Surface Mining and Quarrying Noise 198

7.3.1 Attenuation by the Pit-walls 199

7.3.2 Correction for Pit-wall Reflection 205

7.4 The Development and Evaluation of a Model for the Assessment of Pit-wall Attenuation 207

7.4.1 The Effects of Pit Geometry 209

7.4.2 A Study of Environmental Noise Control in Surface Mines 212

7.5 Summary 214

CHAPTER 8

System Integration and Final Field Validation

8.1 Introduction 216

8.2 The Integration of the Source Power and Attenuation Models for Noise Prediction 217

8.2.1 Ground Absorption and Barrier Attenuation 221

8.2.1.1 The Acoustic Phenomena at the Pit Bottom 222

8.2.1.2 The Acoustic Phenomena at the Pit Walls 223

8.2.2 Experimental Validation of the Combined Pit-wall and Ground Attenuation Model 228

8.3 Final Field Validation of the Noise Prediction System 229

8.3.1 Prediction of Sound Pressure Level Spectra 234

8.3.2 Experimental Noise Measurements at the Test Quarry 238

8.3.3 Directivity Corrections 241

8.3.4 Far Field Noise Prediction Results 245

8.4 Conclusion 246

CHAPTER 9

CONCLUSIONS AND RECOMMENDATIONS FOR FUTURE RESEARCH 249

9.1 Introduction 249

9.2 Conclusions 250

9.3 Recommendations for Future Research 258

REFERENCES 262

APPENDIX 271

Appendix 1 271

A1 List of Important Standards and Guidelines on Noise

Appendix 2 274

A2 Noise Signature of Shovel Dumper Operation 274

Appendix 3 **284**

A3 Experiment over grass covered soft soil 284

A3.1 Experiment 14-1 284

A3.2 Experiment 14-2 288

A3.3 Experiment 14-3 291

B3 Experiment over Settled Quick Sand 293

B3.1 Experiment 14-4 293

B3.2. Experiment 14-5 296

C3 Experiment over Gritty Road Surface 300

C3.1 Experiment: 13-1 300

C3.2 Experiment 13-2 301

LIST OF FIGURES

Figure 1.1	The modelling procedure.	6
Figure 1.2	The main components of the environmental simulation and impact assessment system which incorporates the noise modelling concept.	9
Figure 2.1	Effects of noise on human beings.	11
Figure 2.2	Factors influencing effects of noise on human beings.	12
Figure 2.3	Propagation velocity of sound through dry air at sea level under different temperatures.	15
Figure 2.4	Sound pressure wave at different times for constant amplitude sound at 1 kHz frequency.	18
Figure 2.5	Response curves for A-, B-, C-, D-and SI-weighting (after Wilson, 1989).	24
Figure 2.6	The radiation fields of a noise source (after Bies and Hansen, 1988).	26
Figure 3.1	Noise descriptors.	36
Figure 3.2	Types of noise sources.	52
Figure 3.3	Effect of source type on attenuation due to spreading.	56
Figure 3.4	Frequency of maximum ground attenuation as a function of path height (h) and distance (R).	58
Figure 3.5	Attenuation constant for viscosity at 1 atmosphere and 200 C (after Equation 3.26).	63
Figure 3.6	Effect of temperature gradient (daytime).	64
Figure 3.7	Inverted Temperature Gradient.	65
Figure 3.8	Average wind velocity gradient as a function of the height over the ground (after Ingard, 1953).	67
Figure 3.9	Attenuation due to vegetation.	71
Figure 3.10	Distance adjustment in sound pressure level estimation (after BS: 5228).	76
Figure 3.11	Adjustment of sound pressure level to calculate Leq in dBA.	77

Figure 4.1 The main structure of the models of the noise prediction system developed. 86
Figure 4.2 Components of the surface mining and quarrying noise prediction system developed. 87
Figure 4.3 The principle of Equivalent Acoustic Centre (EAC). 89
Figure 4.4 Techniques of developing the source characterisation model. 95
Figure 4.5 The procedure followed and the flow diagram of the software developed for the source characterisation. 98
Figure 4.6 Plan view of the processing plant and the noise measurement locations. 100
Figure 4.7 Time series of the noise levels at measurement locations, (a) at reference location, (b) at station 3, (c) at station 2, (d) at station 8. 102
Figure 4.8 The flow diagram of the source power model with the Experimental Measurement Technique implemented only-Stage 1(EAC.CPP). 103
Figure 4.9 Predicted noise levels using the EAC concept and the measured values. 103
Figure 4.10 Estimated noise contours near the processing plant. 104
Figure 4.11 The flow diagram of the source power model after the implementation of the Acoustic Database Technique -Stage 2 (EAC.CPP). 107
Figure 4.12 Activity Accounting Technique of evaluating sound power levels of the noise sources in a work zone within a surface mine. 109
Figure 4.13 The flow diagram of the source power model after the implementation of the Activity Accounting Technique -Stage 3 (EAC.CPP). 112
Figure 4.14 Surface plan of the limestone quarry. 115
Figure 4.15 SPL spectrum of 35T RD dump truck (a) being loaded by hydraulic shovel (b) moving with load on level ground (recorded by Larson Davis RTA 2900).118
Figure 4.16 Sound power spectra of the activities of FEL and dump truck operation. 121

Figure 5.1 Combination of reflected and direct sounds at the receiver's location. 126
Figure 5.2 Reflection of an acoustic wave. 128
Figure 5.3 Behaviour of acoustic waves at ground surface: a. Local reaction, b. Extended reaction. 129
Figure 5.4 Refraction of a sound ray at the interface of ground and the atmosphere. 131
Figure 5.5 Effect of terrain conditions over outdoor noise propagation. 134

Figure 5.6 Program structure of the ISO method for determining attenuation due to the ground and a program output. 143
Figure 5.7 The structure of the ground attenuation model developed. 146
Figure 5.8 Theoretical excess attenuation due to ground absorption for different values of flow resistivity and frequencies. 147
Figure 5.9 Scheme of the field experiments. 148
Figure 5.10 Experimental set-up used in determining the excess attenuation due to ground absorption. 149
Figure 5.11 Arrangement of speaker and sound level meters. O: Position of speaker, D: Reference sound level meter at a distance of 1 m from O. A: Recording sound level meter at a distance of 10 m from O. P: Equivalent point source at a distance of 0.239 m from O. P': Image source. 150
Figure 5.12 Experimental and theoretical excess attenuation due to ground absorption over grass covered soft soil. (a). In the direction of wind, (b). Opposite to the wind direction, (c). At 135o to the wind direction. 155
Figure 5.13 Excess attenuation due to ground absorption over settled quicksand, (a) along wind direction, (b) along 45o to wind direction, (c) along 90o to wind direction. 157
Figure 5.14 Excess attenuation due to ground absorption over gritty road surface, (a) at 15o to the wind direction, (b) at 165o to the wind direction. 160
Figure 5.15 Excess attenuation due to ground absorption at different frequencies (f) as a function of distance. 161
Figure 5.16 Effect of distance on excess attenuation due to ground attenuation over (a) Grass-covered soft soil at 135o to the wind direction, (b) Settled quicksand along the wind direction , (c) Gritty road surface at 165o to the wind direction. 162
Figure 5.17 Effect of wind direction on ground absorption. 163
Figure 5.18 Variation of excess attenuation over grass-covered soft soil due to a 180^{o} change in the direction of wind. 164

Figure 6.1 Attenuation due to air absorption (derived from the German Standards VDI 2714/VDI 2720). 175

Figure 6.2 Air attenuation at different atmospheric conditions (drawn after Sutherland et al, 1974). 176
Figure 6.3 Attenuation due to air absorption over a distance of 1000 m, (a) At 25o C, (b) At 50 % relative humidity. 176
Figure 6.4 Effects of wind direction on sound propagation. 178
Figure 6.5 Effect of temperature gradient on acoustic propagation. 179
Figure 6.6 Sound pressure level and distance of propagation under different values of k (After Larson, 1992b). 180
Figure 6.7 Air attenuation model. 185
Figure 6.8 Steps to determine the radius of curvature of acoustic path from source to receiver. 187
Figure 6.9 Sample output of module METEOK.CPP. 187
Figure 6.10 Sample output of METEOK.CPP determining radius of curvature of sound propagation path without wind profile measurement. 188
Figure 6.11 Attenuation due to air of the noise generated in the Primary Crusher Zone of the test quarry. 189

Figure 7.1 The geometry of the sound propagation path over a barrier wall. 193
Figure 7.2 Attenuation due to a thin barrier (after Kurze and Anderson, 1970; Rathe, 1969). 195
Figure 7.3 Barrier attenuation calculated using CONCAWE model for (a) higher values of Fresnel Number and (b) Lower values of Fresnel Number (after Marsh, 1962). 196
Figure 7.4 Diffraction of sound waves at the edge of pit-walls. 198
Figure 7.5 Pit-wall as a noise barrier. 199
Figure 7.6 Sound fields for a noise source at the mine floor. 201
Figure 7.7 A simple geometric model for a surface mine or a quarry. 206
Figure 7.8 Model structure for evaluating attenuation due to pit-wall. 207
Figure 7.9 An example output from the pit-wall attenuation model. 208
Figure 7.10 Comparison of measured and predicted values. 209
Figure 7.11 The effect of distance between noise source and pit-wall on noise attenuation. 210

Figure 7.12 The effect of slope angle of pit-wall on attenuation. 210
Figure 7.13 The effect of safety berm height on noise attenuation. 211
Figure 7.14 Geometric position of the receiver with respect to the pit-wall. 212
Figure 8.1 Steps involved in predicting the noise levels around surface mines and quarries. 217
Figure 8.2 The characteristics of working zones relevant to noise prediction in surface mining and quarrying. 218
Figure 8.3 The noise prediction system developed for surface mines and quarries. 220
Figure 8.4 Pit geometry affecting the attenuation of sound from a pit-bottom source to a pit-top receiver. 222
Figure 8.5 The structure of the combined pit-wall-ground absorption prediction model. 227
Figure 8.6 Theoretical excess attenuation due to the combined effects of pit-walls and ground attenuation. 227
Figure 8.7 Schematic diagram of the pit-wall attenuation experiments carried out. 228
Figure 8.8 Theoretical and measured attenuation due to mound walls. 229
Figure 8.9 The software code written to predict sound pressure level spectra based on the Activity Accounting Technique. 237
Figure 8.10 Program output for noise level prediction based on the Activity Accounting Technique. 238
Figure 8.11 Estimated spectra due to various activities at a selected location under specific atmospheric conditions. 238
Figure 8.12 Measured time series at one of the noise monitoring stations in the test quarry during the experiment. 241
Figure 8.13 The directivity corrections for the EAC based sound pressure levels. 243
Figure 8.14 Combining the significant directivities. 244
Figure 8.15 Comparison of measured and predicted sound pressure levels near the test quarry. 246
Figure 8.16 A GRID overlay of predicted noise levels over the topography, surface structures and geographic features around the test quarry. 247

Figure A2.1 Frequency spectrum of the noise emitted by a 35 t RD dump truck being loaded by hydraulic shovel. 274

Figure A2.1A Frequency spectrum of the noise emitted by a 35 t RD dump truck being loaded by hydraulic shovel. 275
Figure A2.2 Frequency spectrum of the noise emitted by a hydraulic shovel during face dressing. 275
Figure A2.2 A Frequency spectrum of the noise emitted by a hydraulic shovel preparing a face while 35 t RD dump truck moving away. 276
Figure A2.3 Frequency spectrum of the noise emitted by a hydraulic shovel during propelling. 276
Figure A2.3A Frequency spectrum of the noise emitted by the movement of a hydraulic excavator. 277
Figure A2.4 Frequency spectrum of the noise emitted by a 35 t RD dump truck down-the-ramp (35 degree). 277
Figure A2.5 Frequency spectrum of the noise emitted by a 35 t RD dump truck on level. 278
Figure A2.6 Frequency spectrum of the noise emitted by a 35 t RD dump truck on a 35 degree up-ramp. 279
Figure A2.7 Frequency spectrum of the noise emitted by a 35 t RD dump truck on a 35 degree down-ramp. 279
Figure A2.8 Frequency spectrum of the noise emitted by a 35 t RD dump truck near a hydraulic shovel. 280
Figure A2.9 Frequency spectrum of the noise emitted by a 35 t RD dump truck on a ramp near the hydraulic shovel. 280
Figure A2.10 Frequency spectrum of noise emitted by 35 t RD dump truck manoeuvring near hydraulic shovel. 281
Figure A2.10A Frequency spectrum of the noise emitted by a 35 t RD dump truck manoeuvring near a hydraulic shovel. 281
Figure A2.11 Frequency spectrum of the noise emitted by a 35 t RD dump truck during turning on level ground. 282
Figure A2.12 Frequency spectrum of the noise emitted by a dump truck travelling with load on the level ground. 282
Figure A3.1 Excess attenuation (dB) due to ground absorption over grass covered soft soil. 285

Figure A3.1(Contd.) Excess attenuation (dB) due to ground absorption over grass covered soft soil. 286

Figure A3.1 (Contd.) Excess attenuation (dB) due to ground absorption over grass covered soft soil. 287

Figure A3.2 Measured and theoretical excess attenuation (dB) over grass covered soft soil under the wind direction 1800 to that of Experiment 14.1. 288

Figure A3.2(Contd.) Measured and theoretical excess attenuation (dB) over grass covered soft soil under the wind direction 1800 to that of Experiment 14.1. 289

Figure A3.2(Contd.) Measured and theoretical excess attenuation over grass covered soft soil under a condition of wind direction 180° to that of Experiment 14.1. 290.

Figure A3.3 Excess attenuation (dB) over grass covered soft soil along 135° to the wind direction 292

Figure A3.3 (Contd.) Excess attenuation (dB) over grass covered soft soil along 135° to the wind direction. 293

Figure B3.1 Excess attenuation (dB) over settled quick sand along direction of wind. 295

Figure B3.1 (Contd.) Excess attenuation (dB) over settled quick sand along direction of wind. 296

Figure B3.2 Theoretical and measured excess attenuation (dB) over settled quicksand at 45 degree to the wind direction. 297

Figure B3.2 (Contd.) Theoretical and measured excess attenuation (dB) over settled quicksand at 45 degree to the wind direction. 298

Figure C3.1 Theoretical and measured excess attenuation over gritty road surface at 15° to the wind direction. 300

Figure C3.2 Theoretical and measured excess attenuation over gritty road surface for Experiment 13.2. 302

LIST OF PLATES

Plate 4.1	Working conditions at the limestone quarry.	116
Plate 4.2	View of the surface plants of limestone quarry.	116
Plate 5.1	Noise attenuation experiments over grass covered soft soil.	154
Plate 5.2	Noise attenuation experiments over gritty road surface.	157
Plate 5.3	Site of experiments over a gritty road surface.	160
Plate 8.1	General view of the quarrying operations.	232
Plate A2.1	Shovel-dump truck noise experiments.	283

LIST OF TABLES

Table 1.1	Characteristics of surface mines and quarries affecting the noise field in the neighbourhood.	4
Table 1.2	Equipment complexes in different unit operations of various opencast mining systems.	4
Table 2.1	Directivity factor for different positions of noise source (After Norton, 1989).	25
Table 2.2	Recommended noise standards for new railways and new roads (after Walker, 1992).	29
Table 2.3	Land classification scheme and maximum sound levels allowed for outdoor noise.	30
Table 2.4	Noise control programs in the USA (after White, 1975).	30
Table 2.5	Safe sound exposure limits (after White, 1975).	31
Table 3.1	Various noise descriptors (after Peterson and Gross, 1977).	37
Table 3.2	Different models of sound pressure level prediction (compiled from Tonin, 1993).	50
Table 3.3	Excess attenuation coefficients for forest.	71
Table 3.4	Vegetation code for wood of different density.	72
Table 3.5	Distance ratio and equivalent on-time (after BS: 5228).	78
Table 4.1	Noise sources in different phases of surface mining.	84
Table 4.2	Various types of noise near mechanised surface mines (after Wiener, 1960).	85
Table 4.3	Calculated sound power level and the location of EAC at Tara Plant.	100
Table 4.4	Variation of the Equivalent Acoustic Centre of the plant during the observation period.	105
Table 4.5	Noise levels of different machinery (after Bartholomae and Parker, 1983).	108
Table 4.6	The atmospheric conditions during noise monitoring at the limestone quarry.	114

Table 4.7	Octave band analysis of RMS sound pressure levels for various activities with FEL and Dump Trucks (from 2900 RTA).	114
Table 4.8	A-weighted sound pressure levels and the duration of various activities of FEL and dump truck.	117
Table 4.9	Locations of activities and their monitoring stations.	120
Table 4.10	Sound power levels (dB) of different activities for the octave frequencies.	120
Table 5.1	Values of flow resistivity for typical ground surfaces (after Embleton et al, 1983).	135
Table 5.2	Acoustic impedance and propagation constants to be used in Equations 5.30 and 5.31.	137
Table 5.3	The numerical relationship proposed for calculating the numerical distance.	140
Table 5.4	Theoretical excess attenuation for a given source receiver configuration.	145
Table 5.5	Coefficients of correlation between the measured and theoretical excess attenuation over grass-covered soft soil at 10 m for measurements at different directions.	153
Table 5.6	Coefficients of correlation between measured and theoretical excess attenuation for different wind directions.	156
Table 5.7	Coefficients of correlation between measured and theoretical excess attenuation over gritty road surface at a distance of 10m under different wind directions.	159
Table 6.1	Attenuation due to atmospheric absorption (after Sutherland et al, 1974).	175
Table 6.2	Aerodynamic roughness length for some typical terrain types (after Stull, 1988 and Oke, 1987).	182
Table 6.3	Values of Dt under different conditions.	183
Table 6.4	Assumptions in development of the air attenuation module.	186
Table 7.1	Attenuation by thin barriers (after Rathe, 1969).	195
Table 7.2	Predicted and measured values at different locations near the quarry.	209

Table 8.1 General features and the functions of the Larson Davis Noise Level Meters used. 234
Table 8.2 Acoustic emissions of mining activities. 235
Table 8.3 Activities in the excavator-truck operating zone and their hourly duration. 236
Table 8.4 A sample of data recorded by the sound level meter. 239
Table 8.5 The co-ordinates and sound pressure levels at the monitoring stations. 240
Table 8.6 The co-ordinates and the predicted sound power levels of the four Equivalent Acoustic Centres at the test quarry. 242
Table 8.7 Predicted and measured sound pressure levels at different locations near the quarry. 245

Table A3.1.1 Recorded sound pressure levels for Experiment 14-1. 285
Table A3.2.1 Recorded sound pressure levels for Experiment 14-2. 287
Table A3.3.1 Recorded sound pressure levels for Experiment 14-3. 291
Table B3.1.1 Recorded sound pressure levels for Experiment 14-4. 294
Table B3.2.1 Recorded sound pressure levels for Experiment 14-5. 297
Table C3.1.1 Recorded sound pressure levels for Experiment 13-1. 299
Table C3.2.1 Recorded sound pressure levels for Experiment 13-2. 301

List of ACRONYMS

AAT	Activity Accounting Technique
ADA	Acoustic Database Technique
CNEL	Community Noise Equivalent
CNR	Composite Noise Rating
CONCAWE	Oil Companies' International Study Group for Conservation of Clean Air and Water
DOD	The Department of Defence, USA
EAC	Equivalent Acoustic Centre
EPA	The Environment Protection Agency
EMA	Experimental Measurement Technique
FHWA	The Federal Highway Administration, USA
HCA	The Hearing Conservation Amendment
NEF	Noise Exposure Forecast
NNI	Noise and Number Index
NAC	Noise Advisory Committee
NSI	Net Solar Index
OSHA	The Occupational Safety and Health Administration
PEM	Planned Experiments Method
PNC	Preferred Noise Criteria
SEA	Statistical Energy Analysis
TNI	Traffic Noise Index

LIST OF NOTATIONS

a	Radius of a sphere whose centre is the sound source, m
A_a	Attenuation due to atmospheric absorption, dB
A_b	Attenuation due to barriers, dB
A_c	Adjustment due to building coverage, dB
A_d	Adjustment due to distance from the reference location, dB
A_f	Adjustment due to finite segment of road, dB
A_g	Attenuation due to ground absorption, dB
A_n	Adjustment due to n number of noise sources, dB
A_r	Reflection loss, dB
A_v	Attenuation due to vegetation
A_u	Usage factor adjustment, dB
B_h	Height of safety berm, m
c	Velocity of sound, m/sec
CL	Criterion Level, dB
$CNEL$	Community Noise Equivalent Level, dB
d	Distance of receiver's location from road (haulage noise), m
dA	Excess attenuation, dB
DI	Directivity Index
D	Noise Dose
ER	Exchange Rate (tolerable noise level that halves the exposure time)
f	Frequency
f_{max}	Frequency of maximum ground attenuation
F	Attenuation parameter for ground attenuation
h	Mean height of source to receiver path
$G(w)$	Amplitude factor
I	Intensity of sound, Wm^{-2}
i_o	Angle of elevation of sound ray
I_{ref}	Reference intensity, 10^{-12} $wattm^{-2}$
k	Wave number, normalised curvature of ray path

K_d	Distance correction, dB
K_I	Correction for impulse noise
K_T	Correction for operating time of noise source
L	Measured sound pressure level, dB
L_{1h}	Equivalent sound level for 1 hour, dBA
L_{24h}	Equivalent sound level for 24 hours, dBA
L_{AX}	Noise exposure level, dBA
L_{DN}	Day-night sound level, dBA
L_{eq}	Equivalent sound level, dB
L_{eqD}	Equivalent sound level (dBA) for the period of 7.00 A.M. to 10.00 P.M., dB
L_{eqN}	Equivalent sound level (dB) for the period of 10.00 P.M. to 7.00 A.M., dB
L_{max}	Maximum A-weighted sound level, dB
L_o	Reference level of mean energy emission, dB
L_{omean}	Arithmetic average emission level, dB
L_{OSD}	Standard deviation of the emission level of mean energy emission, dB
L_p	Sound pressure level, dB
L_{pd}	Sound pressure level due to direct sound wave, dB
L_{peak}	Peak sound pressure level, dB
L_{pr}	Sound pressure level due to reflected sound wave, dB
L_{pt}	Total sound pressure level, dB
L_{result}	Resultant sound pressure level, dB
L_{sx}	Sound level that exceeds x% of time, dB
L_X	Percentile Exceeded Sound Level, dB
L_W	Sound power level, dB
n	grain shape factor
N	Fresnel number, number of surface elements
ND	Limit of noise dose from noisy activity
NL	Noise level of the noisy activity
NC	Maximum exposure time to noisy activity
NSI	Net Solar Index
p	Sound pressure
p_o	Ambient pressure

P, P_R	Amplitude of pressure fluctuation
pA	A-weighted sound pressure, dBA
p_{rms}	Root mean square pressure level
p_{ref}	Reference sound pressure level, 2×10^{-5} Pa
Q	Number of vehicles per hour
Q, Q_θ	Directivity factor
RR	Rainfall rate, mms^{-1}
R	Universal gas constant, Reflection coefficient
S	Ground surface correction factor for sound pressure due to rain, Vehicle speed
$SENL$	Single event noise exposure level, dB
SR, R, r	Source to receiver distance
S_n	Area of surface element n
S_p	Pore shape factor
SP_r	Sound pressure level due to rain
T	Time, daily exposure time, tortuosity
T_g	Temperature gradient
T_t	Total time
TD	Total noise dose
TNL	Allowable exposure time to the noisy activity
TR	Distance of receiver from the image source
u	Particle velocity, ms^{-1}
V	Average vehicle speed, km/h
W	Wind correction for sound pressure due to rain, Sound power level, Sound
w	Wind Speed , ms^{-1}
W_g	Wind gradient
Z	Acoustic impedance
Z_r	Specific normal acoustic impedance
α_v	Attenuation constant due to viscosity, dB/km
α_a	Attenuation per meter due to air absorption
α_h	Humidity factor on air attenuation
γ	Ratio of specific heats
λ	Wave length, m

ϕ	Phase difference
ϕ_m	Angle of sector of shadow formation due to wind gradient
ξ	Displacement of a particle from equilibrium position, m
ρ	density, kgm^{-3}
ρ_o	Ambient density, kgm^{-3}
Ω	Porosity of air filled pores connected with soil surface
v_n	rms. value of particle velocity in direction *n*, perpendicular to the measuring surface
σ	Flow resistivity of ground surface, $raylsm^{-1}$
ω	Numerical distance
κ	Karman constant

Chapter 1

Introduction and Objectives

1.1 Introduction

Mining involves the operation of machinery and activities generating noise at different frequencies and amplitudes, resulting in noise levels as high as 130 dBA (Derzay, 1972). Apart from direct effects on sensation, hearing, sleeping and masking of speech, exposure to high noise levels can indirectly affect human psychology and physiology, resulting in adverse effects on general performances (Öhrström and Rylander, 1982; Griefahn and Nishi, 1992; Carter *et al*; 1994). A number of ailments have a causal relationship with noise exposure (Yamanaka *et al*, 1982). These facts establish the urgency of estimating the possible noise exposure levels of individuals, and the community in the vicinity of any industrial complex at various phases of its operations. To maintain the noise levels both in near field and far field within the limit prescribed by the standards the land use plans for any industry must be acoustically designed. The

location of plants, machinery and their movements, and road and traffic patterns in a mining complex are planned according to technological and economic requirements. If the acoustic qualities of these are not properly analysed the prevailing noise levels in the neighbourhood may be adversely affected and scope for future expansion or modification may be limited. Noisy workings may lead to violation of environmental guidelines, industrial disputes, and compensation claims. The Control of Pollution Act, 1974 authorises the local authorities to inspect and abate nuisances with the establishment of a Noise Abatement Zone, and entertain complaints if industrial noise levels exceed the standard background noise level by 10 dBA. The Social Security (Industrial Injuries - Prescribed Diseases) Amendment No 4, Regulations 1979 necessitates more measures of noise pollution in industry. The Noise at Work Regulations 1989 (UK) based on the EEC Directive /86/188/EEC have also alerted all sections of industry to the need to measure noise levels at the work place.

The time of occurrence of the numerous noise generating activities associated with mining operations, and variations in the degree and quality of the generated noise, do not follow a simple law. ISO 9613, 3744, 3746, 3891 and 1996 give procedures and guidelines for noise measurement. However, none of these Standards mention noise generated by a group of different equipment performing different activities under various parameters. The influence of conditions pertaining to mining on the propagation of noise from these sources is also not adequately addressed in the existing Standards. The noise sources in any machinery or plant are located at different positions and they work in different cycles, making the determination of exact sound power level of the source very difficult. The noise sources generally emanate sound as a time-dependent functions. Therefore, it is necessary to search for an adequate method for assessing the noise levels in terms of the possible combinations of noise sources and influencing parameters. Tools for prediction of the impact on the noise field after introduction of new machinery into an existing equipment complex at a particular time and location are also not readily available. This problem is further aggravated in mining where technological requirements demand continuous changes in the relative positions of machinery. None the less, the noise levels in a mining complex need to be analysed not

only for proper evaluation of environmental impact but also to incorporate better equipment deployment strategy. The mining industry, therefore, must have access to techniques and prediction systems to assess the noise levels associated with their activities, and have the ability to design their operations with due consideration, to the environment.

1.2 Noise from Surface Mining and Quarrying

The noise level in the near field and the far field of an opencast mine depends on the level of mechanisation. This depends on the geo-mining factors and consequently these factors determine the quality of the environmental noise near the mining areas.

The transfer of energy in the machinery during their operation results in vibrations generating different types of noise. Such vibrations are capable of inducing excess pressure levels in the air medium. An undesirable noise source is one that vibrates to induce a sound pressure level of more than 85 dBA.

There are no records of acoustical analysis of mine designs. However, it is felt that it may become statutory to establish desirable acoustic environments in specified areas near a mining complex. Acoustic design of surface excavations could be possible, provided the variation of the noise field with a change in equipment deployment pattern is established.

A study of the far field noise level is necessary to determine the measures to be taken to minimise noise pollution in the neighbouring residential areas. The noise levels in the near field depend mainly on the acoustic behaviour of the sources. The far field noise levels depend on the layout of these sources in a mine, which determines the sound power levels at the mining faces. The noise levels at a point in the far field depend not only on the sound power levels of the sources, but also on the degree of attenuation during propagation.

Table 1.1 Characteristics of surface mines and quarries affecting the noise field in the neighbourhood.

Characteristics	Influence on Noise Field	Deciding Factors
Depth of ultimate pit	Attenuation by the pit slope as a noise barrier	Geo-mining conditions, mine planning and design
Angle of pit slope	Flatter slopes provide longer distances between the sources and receivers and thus more attenuation by spreading	Stability of the rock mass
Dimension of pit floor	Pattern of distribution of noise sources and reflection and interference of the generated noise	Geology of the reserve, method of mining and quarrying
Spatial extent of the mine	Haulage noise	Design of haul road routing and location of other services and facilities
Location of waste dumps	Haulage noise	Stripping ratio and waste dump design
Work scheduling	Noise field variation with time	Production planning and equipment selection
Machinery deployment pattern	Noise generation and interference	Geo mining conditions, mining economics
Plants, workshop and township	Generation and propagation of noise	Planning of surface layout

Table 1.2 Equipment complexes in different unit operations of various opencast mining systems.

Systems	Unit Operations				
	Drilling and Blasting	Excavation and Loading	Transport	Storage and Dumping	Auxiliary Equipment
Cyclic	1. Drill	Electric Shovel	Dump Truck	Dozer	Dozer, Crane, Grader
	2. Drill	Hydraulic Shovel	Dump Truck	〃	〃
	3. Drill	Dragline	———	〃	〃
Semi-Cyclic	1. Drill	Shovel, Mobile Crusher	Conveyor Belts	Tripper, Spreader, Dozer	〃
	2. Drill	Shovel	Dumper and Conveyor Belt	〃	Semi-Mobile or In-Pit Crusher,
Continuous	1. Drill	Bucket Wheel Excavator, Mobile Transfer Conveyor, Transfer Feeder	Conveyor Belts	Tripper, Spreader, Dozer, Reclaimer	Dozer, Track-Shifter, Crane, Grader, Mobile Crusher
	2. Drill	Bucket Chain Excavator	〃	〃	〃
		Continuous Surface Miner	〃	〃	〃

There are various ways of classifying surface mining activities. All these activities involve a certain amount of noise generation at different phases. Moreover, these activities have certain characteristics that influence the acoustic field in the neighbourhood. These characteristics are determined during the design of the mine considering the prevailing economic and geo-mining conditions. Table 1.1 shows the characteristics of surface mines and quarries, their influence on the noise field and the deciding factors that may control these characteristics. The noise levels in the neighbourhood will also vary during the different phases of the mine under different unit operations. Table 1.2 shows the noise generating equipment complexes for different unit operations in surface mining and quarrying. Thus the surface mining and quarrying noise can be considered mainly as *excavating and loading noise*, *haulage noise*, *drilling and blasting noise* and *material handling noise.*

1.3 Research Objectives

Noise researchers in the past have developed models for the assessment of sound pressure levels and the attenuation around industrial complexes (Tonin, 1993). All of these models, primarily developed for non-mining applications in the field, rely on the determination of sound power level of the noise sources and on the evaluation of attenuation of sound energy during propagation from the source to the receiver. However, although theoretically sound, these models are not directly applicable to a surface mine or a quarry due to the unique nature of mining operations, and other factors specifically:

- the noise sources in a mine are distributed over a wide area and their sound power levels are production dependent and unsteady,
- the noise sources are located at a depth, and the depth varies with time,
- both static and moving sources are present simultaneously,
- the attenuation experienced in different mines varies with geological conditions and mining parameters:
  - ground surface and rock type different than those experienced in most other industrial cases
  - pit-walls behave as a barrier, however the geometry and reflective character of the overall pit shape requires research into this behaviour.
  - wind velocity profiles at different locations around the pit change according to the topographical variations of the mine itself and the surrounding terrain.

Therefore, a model for the prediction of noise levels in the far field of a surface mine or quarry must consider these unique factors listed above.

The main objective of this thesis was to address these problems through theoretical and experimental research, and to develop an environmental noise prediction system applicable in surface mines and quarries. This involved:

1. The development of a Source Power Model to account for the distributed and dynamic nature of the noise sources in mining.
2. The development of a Ground Attenuation Model to incorporate flow resistivities relevant to mining surfaces and rock types.
3. The development of an Air Attenuation Model.
4. The development of a Pit-Wall Attenuation Model to account for the combined characteristics of pit geometry and pit-wall surfaces as a noise barrier.

Figure 1.1 illustrates the modelling procedure followed in this research.

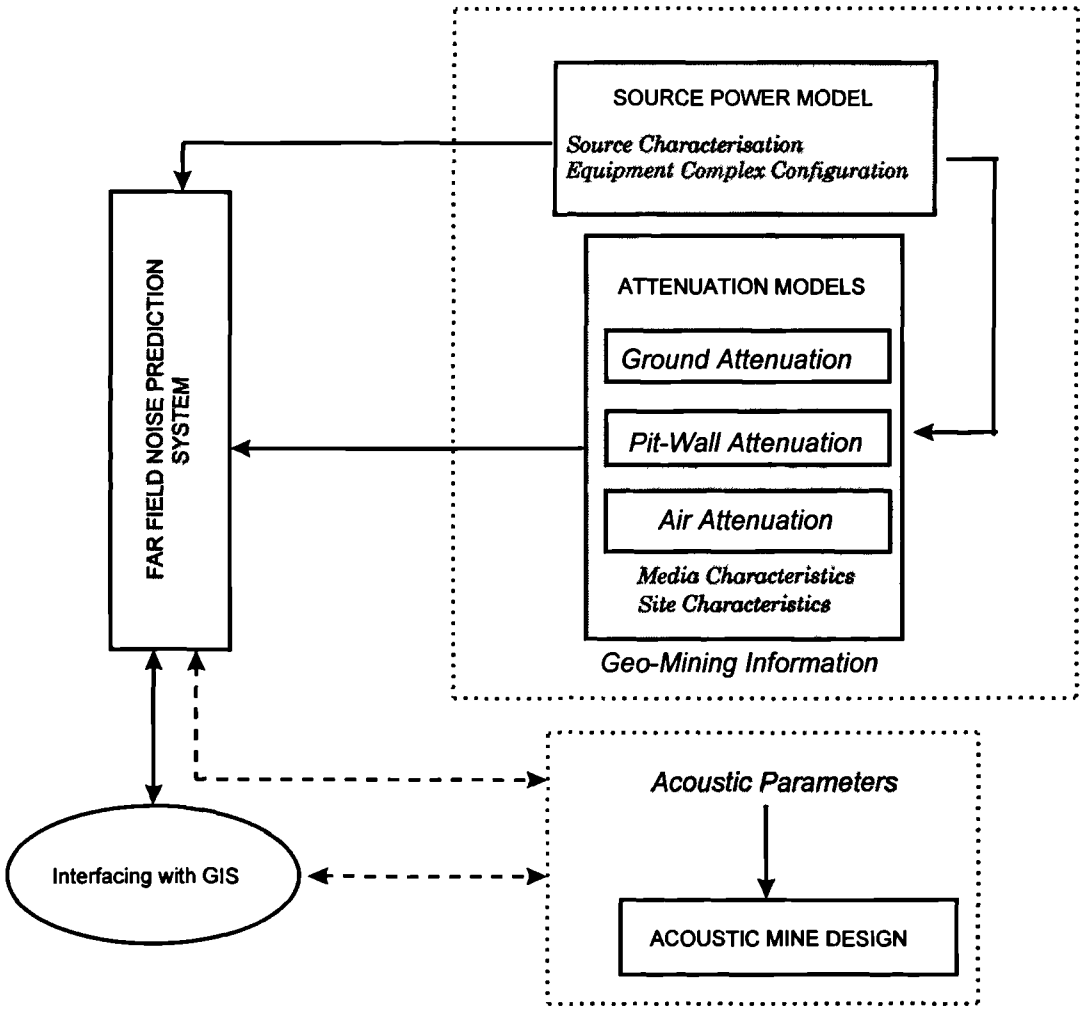


Figure 1.1 The modelling procedure.

An industrial area comprised of a number of noise generators can be represented by an equivalent point source referred to as the Equivalent Acoustic Centre (EAC) characterised by its location, sound power level and Directivity Index (Alster, 1982). Encouraged by the results of a validation test on-site, this method was adopted to develop a source power model for the surface mining noise. The source power model developed determines the sound power level and location of the EAC in terms of sound pressure levels and co-ordinates of EAC definer locations within a noise zone. To apply this model to a mine at its design stage and operating stage, and to emphasise the noise quality prediction in terms of sound pressure level spectra, three complementary techniques namely the Experimental Measurement Technique (EMT), the Acoustic Database Technique (ADT) and the Activity Accounting Technique (AAT) have been developed and implemented in the source power model. Chapter 4 presents the processes involved in these techniques and provides a description of the source power model developed.

The experimentally verified method of Isei (1980) was adopted to calculate the excess attenuation due to ground absorption as a function of the flow resistivity of the ground surface. However, due to the absence of relevant information on the flow resistivities of the type of ground surfaces prevailing near mining areas, systematic experiments involving noise measurement were designed and carried out in three types of mining terrain, namely grass covered loose soil, gritty road surface simulating the haul road and settled quicksand simulating the reclaimed overburden. The results of these experiments form the input data for predicting the noise attenuation by the Ground Attenuation Model. These experiments and the developed model are described in Chapter 5.

Theoretical research on the attenuation of noise in air formed the basis to the development of the Air Attenuation Model to predict attenuation of mining noise by considering the prevailing temperature and relative humidity. The input data was adopted from the work of Sutherland *et al* (1974). The model has incorporated source-receiver configurations in mining conditions receiving its source information from the Source Power Model. Though not tested by field experiments, the model includes the evaluation of ray path curvature directly from experimental wind velocity and

temperature log, or indirectly in terms of the Net Solar Index and the wind velocity. Chapter 6 describes the development of this model.

Considering the noise field within a pit as semi-reverberant, a method was developed to evaluate the loss of sound pressure level due to diffraction at the edge of the pit-wall. The Pit-wall Attenuation Model was developed accounting for the geometric configuration of the source and the receiver with respect to the pit-wall as the input data. The model considers the reflection from the opposite pit-walls to correct the predicted values. Chapter 7 details the initial development of this model. The model is further developed using the theory of image sources and ground absorption, and considering that the barrier effect is independent of the wind speed. Using this model the excess attenuation of sound energy radiated from the pit could be predicted at any location on the surface. This work is described in Chapter 8.

All of the above-mentioned models developed in this research were integrated to form an environmental noise prediction system so that this could be used for the acoustic design of a mine, for the purpose of environmental management. Comprehensive experiments were conducted at a limestone quarry in the Republic of Ireland to test the validity of the models developed. The results of these experiments and the application of the final system to predict noise levels near the quarry are presented in Chapter 8. Chapter 9 summarises the findings of the present phase of surface mining noise research and brings out the henceforth unknown areas where further research are required to fulfil the requirements of environmentally friendly acoustic mine design.

The environmental noise prediction system described in this thesis was developed as one of a number of numerical models to be incorporated in the environmental simulation and impact assessment system currently being completed by the researchers in the Mining and Environment Research Group. The system uses numerical models to predict the environmental impacts of mining operations and utilises a Geographical Information System (GIS) as its spatial database for input, output and spatial operations, and providing a graphical tool for interactive environmental impact assessment. The main components of this system are illustrated in Figure 1.2.

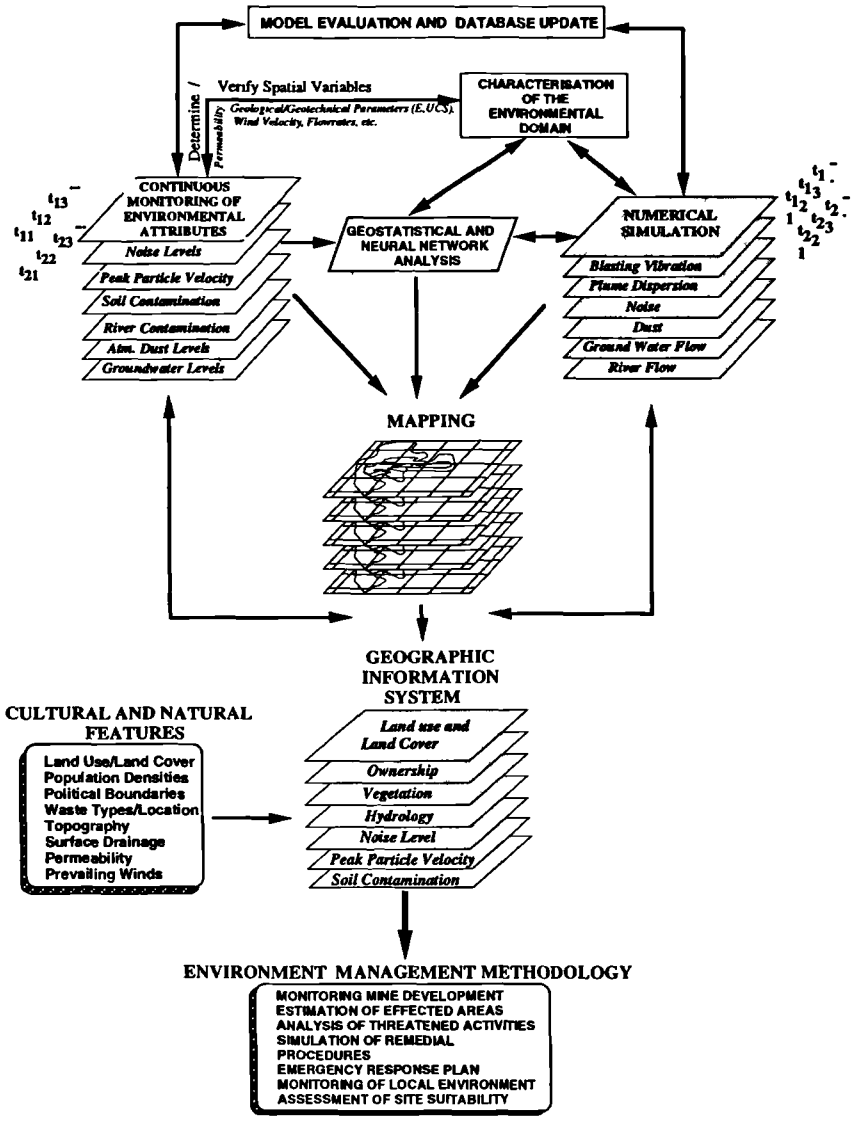


Figure 1.2 The main components of the environmental simulation and impact assessment system which incorporates the noise modelling concept.

Chapter 2

Review of Environmental Acoustics

2.1 Introduction

Numerous scholars have studied sound as a form of energy since the period of Aristotle (384-322 BC) and recognised noise as a health hazard. Ramazzini (1713) studied the effects of noise on the workers engaged in hammering copper and other noisy operations (Green, 1986). Such workers suffered from loss of hearing and became completely deaf in their old age. Bar (1886) conducted similar research on the boiler makers. However, it is only in the 19th century that acoustics has developed as a separate scientific discipline. Chaldni (1756-1824), Helmholtz (1821-1894), Rayleigh (1842-1919), Sabine (1868-1919), etc. were the pioneering scientists (Malecki, 1969). The study of noise during the first half of the current century identified the impacts of noise on human beings. Figure 2.1 illustrates the domain of such effects. Medical researchers (Izumi and Osada, 1988; Rylander *et al*, 1988) have also recognised noise as

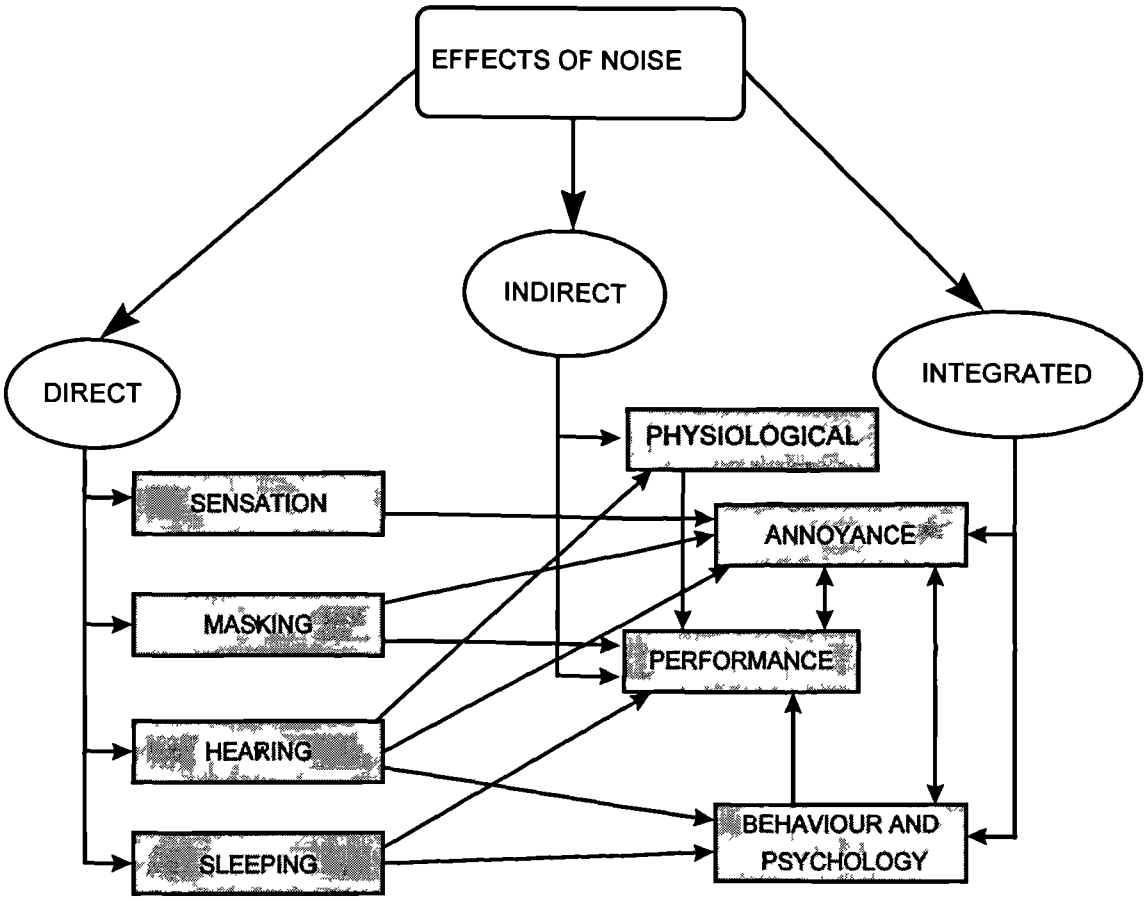


Figure 2.1 Effects of noise on human beings.

an environmental pollutant. Yamanaka *et al* (1982) listed many ailments directly or indirectly related to noise. However, the epidemiological studies have not yet clearly confirmed links between noise levels and physical ailments. White (1975) reported the link of muscular activity with the variation of sound intensity. Griefahn and Nishi (1992) concluded through experimental research that noise evokes physiological responses. These responses are characteristic of stress. Tension increases in muscles at a steady state noise level of 90 dBA. They also reported that long term noise exposures contribute to the genesis of cardiovascular diseases. Effects of environmental noise on sleep and health are still an unresolved issue (Carter *et al,* 1994). Of course, medical science has established that higher noise levels can cause circulatory, digestive and metabolic troubles. Figure 2.2 shows the factors that determine the effects of noise on people. Readers may refer to Kryter (1970), Lord *et al* (1980) and Öhrström and Rylander (1982) for detailed discussions on these issues. The increased awareness of

noise effects resulted in formulation of Standards for the measurement of noise by the national and the international standard organisations. State authorities have also formulated regulations to combat unwanted noise levels.

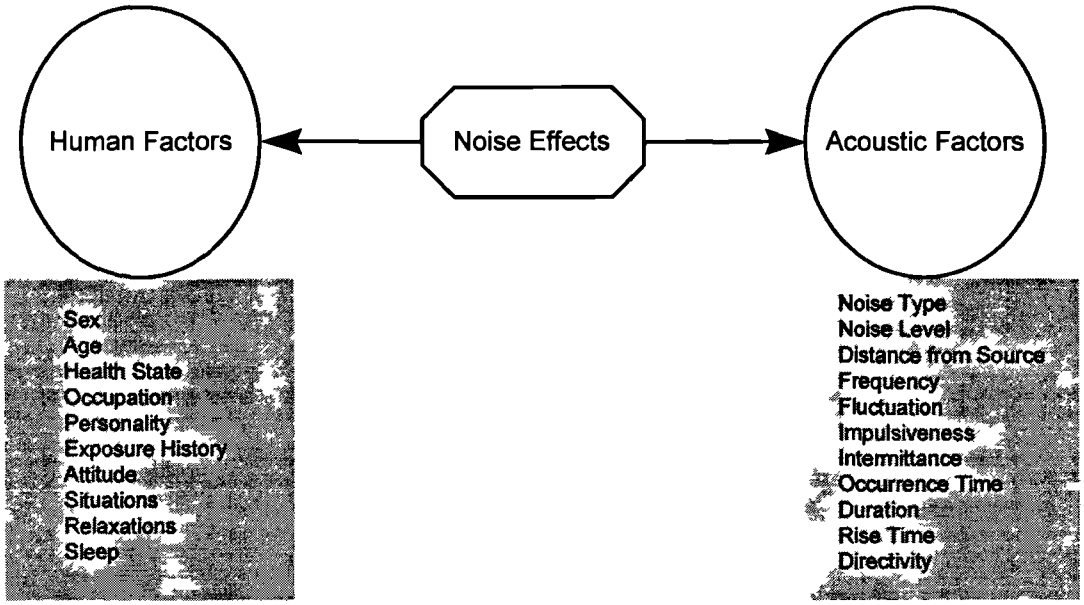


Figure 2.2 Factors influencing effects of noise on human beings.

Noise may cause many physiological, psychological and behavioural problems. Every industry, therefore, should estimate the possible increase in environmental noise level as a result of the industrial activities. Mechanised mining involves a number of machinery and operations that are liable to generate noise at different frequencies and amplitudes. Any residential area near a mining complex also receives other noises indirectly related to mining. Such an area being commercially important for ancillary trades and business, traffic noise increases rapidly. Prediction of mining noise in the residential areas at different phases of mining is indispensable. Mining with acoustically designed land use plans would be more environmentally friendly.

This chapter describes the basic principles of acoustics that are necessary for the study of noise fields near surface mining and quarrying operations. Assessment of industrial noise on the basis these theories will be discussed in the next Chapter.

2.2 Basic Concepts

Human ears perceive certain modulations of the atmospheric pressure as sound. Such modulations result from propagated vibration of an elastic medium or superposition of such vibrations. These vibrations cause an alteration in pressure, stress, particle displacement, or particle velocity of the medium. Sound propagates through the medium as a wave. In the absence of acoustic energy in a particular space the air molecules move about in random thermal motion. There occur frequent collisions amongst the molecules without loss of energy. The net result is an equilibrium condition with characteristic absolute temperature and pressure. On introduction of a vibrating surface the molecules gain additional momentum by momentum transfer and the disturbance propagates into the space with a velocity essentially equal to the thermal speed of individual molecules. If the vibrating surface is a pulsating sphere the sound wave spreads out spherically with a wave of single frequency. This disturbance spreads by momentum transfer. The disturbance induces displacement of the individual particles of the medium. The particles attain velocities in the direction of propagation. These bring changes in absolute pressure and temperature. Human ears or microphones detect this pressure change as sound.

2.2.1 Acoustic Variables and their Relationships

The important variables to describe a sound wave are pressure (P), velocity (U), density (ρ), and temperature (T). Each of these has a mean and a fluctuating component (Bies and Hansen, 1988). In a plane wave all these properties are uniform in a plane perpendicular to the direction of sound propagation.

The equation for pressure fluctuation is:

$$p(x,t) = P_R \sin(kx - \omega t + \phi) \tag{2.1}$$

where,

P_R : amplitude of the pressure fluctuation
ϕ : phase of sound signal being measured relative to some reference
ω : frequency in rads^{-1} defined as:

$$\omega = \frac{2\pi}{T} = 2\pi f \tag{2.2}$$

f : frequency of pressure change within the cycle time, T

The notations for the vectors have been omitted in this thesis and symbols themselves are used to imply vectors. The velocity of propagation of sound wave, c, and wave length, λ is related as:

$$\lambda = \frac{c}{f} \tag{2.3}$$

Wave number, k in Equation 2.1 is defined as:

$$k = \frac{\omega}{c} \tag{2.4}$$

The one dimensional wave equation of propagation of sound in air is:

$$\frac{\delta^2 \xi}{dt^2} = -c^2 \frac{\delta^2 \xi}{\delta x^2} \tag{2.5}$$

Where,

ξ : displacement of a particle for equilibrium position, m
c : velocity of propagation of sound, ms^{-1}

c is determined as:

$$c = \left(\frac{\gamma p_o}{\rho_o} \right)^{0.5} \tag{2.6}$$

Where,

γ : ratio of specific heats, which is equal to 1.4 for air
p_o : ambient pressure
ρ_o : ambient density

Air behaves like an ideal gas at normal temperature and pressure. Therefore, one can write:

$$p_o = \rho_o RT \tag{2.7}$$

where,

R : universal gas constant

and from Equations 2.6 and 2.7:

$$c = \sqrt{\gamma RT} \tag{2.8}$$

To calculate the velocity of sound, c at sea level in dry air R is taken as 28 $Nmkg^{-1}K$. The equation to determine c in ms^{-1} is:

$$c = 20.04(T + 273.16)^{0.5} \tag{2.9}$$

Figure 2.3 shows the variation of speed of sound in air with temperature.

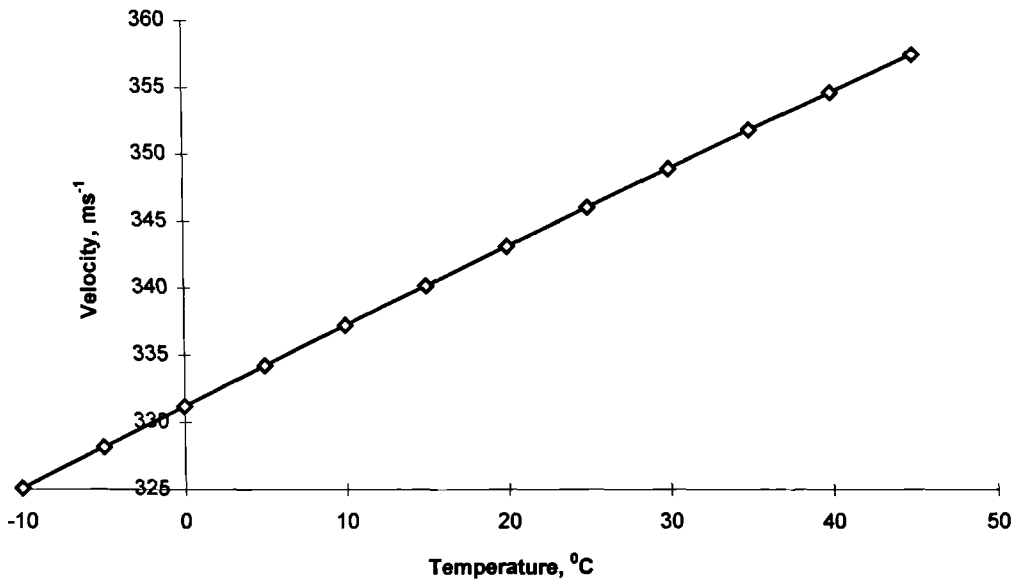


Figure 2.3 Propagation velocity of sound through dry air at sea level under different temperatures.

Newton (1687) assumed that propagation of sound in air is an isothermal process. Later Laplace and Poisson assumed the process as adiabatic (Wilson, 1989). The time interval between compression and expansion of 1 kHz sound wave is one-half period or (1/1000x1/2)=1/2000 second. During this time the thermal speed of sound is 343 ms^{-1} and wavelength is 343 mm. Comparing the half period length (171 mm) with the thermal wave progress, one concludes that heat exchange between compression and expansion is negligible. Thus, the process is taken to be adiabatic .

The general solution of the one-dimensional wave equation of airborne sound is:

$$p = F_1(x - ct) + F_2(x - ct) \tag{2.10}$$

Here,

p : sound pressure that is the difference between instantaneous pressure and ambient pressure

The first term of Equation 2.10 represents the forward propagating noise and the second term represents the backward travelling wave. One determines mean-square sound pressure from the following equation:

$$p_{rms}^2 = \frac{1}{T}\int_0^T p^2 dt \tag{2.11}$$

Here, p is a sound pressure as a function of time. For pure tone the averaging period T is one period or any integer number of periods. For a sinusoidal sound wave of pure tone with amplitude P the root mean square pressure is:

$$p_{rms} = \frac{P}{\sqrt{2}} \tag{2.12}$$

Pressure amplitude due to a spherical sound wave generated by the surface of a radially vibrating sphere depends on the radius (a), amplitude (U_0) of pulsating speed and frequency (ω). The following equation calculates the pressure at distance (Kinsler *et al*, 1982):

$$p(r,t) = \frac{\rho_0 c U_0 a}{r} \exp\left[j(\omega t - k(r-a) + \phi) \right] \tag{2.13}$$

A sound wave is freely propagating when the particle velocity is in the direction of wave propagation and when the pressure and particle velocity reach their maximum and minimum values simultaneously. This occurs when

$$k^2 r^2 >> 1 \tag{2.14}$$

where,

k : wave number
r : distance from the centre of the source
a : characteristic dimension of the source

r is normally much larger than a in most of the environmental acoustical situations. Such a wave may be a plane wave or a spherical wave. For spherical wave propagation from a point source the pressure perturbation is derived as:

$$p(r,t) = \left(\frac{A}{r}\right) \cos 2\pi \left(ft - \frac{r}{\lambda} \right) \tag{2.15}$$

where, A is the amplitude and the air particle velocity expressed is:

$$u = \left(\frac{A}{r}\right) \frac{\left[1 + (2\pi r/\lambda)^2\right]^{1/2}}{\rho c (2\pi r/\lambda)} \cos 2\pi \left(ft - \frac{r}{\lambda} - \frac{\theta}{2\pi} \right) \tag{2.16}$$

where the root mean square pressure, p_{rms}, is:

$$p_{rms}^2 = \frac{A^2}{2r^2} \tag{2.17}$$

Figure 2.4 shows the plot of sound pressure waves at different times for constant amplitude sound at 1 kHz frequency. This illustrates that the wave repeats on increase of the distance by wavelength, λ.

The ratio of the acoustic pressure in a media to the associated particle speed is termed as specific acoustic impedance, Z. For a plane sound wave this is called characteristic impedance of the medium and expressed as:

$$Z = \pm \rho c \tag{2.18}$$

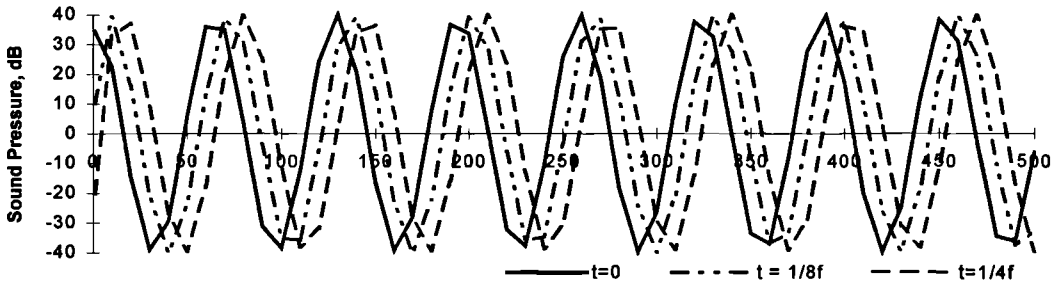


Figure 2.4 Sound pressure wave at different times for constant amplitude sound at 1 kHz frequency.

The sign is selected depending on the direction of propagation. *Intensity* (I) of sound is the average amount of acoustic power passing through a unit area of the medium that is perpendicular to the direction of propagation of sound. For a freely propagating spherical sound wave of single frequency it is as given below:

$$\begin{aligned} I &= \frac{1}{T}\int_0^T p(r,t)\cdot u(r,t)\,dt \\ u(r,t) &= \frac{p(r,t)}{\rho_o c} \end{aligned} \tag{2.19}$$

By definition, acoustic or sound power (W) of a sound source is the acoustic energy generated per second by the source and it is calculated in watts as:

$$W = I 4\pi a^2 \tag{2.20}$$

where,

a : radius of a sphere whose centre is the sound source

If p_{rms} is the rms sound pressure at a distance, R from a spherical source the acoustic power will be:

$$W = \frac{p_{rms}^2}{\rho_o c} 4\pi R^2 \tag{2.21}$$

For an arbitrary source radiating sound non uniformly W can be obtained as:

$$W = \sum_{n=1}^{N} \frac{\left(\bar{p}^2\right)_n S_n}{\rho_o c} \tag{2.22}$$

where,

N : number of surface elements
S_n : area of each surface element
$\bar{p}_n$: average rms acoustic pressure over each surface element

There are extensive studies on sound waves as plane waves and spherical waves. Various solutions of wave equations of acoustic propagation are available. There is numerous literature treating sound propagation by one dimensional and three dimensional wave equations. Depending on the purposes defined by the boundary conditions there are treatments of wave equations as linear or non-linear. Readers may find detailed discussions in Kinsler *et al* (1982) and Norton (1989).

2.2.2 Decibel Scale

Human ears can hear sounds of root mean square sound pressure ranging from 20 μPa to 200 Pa. Because of such a large range, it is customary to report sound measurements in decibels. A decibel level is ten times of the logarithm (base ten) of a power ratio. To measure sound pressure, sound power and sound intensity in decibels one requires their standardised reference values. American National Standards Institute (ANSI) and International Standard Organisation (ISO) define these reference values as:

$p_{ref} = 2 \times 10^{-5}$ Pa
$W_{ref} = 10^{-12}$ Watt
$I_{ref} = 10^{-12}$ Wattm^{-2}

The following equation gives Sound Pressure Level (SPL) in terms of reference pressure (p_{ref}) and root-mean square sound pressure:

$$L_p = 20\log\left(\frac{p}{p_{ref}}\right) \tag{2.23}$$

The reference pressure (20 μPa) is the nominal threshold of hearing. The above definition puts the sound pressure level of the nominal threshold of hearing at 0 dB. A doubling of mean square sound pressure corresponds to approximately 3 dB increase in sound pressure level (SPL). The following equation is used to determine the root mean square sound pressure from the SPL:

$$p_{rms} = 2 \times 10^{\left(L_p - 100\right)/20} \tag{2.24}$$

The amplitude of the sound wave is expressed by Equation 2.12 as:

$$P = \sqrt{2} p_{rms} \tag{2.25}$$

By definition, the standard atmosphere has an absolute pressure of 101,325 Pa. The sound pressure of a loud sound of level 90 dB is thus less than 1/100000th of one atmospheric pressure.

2.2.3 Sound Power

Sound power is the rate at which a machine produces sound energy. Ordinarily only a very small fraction of the input energy of a machine is converted to sound power. However, in many situations a fraction of a Watt can create objectionable noise levels. Determination of sound power is important for the prediction of noise levels and the evaluation of noise control measures.

Sound power level is defined as the ratio of sound power to a reference power as follows:

$$\begin{aligned} L_W &= 10\log\left(\frac{W}{W_{ref}}\right) \\ &= 10\log\left(\frac{W}{10^{-12}}\right) \\ &= 10\log W + 120 \end{aligned} \tag{2.26}$$

where,

L_W : sound power level, decibel
W : sound power of the source, watt
W_{ref} : reference sound power, watt

If the sound pressure level at a point at a distance r from the source is L_p in dBA, the intensity at that point is:

$$I = 10^{-12} \times 10^{L_p/10} \tag{2.27}$$

To provide this intensity at a distance r the source must have a power, W given by:

$$W = 4\pi r^2 I \tag{2.28}$$

Sound pressure level at that point is:

$$L_p = 10\log\left(\frac{W/4\pi r^2}{10^{-12}}\right) = L_W - 20\log r - 11 \tag{2.29}$$

If the source is near the ground and sound transmits hemispherically, the expression reduces to:

$$L_p = L_W - 20\log r - 8 \tag{2.30}$$

Thus, estimation of sound pressure level at a location is possible from the known values of sound power level. Development of a method to determine the sound power level for noise sources in surface mining and quarrying operations was the major objective of the present work and the principle of the modelling techniques developed will be discussed in Chapter 4.

2.2.4 Combined Effects of Sound

When two pure tone sounds occur at the same time, the combined effect depends on the phase relationship at the receiver. There may be cases of reflection where a noise source is emitting a sound wave. Such reflection may give rise to correlated sound waves which have a precise time and frequency relationship. Let there be two sound waves:

$$p_1 = P_1 \cos(\omega_1 t + \phi_1) \tag{2.31}$$

$$p_2 = P_2 \cos(\omega_2 t + \phi_2) \tag{2.32}$$

where,

p : instantaneous sound pressure
P : sound pressure amplitude
ω : angular frequency
ϕ : phase angle

The instantaneous sound pressure due to the two waves is given by the sum of the two instantaneous sound pressures. Mean square sound pressure of the combined wave is:

$$p_{rms}^2 = \frac{1}{T}\int_0^T (p_1 + p_2)^2 dt \tag{2.33}$$

where,

T : averaging time which is equal to an integer number of periods at both frequencies

T should include many periods so that any contribution from fractional periods is insignificant. Therefore,

$$T >> \frac{1}{f_{\min}} \tag{2.34}$$

where,

$f_{\min}$: lower frequency

The integration in the Equation 2.33 results in the following relationships (Wilson, 1989):

$$p_{rms}^2 = \frac{\left(P_1^2 + P_2^2\right)}{2} + P_1 P_2 \cos\left(\phi_1 - \phi_2\right), \quad \omega_1 = \omega_2$$
$$p_{rms}^2 = \frac{\left(P_1^2 + P_2^2\right)}{2} = p_{rms1}^2 + p_{rms2}^2, \quad \omega_1 \neq \omega_2 \tag{2.35}$$

For correlated sounds the frequencies are equal. Thus the first of the above equations is applicable. This shows that if two sound waves with same amplitude and frequency occur together at a phase difference of 180° at an observer then the sound pressure at the observer will be theoretically zero. This principle is used in active noise control.

Like most of the industrial noise, the noise generated during surface mining operations represents a combination of many uncorrelated sources. The amplitudes and frequencies of the sound waves generated by these sources vary randomly. Thus the second relationship shown in Equation 2.35 is applicable. If the sound pressure levels contributed by the noise sources are known their combined effects is calculated as:

$$L_{pT} = 10\log\left(10^{L_{p1}/10} + 10^{L_{p2}/10} + \cdots\right) \tag{2.36}$$

where,

L_{pT} : combined sound pressure level due to the sources
L_{pi} : sound level of the ith source

2.2.5 Frequency Weighting

Industrial noise is the result of contributions from a number of sources. Therefore, it may have sound pressure waves of different frequencies. Perception of loudness by the human ear varies with the frequency of sound. A noise appears to be louder if the concentration of energy is in the middle frequencies. Let there be two cases of noise. In the first case the energy concentration is in the middle frequency, that is near 1 kHz. In

the second case it is near the low frequency (31.5 Hz). The noise in the first case here appears to be louder. Sound at frequencies near 1000 Hz seems to be louder than sound at higher frequencies (near 20 kHz). The effect of frequency is more prominent with soft sounds than it is with loud sounds.

Frequency weighting takes typical human response into account when all the audible frequency components of noise samples are to be described by a single number. There are five types of weightings *viz* A, B, C, D and SI as shown in Figure 2.5.

Adjustment of sound levels in each frequency band to correspond to the approximate response to soft sounds provides A-weighted sound level. B-weighting and C-weighting correspond, respectively, to human responses to moderate and loud sounds. The C-weighting is relatively flat in the middle range of frequencies. In this system less than 1 dB is subtracted from levels measured in the frequency bands from 63 Hz to 4 kHz. D-weighting has been used to approximate perceived noisiness of aircraft. Speech Interference (SI) weighting evaluates noise in terms of speech interference considering the fact that sounds less than 100 Hz or more than 7.5 kHz are not important for speech interference.

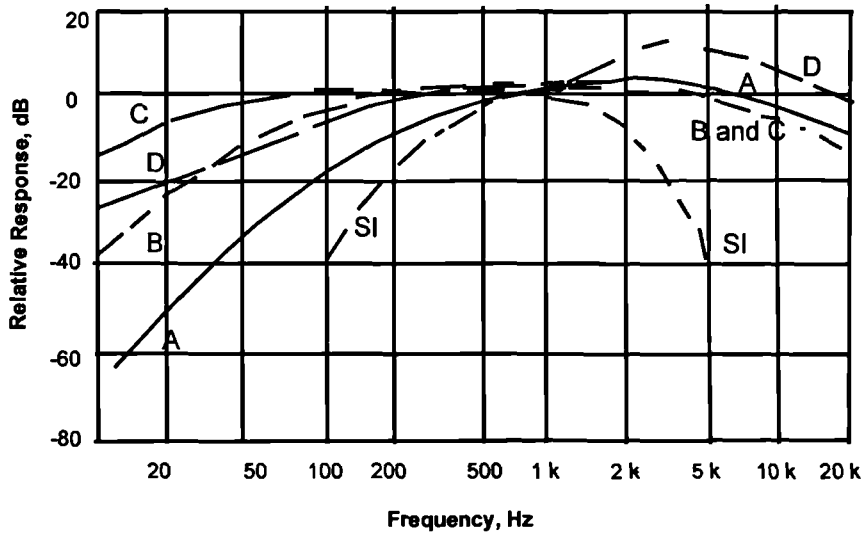


Figure 2.5 Response curves for A-, B-, C-, D-and SI-weighting (after Wilson, 1989).

2.2.6 Directional Characteristics of Sound Sources

If the dimension of the sound source is smaller than the wave-length of the radiated sound wave then the source is omni-directional. In most cases the size of sound source is comparable with the wave-length and hence directionality is to be taken into account in any analysis.

A Directivity Factor Q_θ, of a directional noise source of power W, defines the ratio of the sound intensity I_θ, at some distance r, from the source and at an angle θ, to a specified axis to the sound intensity I_s, at the same distance due to a uniformly radiating sound source of equal power. Thus,

$$Q_\theta = \frac{I_\theta}{I_s} \tag{2.37}$$

The directivity factor is a function of both angular position and frequency. Directivity Index is defined as:

$$DI_\theta = 10\log Q_\theta \tag{2.38}$$

Ignoring the effect of atmospheric attenuation, absorption by vegetation and terrain conditions the sound pressure level at a point of observation can be related to the sound power level of the source and the directivity factor as:

$$L_p = L_W - 10\log\frac{4\pi r^2}{Q_\theta} \tag{2.39}$$

Table 2.1 Directivity factor for different positions of noise source (After Norton, 1989).

Position	Directivity Factor	Directivity Index
Free space (e.g. near the centre of a large room)	1	0
Centre of a large flat surface (e.g. centre of a wall, floor or ceiling)	2	3
Intersection of two large flat surfaces (e.g. intersection of a wall and a floor)	4	6
Intersections of three large flat surfaces (e.g. corner of a room)	8	9

Table 2.1 gives the values of directivity factors for different positions of noise source. Given the sound power level L_W, and the directivity index DI, the sound pressure level L_p, can be evaluated at any position, relative to the source.

2.2.7 Sound Field

Noise generated by a vibrating surface of any form travels through the surrounding medium as waves propagating in all directions spatially. The particles of the medium transmit the sound waves to the receiver. Reflection of the propagating sound waves occurs wherever and whenever they come across other surfaces or materials in the path of propagation. Sound field is the space in which the sound waves exist as a disturbance caused by the noise sources, reflecting surfaces and other influencing factors in the medium. Measurements of sound pressure levels at close grid points can give a complete description of sound field. Such surveys enable us to predict the type of source and its location. This helps also in computing the sound power radiated from the source. There are three types of radiation field of a sound source, namely hydrodynamic near field, geometric near field and far field. Figure 2.6 shows these fields.

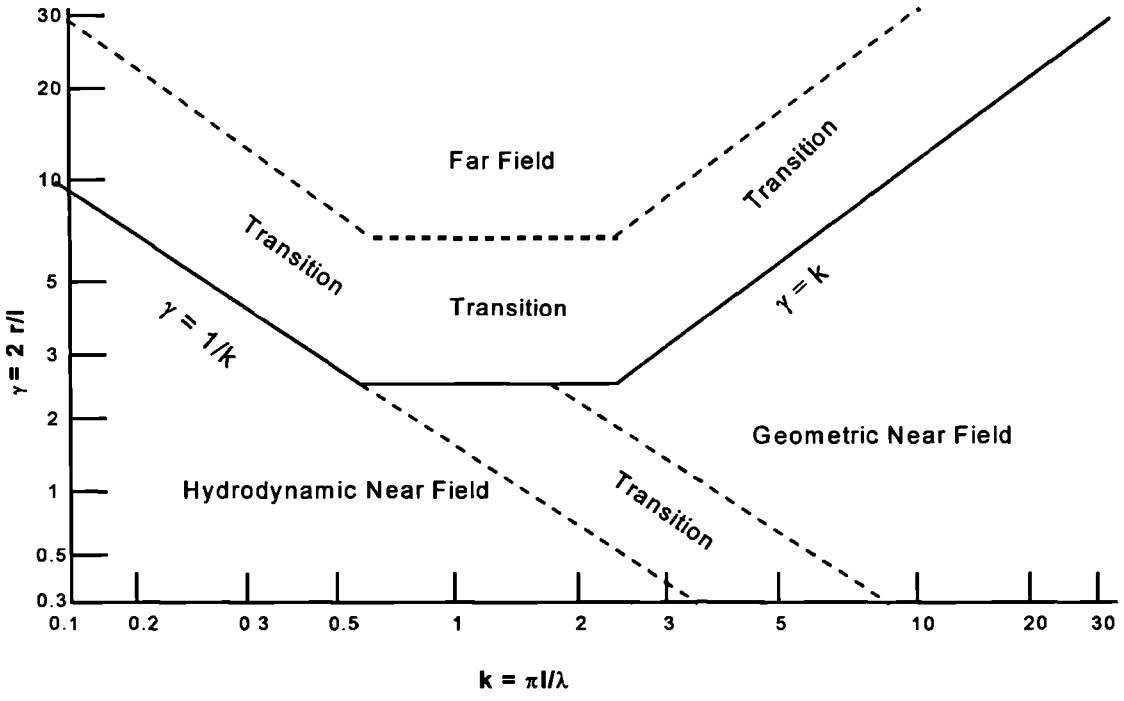


Figure 2.6 The radiation fields of a noise source (after Bies and Hansen, 1988).

The hydrodynamic near field is the region immediately near the vibrating surface of the source. This field extends outward to a distance much less than one wavelength. There is no fluid motion directly associated with sound propagation in this region. Near the vibrating surfaces the acoustic pressure and the local particle velocity are out of phase. The acoustic pressure amplitude measured in the near field does not give a true indication of the sound power level of the source.

The sound field next to the hydrodynamic near field is the geometric near field. Effects of interference are more prominent in this region. The sound pressure level does not decrease here monotonically at the rate of 6 dB per doubling of distance. Instead, there may be relative maxima and minima. This effect is greater for single frequency sound than for band noise. However, the particle velocity and pressure are always in phase. It is possible to calculate the radiated power from extensive sound pressure measurements in the geometric near field. However, due consideration to directivity is necessary.

The region beyond the geometric near field that extends to infinity is the far field. In this region, sound pressure level decreases monotonically at the rate of 6 dB per doubling of distance from the source. Bies (1976) forwarded three conditions for far field. These are:

$$r >> \frac{\lambda}{2\pi}, \qquad r >> l, \qquad r >> \frac{\pi l^2}{2\lambda} \tag{2.40}$$

where, r is the distance from the source to measurement position, λ is the wavelength of the radiated sound and l is the maximum source dimension. The phrase, "much greater than" (>>), in the above conditions refers to a factor of three or more. The two factors, γ and K can be defined as:

$$\gamma = \frac{2r}{l}, \qquad K = \frac{\pi l}{\lambda} \tag{2.41}$$

The new criteria will be:

$$\gamma >> \frac{1}{K}, \qquad \gamma >> 2, \quad \gamma >> K \tag{2.42}$$

The sound field surrounding a noise source can also be a direct radiation or reverberant field. Simple sources exhibit the direct radiation or free field. In such a field, sound pressure level decreases at the rate of 6 dB per doubling of the distance from the centre of the source (Norton, 1989). The reverberant field exists at a distance where a multiple reflection from bounding surfaces becomes important. The sound field is a function not only of the source but also of the characteristics of the space surrounding the source.

Broad bands of frequencies of periodic, aperiodic and impulse sounds constitute industrial and community noise. Depending on its quality, noise can be ambient or background noise, steady-state noise, fluctuating or intermittent noise or impulsive noise. Ambient or background noise is the noise in an environment from both near and far sources. Usually it refers to minimum levels when no strong sources of noise or sound are present. Steady-state noise often refers to machinery or apparatus where sound levels are reasonably constant. In fluctuating noise sound may vary in levels but remains for longer duration than the integration time of the human ear (about 200 μsec). An impulsive noise is of very short duration for its peak pressure levels (change in rms pressure levels greater than 40 dB per 0.5 sec). White (1975) and Bies and Hansen (1988) elaborately discussed these subjects.

2.3 Present Status of Noise Awareness

State authorities try to control the noise level from various industries by specifying standard values of acceptable noise. Table 2.2 shows the recommended A-weighted equivalent noise levels for newly constructed roadways and railways. Table 2.3 shows the recommended values for different areas (Walker, 1992).

British Standards 5228:1984 reports the method of estimating noise for construction sites. Part 1 describes the procedure for estimation of site noise. This document also provides the sound power levels of different types of earth moving machinery. Part 3 of this document describes the code of practices for noise control applicable to surface coal mines. Other related documents and standards are listed in Appendix 1. However, these documents do not reveal a ready to use model for applying by the mining industry.

Table 2.2 Recommended noise standards for new railways and new roads (after Walker, 1992).

Country	Standards, Guidelines or Recommendations	Road Facade (F) Free-field (FF) L_{Aeq} (or as stated)	Railway Facade (F) Free-field (FF) L_{Aeq} (or as stated)	Duration in a day	Note
Denmark	G	58(F)	63(F) 88 L_{Amax}	24 h 24 h	
Norway	R	-	60(F)	24 h	
Sweden	S	-	63(F) 30(indoor, living) 50 L_{Amax}(indoor, bed)	24 h 24 h 2200-0600	
France	R	60(F)	65-70(F)	0800-2000	1
Germany	S	59(FF) 49(FF)	59-64(FF) 49-54(FF)	0600-2200 2200-0600	1
Netherlands	S	- 55(F) 50(F) 45(F)	60(F) 60(F) 55(F) 50(F)	24 h 0700-1900 1900-2300 2300-0700	1, 2 1, 2 1 1
Italy	R	**			
Switzerland	S	55 45	60(FF) 50(FF)	0600-2200 2200-0600	1 1
UK	S: Road R: Railway	68 L_{A10},18h	68(F) 63(F)	0600-2400 2400-0600	1 1

1: Insulation to property provided when those levels exceeded.
2: These limits to be reduced to 57 dBA on 1 January, 2000.

The Noise Abatement Act, 1960 is an example of attempts to combat environmental noise. Noise Advisory Council of Royal Committee on Environmental Pollution, Department of the Environment, Building Research Station and Ministry of Public Building and Works have conducted studies on the effects of noise and how to control them. International Standards 1996 Part 1 covers the basic quantities and procedures for description and measurement of environmental noise. The Part 2 deals with norms of data acquisition and Part 3 gives the standards to follow while conducting a noise survey. It specifies how to write noise survey reports. ISO-3741-3746 covers various aspects of noise measurement and environmental noise assessment. ISO 6081: 1986 offers the statistical methods for determining and verifying stated noise emission values of machinery and equipment.

Table 2.3 Land classification scheme and maximum sound levels allowed for outdoor noise.

Land Areas	Maximum L_{eq} (dBA)	
	Day (6.00 - 22.00)	Night (22.00 - 6.00)
1. Particularly Protected Areas	50	40
2. Mostly Residential Areas	55	45
3. Mixed Areas	60	50
4. Areas of Intense Human Activity	65	55
5. Mostly Industrial Areas	70	60
6. Exclusively Industrial Areas	70	70

Environmental Protection Agency (EPA) of the USA through its Office of Noise Abatement and Control has worked for developing noise standards since 1970. EPA had to conduct a full and complete investigation and study of noise and its effects on public health and welfare under Title IV of Public Law 91-604. Table 2.4 shows the various noise control programs conducted by different agencies in the USA.

Table 2.4 Noise control programs in the USA (after White, 1975).

Agencies	Noise Control Program
Department of Agriculture	Research on noise reduction from vegetative screen etc. Clark-McNary Act of 1942, McSweeny- McNary Forest Act of 1928, and Agricultural (Smith-Lever Act of 1955).
Department of Commerce	Noise standards; materials research and subjective studies are undertaken by the National Bureau of Standards.
Department of Defence, US. Air Force	Noise abatement in propulsion systems, and bio-acoustics.
US. Army	Hearing conservation and occupational noise control. Biomedical effects of noise, auditory perception and, and siting of military activities.
US. Navy	Noise reduction of operating and testing aircraft.
Department of Health, Education and Welfare	Occupational health, industrial safety, diagnosis of hearing loss, and training.
Department of Housing and Urban Development	Housing site selection, structural characteristics of buildings, and noise emission ratings for appliances and equipment.
Department of Interior	Bureau of Mines training program and study of sonic booms.
Department of Labour and Health Act (OSHA).	Walsh-Healy Contract Act and Occupational Safety
Department of Transportation	Transportation noise, including aircraft
National Aeronautics and Space Administration	Aircraft noise research, audiometric testing programs; The Aircraft and Noise Reduction Laboratory (Hampton,Va).

Numerous experimental studies have established the safe duration of exposure to different A-weighted levels as shown in Table 2.5. General recommendation is that the industry must have an effective hearing conservation program if the noise levels exceed

these values. According to the present norms the exposure to impulsive or impact noise should not exceed 140 dB peak sound pressure level. When the daily noise exposure is composed of two or more periods of noise exposure of different levels, their combined effects should be considered, rather than the individual effects of each. The condition for safe exposure is:

$$C_1/T_1 + C_2/T_2 + \ldots + C_n/T_n < 1.0 \tag{2.43}$$

where,

C_n : total time exposure for nth noise events, (n=1,2,3...)
T_n : time of exposure at that event

Readers may refer to the various laws and acts for detailed information on environmental noise awareness. Hughes (1989) reviewed the existing Acts and the possibility of their application in noise related cases.

Table 2.5 Safe sound exposure limits (after White, 1975).

Duration per day (hours)	Sound level dBA (slow response)
8.0	90
6.0	92
4.0	95
3.0	97
2.0	100
1.5	102
1.0	105
0.5	110
0.25 or less	115

2.4 Summary

The basic theory and concepts of acoustics related to the study of environmental noise are briefly discussed in this Chapter. It has been observed that the problems of environmental noise has been addressed by various authorities and attempts have been made to develop standard practices for measurement and control of noise. However, very little information is available on mining noise. So far, not many attempts have been

made to model mining noise in order to develop input data for mine planning and design purposes. The author has attempted to develop a method of prediction and modelling of surface mining and quarrying noise. This type of model can be used for planning equipment deployment patterns and production scheduling. Through the application of such a model the impact on the environment could be kept within the required limits. The current techniques of noise assessment will be discussed in the next Chapter. The subsequent chapters will reveal how this knowledge has been applied to develop a model for the assessment and prediction of noise levels near surface mining and quarrying operations.

Chapter 3

Current Techniques of Industrial Noise Assessment

3.1 Introduction

The development of theories regarding generation, propagation and attenuation of acoustic waves resulted with the techniques of measurement of sound energy. The basic principles were discussed briefly in Chapter 2. This chapter discusses the currently practised methods of noise estimation.

The noise generating operations in any industrial site are large in number and do not follow a simple relationship amongst them so far as their time of occurrence and variations in noise generation are concerned. Two industrial sites having the same acoustic characteristics will be rare. Therefore, it has always been of great interest to search for an adequate method of assessing the industrial noise level for all the possible combinations of noise sources and influencing parameters. British Standards 5228: Part 1: 1984 laid out the prevailing methods for assessment of noise from industrial sites. Acoustic disturbances arising from the use of industrial machinery are analysed by using

the principles of wave acoustics, ray acoustics or energy acoustics. The wave acoustics approach describes wave propagation using the particle model. In ray acoustics wave propagation over large distances like that in atmosphere is described taking due considerations for the effects of temperature gradient and wind velocity. Energy acoustics uses statistical energy analysis (SEA) techniques to describe the propagation of sound wave as transfer of energy of different parameters. Statistical energy analysis is a modelling procedure for the theoretical estimation of the dynamic characteristics, the vibration response levels and the noise radiation in complex, resonant, built-up structures using energy flow relationships. It has been accepted as a prediction model for industrial machine noise and vibration as well as for optimisation of their control, particularly in high frequency regions where a deterministic analysis of all the resonant modes of vibration is not practical. Lyon (1975), Woodhouse (1981), Stimpson *et al* (1986) and Norton (1989) discussed various aspects of this method for predicting sound power of sources. The SEA method has become more popular for analysing in-plant industrial noise and vibration problems. However, this technique needs rigorous experimental studies for determining various loss factors. The use of this technique will not be simple and cost effective for environmental noise assessment for surface mining and quarrying operations. The methods of wave acoustics are the most fundamental. The method of ray acoustics is more relevant for long distance outdoor propagation of noise.

The objective of the present work is to develop a method of estimating noise level near surface mines and quarries. Most of the present methods are based on noise measurements. This Chapter reviews the existing methods of industrial noise assessment and highlights the existing modelling procedures. The subsequent chapters describe the predictive methods developed in this research.

3.2 Noise Measurement

As discussed in Chapter 2, the sound level measuring instruments use different weightings or filter networks to account for the variations of loudness with sound pressure levels. For noise measurement purposes A-weighting network has been industrially accepted and the unit of noise measurement is often written as dBA. Noise

level at a point in the far field of a noise source depends primarily on the sound power level of the source and the influence of external factors. The prediction of noise level, therefore, involves the measurement of the sound power of the source. Developments in instrumentation during the last three decades have made it possible to precisely detect the variation of our acoustic environment. Noise measurements are carried out either as sound pressure level measurements or sound intensity measurements by using sound level metres. Instruments are available for real time frequency analysis of the acoustic waves. Noise measurements may be carried out as precision measurements, engineering measurements or survey measurements as specified in the British Standard BS 4196. Yang and Ellision (1985) classified the measurement procedures in these Standards according to the method of measurement, test environments, characteristics of measured noise and obtainable sound power level. Ellison *et al* (1969) discussed the methods of measurement of radiated noise from an electric machine. Hassal and Zaveri (1979) described the sound measurement procedures for free field environment in detail. A number of researchers have made important contributions in the field of noise measurement (Land, 1973; Schultz, 1986; Holmer, 1977; Hübner, 1977). Readers may refer to more information on noise measurement principles and techniques in Peterson and Gross (1977).

For noise estimation purposes measured noise levels are expressed in terms of different indices. The index is selected based on the purposes. Commonly used noise estimation indices are described below.

3.2.1 Index for Noise Estimation

Noise is described objectively in terms of sound pressure level or sound intensity levels at the receivers and as sound power level at the source. Loudness, annoyance, sleep-interference and masking are some subjective descriptions of noise. However, these measurements do not give an overall impression of total noise exposure of a listener. Therefore, it was necessary to evolve a method for comprehensive representation of the time history of sound exposure. Commonly used noise descriptors can be represented in general by Figure 3.1.

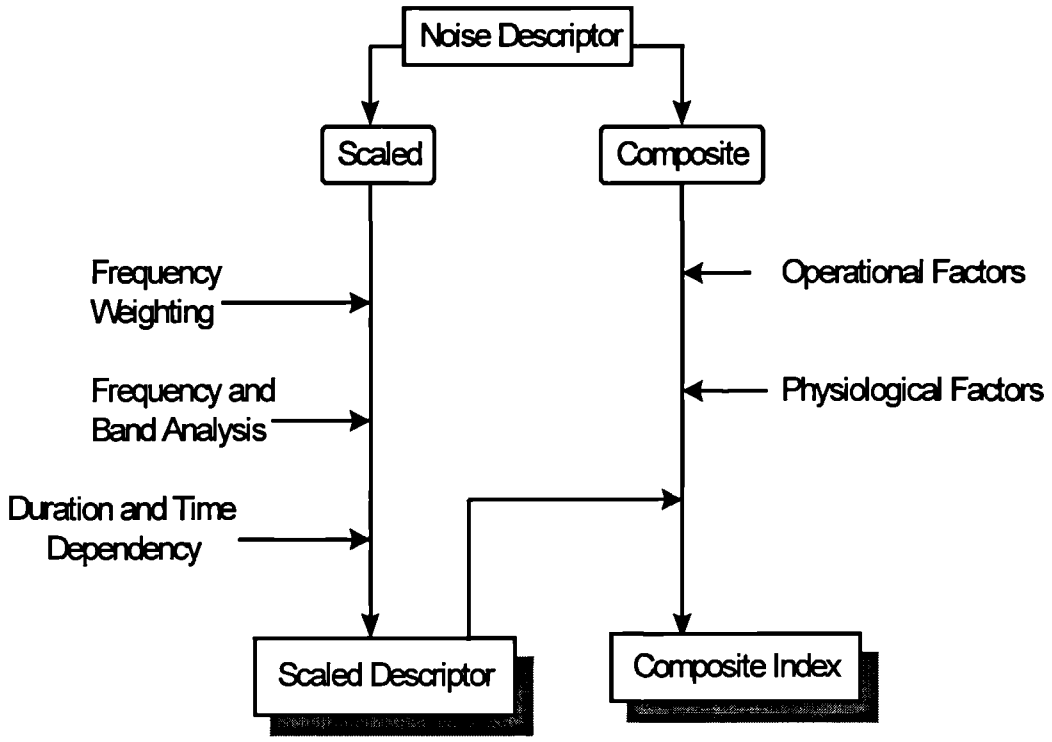


Figure 3.1 Noise descriptors.

Table 3.1 shows the various descriptors of noise used for measurement and representation of noise levels. There are various methods of converting the noise-level-vs.-time information to simplified indices. Some commonly used indices are discussed below.

3.2.1.1 Sound Pressure Level, L_p

Sound pressure level is defined in decibels as 20 times the logarithms (to the base 10) of the ratio of root mean sound pressure to the reference sound pressure of 20 μPa. This must be stated along with the frequency bandwidth.

$$L_p = 20\log\left(\frac{p_{rms}}{p_{ref}}\right) \tag{3.1}$$

where,

p_{rms} : root mean squared pressure value
p_{ref} : reference value

Table 3.1 Various noise descriptors (after Peterson and Gross, 1977).

Descriptor	Abbreviation	Base Measure	Adjustment to Base Measure	Derivation	Relation to other Descriptor	Application
Weighted sound level	L_A, L_B, L_C ,L_D ,L_E	1. Octave or 1/3 octave band 2. Measured directly from a sound level metre.	None			General
Phons, Sones	LL_S (Steven's procedure) LL_Z (Zwicker's procedure)	1. Octave or 1/3 octave band 2. Equal loudness contour	None	S=Sm+f(ΣS-Sm) P=40+10log 2St		Loudness
Perceived Noise Level	L_{PN}	1. Octave or 1/3 octave band 2. Equal noisiness contour	None	PNt= PNm + f(ΣPN-PNm) L_{PN}= 40 + 10log2PNt	$L_{PN} = L_D + 7$ $L_{PN} = L_A + 13$	Noisiness
Effective Perceived Noise Level	L_{EPN}	L_{PN}	1. Duration 2. Tone	$L_{EPN} = L_{PN} + C + D$		Noisiness
Articulation Index	AI	1/3 octave band	None	ANSI, 1969		Speech Interference
Speech Interference Level	SIL	Octave Bands	None	Average Octave Bands with Centre Frequencies of 500, 1000, 2000 and 4000 Hz.	$SIL = L_A + 7$	Speech Interference

Table 3.1 Contd.

Descriptor	Abbreviation	Base -Measure	Adjustment to Base Measure	Derivation	Relation to other Descriptor	Application
Preferred Noise Criteria	PNC	Octave Bands	None	See Beranek *et al*, 1971		Interior Room Noise
Statistical Sound Levels	L_X	L_A	None	Time-history		Community Noise
Traffic Noise Index	TNI	L_{10}, L_{90}	None	$TNI= 4(L_{10} - L_{90})+ L_{90} -30$	$TNI= 4(L_{10} - L_{90})+ L_{90} -30$	Traffic Noise
Equivalent Sound Level	L_{eq}	L_A	None	$L_{eq} =10 \log (1/T)\Sigma 10Li/10$	$L_{eq} =L_{50} +0.115\sigma 2$	Community Noise
Noise Pollution Level	L_{NP}	L_{eq}	Variability	$L_{NP} = L_{eq} + 2.56\sigma$	$L_{NP} = L_{eq} +(L_{10}-L_{90})$ $=L_{50} + (L_{10}-L_{90})+ (L_{10}-L_{90})2/60$	Community Noise
Composite Noise Rating	CNR	L_{PN}	1. Number of events 2. Time of day	$CNR = PNL_{max} +N+K$	$CNR \approx NEF + 70$ $\approx L_{dn} + 35$ $\approx CNEL + 35$	Aircraft Noise
Noise Exposure Forecast	NEF	L_{EPN}	1. Number of events 2. Time of day	$NEF = L_{EPN} +N+K$	$NEF \approx CNR - 70$ $\approx L_{dn} - 35$ $\approx CNEL - 35$	Aircraft Noise

Table 3.1 Contd.

Descriptor	Abbreviation	Base -Measure	Adjustment to Base Measure	Derivation	Relation to other Descriptor	Application
Noise and Number Index	NNI	L_{PN}	Number of events	$NNI = P\overline{NL}_{max} + 15\log N - 80$	NNI = $10\log L_{PN}/10+15$ logN- 80	Aircraft Noise
Community Noise Equivalent Level	CNEL	L_{eq}	1. Time of the day 2. Optional: number of events	CNEL = $10\log[A + B+C]$ $A = \left(\frac{1}{24}\right)\left(12x10^{Ld_{10}}\right)$ $B = 3x10^{\left((Le+5)_{10}\right)}$ $C = 9x10^{(L_n+10)/10}$	$CNEL \approx L_{dn}$ $\approx NEF+35$ $\approx CNR-35$	Community Noise
Day and Night Average Sound Level	L_{dn}	L_{eq}	1. Time of the day 2. Optional: number of events	L_{dn}=10 log(1/24)[(15x10Ld/10)+(9 x10(Ln+10)/10)]	$L_{dn} \approx CNEL$ $\approx NEF + 35$ $\approx CNR - 35$	Community Noise
Isopsophic Index	N	LPN	1. Time of the day 2. Number of events	$Nd = \overline{PNL}_{max} + 10 \log Nd - 30$ $Nn = \overline{PNL}_{max} + 6 \log(3N_1+N_2) - 31$	$N=10 \log 10^{L_{PN}/10} + 10 \log N - 30$ $N=CNR-18$	Aircraft Noise
Weighted Equivalent Continuous Perceived Noise Level	WECPNL	L_{EPN}	1. Seasonal weighting 2. Time of the day 3. Number of events		$WECPNL = 10\log 10^{L_{EPN}/10} + 10\log N - 39.4$	Aircraft Noise

Table 3.1 Contd.

Descriptor	Abbreviation	Base -Measure	Adjustment to Base Measure	Derivation	Relation to other Descriptor	Application
Mean Annoyance Level	Q	L_A	Duration	$\overline{Q} = 13.3 \log \sum \frac{\left(10^{L_{Ai}/13.3} xti\right)}{T}$ $= \frac{13.3 \log\left(10^{L_{Ai}} xfk\right)}{100}$	$\overline{Q} = 13.3 \log 10^{L_{PN}/10} + 13.3 \log N - 39.4$	Aircraft and Traffic Noise
Noisiness Index	NI	1. L_A 2. 1/3 Octave bands	1. Time of the day 2. Season 3. Duration	$\overline{NI} = 10 \log \sum_i^n anti\log[A]$ $A = \frac{B}{10}$ $B = L_{AT} + 10 \log\left(t/t_o\right) + G + S$	$\overline{NI} = 10 \log 10^{(L_{PN}-13)/10} + 10 \log N - 39.4$	Aircraft Noise
Total Noise Load	B	L_A	1. Time of the day 2. Number of events	$B = 20 \log[C] - K$ $C = \sum_i^n W x 10^{L_{Ai}/15}$	$B = 20 \log 10^{(L_{PN}-13)/15} + 20 \log N - K$	Aircraft Noise
Rating Sound Level	L_r	L_A, L_{eq}	1. Impulsiveness 2. Tones 3. Duration 4. Time of the day 5. Zoning	L_r={LA+I+C+D(steady state noise) L_{eq}+ I +C (fluctuating noise)		Community Noise

The maximum instantaneous sound pressure level, during a stated time period or event is called peak sound pressure level, L_{peak}

3.2.1.2 Equivalent Sound Level, L_{eq}

Equivalent sound level is an energy average, ordinarily based on A-weighted[1] measurements. It is a single-number descriptor of time-varying noise used in noise codes, environmental impact statements and other documents.

It is defined as the steady sound level that contains the same amount of acoustic energy as the fluctuating level over the prescribed period of time. Commonly used periods are 1 hour (L_{1h}), 24 hour (L_{24h}), the day time hours (7:00 a.m. to 10:00 p.m., L_{eqd}), and the night time hours (10:00 p.m. to 7:00 a.m.., L_{eqn}).

Mathematically,

$$L_{eq} = 10\log\left[\frac{1}{T_2 - T_1}\int_{T_1}^{T_2}\frac{p_A^2(t)}{p_{ref}^2}dt\right] \tag{3.2}$$

where,

$p_A(t)$: A-weighted sound pressure (Pa) as a function of time

If L is sound pressure level measured in dBA,

$$L_{eq} = 10\log\left[\frac{1}{T_2 - T_1}\int_{T_1}^{T_2}10^{L/10}dt\right] \tag{3.3}$$

For the calculation of L_{eq} due to the operation of a number of individual and composed sources, the individual events need to be characterised in such a way that their effects

[1] Certain values are added to the measured sound pressure levels (dB) spectrum for converting them to replicate human response. This is A-weighting.

can be combined. Characterisation of the individual events may be required for diagnostic purposes.

According to the "Code of practice for reducing the exposure of employed persons to noise" (HMSO, 1975) noise exposure is to be quantified in terms of L_{eq}. This value can be used as reasonable predictor of hearing loss (Beckenbauer, 1992).

L_{eq} can be measured with the three options of time constants[1], namely FAST, SLOW and IMPULSE. In Germany, the measurement for L_{eq} is done with time constant FAST. If measured with SLOW, L_{eq} is referred to as L_{eqs}. L_{eq} and L_{eqs} differ significantly.

For impulsive noise or considerably fluctuating noise that is characterised by large variations of level at short time intervals, the time constant FAST is too long. The actual energy content of the sound begins to be underrated, causing an error of several dB. In this case the time constant IMPULSE should be used.

The rise time constant at 35 μs is considerably shorter than that at the time constant FAST, whereas the decrease time constant at 1500 μs is considerably longer. This leads to typical slopes in the time history of the sound pressure level. The time weighting IMPULSE consequently reproduces the occurrence concerning the formation of loudness in the human ear, but only in a very loose approximation. Nevertheless, with time constant IMPULSE, energy is slightly over estimated but the effect of noise is covered better. Correction for impulse noise is given as:

---

[1] *Time constants* when choosing a suitable time constant for the measurement, the characteristics of the noise must be taken into account. The level of noise always varies to certain extent. The display of the measuring instrument has a certain time constant and cannot follow rapid fluctuations of sound levels. In addition human eye cannot follow rapid movement. Therefore, the display of a sound level meter is deliberately damped. There is normally a choice between three standardised time constants or damping:

1. SLOW : This has high damping giving a slow display movement. The effective averaging time is approximately 1 sec.
2. FAST : This has low damping giving a more rapid display movement. The effective averaging time is approximately 0.125 sec.
3. IMPULSE : This has a very fast rising time constant and very slow falling time constant. This is intended to present a value which represents how loud the human ear judges a short duration sound. It is aimed at annoyance rather than hearing damage risk. (Bruel and Kjaer, 1982).

$$K_I = L_{Aeq(IMPULSE)} - L_{Aeq(FAST)} \cong 3 \text{ to } 6 \ dB \tag{3.4}$$

Correction for tonal sound is taken as 3 or 6 dB and correction for rest hour (that is 6.00 a.m. to 7.00 a.m. and 7.00 p.m. to 10.00 p.m.) is taken as 6 dB.

3.2.1.3 Percentile Exceeded Sound Level, L_x

Percentile Exceeded Sound Level is defined as the sound level that exceeded X percentage of the time. L_{50} and L_{10} are the two commonly used percentile exceeded sound levels. This index is used in estimation and representation of traffic noise level.

3.2.1.4 Day-Night Sound Level, L_{DN}

Day-night sound level is used as a descriptor when night time noise is particularly objectionable. This index is generally preferred for noise assessment near residential areas. To calculate this index 10 dBA is added to an A-weighted sound level measured between the hours of 10.00 p.m. and 7.00 a.m. Day-night sound level is then commuted from the adjusted night-time sound level along with the unadjusted day-time values using the following equation:

$$L_{DN} = 10\log\left[\frac{1}{24}\left(\int_{7A.M.}^{10P.M.} 10^{L/10}dt + \int_{10P.M.}^{7A.M.} 10^{(L+10)/10}dt\right)\right] \tag{3.5}$$

where, L is the measured or predicted sound level (dBA).

If representative equivalent sound levels have been determined for the daytime and night-time periods, Equation 3.5 can be written as:

$$L_{DN} = 10\log\left[\frac{1}{24}\left(15\times 10^{L_{eqD}/10} + 9\times 10^{(L_{eqN}+10)/10}\right)\right] \tag{3.6}$$

where,

L_{eqD} : equivalent sound level for the 15-hour period from 7.00 a.m. to 10.00 p.m.
L_{eqN} : equivalent sound level for the 9-hour period from 10.00 p.m. to 7.00 a.m

3.2.1.5 Community Noise Equivalent Level, *CNEL*

This noise index is used in aircraft noise prediction. The community noise equivalent level is based on single-event noise exposure level, which is approximated as:

$$SENL = L_{\max} + 10\log\left(\frac{t(2)-t(1)}{2}\right) \tag{3.7}$$

where,

$SENL$: single event noise exposure level (dBA).
$L_{\max}$: maximum A-weighted sound level during a flyover

Community Noise Equivalent Level is defined as the highest sound level measured on a sound level metre, during a designated time interval or event, using fast time-averaging and A-weighting. The term t(2) - t(1) represents the effective event duration (sec) given by the interval between the 10-dBA down points.

Community Noise Equivalent Level (CNEL) is given by:

$$CNEL = SENL_{mean} + 10\log\left(N_d + 3N_e + 10N_n\right) - 49.4 \tag{3.8}$$

where,

$SENL_{mean}$: energy average SENL (dBA), that is, SENL for one typical flyover
N_d : number of flyover between 7 a.m. and 7 p.m.
N_e : number of flyover between 7 p.m. and 10 p.m.
N_n : number of flyover between 10 p.m. 7 a.m.

It is necessary to convert forecasts in terms of $CNEL$ to L_{DN}. The approximate relationship is:

$$L_{DN} = CNEL \pm 3 \tag{3.9}$$

3.2.1.6 Day Average Sound Level, L_D

The equivalent continuous sound level in decibels over the 15 hour time period from 7:00 a.m. to 10:00 p.m. is referred to as day average sound level.

3.2.1.7 Noise Exposure Level, L_{AX}

The level of the time integral of the squared, A-weighted sound pressure level over a stated time interval or event with reference to the squared reference sound pressure (20 μPa) and a reference duration of 1 second is termed as noise exposure level. If the sound energy associated with a single event is known it is easy to calculate L_{AX} for the event and hence L_{eq} for any number of events. L_{AX} values for contributing noise sources can be considered as individual building blocks being used in the construction of a calculated value of L_{eq} for the total noise.

$$L_{AX} = 10\log \int_{-\infty}^{\infty} \frac{p_A^2(t)}{p_{ref}^2} dt / \tau_{ref} \tag{3.10}$$

where τ_{ref} is 1 sec. The equivalent form of this equation is

$$L_{AX} = 10\log \int_{-\infty}^{\infty} 10^{L_A(t)/10} dt / \tau_{ref} \tag{3.11}$$

The value of L_{eq} due to the combined effect of n events each with its own single event noise exposure level L_{AX_i} is calculated as:

$$L_{eq} = 10\log\left[\frac{\tau_{ref}}{T}\sum_{i=1}^{n} 10^{L_{AXi}/10}\right] \tag{3.12}$$

where T is the total time period in seconds and τ_{ref} is 1 second.

For n events of same L_{AX}, L_{eq} can be written as:

$$L_{eq} = L_{AX} + 10\log n - 10\log T \tag{3.13}$$

If n is given as q per hour (in case of say automobiles etc.),

$$L_{eq} = L_{AX} + 10\log q - 35.5 \tag{3.14}$$

3.2.1.8 Day Average Sound Level, L_d

The equivalent continuous sound level in decibels over the 15 hour time period from 7.00 a.m. to 10.00 p.m. is called the day average sound level.

3.2.2 Errors in Noise Measurements

Noise assessment involves large scale noise measurement. Accuracy of the statistical conclusions from such measurements depends on the evaluation of the errors in measurement. Yang and Ellision (1985) discussed error estimation in detail.

Following errors are generally needed to be accounted for in noise measurements:

- Errors due to limited number of measuring points,
- Errors due to far-field assumptions,
- Errors due to ground reflection.

Estimation of these errors and necessary corrections need to be carefully carried out. To calculate the errors due to limited number of measurements the following steps are needed:

a. Measure n number of sound pressure levels (L_i, $i = 1,2,3,\ldots, n$).
b. Calculate

$$\frac{p_i^2}{p_{ref}^2} = 10^{L_i/10} \tag{3.15}$$

where,

p_i : sound pressure in Pa

p_{ref} : reference sound pressure

c. Calculate

$$\frac{\left(p_{av}^2\right)}{p_{ref}^2} = \frac{1}{n}\left(\sum_{i=1}^{n} 10^{L_i/10}\right) \tag{3.16}$$

where,

p_{av} : average sound pressure in Pa.

d. Calculate the difference of the values calculated in (b) and (c)
e. Calculate the square of values obtained in (d).
f. Calculate the sum of the values of (e).
g. Calculate the standard deviation of the values in (b) as

$$\sigma_E = \sqrt{\frac{(f)}{n}} \tag{3.17}$$

h. Find the value of Student's t at the required confidence level and (n-1) degrees of freedom from table.
i. Calculate Error as:

$$Error = 10\log\left[1 + \frac{n\sigma_E t}{\sqrt{(n-1)\sum_{i=1}^{n} 10^{L_i/10}}}\right] \tag{3.18}$$

j. Add error from (i) to the measured sound power level.

Assumptions made during deriving the equations for measurements of sound power are:

1. The instantaneous sound pressure and particle velocity at all measuring points are in phase with each other,
2. The measuring surface at every point of measurement is perpendicular to the direction of sound propagation, and
3. Sound intensity is equal to:

$$\frac{p^2}{\rho c} \tag{3.19}$$

However, in most practical cases there is a phase difference between the particle velocity and instantaneous sound pressure. Intensity need to be expressed not merely as $\frac{p^2}{\rho c}$, but is expressed as:

$$I_n = pv_n \cos\phi \tag{3.20}$$

where,

p : rms value of sound pressure
v_n : rms value of particle velocity in direction n, perpendicular to the measuring surface
ϕ : phase angle between the pressure and velocity

Therefore, the above assumptions made in calculations induce an error due to the real nature of the measurements. Evaluation of this error is rather complicated. Yang *et al*, (1985) summarised on the basis of studies of Ellison *et al* (1969) and Hübner (1977) that this error can be calculated as:

$$Error_{far\ field} = 10\log\left(\cos\phi_{ref}\right) \tag{3.21}$$

The reference phase angle ϕ_{ref} is determined from the graph of phase angle between pressure and velocity vs. the product of wave number and measuring surface radius for various vibration modes usually derived for small machines.

Therefore the steps in calculating this error are:

- For the given sound wave find the wave number from the information of frequency and sound velocity.
- For the given mode of vibration find the reference phase angle from the standardised graph.
- Use equation (3.21) for calculating the error.

For a noise source over a hard reflecting surface the receiver gets the superimposed sound waves from the source and its reflection from the ground. This error is evaluated as the difference of sound power levels measured by the spherical and hemispherical surface methods. The steps for calculation are:

a. Tabulate the measurement locations (x_r, y_r, z_r) for each point and find the value of h, the height of the source above the ground.
b. From the frequency and sound velocity find out the wavelength as

$$\lambda = \frac{c}{f} \tag{3.22}$$

c. Find for each point the value of the angle of incidence as

$$\theta = \tan^{-1}\left(\frac{z_r}{x_r}\right) \tag{3.23}$$

d. For each point calculate:

$$\cos^2\left(\frac{2\pi h \sin\theta}{\lambda}\right) \tag{3.24}$$

e. Find the sum of all the values of (d), i.e.

$$\sum_{i=1}^{n}\cos^2\left(\frac{2\pi h \sin\theta_i}{\lambda}\right) \tag{3.25}$$

f. Calculate the error due to ground reflection as:

$$Error_{reflection} = 10\log\left[\frac{2}{n}\sum_{i=1}^{n}\cos^2\left(\frac{2\pi h \sin\theta_i}{\lambda}\right)\right] \tag{3.26}$$

g. From the measured SPL on a hemispherical surface calculate the mean level as:

$$\bar{L}_{p,h} = 10\log\left(\frac{1}{n}\sum_{i=1}^{n} 10^{0.1L_{pi}}\right) \tag{3.27}$$

h. The sound power level of the source will be (f) + (g) taking the error due to ground reflection into account.

The present work has not adopted the statistical method for noise estimation. However, experimental methods involve analysis of measured noise levels and therefore it is necessary to be careful about all probable errors in measurements.

3.3 Noise Assessment

A number of researchers have developed models for the assessment of sound pressure levels and the attenuation around industrial complexes (Tonin, 1993). A generalised equation of these models takes following form:

$$L_p = \sum_{sources}^{\log}\left[L_W - \sum_i (A_i)\right] \tag{3.28}$$

where,

L_p : resultant sound pressure level at a point in the noise field

L_W : sound power level of the source

A_i (i=1, 2, 3...): attenuation applicable in the site under consideration

Thus all noise estimation models rely on the determination of sound power level of the noise sources and evaluation of the attenuation of sound energy during propagation from the source to the receiver. Various noise estimation models are presented in Table 3.2.

These models are not directly applicable to a surface mine or a quarry due to the following reasons:

- The sound power level of the sources distributed in the mine cannot be represented uniquely,
- The location of the sources keeps on changing with time. Thus the directive sources affect the noise level at the receiver points differently,
- The noise sources are located at a depth and the depth varies with time,
- Both static and moving sources are present simultaneously,
- Due to geo-mining conditions no two individual mines offer the same amount of attenuation,
- Wind velocity profiles at different locations around the pit change according to the topographical variations of the mine and the surface surrounding it.



Table 3.2 Different models of sound pressure level prediction (compiled from Tonin, 1993).

SL. No.	Name of the Model	Basic Equation
1	Oil Companies Materials Association (OCMA) Model.	$L_p = \sum_{\text{all sources}}^{\log}\left(L_W - K_1 - K_2\right)$ L_W is the sound power level, K_1 is the attenuation due to spreading and soil type, K_2 is the attenuation due to ground and meteorological effects.
2	VDI 2714/VDI 2720 (German Draft Standard)	$L_p = L_W + DI + K_0 - D_s - D_L - D_{BM} - D_D - D_G - D_e$ L_W is the sound power level, DI is directivity index, K_0 is the solid angle reflection index, D_s is the attenuation due to geometric spreading, D_L is the air absorption factor, DBM is the ground and meteorological attenuation, D_D is the attenuation due to vegetation, D_G is the attenuation due to built-up areas, D_e is the attenuation due to barriers.
3.	Oil Companies' International Study Group for Conservation of Clean Air and Water (CONCAWE) Model.	$L_p = \sum_{\text{all sources}}^{\log}\left(L_W + D - K_1 - K_2 - K_3 - K_4 - K_5 - K_6 - K_7\right)$ L_W is the sound power level, D is directivity index of source, K_1 is attenuation due to geometric spreading, K_2 is atmospheric absorption, K_3 is attenuation due to ground effect, K_4 is attenuation due to meteorological effects, K_5 is correction for source height above ground, K_6 is the barrier shielding and K_7 is the in-plant screening.
4	BBN/EEI (Bolt Beranek and Newman Inc. Ltd./Edision Electric Institute)	$L_p = L_W + D - 10\log\left(4\pi d^2\right) - \left[\frac{d}{100}\left(a_m\right) + \frac{d}{100}\left(a_a\right)\right] - [-3]$ L_W is the sound power level, D is directivity index of source, d is the distance from the acoustic centre of a point source to receiver, a_m is the molecular absorption rate in dB per 100m, a_a is the anomalous excess attenuation rate in dB per 100m.
5	NORDFORSK Noise Model (by Lydteknisk Laboratorium, Denmark)	$L_p = L_W + \Delta L_\varphi - \sum \Delta L$ The second term accounts for the directivity and the third term accounts for various types of attenuation.
6	ENM (Environmental Noise Model by RTA Technology Pty. Ltd.)	$L_p = \sum_{\text{all sources}}^{\log}\left(L_W + D - A_1 - A_2 - A_3 - A_4 - A_5\right)$ L_W is the sound power level, D is directivity index of source. Types of attenuation accounted are geometric spreading, barrier attenuation, air absorption, wind and temperature effects and ground attenuation.

Therefore, for predicting noise levels in the far field of a mine or a quarry requires site specific studies. Hohenwarter (1990) developed a noise propagation model to calculate

sound event level[1] and energy equivalent level for short distance propagation of railway noise. Event wise energy accounting seems suitable for railway noise considering every passage of a train as an event. However, such an approach for mining noise will require handling of a large number of varied activities. The mining activities will have to be represented suitably considering the production schedules and equipment deployment strategy.

Güdesen (1990) reported the application of underwater sound propagation models for atmospheric sound propagation. The model is, however, most suitable for stationary, homogeneous and horizontally stratified layers. This model proved that meteorological data are more relevant for heights up to about 200 metres. Davies (1978) developed a sound propagation model for streets considering multiple reflection and scattering. Such approach may be useful for accounting for the multiple diffusion taking place in a mining environment. However, the available model does not readily include such situations. Similar approaches considering geo-mining conditions can provide a suitable method for noise field modelling near surface mining and quarrying operations.

The noise propagation model developed by ISVR uses the CONCAWE model (Pinder, 1995). This model can draw the noise contours around a noise source. However, the application of the model for mining conditions needs further modifications.

3.4 Industrial Noise Assessment and Prediction

Assessment of industrial noise largely depends on proper evaluation of noise sources. Industrial noise sources are random composition of various sources. They behave differently depending on their mobility, periodicity and characteristics. Accordingly, there are various types of sources as shown in Figure 3.2.

Therefore, a careful and systematic approach is necessary for reliable assessment and prediction of environmental noise due to such sources. The procedures applied and the

[1] Sound event level is the energy content of an event for a second to provide the total energy of the event for the whole period. Energy equivalent level depends on the number of events per hour.

influencing factors are discussed in this section. The essential steps of noise assessment are:

- Quantification of the noise output of the sources by sound power levels in frequency bands (usually octaves or one-third octaves) and directivity factors,
- Calculation of sound pressure levels at the receivers in each band due to each source, making allowance of the variety of factors affecting propagation,
- Conversion of the frequency band sound pressure levels at the receiver for each source to A-weighted values and adding these logarithimically to the operation time for each of the sources to give L_{eq}

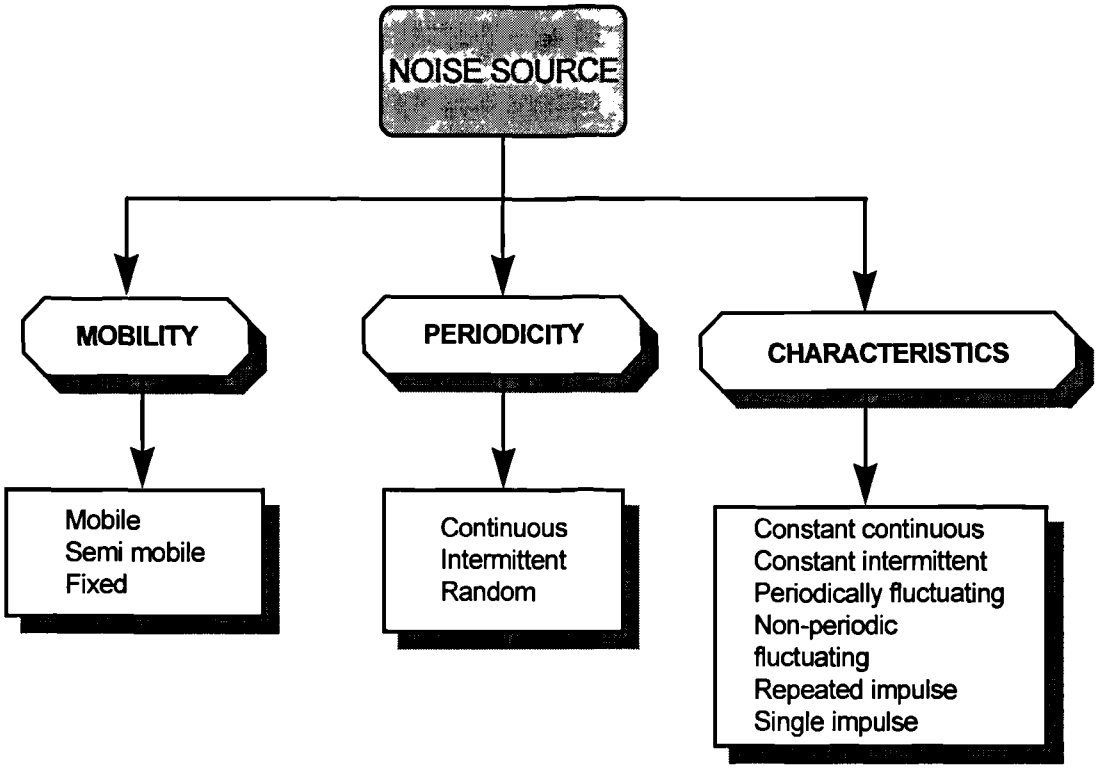


Figure 3.2 Types of noise sources.

The following factors are to be evaluated for assessing industrial noise:

a. Sound output of processes and plants
b. Attenuation of noise levels
d. Meteorological conditions
e. Interference with other sounds

3.4.1 Sound Output of Processes and Plants

The noise field around an industrial site largely depends on the characteristics of its processes and plants. The sound output of any process or plant is characterised by sound power level, frequency content and duration of generation. Environmental noise assessment is based on the sound power output of the various noise sources associated with the processes and plants. The sound power level of a machine or source of noise can be determined by carrying out measurements for the sound pressure levels over an enveloping surface surrounding the machine. Yang and Elision (1985) have described the detailed methods of such measurements. British Standards (BS 5228: 1984) has laid out general methods for three types of noise sources: Stationary, Haul Roads and Mobile Plants. However, the standard does not provide any guidelines for modelling the complex nature of surface mining and quarrying noise. Such noises are generated during the operation of different machinery working in number of different combinations. Rzhevsky (1985; 1987) described the equipment complexes deployed for various unit operations of surface mining and quarrying. However, acoustic performance of any such combinations have not ever been studied.

Because of the growing concerns on the impact of industry on the environment, the noise generated in surface mining and quarrying operations was studied in this research. The sound power levels of the working processes and plants within a pit have been evaluated by following different approaches derived from the existing methods of noise measurements applied elsewhere. Chapter 4 presents a detailed description of these approaches and their applications.

Modelling of the excitations of the acoustic media by the processes and plants is not straightforward and simple. Most of the processes and plants in any industrial site work with a specified cycle time. However, some of them operate perfectly at random. Correspondingly, noise fields can be stochastic or deterministic. Based on the cycle of operations of the noise source, the air medium is excited simultaneously or in sequence. Therefore, time averaging techniques of acoustic energy measurement have been internationally accepted for assessing the noise environment. The index for noise

assessment for a particular industry is selected according to the period of operation of its processes and plants.

Considering the period of operation of processes and plants, the author has developed a technique referred to as the Activity Accounting Technique (AAT) for determining the resultant environmental noise. This is discussed in Chapter 4 along with the results of field experiments.

3.4.2 Attenuation of Noise Level

The difference of sound energies at the source and the receiver gives the total attenuation of sound energy during propagation. There are many factors of noise attenuation. Sound propagation models referred to in Section 3.3 attempts to determine the attenuation caused by these factors. The predominant attenuation factors are:

- Geometric spreading or source-receiver distance
- Influence of underlying ground surface
- Absorption of acoustic energy in air
- Sound reduction by barriers on source-receiver path

3.4.2.1 Attenuation by Spreading

Sound energy is attenuated during its propagation through a medium. Therefore, the distance between the source and the receiver is an important factor in assessing noise environment. The effect of distance has been referred to as *attenuation due to spreading*. This attenuation depends on the frequency content of the sound wave and the directionality of source. Over a distance, there are changes in the conditions of the medium and the terrain over which the sound wave propagates. Height of the source above the ground surface is also important.

Attenuation due to spreading depends on the type of source. For spherical radiation from a point source attenuation is 6 dB per doubling of distance from the source. Rathe (1977) has shown that for a dipole line source such attenuation is 6 dB per doubling of the distance near the source. It is 3 dB in an intermediate zone. At a large distance this

attenuation is again 6 dB per doubling of the distance. Most of the available models calculate geometric spreading as:

$$\text{Geometric Spreading} = 10\log\left(4\pi d^2\right) \tag{3.29}$$

where, d is the distance from the source to the receiver.

Norton (1989) discussed attenuation due to spreading for various conditions of point source, line source and plane source. It was shown that for a uniform infinite line source in free space with sound waves radiating as concentric cylindrical waves, sound pressure level decays by 3 dB for every doubling of distance rather than 6 dB as is the case for spherical sources. The sound pressure level, L_p at a distance, R from a source is determined from the knowledge of sound power level, L_W of the source using the equation:

$$L_p = L_W - 10\log R - 8 \tag{3.30}$$

If the line source is at the ground level, the equation becomes:

$$L_p = L_W - 10\log R - 5 \tag{3.31}$$

This is because for a ground mounted source the radiating surface area is halved. That is why for a free spherical point source in free space the sound pressure level at a distance R is given as:

$$L_p = L_W - 20\log R - 11 \tag{3.32}$$

If the source is mounted on the ground surface then the equation will be:

$$L_p = L_W - 20\log R - 8 \tag{3.33}$$

If a source is located very close to the ground, there occurs an attenuation of 12 dB for every doubling of source-receiver distance when the receiver is at a considerable distance from the source. For spherical divergence, however, an attenuation of 6 dB is observed. Thus, effects of ground absorption and distance are to be considered together.

The behaviour of attenuation by spreading is also affected by the nature of the source. Sound waves from a point source, a line source and an area source undergo different degrees of attenuation due to spreading.

For large sources, the inverse square law does not apply close to the source. As shown in Figure 3.3, in the case of a line source of length a the rate of attenuation due to spreading is 3 dB per doubling of distance up to a distance of a/π from the source. There after, the attenuation is again 6 dB per doubling of distance. For a plane source with length b and width c, the attenuation is 0 dB up to a distance of c/π. Thereafter, it follows a reduction of 3 dB per doubling of distance up to a distance of b/π. Then it undergoes attenuation of 6 dB per doubling of distance.

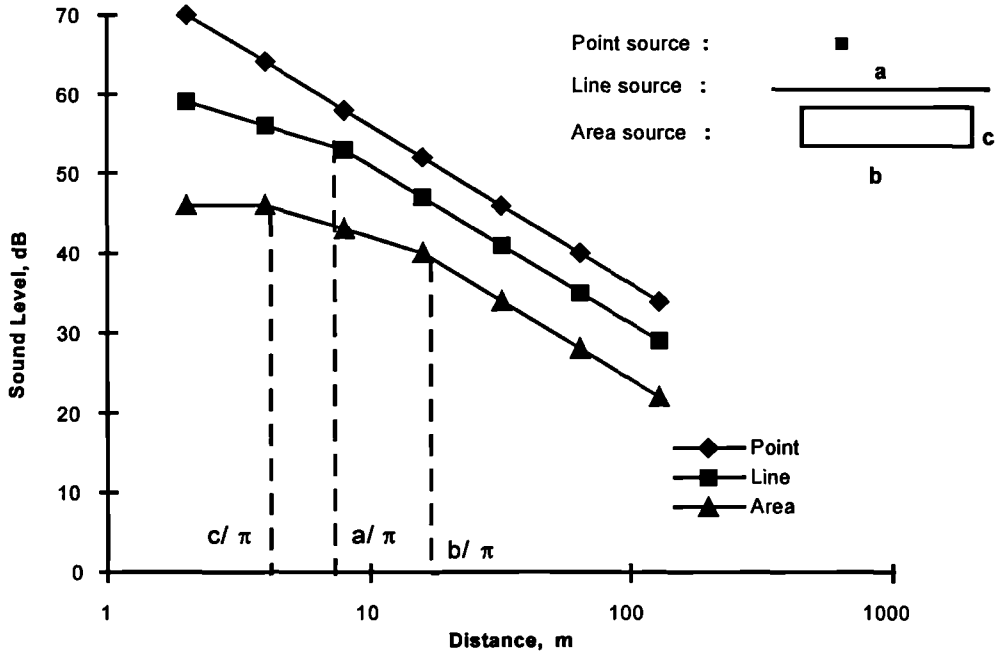


Figure 3.3 Effect of source type on attenuation due to spreading.

3.4.2.2 Influence of Ground Surfaces

Presence of reflecting surfaces and ground surface influences the overall noise field considerably. Complex reflecting surfaces induce more difficulties in modelling the

noise field. Ground reflection has been studied by various researchers in connection with the ground absorption and barrier performance.

Sound energy is attenuated as it travels over the ground. Calculation of ground absorption in terms of ground impedance is an established practice (Ingard, 1951, Rudnick, 1947). Ingard (1953) determined the contour lines of constant sound pressure level for point sources located at a certain height above the ground. Determination of ground absorption uses the semi-empirical equations developed by Delany and Bazley (1970b). These methods treat ground as comparable to a porous substance. Sutherland (1994) developed a new model for determination of acoustic impedance of ground under grass surfaces. However, the basis of this modelling still remains the flow resistivity of the ground surface.

Assessment of noise field in the industrial site should consider the effects of the ground on the sound propagation. This effect depends on the positions of the source and receiver relative to the ground. Attenborough (1982) used normal surface impedance of ground to predict ground effects on the highway noise propagation. The acoustical properties of the ground surface are particularly important at frequencies less than 500 Hz. At higher frequencies wind, temperature gradients and turbulence influence noise-propagation in such a way that the effects of the ground becomes almost insignificant (Glaretas, 1981). The acoustical behaviour of isotropic and homogeneous air-filled soils and sand can be described by flow resistivity, porosity and the ratio of grain shape factor and pore-shape factor. Attenborough (1985) used the theory of predicting the acoustical characteristics of rigid porous materials in terms of the four physical parameters to provide impedance versus frequency models for various types of ground surface. Behaviour of ground surface as an acoustic absorbent has been discussed in detail in Chapter 5.

The objective of assessing ground absorption is to evaluate the excess attenuation of sound energy propagating over it. This excess attenuation due to ground surface depends on source and receiver heights above the ground surface. The attenuation also depends on the frequency content of the sound.

The frequency of maximum ground attenuation is given as:

$$f_{\max} = \frac{1500}{h\log\left(r/0.3\right)} \tag{3.34}$$

where,

h : mean height of source to receiver path, m.
r : distance between the source and the receiver, m

Figure 3.4 shows the above relationship graphically. Thus, the attenuation due to ground absorption has a peak value at $f_{\max}$. The value of $f_{\max}$ reduces with an increase in distance and mean height of the propagation path.

The attenuation in the octave band containing $f_{\max}$ is obtained as:

$$A_g = 15\log\left(0.065r/h\right) \tag{3.35}$$

If 0.065 rh^{-1} is less than 1, A_g =0.

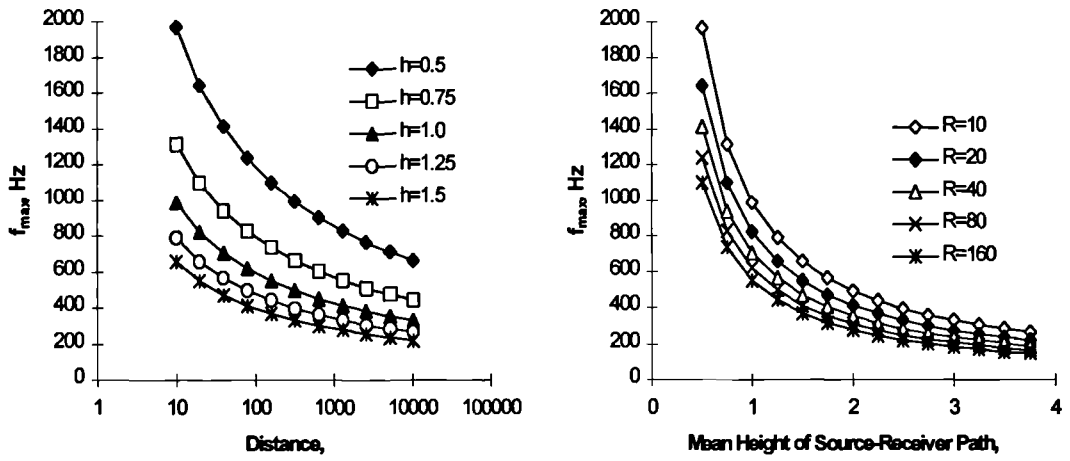


Figure 3.4 Frequency of maximum ground attenuation as a function of path height (h) and distance (R).

In the two octave bands adjacent to that of maximum attenuation, the attenuation is half of the maximum value; in all other cases it is zero. In the presence of a barrier, allowance for the ground absorption is not necessary.

3.4.2.3 Absorption by Air

Absorption of sound energy in the air medium has been studied by a number of researchers during the last 150 years after Stokes (1845; 1851) published his theoretical treatment of the influence of heat radiation and internal friction on heat radiation and internal friction on the propagation of elastic waves. Knudsen (1933) studied the absorption of sound in air, oxygen and nitrogen. Thus, the loss of sound energy during its propagation through the atmosphere is well established. This loss is due to a relaxation process. Such loss is significantly influenced by temperature and humidity. Moreover, the degree of attenuation depends on the frequency of the propagated wave. It was established that frequency and humidity affect attenuation per metre as per the following equation (Smith, 1971):

$$\alpha_a = kf^2 + \alpha_h \tag{3.36}$$

where,

α_a : attenuation per metre
k : constant given as, $k = 14.24 \times 10^{-11}$
f : frequency, Hz
α_h : humidity dependent factor

Typical values are 3 dB per 100 metre, at 4000 Hz to 0.3 dB per 100 metre, at 1000 Hz.

Fog and smoke particles cause additional attenuation. It has been observed that fog particles are less significant for frequencies above 300 Hz. Generally, background noise level decreases with the presence of fog or snow resulting in less masking and sound can be distinguished at lower intensities even at a greater distance.

Development in the theory of molecular absorption helped to determine the coefficients of air absorption for a wide range of frequencies, humidity and temperature. Sutherland *et al* (1974) studied attenuation of acoustic energy in atmosphere experimentally. ISO 3891 provides the corrections for air absorption to apply in noise prediction models. German Standards (VDI 2714) calculates air absorption as proportional to the distance

from the source to the receiver. The constant of proportionality for octave bands in dB per m is:

$$\alpha_{L,\ octave} = \left[0.02 + 0.36f(kHz) + 0.036\left(f(kHz)\right)^2\right].10^{-2} \quad (3.37)$$

ANSI 1978 provides the necessary tables for calculating air attenuation at different temperatures and humidity under octave bands. Chapter 6 describes the application of the methods of determination of this attenuation for predicting noise levels near surface mining and quarrying operations.

3.4.2.4 Presence of a Barrier

Presence of a barrier between the source and the receiver modifies the noise field over a region. The barrier modifies the noise field towards the source by sending reflected waves. The edges of the barrier cause diffraction of sound waves towards the receiver. This diffraction may result in the formation of a shadow zone. Thus, the position of the source and the receiver with respect to the barrier(s) is an important factor in assessing industrial noise. Isei *et al* (1980) calculated the sound field behind a barrier using five different theories and showed the significance of the site geometry, source spectrum and acoustic characteristics of the ground. The attenuation caused due to the insertion of a barrier is called insertion loss. Redfearn (1940) expressed barrier insertion loss as a function of the non-dimensional ratio of the length of the perpendicular from the edge of the barrier to the line between the source and the receiver. Fehr (1951) used the Fresnel number to evaluate barrier attenuation. Maekawa (1962; 1968) developed a chart for calculating the barrier loss. In this chart barrier attenuation is a function of the Fresnel number, calculated as:

$$N = \pm \frac{\text{path length difference}}{\left(\frac{\lambda}{2}\right)} \quad (3.38)$$

where λ is the wavelength.

Kurze and Anderson (1971) also developed a chart similar to that of Maekawa. Following the technique of image source various authors studied barrier performance considering absorption of acoustic energy by the barrier surface. Works of Fujiwara *et al* (1976) and Yuzawa (1977) may be referred to in this regard. Jonasson (1972a), from his theoretical and experimental studies, concluded that sound propagation patterns may change appreciably from one type of ground surface to another. He noticed that this is most pronounced in the frequency range of 250-1000 Hz. Continued research in this area has proved that the effect of the ground on barrier performance is bigger than other factors, such as the absorptive properties of the barrier or of obliquity of incidence at the barrier. Correction for the effects of rigid, thin barriers with thickness less than the wave-length is expressed as:

$$A_b = 10\log(3 \pm 20N)$$
$$N = \frac{2}{\lambda}(a + b - R) \tag{3.39}$$

where,

λ : acoustic wave-length in metre, for the band centre frequency
a : distance from the source to the edge of barrier, m
b : distance from the receiver to the edge of barrier, m
R : the straight line distance from the source to the receiver, m

The minus sign with A_b is used if the receiver is above the shadow zone of a barrier. Attenuation due to barriers is a combination of ground absorption and loss due to the insertion of a screen.

Jonassion (1972b) studied the barrier effect of depressed roads. Elizabeth and Russel (1977) studied attenuation of sound by wide barriers. The Department of Transport, UK prepared guidelines for calculating barrier loss for depressed roads (HMSO, 1988). These procedures provide the basic theories and methodologies for determining the attenuation of sound energy during propagation from pit bottom to the surface level in surface mining and quarrying conditions. However, careful consideration of the geo-mining factors is necessary to apply them for predicting mining noise.

In surface mining and quarrying, the slope of the pit behaves as a barrier. Chapter 7 describes the detailed method of applying the theories of barrier attenuation for evaluating the reduction of noise level by the pit slope.

3.4.3 Meteorological Conditions

Meteorological conditions of the atmosphere influence propagation of sound. Scientific study on weather effects on sound propagation started towards the end of eighteenth century. Ingard (1953) referred to the work of Dr Derham of England who investigated in 1704, in collaboration with Joseph Averiani of Italy, to prove that the statement "sound appeared to be heard much better in Italy than in England" was not correct.

Studies on the propagation of sound were encouraged by the Light House Boards and Fog Signal Committees with the objective of making a siren that will be heard at a longer distance in difficult meteorological conditions. During the first two decades of this century important research was carried out by Lord Raleigh of England and L. V. King of Canada. In 1913, King reported his experimental results and fundamental discussions on the propagation of large amplitude waves. In his review paper Ingard (1953) mentioned the important work carried out by Schilling, Blockhintzev and Eyring in the forties. Piercy and Isei (1977) verified the influence of atmospheric temperature and wind gradient as well as of ground surface on the noise levels. Li *et al* (1994) examined sound propagation in moving stratified atmosphere and studied the effects of porous ground surface. All these studies reveal that for environmental noise prediction purposes the following meteorological conditions influencing sound propagation are to be considered:

a. Viscosity
b. Humidity
c. Rain and Fog
d. Temperature
e. Wind
f. Turbulence

3.4.3.1 Viscosity

Experiments conducted in the laboratory during the first half of this century revealed that attenuation due to viscosity increases with the square of the frequency. However, the attenuation is very small, even at 5 kHz it is less than 0.5 dB in 100 m. Such a small attenuation can be neglected in all practical purposes. White and Walker (1982) expressed attenuation constant (in dBm^{-1}) due to viscosity (α_v) at frequency of f Hz in air at 1 atmosphere and 20 ^{0}C as:

$$\alpha_v = 8.5 \times 10^{-8} f^2 \tag{3.40}$$

The effects of viscosity are insignificant at low frequencies. This can be seen from Figure 3.5.

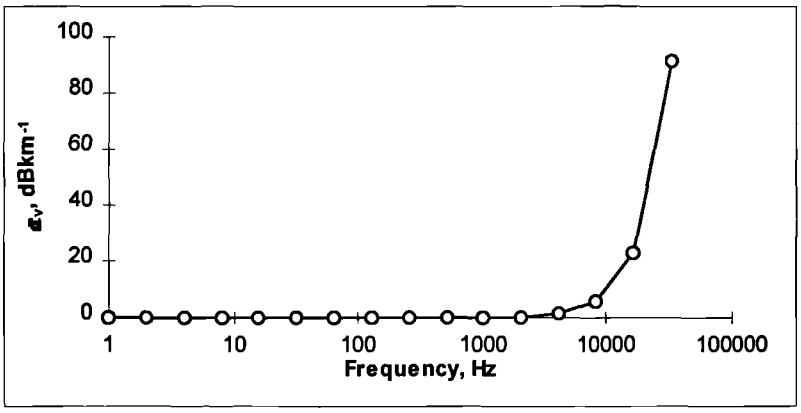


Figure 3.5 Attenuation constant for viscosity at 1 atmosphere and 20^0 C (after Equation 3.26).

3.4.3.2 Humidity

Studies have shown that the effect of humidity is also negligible unless at high frequencies and certain unusual comparatively small values of relative humidity. The curves developed by Knudsen (1933) and Kneser (1933) for the attenuation of sound in air caused by relaxation effects show the attenuation in air as dB/100 metre as a function of relative humidity with frequency as a parameter. At 50% relative humidity and frequency below 2 kHz, attenuation is less than 1 dB. Humidity is considered while estimating sound absorption in air. Chapter 6 presents the detailed effects of humidity on air absorption of acoustic waves.

3.4.3.3 Rain and Fog

Ingard (1953) gives an extensive review of studies on the effects of rain and fog on propagation of sound. Experimental studies in the eighteenth century claimed that rain and fog do not interfere with sound propagation noticeably. However, fluctuations of sound-signals were noticed in such situations. This was attributed to the reflections from clouds and layers with different humidities. Attenuation of a 500 Hz sound wave in foggy weather was reported to be of 1.1 dB per 100 metre. Sound pressure level (SP_r) due to rainfall rate has been estimated empirically as per the following equation (Bies and Hansen, 1988):

$$SP_r = 52 + 10\log\frac{RR}{2.54} + S + W \tag{3.41}$$

where,

SP_r : sound pressure level due to rainfall, dBA
RR : rainfall rate in cms^{-1}.
S : ground surface correction factor
$S = 0$ for lawns and porous ground
$S = 12$ for large leafed vegetation.
W : wind correction
$W = 0$ to 6 dBA depending on wind speed and foliage type.

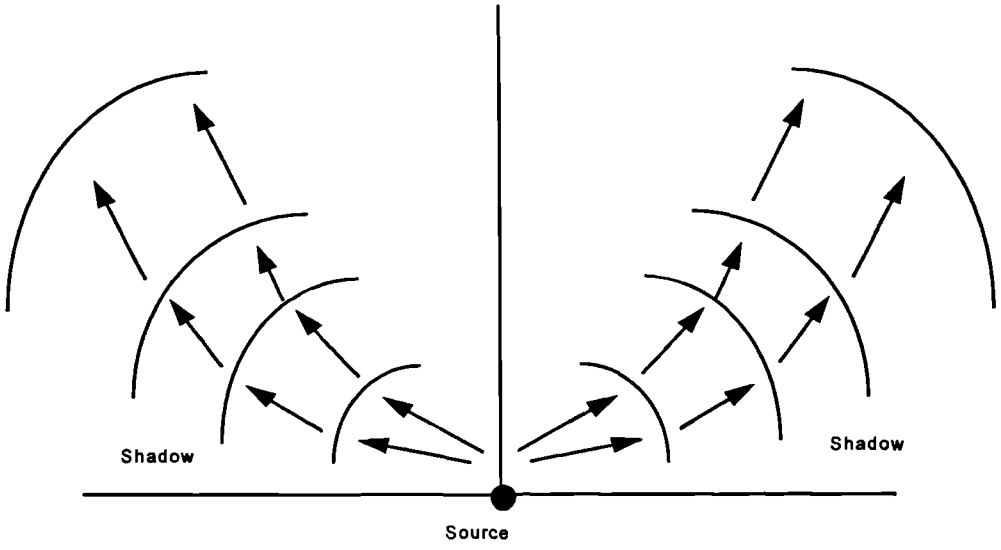


Figure 3.6 Effect of temperature gradient (daytime).

3.4.3.4 Temperature

Air temperature varies with altitude. This variation induces an acoustic shadow zone. Acoustic velocity is proportional to the square root of temperature. Temperature decreases with height and therefore the velocity of sound also decreases. Thus, the path of sound becomes curved instead of straight in the presence of a temperature gradient in the medium. The radius of curvature of the path at any point is inversely proportional to the velocity gradient at this point. With the temperature decreasing upwards (daytime), sound rays will be refracted upwards. This phenomenon results in the formation of a shadow zone as shown in Figure 3.6. If the temperature gradient is 1 °C per 100 m, the radius of curvature is 56 km.

At night, inversion of temperature gradient causes sound rays to bend downwards as shown in Figure 3.7. With no ground absorption and obstruction the intensity distribution would be the same as the unperturbed one. The inversion of the temperature gradient causes sound to propagate to a larger distance during the night. Ingard (1953) presented a contour plot showing how the temperature gradient varies with the time of the day and the time of the year. With the advent of better instruments for meteorological monitoring, reliable data for temperature gradient and wind velocity gradient are now available. Larsson (1992b) studied the radius of curvature of the sound path under various meteorological conditions.

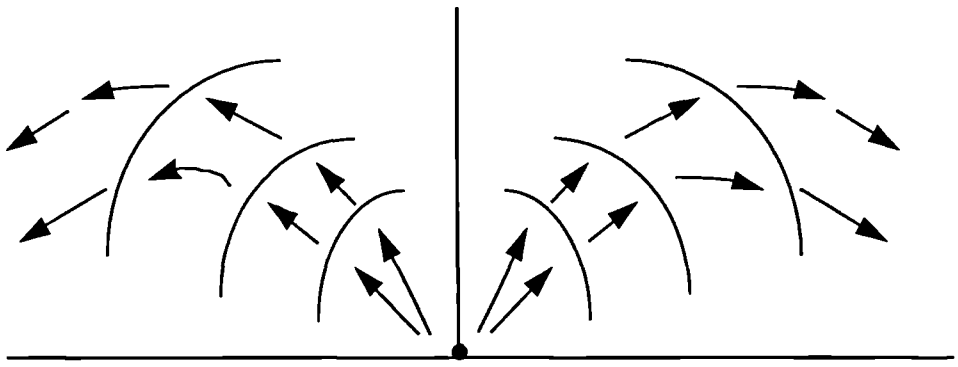


Figure 3.7 Inverted Temperature Gradient.

Atmospheric attenuation at a temperature of 20° C and 50% relative humidity is calculated as:

$$A_a = 0.148 f^2 r \times 10^{-8} \tag{3.42}$$

where,

f : octave band frequency, Hz
r : distance from the source to the receiver, m.

For a temperature of 20 ±10 °C the value of A_a is given as:

$$A_a = \frac{0.148 f^2 r \times 10^{-8}}{1 + \beta \Delta t f} \tag{3.43}$$

$$\beta = 4 \times 10^{-6} \text{ for } t \text{ in } ^\circ\text{C}.$$

Characteristic impedance of air varies with temperature resulting in different values at different heights. The nature of this variation and its effect on sound transmission is not readily predictable. However, the general effect is that the sound wave is deflected downwards. This deflection may occur at a considerable height and may be received at a point much beyond the point where the normal sound waves get completely attenuated.

3.4.3.5 Wind

Acoustic velocity is a velocity relative to air velocity. In the presence of wind, the wind velocity needs to be added to the acoustic velocity to obtain the latter with respect to the ground. Generally, wind velocity is much smaller than the velocity of acoustic wave. However in gale conditions it becomes significant. Wind increases the background noise level by inducing vibrations to many items in the environment like leaves, lighter structures, etc. Wind velocity (near ground) increases with an increase in height. The sound velocity increases with height downwind and decreases with height upwind. A wave is transmitted in such a way that the direction of propagation at any point is always at right angles to the wave front at that point. So the distortion in the wave front due to variation in the velocity leads to a deflection of the direction of propagation. In

the downwind direction the sound is deflected downwards and the reverse is the case in the upwind direction. This may induce a shadow zone in the upwind direction.

The above effects on transmission are negligible in the near-field. In the far field, their influences are significant. Normally, wind speed increases with height over the ground depending on the season. Sound rays travelling in air bend downwards in the wind direction and upwards against the wind. The curvature of the rays is inversely proportional to the velocity gradient of the wind. Figure 3.8 shows wind velocity gradient as a function of the height over the ground.

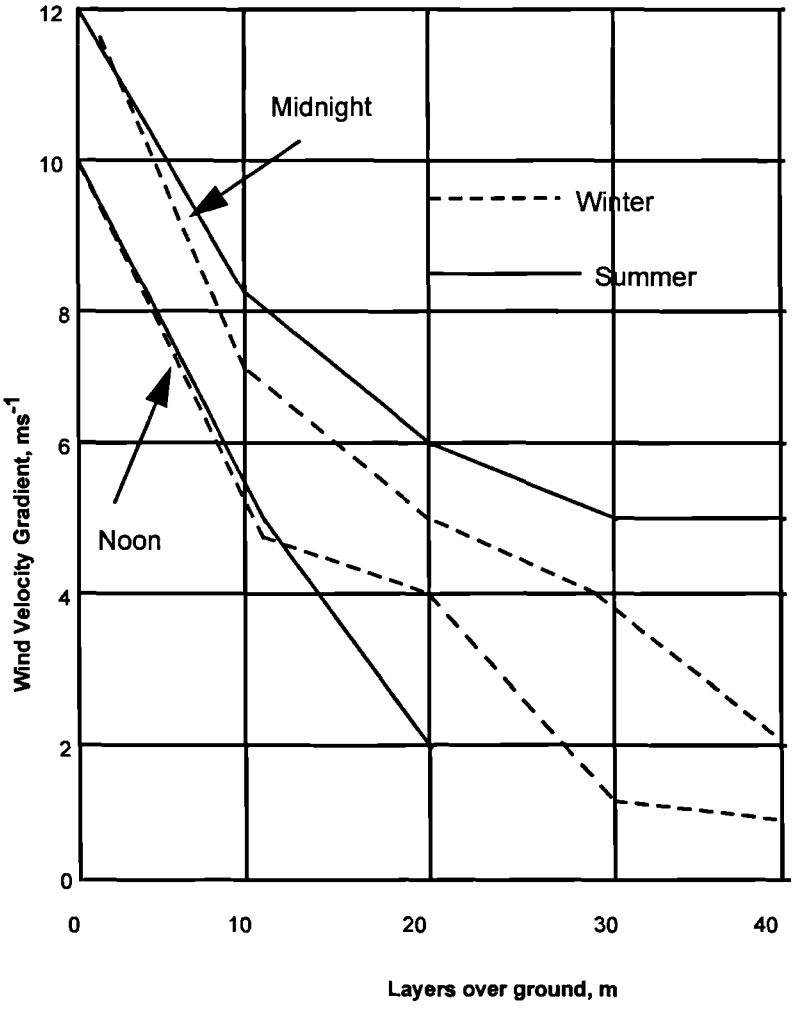


Figure 3.8 Average wind velocity gradient as a function of the height over the ground (after Ingard, 1953).

In a combined field of temperature and wind gradient, cancellation of the influence of each factor takes place. This occurs when the wind gradient is equal to 0.6 times the temperature gradient and assuming a horizontal sound ray in the wind direction.

The wind has no effect on a sound ray at right angles to the wind direction. For rays within 0 to 90 degrees, the component in the direction of the ray only affects to induce curvature to the ray path.

If wind gradient is larger than 0.6 times the temperature gradient there will be a sector within which the sound rays will be bent downwards thus eliminating possible shadow formation. In a combined field of wind and temperature gradients, the angle of the sector of shadow formation is given by the formula (Ingard, 1953):

$$\cos\phi_m = \left(c_o / 2T_o\right)\left(\frac{W_g}{T_g \sin i_o}\right) \tag{3.44}$$

where,

W_g : wind gradient
T_g : temperature gradient
i_o : angle of elevation of the sound ray

In the direction opposite to the wind direction, wind and temperature gradients both occur in the same direction and shadow zone occurs relatively close to the ground. The intensity of the sound field outside a shadow zone is just about the same as that obtained without wind and temperature gradient.

Thus, wind makes sound propagation anisotropic. Sound speed depends on the direction of propagation relative to wind-direction. Raspet *et al* (1985), Lee *et al* (1986), Franke *et al* (1988), Franke and Swenson (1989) and West *et al* (1991) studied the problem of sound propagation under the influence of wind. Li *et al* (1991) used the effective sound-speed profile as:

$$c(z) = 331.5\sqrt{\frac{T+273.15}{273.15}} + w\cos\left(\theta_D - \theta_W\right) \tag{3.45}$$

where,

T : temperature in ^{o}C
θ_D : azimuth angle of the detector
θ_W: azimuth angle of the wind, aligned with the direction of air flow
W : wind speed, ms^{-1}

Nijs and Wapenaar (1990) modelled sound propagation with wind and temperature effects but the effect of cross wind was neglected. Li *et al* (1994) developed a program for the computation of the near-field and far-field sound pressure due to a point source embedded in a layered medium, in each layer of which the magnitude and direction of wind is arbitrary but constant. However, the applicability of these methods have not yet been tested over mining conditions. The modification of wind velocity over the pit is yet to be modelled. Therefore, the wind effects on sound propagation have not been covered in the prediction models. However, the effects of wind velocity on the absorption of sound energy by ground surface were experimentally studied in this research. The results of these studies are presented in Chapter 5.

3.4.3.6 Turbulence

Sound levels at the receiver positions fluctuate with gustiness, i.e. increased wind velocity. Gustiness can cause average attenuation of 4 to 6 dB per 100 m. This may even be as high as 20 dB. However, it is yet to be known how the total noise field varies with the change of wind pattern and there are not enough conclusive studies to estimate how much noise the gustiness may induce in any noise field.

Gustiness is caused by eddies of various sizes that travel along with the wind. The velocity of rotation of eddies may add to or subtract from the average velocity thus causing fluctuations. The rapidity of the fluctuations is a measure of the size of the eddies at a given average velocity. Average size of eddy diameter is 2-8 m. However, sometimes eddies of diameter of 1000 or more may occur.

A sound beam striking an eddy is deviated up to 2^{o} or more. A larger number of eddies may deflect the sound from the direction of the receiver. With eddies changing continuously the net result at any moment may be that a receiver in a particular direction

may not at least momentarily hear a particular sound. Eddy size and direction as well as its influence on sound propagation is dependent on the wind structure. It was found that attenuation due to eddies is essentially the same in all directions.

3.4.4 Presence of Other Sources

An industrial site comprises of a multiple number of sets of noise sources. The assessment of the combined effect of all these requires a careful treatment of the characteristics and the location of the sources and the media. Alster (1982) described a method of equivalent acoustic centres to represent the combined effect of a number of distributed noise sources. In the field of acoustic diagnostics considerable developments have been made to identify the source of noise. The identification of a problematic noise source from the data of combined noise fields is attempted and the acoustic analysers currently available can separate the noise levels from moving sources and static sources. However, the characteristics of combined effects environmental noise generating from a number of distributed industrial sources are still not very well understood. The concept of Equivalent Acoustic Centre (EAC) used in assessing the combined effects of various noise sources is discussed in more detail in Chapter 4.

3.4.5 Other Attenuation

Propagating sound energy gets attenuated by vegetation and built up areas. Prediction of noise from mining operations needs to consider this attenuation in places where there is sufficient vegetation. Noise level in residential areas is influenced by the attenuation due to built-up areas. Figure 3.9 shows a possible case that may exist near a mining area. The noise is emitted from the source located at the pit. The receiver is located beyond the screen of trees. Attenuation due to vegetation A_v is calculated according to the following equation:

$$A_v = \alpha_v . S_D \tag{3.46}$$

where, S_D is the ray path through vegetation as shown in Figure 3.9. The factor α_v depends on the frequency and the height of the source and is determined as:

$$\alpha_v = 0.006\left(\frac{f}{H_s}\right)^{1/3} \tag{3.47}$$

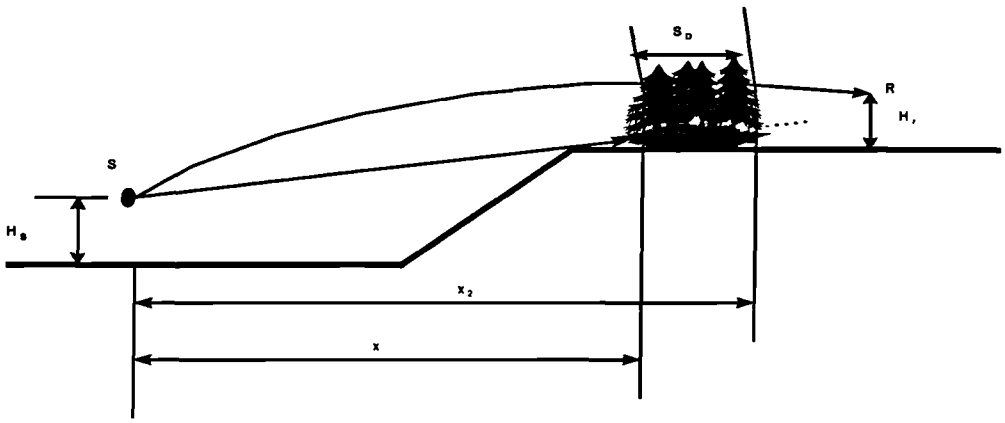


Figure 3.9 Attenuation due to vegetation.

BBN/EEI model of noise prediction (Tonin, 1993) determines attenuation due to vegetation by two different schemes. For forests, attenuation is given in dB per 10 m of growth by the following equation:

$$A_v = 1.8\log(f) - 3.1 \tag{3.48}$$

If the density of forest varies then the attenuation is calculated as:

$$A_v = \frac{Coefficient \times Vegetation\ Code}{3.048} \tag{3.49}$$

The coefficients of Equation (3.49) depend on frequency and are taken from Table 3.3.

Table 3.3 Excess attenuation coefficients for forest.

Freq.(Hz	31.50	63.00	125.00	250.00	500.00	1000.00	2000.00	4000.00	8000.00
Coeff.	0.40	0.50	0.63	0.79	1.00	1.10	1.25	1.40	1.60

The value of the vegetation code depends on the forest zones and its density. The forest is classified into three zones for noise attenuation purposes. These are:

- Zone 1: Extent of vegetation intersected by the source receiver line.
- Zone 2: Intersected by imaginary line of 3.3 m above the source receiver line.
- Zone 3: Intersected by imaginary line of 6.6 m above the source receiver line.

Table 3.4 shows the values of the vegetation code for different densities of forest. By selecting the value of the coefficient and the code, attenuation due to such vegetation can be evaluated.

Table 3.4 Vegetation code for wood of different density.

Density	Zones completely covered by growth		
Category	Zone 1	Zones 1 and 2	Zones 1, 2 and 3
Low	0.3	0.7	1
Medium	0.6	1.4	2
High	0.9	2.1	3

Attenuation due to vegetation in the winter period is corrected by a factor of 0.7.

3.5 The Calculation of Noise Levels near Industrial Complexes

BS 5228: 1984 provides the method for the calculation of noise levels from different activities and plants which vary with time and location. This procedure, as well as other procedures mentioned in different standards, gives a reasonable assessment of the noise levels. ISO 1996-2:1987 (E) stated that a universally agreed prediction model does not exist and a method adopted should be carefully described in each case. For the calculation of noise level of an industrial complex, say an opencast coal mine, a plan showing all the machinery and facility in the site including the haul roads is to be drawn. The site elements of interest may include the following:

a. Access points,
b. Baffle mounds,
c. Bunker storage and rail loading facilities,
d. Car parking facilities,
e. Coal handling plant and washery,
f. Internal haul roads,
g. Office complexes,
h. Overburden mounds,
i. Plant yards and maintenance yards,
j. Expected machinery locations.

The noise level of the mine will be varying depending on the method of mining and geo-mining conditions. For the estimation of noise at a particular phase of mining the plan of the mine at that phase showing all the details of acoustic components as mentioned above will have to be made. Internationally accepted standards have

specified generalised methods of noise estimation. However, no application models have been prepared for applying these methods to surface mining and quarrying operations. The available methods are briefly reviewed here.

3.5.1 Activity L_{eqA} Method.

BS: 5228: Part 1 1984 suggests the Activity L_{eqA} method for determination of A-weighted equivalent continuous sound pressure level (L_{eqA}) at a distance from a source on the basis of measured L_{eqA} levels at a distance of 10 m from the same source. This method is developed for clearly defined stationary and quasi-stationary activities. Thus this procedure will be appropriate provided the working pattern of the noise source does not vary with time. In this method partial Noise Exposure Index due to a source is determined from an established Nomogram on the basis of the measured equivalent sound pressure levels and duration. Summation of the Noise Exposure Indices of all the sources give the total Noise Exposure Index. Knowing this index, the combined equivalent sound level is determined from the Nomogram.

This procedure does not suggest its applicability when a group of machines are performing an activity. Such activities are common in mining operations. Therefore the author has modified this method to evolve a new technique referred to as the Activity Accounting Technique (AAT) in which the different activities performed by a group of machinery has been identified. Using the techniques of measurement of sound pressure levels, the equivalent sound power level of each of the activities could be determined. Chapter 4 presents detailed description of this method.

The Activity L_{eqA} method given in the Standard can be adopted for prediction of noise from small mines and quarries with a limited number of machinery and activities. This will involve the following steps:

1. *Tabulation of the activities of items of the plant*: Activities involved in operations of the machinery like excavators, drills, draglines, compressors and rock breakers, in-pit crushers, belt conveyor, bucket wheel excavators are tabulated.
2. *Determination of the activity* L_{eq}: For the activities enumerated in (1) L_{eq} levels at a distance 10 m from the source are to be determined. This should be

obtained experimentally. Alternatively, these may be extracted from a standard table, e.g. Appendix C of BS 5228: Part 1: 1984. These values may be evaluated by other methods suitable for the measurement L_{eq} of machinery.

3. *Source-Receiver distances*: The distances of the noise sources from the point of estimation are then determined.
4. *Distance correction*: Sound pressure levels are measured at a standard distance of 10 m. Therefore, they need to be corrected for the location where one wants to predict the noise level. The standard suggests that this allowance may be expressed as:

$$K_d = -20\log\frac{R}{10} \tag{3.50}$$

where, R is the distance from the prediction point to the geometric centre of the activity, m. This can be calculated from the given co-ordinates of the two points.

5. *Barrier correction*: For each of the L_{eq} of the activities or sources, allowance for the screening effects by any barrier in between the source and the point of estimation will have to be determined. The standard assumes this allowance to be 5 dBA when the noise source is visible to the observer and 10 dBA when it is not visible. The effects of a barrier which in the case of an opencast coal mine may be a slope of multiple berms or a baffle mound need to be evaluated. Barrier corrections may be applied as a function of path difference as suggested in the memorandum published by the Department of Transport[1] .
6. *Reflection adjustment*: Depending on the position of the activity or source and the position of the receiver different situations of interference of reflected sound wave with direct sound wave may arise. Impact of the reflection is then to be included as an adjustment. BS 5228 takes an allowance of +3 dBA to the calculated L_{eq} if the point of interest is within 1 m of the facade of a building.
7. *Summation*: Resultant of the measured L_{eq} and the allowances is then evaluated.
8. *Duration of activities*: The duration of activities is then noted. This can be determined from the cycle time of the machinery. If these are not available they will have to be determined by carrying out work studies.
9. *Determination of Work-Factor*: The duration of activities is expressed as the percentage of the duration on which basis noise is to be estimated.
10. *Determination of Partial Noise Exposure Index*: BS 5228: part 1:1984 provides a Nomogram to find the value of partial Noise Exposure Index for each activity. Summation of them would give the total Noise Exposure Index. Corresponding to this value, the combined equivalent continuous sound level for the activities should be obtained.

[1] Calculation of road traffic noise
Department of Transport, Welsh Office, HMSO publication, 1988

3.5.2 Plant Sound Power Method

This is a method of estimation of equivalent noise level, L_{eq} at a point of interest. Noise level prediction by this method depends on the sound power levels of the noise sources. However, in the prescribed method the directivity of the sources are not taken into consideration. Moreover the influence of the noise emitted by various sources is not taken into consideration. Therefore, it is expected that this method will be suitable only when there are less sources. This method may be applicable in certain construction sites. However, in mining and quarrying operations large numbers of machines of different categories work together and noise prediction in such operations must take their combined effects and directivities into consideration.

The author has adopted the concept of Equivalent Acoustic Centre (Alster, 1982) for determining the sound power level of working zones within a quarry. The method has been tested for its applicability to account for the combined effects of large number of distributed sources and resultant effects of directivity. Chapter 4 presents a detailed description of the developed method.

In the plant power method described in the Standard the sound power levels of the stationery or quasi-stationary noise sources are determined first. This method is especially used if data for calculating activity L_{eq} are insufficient. The basic procedures of this method are stated below:

1. The available noise sources influencing the noise level at the receiver's position are listed and their sound power levels, L_W, are either determined by experimentation or taken from available references.
2. Note the effective working hours, i.e. the 'on-time' of each of the noise sources. If the source is producing noise varying with time, average percentage 'on-time' is to be obtained. This time refers to the percentage time that the noise levels of the individual item of the plant are at or within 3 dBA of the maximum.
3. Determine the distances from the sources to the receiver points. If the source is moving within a limited area, the distances are to be calculated as time-weighted averages. For example, let a dozer be working within an area. During a period, T, let it be located at (x_i, y_i, z_i) for a duration of t_i. In this case the distance, R to a receiver at a location (x_r, y_r, z_r) will be calculated as:

$$R = \frac{\sum_{i=1}^{n} r_i t_i}{\sum_{i=1}^{n} t_i} \tag{3.51}$$

where,

$$r_i = \sqrt{\left\{(x_r - x_i)^2 + (y_r - y_i)^2 + (z_r - z_i)^2\right\}} \tag{3.52}$$

4. For the sound-power levels of step 1 and corresponding distances obtained in step 3 sound pressure level, L_p, is calculated. One way of getting L_p is by subtracting a distance allowance in dBA from the L_W value.
The distance allowance is given by BS 5228 as:

$$K_d = 20 \log R + 8 \tag{3.53}$$

This value needs to be corrected for directivity of the sources. Other factors such as ground conditions and meteorological conditions may further modify this equation. The above equation for reduction due to distance is developed considering the source as a spherical point source located in the ground plane. It is assumed that this source radiates sound energy through a hemispherical surface centred on the source. Figure 3.10 shows the distance adjustment for different cases.

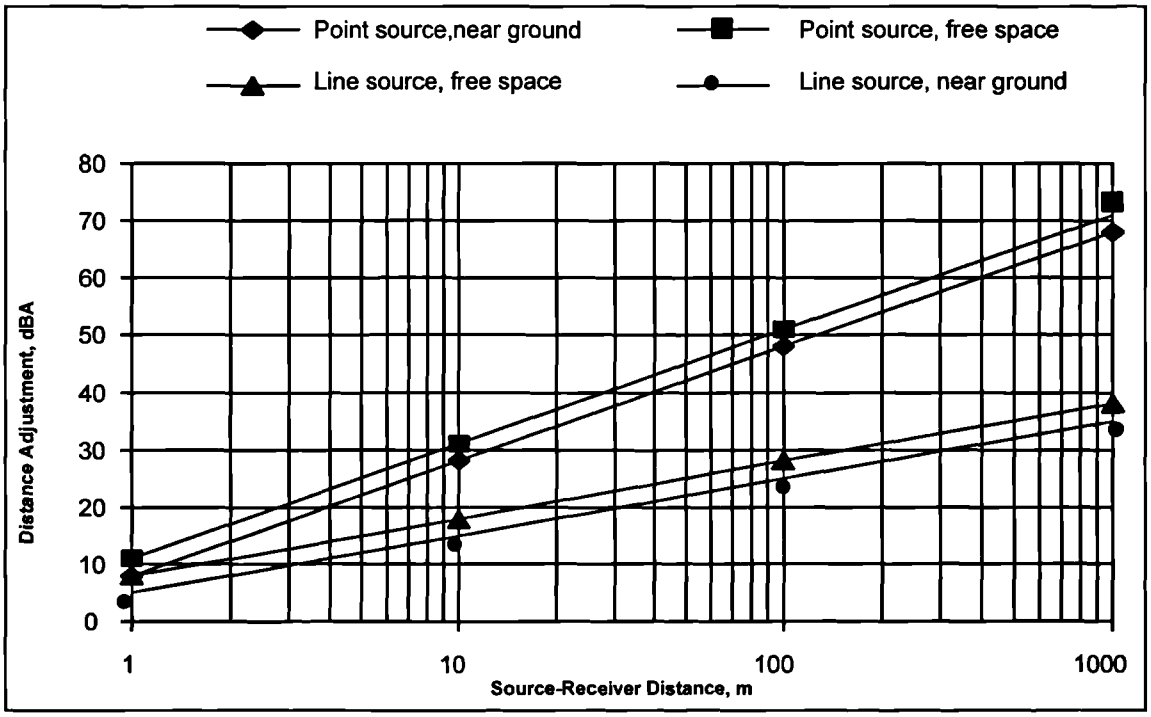


Figure 3.10 Distance adjustment in sound pressure level estimation (after BS: 5228).

5. Determine the allowance for screening effects and ground reflections and apply to L_p.
6. Use percentage ontime of a particular source to determine an adjustment (K_T) value to be subtracted from the L_p. of that source. BS 5228: Part 1:1984 suggests subtraction of adjustment K_T to calculate activity L_{eq} in dBA as::

$$L_{eq} = L_p - K_T \tag{3.54}$$

   K_T can be obtained from the chart in Figure 3.11.
7. Estimate the percentage of the assessment period for which each activity takes place.
8. For the L_{eq} and the percentage of duration determine partial Noise Exposure Index from nomogram or by calculating for each of the activities and then determine their sum total.
9. From the summed Noise Exposure Index using nomogram again the combined equivalent continuous sound level can be obtained.

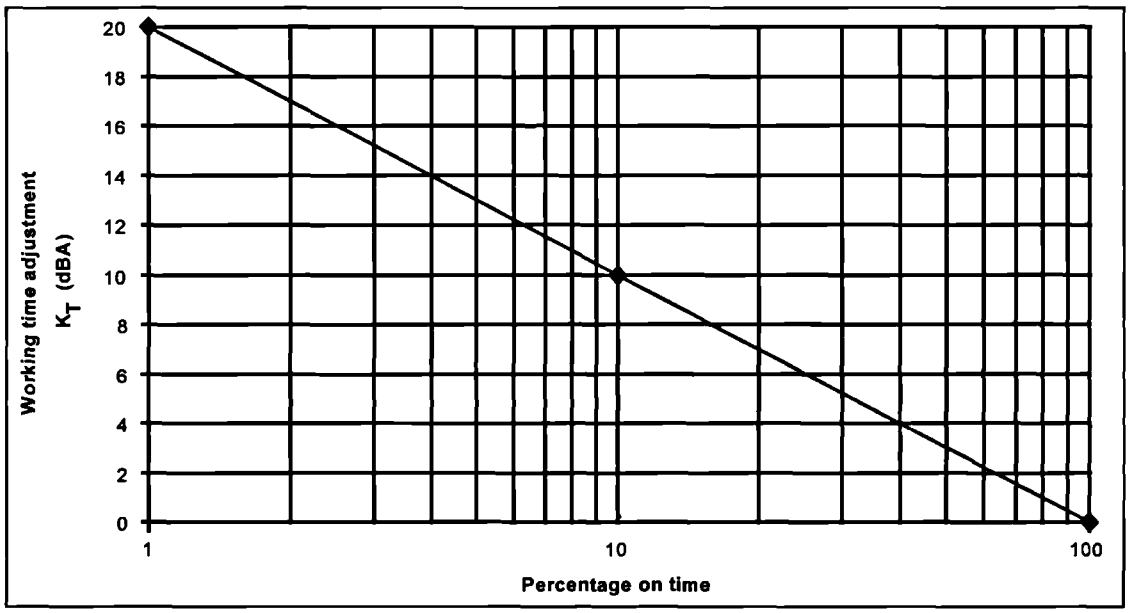


Figure 3.11 Adjustment of sound pressure level to calculate L_{eq} in dBA.

3.5.3 Calculation of L_{eq} for Mobile Plant

An opencast mining site involves mobile plants of two types, namely,

a. Mobile machinery operating in a small area
b. Mobile machinery operating on a regular route

Haulage machinery moves on regular routes. The noise due to haulage machines may be determined following the procedures of traffic noise laid out in the standards with the necessary modifications. The standardised procedure is outlined below.

3.5.3.1 Mobile Plants within a Small Area

Sound power levels of the mobile plants are determined by experiments prior to the assessment of noise level at a receiver's location. Like the activity L_{eq} method the estimation suffers from an error as the orientation of the noise source varies relative to the receiver locations. The method of finding out the exact error in estimating noise for a moving plant is still unknown. Establishing a relationship for the estimation of noise level as a function of the ratio of traversing distance of the mobile plant to the minimum distance between the moving source and the receiver may be useful.

Table 3.5 Distance ratio and equivalent on-time (after BS: 5228).

Distance Ratio, D	Equivalent on-time
0.5	1.00
0.7	0.80
1.0	0.63
1.5	0.50
2.0	0.40
3.0	0.32
4.0	0.20
5.0	0.16
6.0	0.13
7.0	0.10
8.0	0.10
9.0	0.08
10.0	0.08

The Standard suggests a method for a slow moving plant typically of a speed of 5 to 10 kmh^{-1} working over short traverses. The method involves the following steps:

1. Find the sound power level of the moving plant.
2. Determine the sound level at the receiver's location for the closest position of the moving plant as is done for stationary sources using sound power method, considering all allowances needed.
3. Determine the ratio of the traverse length to the minimum distance to the receiver's position. This ratio is used for finding the equivalent 'on-time' for slow moving plants as shown in Table 3.5.
4. Find the duration of activity for the correction of equivalent 'on-time'.
5. Determine the corrected 'on-time' as:

$$t_c = T_t \times t_o \tag{3.55}$$

where,

t_c : corrected on-time

T_t : total working time for the moving plant during the period of interest

T_o : equivalent 'on-time'

6. From the values of L_p and percentage 'on-time', noise-exposure index is determined for each of the moving plants. From the total value, L_{eq} is determined for the duration of the assessment period.

3.5.3.2 Mobile Plants on Regular Routes

Estimation of L_{eq} for mobile plants on a regular route like a haulage truck in an opencast mine can be done as per the British Standard. The procedure includes the following steps:

1. Determine the following:
   a) Number of vehicles per hour, Q
   b) Average vehicle speed, V
   c) Distance of receiver's location from the centre of the haul road, d
   d) Sound power level of the plant, L_W
2. From the above values calculate the L_{eq} along side the haul road using the following equation (for single engine plants):

$$L_{eq} = L_W - 33 + 10\log Q - 10\log V - 10\log d \tag{3.56}$$

For twin engine plants a correction of +3 dBA is added to the above L_{eq} value.

3. Depending on the situation other corrections for screening, reflection and absorption are then applied.
4. Steps 1, 2 and 3 are repeated for each of the moving plants.
5. Find the duration of each activity and estimate the percentage of the assessment periods and determine the noise level due to the combined effects of all the activities.

3.5.3.3 Road Traffic Noise

In case there are different categories of vehicles, noise exposure level for the traffic noise is calculated as:

$$L_X = L_0(v) - 10\log v - 10(F-1)\log d + 10\log\theta + 5.5 \tag{3.57}$$

where,

$L_0(v)$: A-weighted SPL as measured at 7.5 m from the vehicle centre line, expressed as a function of vehicle speed v in kmh^{-1}; varies with vehicle category
F : attenuation parameter depending on the ground conditions
d : shortest distance from the receiver's position to the vehicle trajectory, m
θ : angle subtended by the vehicle trajectory, in degrees

Measuring the noise exposure levels, L_X for the light and the heavy vehicles, L_{eq} is calculated as:

$$L_{eq} = 10\log\left\{\frac{1}{T}\frac{N}{100}\left[p.10^{L_{X2}/10} + (100-p)10^{L_{X1}/10}\right]\right\} \qquad (3.58)$$

where,

p : % of heavy vehicles
L_{X1} : noise exposure levels of heavy vehicles
L_{X2} : noise exposure levels of light vehicles

To estimate the propagating noise Jonasson (1973) discussed corrections for the effects of distance, barrier, etc. These corrections refine the values of L_X to calculate L_{eq}.

The present work has not covered the haulage noise in a surface mine in detail due to the limited time of research.

3.6 Summation of Sound Levels

The total impact of all the sound sources on a particular location of receiver would be estimated by summation of all of the above estimated noise levels. Two situations may arise:

a. Conditions in the site remain constant during the assessment period.
b. Conditions vary during the assessment period.

The acoustic conditions of a site may not significantly change during the period of assessment. This may happen in small scale operations where the activities are limited. To obtain the resultant effects of the sound exposure in such a situation one follows addition of quantities in decibels.

Acoustic environment of an industrial site may vary due to random behaviour of activities, introduction of noisy machinery or modification of performance of existing machines. In such cases equivalent continuous A-weighted sound pressure levels of each of the noise sources will have to be determined for the duration of their operations. Then the following equation gives the estimation of the combined effect:

$$L_{eq,T} = 10\log\frac{1}{T}\left(\sum t_i 10^{L_{eq,i}/10}\right) \tag{3.59}$$

where,

$L_{eq,T}$: the combined equivalent continuous A-weighted sound pressure level over a given period of time.

$L_{eq,i}$: individual equivalent continuous sound level for an item of moving plant or activity during the period t_i.

3.7 Summary

Current techniques of industrial noise assessment have been discussed in this Chapter. Industrial noise differs from industry to industry. As a result it has not been possible to generalise the procedure for noise prediction. The internationally accepted Standards have laid out the basic principles for noise measurement, estimation and modelling. However, these standards require modifications to apply to a particular industry. Surface mining and quarrying operations involve a number of distinctive features such as spatial and random distribution of the noise generating machinery over a wide area. Their behaviour and characteristics change with time. At the same time the geo-mining conditions also vary depending on the production plans. Moreover, the periodic variations in the characteristics of acoustic media, that is the atmosphere, are still not fully resolved. The acoustic influence of the spatially variable terrain conditions, especially in mining and quarrying sites are yet to be determined. Therefore, the procedures given in the standards or applied by other industries cannot be adopted exactly for predicting environmental noise near surface mining operations. To apply these methods for assessing noise levels in such situations, one must pay site specific attention to include the effects of terrain conditions, equipment deployment strategy,

ground absorption, pit geometry, etc. An adequate general method to determine the error in noise estimation as a function of influencing parameters is yet to be standardised.

The author has considered some of these problems in estimating surface mining and quarrying noise. The core of all noise prediction models is the sound power level of the noise source. Therefore, the present work was concerned foremost with the determination of the sound power level of the noise generating operations within a pit. New techniques for representing the sources of environmental noise due to mining and quarrying operations have been evolved. These methods and the results of some experiments conducted by the author to validate them are described in Chapter 4. The subsequent Chapters discuss the next important features of a noise prediction model, i.e. the prediction and modelling of the attenuation during propagation of noise from the source to the receiver in a mining situation.

Chapter 4

The Development of a Source Characterisation Model for Surface Mining and Quarrying Noise

4.1 Introduction

Development of a model for predicting the noise level near surface mining and quarrying operations was the primary objective of this research. Noise levels near such operations vary with site conditions depending on the selected mining systems. As shown in Table 4.1, noise sources and exposed areas vary with the phase of mining. Each phase is associated with various types of noise as shown in Table 4.2. These features are not easily quantifiable. As a result, studies on mining noise were mainly limited to the study of noise from particular machinery (Bartholomae and Parker, 1983; Chakravarty, 1973; Lynch, 1973) or survey of noise levels near mining areas and representations of the data surveyed by using commercially available software (Turner, 1986; Tompsett, 1992). In the past the mining industry was more interested in protecting the work force in the mines than the environmental noise impact (Anderson,

1971; Derazay, 1972; Weglo, 1973). Therefore, not much emphasis was given to developing a model for predicting noise levels around surface mining operations.

Table 4.1 Noise sources in different phases of surface mining.

Phases	Works	Noise Sources	Exposed Persons and/or Area
Preparation	Clearance of wood Timber felling and stumping Drainage network construction Top-soil excavation and storage Infra-structure development Construction of erection yard Approach road construction Electricity supply system construction Temporary and permanent building construction	Power saw Construction machinery Shovel Dragline (civil work) Construction machinery Compactor Crane Construction machinery Impact noises	Machinery operators Bystanders Neighbouring residents Forest fauna
Construction phase	Removal of overburden Drilling Blasting Excavation Transportation Dumping Dump yard construction Levelling	Automobiles Drills Explosions Excavators Electric shovel Hydraulic shovel Bucket wheel excavator Continuous miner Dragline Auxiliary machines Mobile crusher Mobile transfer conveyor Transfer feeder Dozer Transport machinery Dumper Conveyor Locomotive Dump yard machinery Dozer Tripper Spreader	Workers in the mine Persons visiting the mine Neighbouring dwellers
Development phase	Overburden removal Mineral/ore excavation Work is similar to construction phase with additional machinery	Same as above More machinery addition Reclaimer Processing plant (optional)	Same as above More persons exposed
Exploitation phase	Full set of machinery for targeted production Excess noise of ageing machines More noise from the maintenance workshops due to increased work load	Machinery noise	Persons in mine Persons of neighbouring area with increased population density. Expansion of noise field with the expansion of mining area and allied work centres.
Reconstruction phase	Replacement of old machines or technology	Impact noises	Persons involved in breaking/disposal of machines
Extinction phase	Reclamation works	Construction machinery Shifting of machinery and materials.	Working personnel Neighbouring settlers

The present research has developed a model for analysing environmental impact of noise due to surface mining or quarrying operations based on acoustical theories and experimentally verified rules. These theories and rules can evaluate different factors contributing to the total sound energy received at a particular location near such operations.

Table 4.2 Various types of noise near mechanised surface mines (after Wiener, 1960).

Type of Motion and Source	Inherent Characteristics of Sound and Vibration	Incidental Characteristics of Sound and Vibration
Rotating Motion		
Fan Blower Turbine Centrifugal pumps Centrifugal compressor	A tone of frequency *f=rpm/60 Number of blades on wheel or impeller (and other harmonics)*	Aerodynamic roar (broad band). Dynamic imbalance with vibration frequency *f=rpm/60* and higher harmonics
Motors, Generators	Whine of frequency f=rpm/60 or some multiple	Same and cooling fan noise
Gears	Whine of frequency *f=rpm/60* X number of teeth or some multiple	Vibration with frequency similar to inherent noise. High speed impact and sliding noise, broad band, grinding and screeching
Bearing	'Squeal' of frequency *f=rpm/60* X some multiple	Same
Reciprocating IC Engine	A roar of frequency of firing rate Exhaust noise	Cooling fan and pump noise, valve chatter, air noise, dynamic imbalance with vibrating frequency
Compressors, Pumps	Same, intake and exhaust noise	Same, pressure pulses in gas and fluid lines, frequency related to inherent sound frequency
Vibrating Transformer Rectifiers	Relatively pure tone of frequency *f= 2 X cps of ac* or some harmonic	Sympathetic vibration of housing, casings and attachments, some multiple of inherent sound
High speed vibrators and vibrating conveyors	Vibration or buzz or rattling	Same
High speed shakers	Essentially broad band	
Impacts Hammers Machine operation Collisions	Hammering, rattling, pounding, thumping, banging, etc. Essentially broad band	Vibration, broad band in frequency
Flow noise Airflow in ducts Fluid flow in pipes	Rushing of flow sound, relatively broad band	Cavitating pumps or supply/return imbalance create squeals and pulsating

As shown in Figure 4.1 the main components of the noise prediction system developed are the source power model, the ground attenuation model, the air attenuation model and the pit-wall attenuation model. The source power model determines the sound power

level of the noise sources. The attenuation models provide the attenuation of sound energy under the prevailing mining and environmental conditions. These models were integrated to enable the prediction of the noise levels at any location near the mining area.

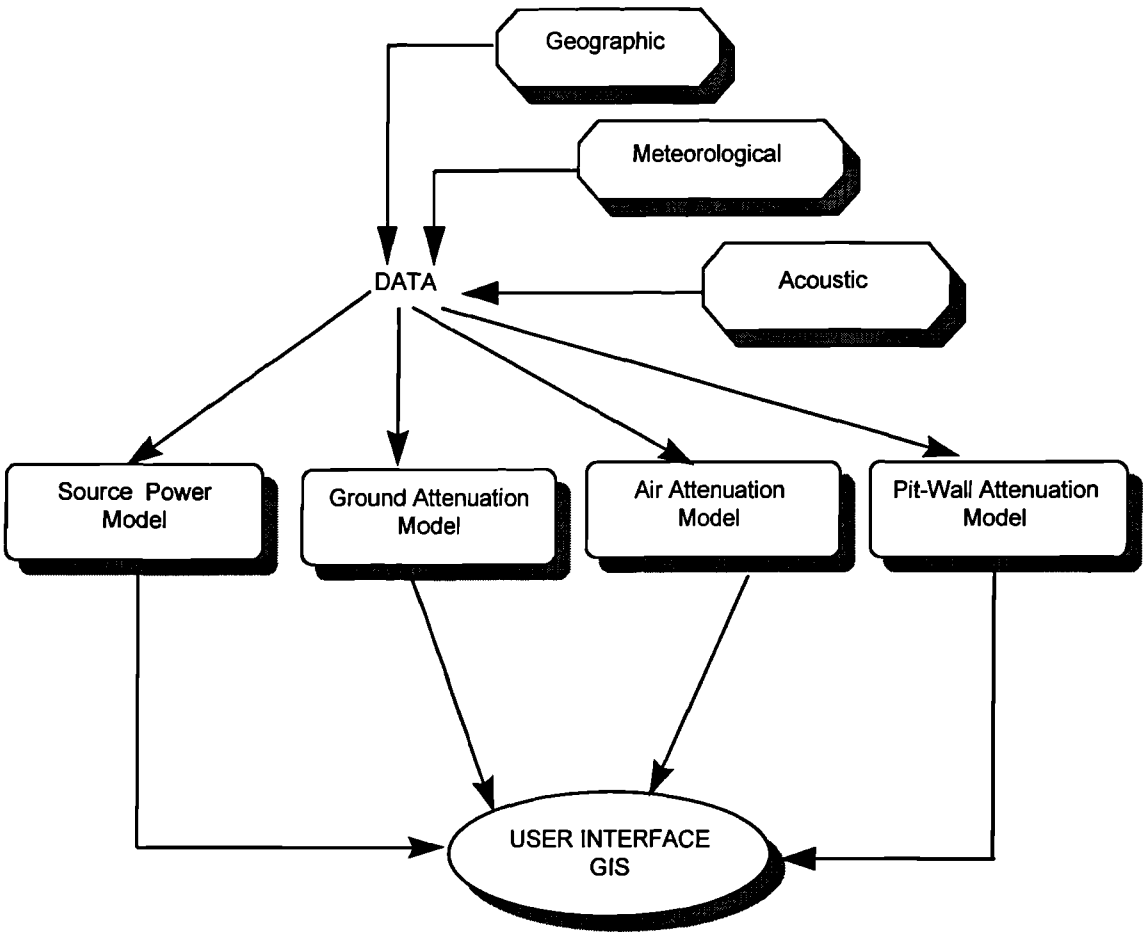


Figure 4.1 The main structure of the models of the noise prediction system developed.

The noise prediction system must have proper ways of data acquisition. Easy-to-understand method of output presentation is also very important for such systems. In other words, the system must incorporate a user interface for input and output handling. Since this system depends on continually changing mining, geo-technical and environmental data, it is essential to have a verification of the predicted levels at definite intervals and the prediction rules need to be modified accordingly. Therefore, the systems need to incorporate different instruments for the measurement of sound levels and meteorological data. It is the Mining and Environment Group's policy to use

ARCINFO, a general purpose Geographical Information System (GIS), as the graphical user interface to present final output of the environmental models developed in the Department. Therefore, provision was made to transfer the output files of the noise prediction model to the workstation platform for further environmental impact analysis purposes using the relevant map data and other geographic and environmental features in a mining region. A brief discussion and example of how GIS is utilised with the predicted noise data is presented in Chapter 8.

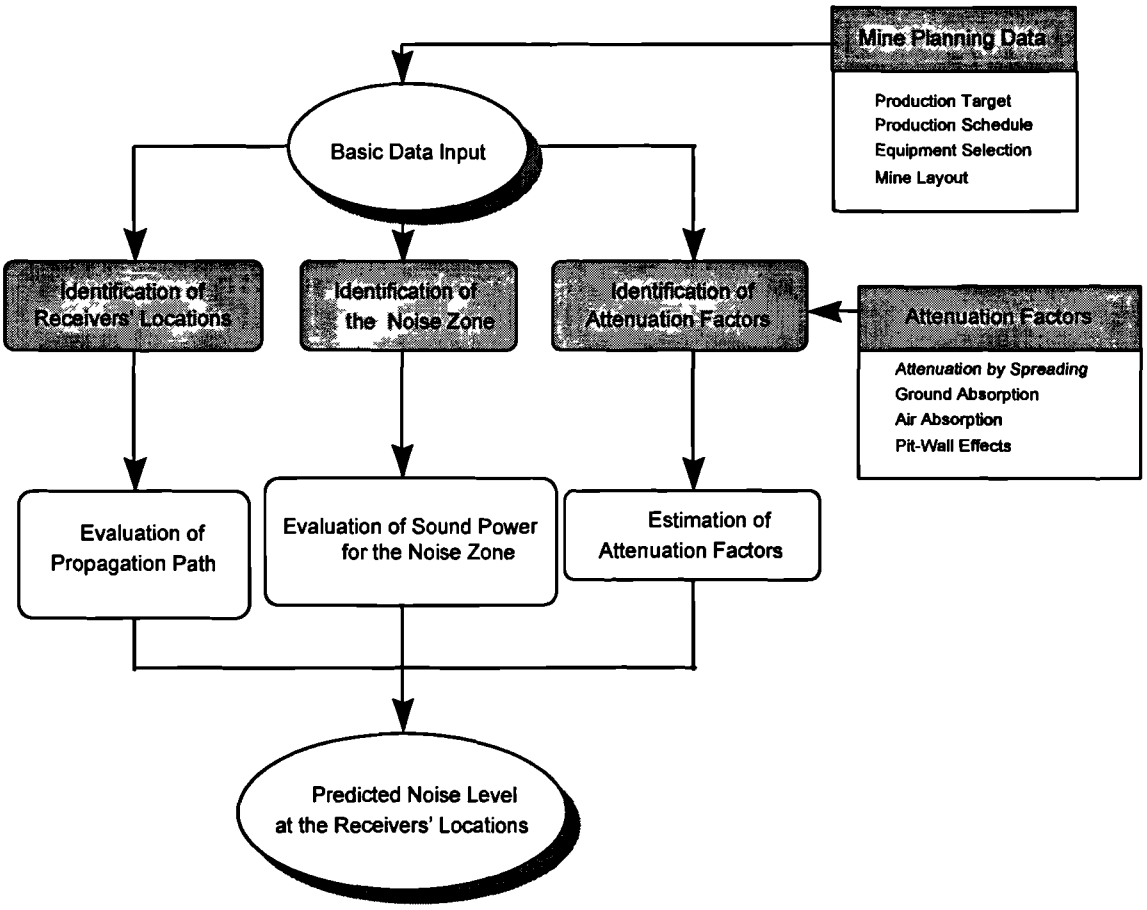


Figure 4.2 Components of the surface mining and quarrying noise prediction system developed.

As discussed in Chapter 2 a noise prediction model involves the determination of sound power level of the noise sources, evaluation of attenuation factors and the combined analysis of these for the specific noise propagation path. Figure 4.2 shows these

components incorporated in the noise modelling system developed in this research for predicting surface mining and quarrying noise.

The starting point of the development of the model was to evolve a system for the determination of the sound power level of the work zones within the mine or quarry. Sound power levels of various mining machinery can be obtained from the manufacturer's catalogue or other compiled work (Bartholomae and Parker, 1983; BS: 5228, 1984). However, these data are incomplete as they do not suggest the variation of these levels with age, maintenance level, working conditions, working strategy, loading conditions and under the influence of other machines working in the neighbourhood. As a result these data cannot be directly considered as the input data for a noise prediction model.

For the purpose of the present model development it is defined that the environmental noise level due to surface mining or quarrying operation is the noise level due to the steady state operation of the machinery working together for producing the targeted output. It is assumed that the equivalent continuous sound pressure level (L_{eq}) for a period at a particular location near the mining area is the overall impact of all the operations producing noise during that period. The predicted level can be considered as the maximum level that may appear due to the operation of the surface mining or quarrying. To develop this model the author has followed the concept of Equivalent Acoustic Centre (EAC) of large sources (Alster, 1982).

The development of the source power model for predicting noise near surface mines and quarries will be discussed in this chapter.

4.2 Theory of Equivalent Acoustic Centre (EAC)

Alster (1982) suggested that a large noise source comprising of a number of noise sources can be represented as an equivalent point source called the Equivalent Acoustic Centre (EAC). The method relies on the determination of the location and sound power level of such an imaginary point source and its directivity indices in different directions.

The EAC is determined on the basis of known sound pressure levels at a number of locations within a noise zone as illustrated in Figure 4.3.

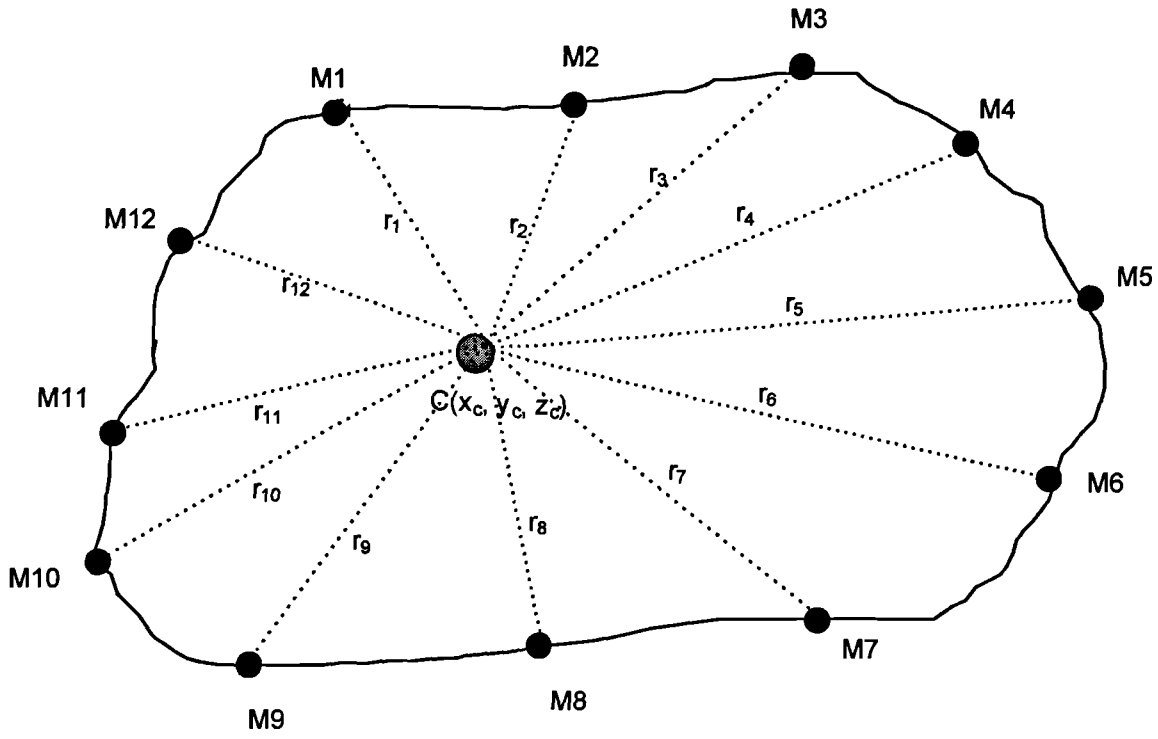


Figure 4.3 The principle of Equivalent Acoustic Centre (EAC).

Let L_W be the sound power level of a noise source and L_p be the sound pressure level due to this source at a distance r. Let the directivity factor of the source be Q. Neglecting the attenuation caused by atmospheric and terrain conditions the relationship between the above parameters can be written as:

$$20\log\left(r10^{L_p/10}\right) = L_W - 10\log\left(\frac{4\pi}{Q}\right) \tag{4.1}$$

For n different measuring points surrounding a point source C, as shown in Figure 4.3, the equations involved are:

$$
\begin{aligned}
20\log\left(r_1 10^{L_{p1}/10}\right) &= L_W - 10\log\left(\frac{4\pi}{Q}\right) \\
20\log\left(r_2 10^{L_{p2}/10}\right) &= L_W - 10\log\left(\frac{4\pi}{Q}\right) \\
&\cdot \\
20\log\left(r_n 10^{L_{pn}/10}\right) &= L_W - 10\log\left(\frac{4\pi}{Q}\right)
\end{aligned}
\tag{4.2}
$$

In these equations the right hand sides are all the same. This indicates:

$$\log(r_1 10^{L_{P1}/20}) = \log(r_2 10^{L_{P2}/20}) = \cdots = \log(r_n 10^{L_{Pn}/20}) = c \tag{4.3}$$

Here c is a constant. Thus the products $r_i \times 10^{L_{Pi}/20}$ are constant. This implies that the equivalent acoustic centre will be located near the source with higher sound pressure level. However, in real life situations these values will not be constant due to variations in Q and the equivalent source may not be necessarily a point source. Let us assume the deviations from the constant value are ε_i. For an area source, the terms of Equation 4.3 will differ from c. The error in estimation will be given as:

$$\log(r_1 10^{L_{P1}/20}) - c = \varepsilon_1,\ \log(r_2 10^{L_{P2}/20}) - c = \varepsilon_2,\ \cdots,\ \log(r_n 10^{L_{Pn}/20}) - c = \varepsilon_n \tag{4.4}$$

The values of the estimation errors will depend on the location (x_c, y_c, z_c) of the source C. The best position of a point source representing the whole noise zone will be at a location where the sum of all the above error terms will be zero and the sum of the squares of the errors is the least. This position is defined as the equivalent acoustic centre, EAC. Now, let a term S be defined such that

$$S = \varepsilon_1^2 + \varepsilon_2^2 + \cdots + \varepsilon_n^2 \tag{4.5}$$

where,

n : number of sources or points of measurements

Expanding this equation we get:

$$
\begin{aligned}
S &= \varepsilon_1^2 + \varepsilon_2^2 + \cdots + \varepsilon_n^2 \\
&= \left(r_1 10^{L_{P1}/20} - c\right)^2 + \left(r_2 10^{L_{P2}/20} - c\right)^2 + \cdots + \left(r_n 10^{L_{Pn}/20} - c\right)^2 \\
&= r_1^2 10^{L_{P1}/20} + r_2^2 10^{L_{P2}/20} + \cdots + r_n^2 10^{L_{Pn}/20} - nc^2
\end{aligned} \tag{4.6}
$$

Now, let the measuring points or the location of the sources be given as (x_i, y_i, z_i). Distances r_i from the equivalent source will be given as shown in Equation 4.7.

$$
\begin{aligned}
r_1^2 &= \left(x_c - x_1\right)^2 + \left(y_c - y_1\right)^2 + \left(z_c - z_1\right)^2 \\
r_2^2 &= \left(x_c - x_2\right)^2 + \left(y_c - y_2\right)^2 + \left(z_c - z_2\right)^2 \\
&\cdot \\
r_n^2 &= \left(x_c - x_n\right)^2 + \left(y_c - y_n\right)^2 + \left(z_c - z_n\right)^2
\end{aligned} \tag{4.7}
$$

After substituting these values of r_i into the Equation 4.6 the values of x_c, y_c, and z_c can be obtained by taking the partial derivatives of S and equating to zero. The results are shown in Equation 4.8. Thus, determining the sound pressure levels at different positions one can determine the position of the equivalent acoustic centre.

$$
\frac{\delta S}{\delta x_c} = 0 \Rightarrow x_c = \frac{\sum_{i=1}^{n} x_i 10^{L_{pi}/10}}{\sum_{i=1}^{n} 10^{L_{pi}/10}} \tag{4.8a}
$$

$$
\frac{\delta S}{\delta y_c} = 0 \Rightarrow y_c = \frac{\sum_{i=1}^{n} y_i 10^{L_{pi}/10}}{\sum_{i=1}^{n} 10^{L_{pi}/10}} \tag{4.8b}
$$

$$
\frac{\delta S}{\delta z_c} = 0 \Rightarrow z_c = \frac{\sum_{i=1}^{n} z_i 10^{L_{pi}/10}}{\sum_{i=1}^{n} 10^{L_{pi}/10}} \tag{4.8c}
$$

4.2.1 Determination of Sound Power Level at the EAC

The sound power levels corresponding to the sound pressure levels, L_{pi} at different locations (x_i, y_i, z_i) are given as:

$$L_{Wi} = L_{pi} + 10\log\left(\frac{4\pi r_i^2}{Q}\right) \tag{4.9}$$

Therefore, the average acoustic power level can be written as:

$$L_W = 10\log\left[\frac{4\pi\left(r_1^2 10^{L_{p1}/10} + r_2^2 10^{L_{p2}/10} + \cdots + r_n^2 10^{L_{pn}/10}\right)}{nQ}\right] \tag{4.10}$$

Substituting the values of r_i from Equation 4.7 into Equation 4.10 the acoustic power level, L_W, at the EAC is expressed as:

$$L_w = 10\log\left[\frac{4\pi}{nQ}\begin{pmatrix}\left\{(x_c-x_1)^2+(y_c-y_1)^2+(z_c-z_1)^2\right\}10^{L_{p1}/10} \\ +\left\{(x_c-x_2)^2+(y_c-y_2)^2+(z_c-z_2)^2\right\}10^{L_{p2}/10} \\ +\cdots+\left\{(x_c-x_n)^2+(y_c-y_n)^2+(z_c-z_n)^2\right\}10^{L_{pn}/10}\end{pmatrix}\right] \tag{4.11}$$

or,

$$L_W = 10\log\left[\frac{4\pi}{nQ}\left(\sum_{i=1}^{n} A\times 10^{L_{pi}/10} + B\times\sum_{i=1}^{n}10^{L_{pi}/10} - \sum_{i=1}^{n}10^{L_{pi}/10}\times C\right)\right] \tag{4.12}$$

Where,

$$\begin{aligned} A &= \left(x_i^2 + y_i^2 + z_i^2\right) \\ B &= \left(x_c^2 + y_c^2 + z_c^2\right) \\ C &= \left(x_c x_i + y_c y_i + z_c z_i\right) \end{aligned} \tag{4.12a}$$

Substituting the values of x_i, y_i, z_i from the expressions of x_c, y_c, and z_c this expression reduces to:

$$L_W = 10\log\left[\frac{1}{n}\left(\frac{4\pi}{Q}\right)\left\{\sum_{i=1}^{n} A\times 10^{L_{pi}/10} - B\times \sum_{i=1}^{n} 10^{L_{pi}/10}\right\}\right] \quad (4.13)$$

After calculating the sound power level at the EAC, directivity indices at each of the measuring points (M_i, i =1, 2,..., n) can be determined as:

$$DI_i = L_{pi} - L_W + 10\log\left\{\left(\frac{4\pi}{Q}\right)\left[(x_c - x_i)^2 + (y_c - y_i)^2 + (z_c - z_i)^2\right]\right\} \quad (4.14)$$

Thus, in this method one needs to determine the sound pressure levels in the near field of the combined sources and the location of the points of measurement. Sound pressure levels in a quarry or opencast mine can be obtained by direct measurement using sound level meters or from the noise data of the deployed equipment. From these values the sound power level and the location of the EAC are calculated for evaluating the far field noise levels.

Alster (1982) has shown that errors associated with the above method depend on the distance of the measuring points from the noise source. Such errors generally diminish with increasing distance between the equivalent centre and the measurement stations. It was also proved that error is minimal when the method is applied to determine equivalent sources for a number of point sources radiating acoustic energy over an area. The error was found to be minimum when applied within a smaller area. This method may yield some errors when applied to large area noise sources, however, the error can be minimised by increasing the number of measuring points. For strongly directional sources, however, this method may give rise to larger errors. Alster also proved that the error involved in representing the noise sources operating over an area by the equivalent acoustic centre is larger if the sound power emission is uniformly distributed over the area of the sources.

The working zone of a quarry or opencast mine can be considered as a volume source emitting different levels of sound power from its different points. Therefore, the sound power is not uniformly distributed over the area of the zone. If sound pressure levels are measured at a number of spatially distributed points around the working machinery

within a zone there will be negligible error in the determination of the location and sound power level of the EAC.

In this research the EAC concept was used in developing a model for predicting noise level near a quarry at steady state. It is assumed that:

- All the machines in the mines are working simultaneously and producing steady state noise levels.
- Each equipment complex is equivalent to a large volume source with sounds uniformly distributed and reducible to a point source for a far-field observation point.
- Effects of wind and other meteorological parameters are negligible.
- No external noise source influences the noise due to steady state operation of the machinery working within a noise zone.
- Location of the EAC remains constant during the steady state operation within the noise zone.

4.3 The Development of Source Characterisation Model

The above theory of equivalent acoustic centre has been used by the author for developing the source power model of the noise prediction system. The noise sources in mining and quarrying operations generate either *operational noise* or *haulage noise*. The production machinery, handling machinery and auxiliary machinery are the main sources of operational noise. Haulage noise comes mainly from the hauling equipment moving on the haul roads. Operational noise includes the noise from the hauling equipment while being loaded or manoeuvring near the working face.

There are a number of problems associated with the prediction of the sound power level of a surface mine for environmental noise assessment. Noise sources are distributed over a number of areas in the mine. The generation of noise from these sources varies with time depending on the working pattern of the mine. However, every mine has some specific work zones in which there are a concentration of activities and generation of noise. From the theory of combining noise from uncorrelated sources it is known that when one of the sound pressure levels is 10 or more decibels below the other, its effect on the total is less than 0.5 dB (Wilson, 1989). Therefore, it is assumed that the total noise impact at a location can be considered as the noise due to the higher noise levels generated at the work zone. Therefore, the problem of determining the sound power

level of a surface mine can be reduced to the determination of the sound power level of the work zones within the mine enabling the application of the Equivalent Acoustic Centre (EAC) principle to develop a point source model for the noise generated in the work zones of a mine or quarry.

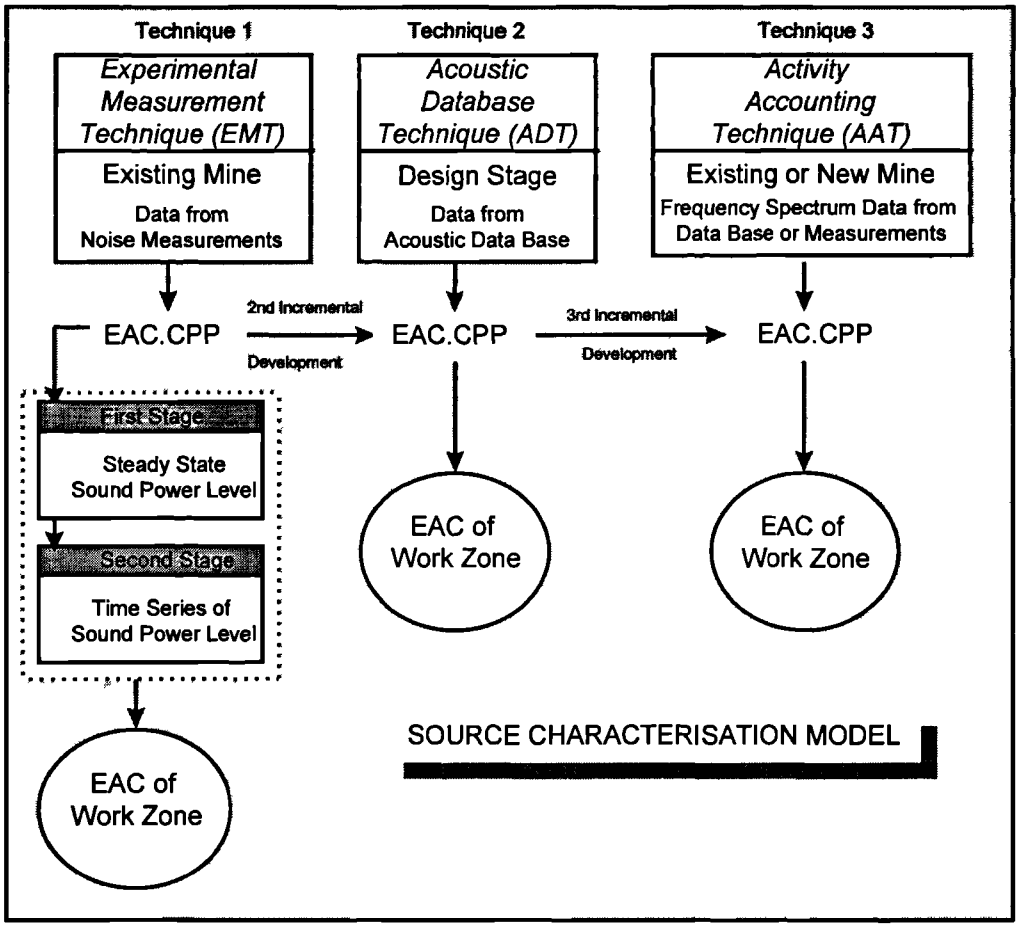


Figure 4.4 Techniques of developing the source characterisation model.

Moreover, the purpose of noise prediction also may be different. In certain cases the objective may be to determine the continuous equivalent sound pressure level (L_{eq}) at a location for a specified period. Sometimes, one may be interested to know how this sound power level of a source is changing with time. In an another situation the objective may be to determine the quality of noise level at a specific location and distance from the mine. The necessity of noise prediction may arise at the design stage of a mine, or for an existing mine. However, there is no unique model for predicting the sound power level of the noise sources for all these purposes. Research into the

characterisation of the noise source involved incremental development of a source power model addressing various important aspects and characteristics of mining noise. This section discusses the development of a source power model for the operational noise in a surface mine or quarry.

The author has developed three techniques for this purpose. These are:

- Experimental Measurement Technique (EMT)
- Acoustic Database Technique (ADT)
- Activity Accounting Technique (AAT)

As shown in Figure 4.4 these techniques are used for determining the equivalent acoustic centres of work zones in a mine depending on the specific situation. All the models were coded in C++. The following sections will discuss the development and application of these techniques. The techniques developed were experimentally verified and the model was finalised.

4.3.1 Experimental Measurement Technique (EMT)

Extensive noise level measurements are common in environmental noise studies. Predictions in such cases are based on the statistical analysis of the measured noise levels. The measurements of noise levels can be used for evaluating the sound power level of the noise source. The current practice is to measure the noise level at a number of locations and interpolate the noise levels to draw the noise contours. This method does not provide quantitative noise prediction as very little information on the sound power level of the sources is available. Many commercial noise estimation packages yield noise contours based on the sound power level of the individual sources (Tonin, 1993).

In order to determine the *in situ* sound power level of noise sources by noise surveys, the sound pressure levels are measured at specific measuring distances from various noise sources. This is carried out considering hours of the day, days of the week, weeks of the month and months of the year as a basis. Such evaluation depends on the quality

and continuity of the noise source. Such values are correlated with the variations of the surrounding conditions related to noise generation, absorption and propagation.

The noise survey may be carried out for individual machines, for its various components or for a group of machines working together. Following a controlled noise measurement scheme the directivity information of the machine or its components is also evaluated.

The survey reports reveal the significant and non significant noise sources involved in the mining operations. This also provides the duration of criticality of certain machines or components. This technique may be useful for qualitative judgement of future noise events. However, without extra tools for noise analysis this method cannot enable the prediction of noise levels near the mining operations.

For developing the environmental noise prediction model the noise survey method has not been selected. This method would require large number of noise measurements and data handling. Therefore the author has developed a method referred to as the Planned Experiment Method (PEM).

The Planned Experiment Method (PEM) for the evaluation of sound power level of a noise source is developed for noise prediction purposes. The method is based on a series of experiments designed for a specific site. These experiments are of two broad categories, namely source characterisation experiments and site characterisation experiments.

Source Characterisation Experiments

Surface mining or quarrying involves the operation of a large number of equipment distributed over a large area. The whole complex can be considered as a large noise source. For the purpose of noise prediction the sound power level of the source should be evaluated. The nature of mining and quarrying favours noise zoning. The whole mining complex can be divided into a number of work zones. The source characterisation experiments are designed to determine the equivalent acoustic centre of the zone. The concept of equivalent acoustic centres of large sources was extended to develop the theoretical model for determining the location and sound power level of the

equivalent acoustic centre of the working zone. Thus the experiments need to be planned for determining a point source equivalence of the working zone. The locations of experimental noise measurements are determined considering the site conditions. The measurement locations need to be such that the influences of the adjacent noise zones are minimised. The geometrical locations of machines, nature of equipment deployed and their directivity characteristics are to be carefully observed before conducting any experiments. This helps in subjective decision making. In the present work experimental locations for the measurements were fixed at a distance from the edge of the source. This distance was equal to half the largest separation of two simultaneously working machines within the same zone. In certain situations it was equal to the largest dimension of the noise generators within the zone.

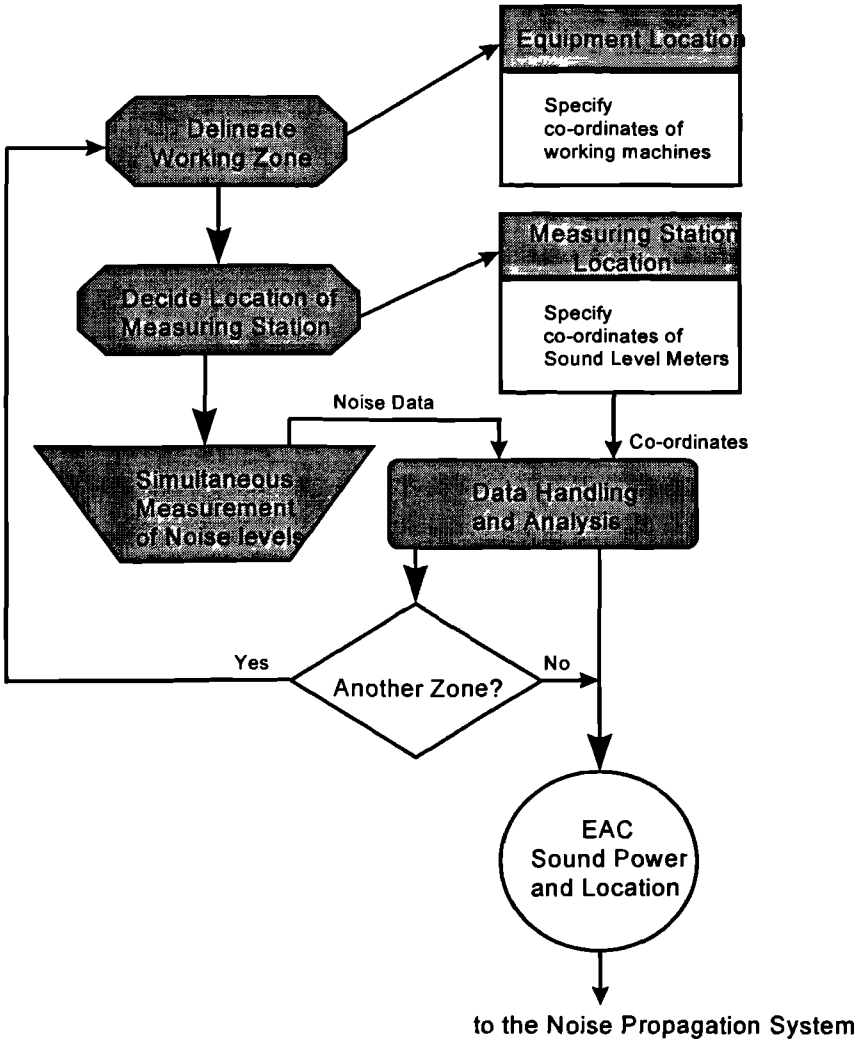


Figure 4.5 The procedure followed and the flow diagram of the software developed for the source characterisation.

The experiments were planned for the steady state operations of the workzones. Sound power levels of the workzones are normally a time varying function. Far field noise prediction aims at predicting the L_{eq} values. Predicted sound pressure levels at experimentally measured steady-state sound power level may give a sound pressure level higher than the exactly measured L_{eq}. The purpose of noise prediction may be to provide decision support for mine planning. Planning of mining activities for the predicted sound pressure level may result in slightly lower L_{eq} at the far field provided other external noise does not alter the situation. The procedure followed in source characterisation experiments is shown in Figure 4.5. The experimental data can be used as input to the source power model (EAC.CPP) to determine the sound power model developed by the author to determine the sound power level of the equivalent acoustic centre for the work zone. The location of this centre and its directivity characteristics depend on the site conditions and patterns of equipment deployment.

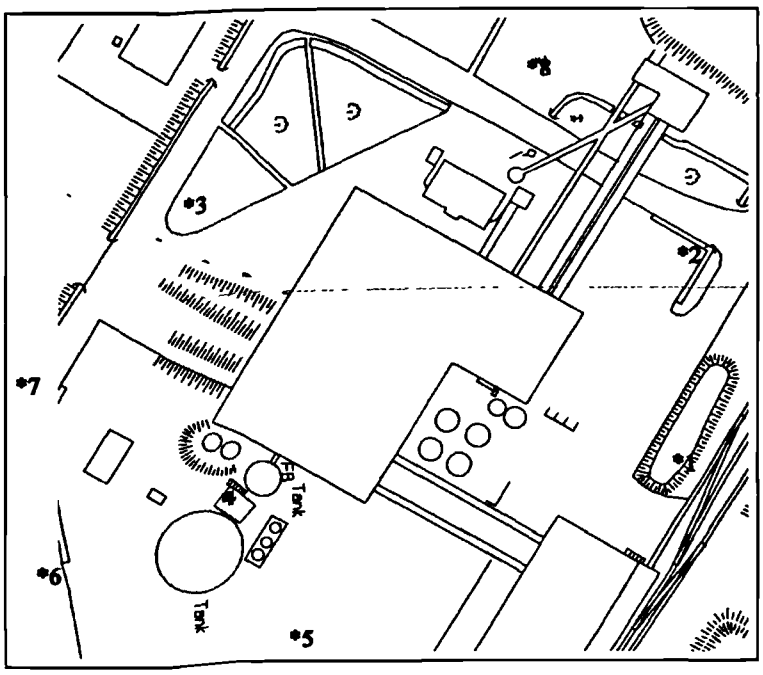
Site Characterisation Experiment

The far field noise level depends on the behaviour of the acoustic waves propagating from the source. The absorption of acoustic energy during propagation will be discussed in the next chapter. An example site characterisation experiment will be discussed there as a part of the development of the Attenuation Model.

4.3.1.1 The Application of Experimental Measurement Technique to determine the EAC of Tara Mines

In order to assess the validity of the principle of Equivalent Acoustic Centre (EAC) a set of experiments were conducted at a large complex comprising of a number of simultaneously operating sources. These experiments were carried out to determine the EAC to represent the sound power level of the processing plant at Tara Mines in the Republic of Ireland.

The noise field surrounding the processing plant is the result of many noise sources working simultaneously within an enclosed housing. The purpose of this experiment was to predict the sound pressure levels around the plant based on experimentally determined EAC.



*3 Noise measurement station

Figure 4.6 Plan view of the processing plant and the noise measurement locations.

Table 4.3 Calculated sound power level and the location of EAC at Tara Plant.

Measuring Station No.	X	Y	Z	Measured SPL, dBA	DI
1	285197	267818	1581.65	55.3066	-1.49535
2	285147	267733	1580.59	54.0194	-2.14247
3	285083	267798	1581.13	65.2591	2.95599
4	285059	267946	1578.27	64.6908	0.91606
5	285001	267959	1576.37	63.1316	1.60430
6	285032	267726	1578.95	52.5318	-5.00141
7	284930	267894	1577.62	59.7757	0.00207
8	284972	267790	1577.60	58.5881	-1.50425
EAC	285044	267875	1578.87	102.9960*	

*Sound Power Level, dBA

Figure 4.6 shows the plan view of the plant. Eight measurement locations were selected for the determination of the equivalent acoustic centre of the plant. These locations were selected considering the influence of reflecting surfaces in the field, wind directions, constituent source locations, sound absorption by green coverage, terrain and minimum interference of external sources. Table 4.3 gives the co-ordinates of the measurement locations along with the representative sound pressure levels measured at these stations.

The noise measurements experiments were carried out during the steady operation of the plant using five sound level meters with data storage facilities. One of the measuring stations was considered as the reference station. The sound level meter at this position was coupled with a wind speed and direction monitor (Larson Davis Model-2140). The data stored in the sound level meter was downloaded to a PC and analysed for the time histories and other descriptors of noise level such as L_{eq}, L_{max}, L_{peak}, etc.

The exact co-ordinates of the measurement locations were obtained from the survey department of the mine. Additional measurements of noise levels were carried out at a number of other stations surrounding the plant to compare with the predicted values on the basis of the resultant EAC. The mill was running with normal operations generating fairly steady noise and the atmospheric conditions during the experiments were:

- The cloud level was 0 to 1.0.
- Atmospheric temperature was within 10^0-15^o C.
- Average wind velocity was between 0.1 and 0.7 $msec^{-1}$, predominantly in the SSW direction.

Noise levels in dBA were continuously monitored at each of the measurement locations. The data stored on the sound level meters were down loaded to a PC and the time series of the observation period were obtained. Figure 4.7 shows the time series of the noise levels observed at four of the measurement stations. These show that during the experiments the noise levels generated by the mill were fairly steady. A hand-held sound level meter (Larson Davis SLM 820) was used to measure noise levels at different locations while monitoring noise continuously at the fixed noise measurement stations. Figure 4.8 illustrates the structure of the model developed for the determination of the EAC from the experimental data. Figure 4.9 shows the comparison of measured and predicted noise levels at different stations. This prediction considered only the attenuation due to spreading. The distances to the measurement stations from the source were less than 100 m. Therefore, the effect of meteorological factors and the attenuation by air absorption could be neglected.

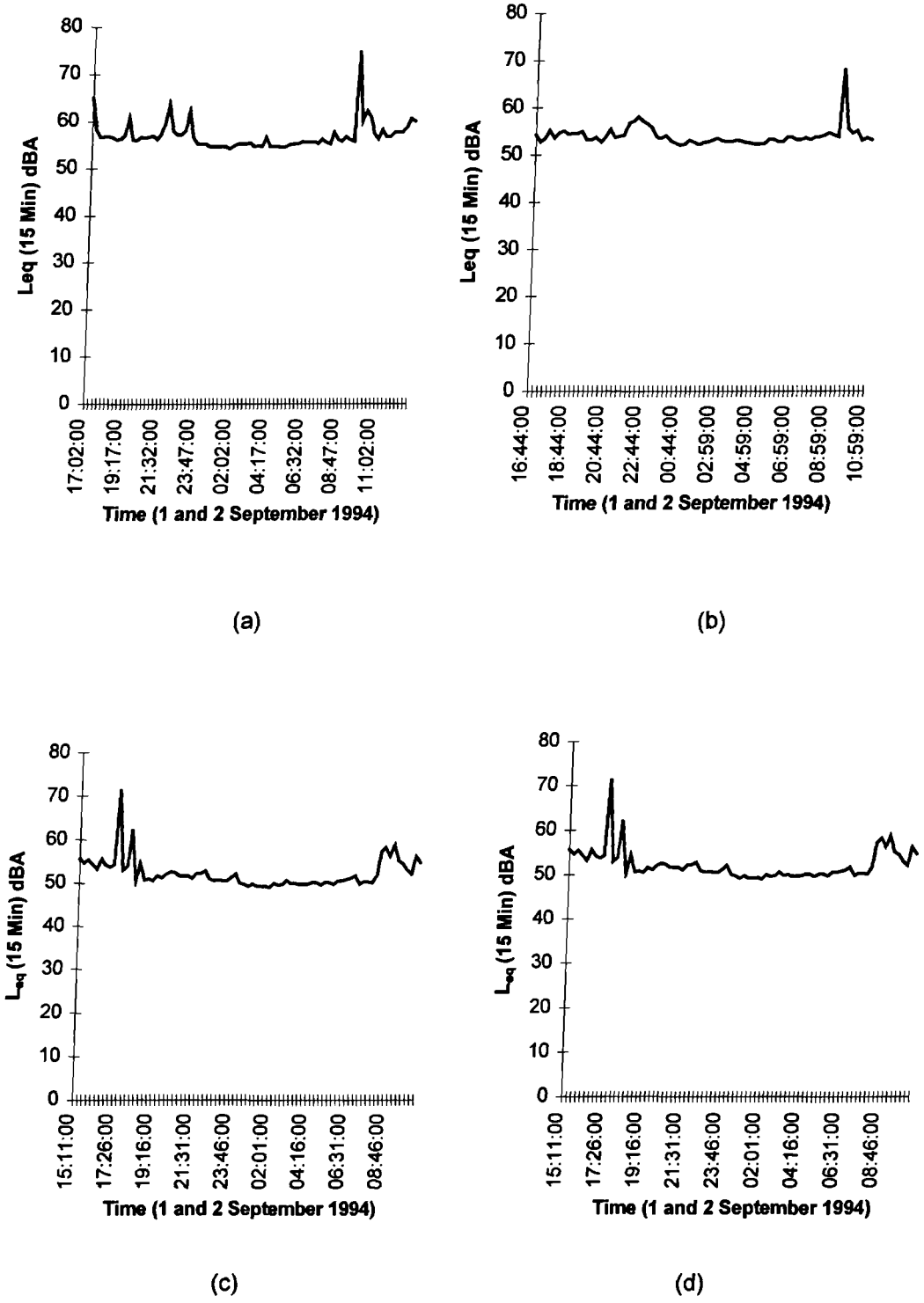


Figure 4.7 Time series of the noise levels at measurement locations, (a) at reference location, (b) at station 3, (c) at station 2, (d) at station 8.

The EAC data determined were used to predict the sound pressure levels at a regular grid around the processing plant. These predicted values were used for drawing contour

maps to show the noise levels. Figure 4.10 shows such a contour map plotted by using UNIMAP.

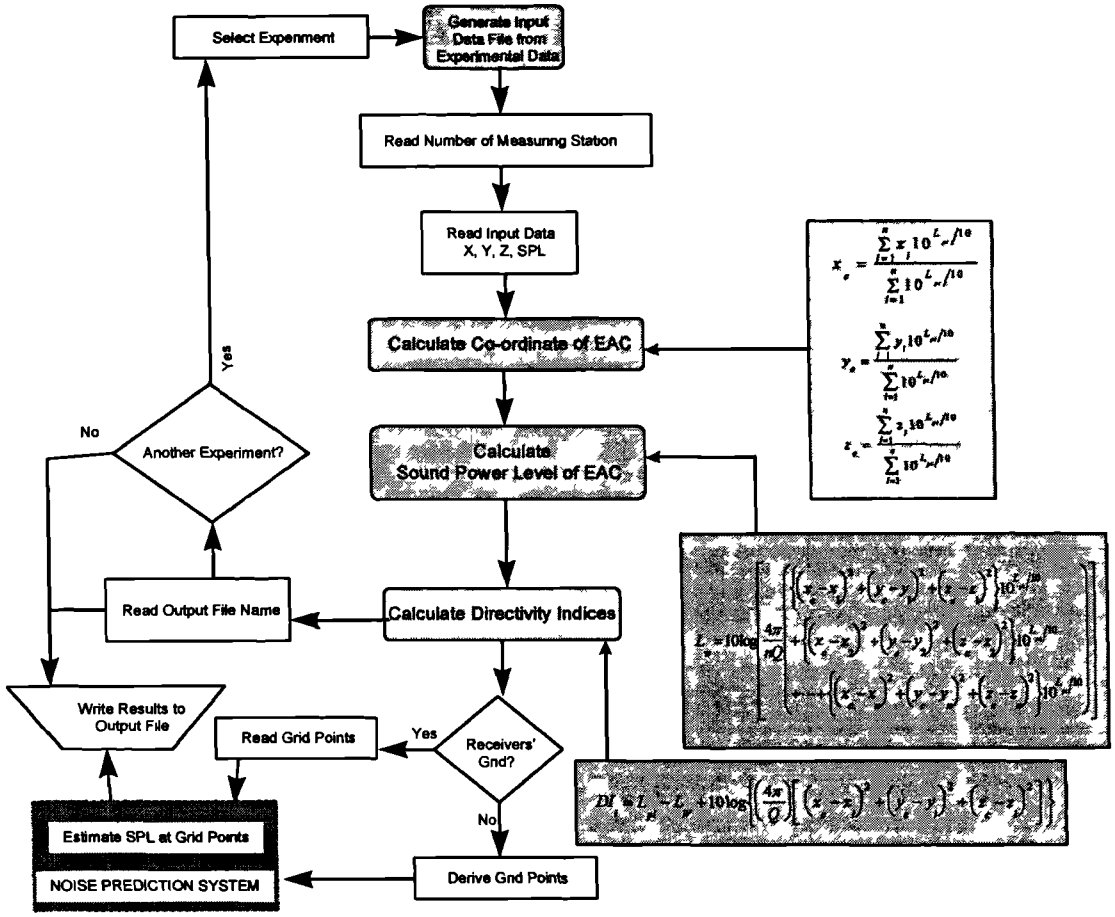


Figure 4.8 The flow diagram of the source power model with the Experimental Measurement Technique implemented only-Stage 1(EAC.CPP).

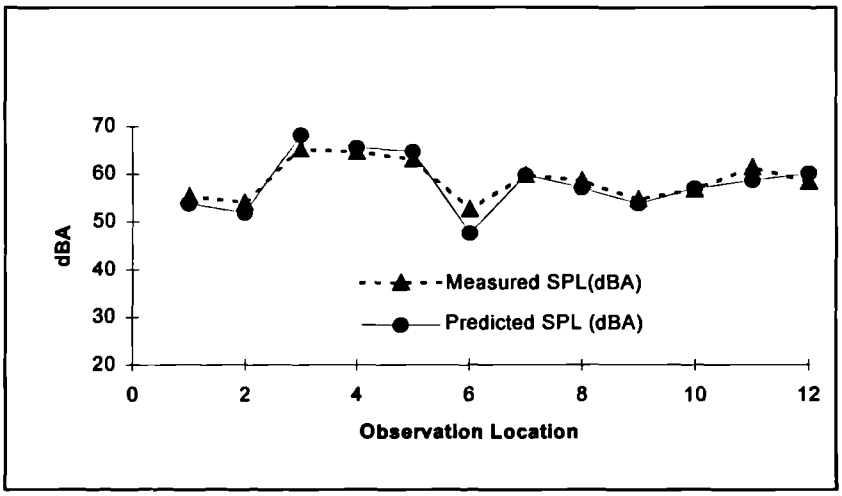


Figure 4.9 Predicted noise levels using the EAC concept and the measured values.

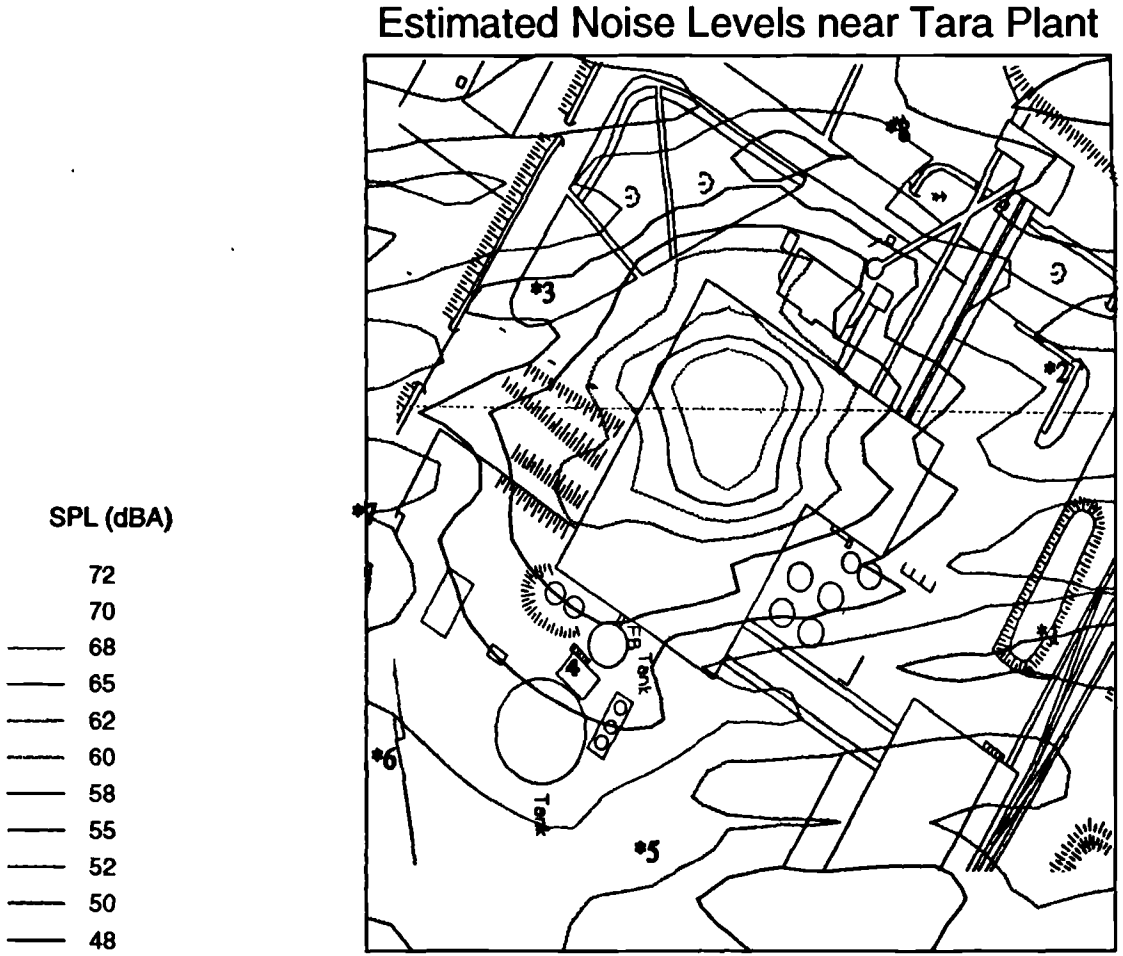


Figure 4.10 Estimated noise contours near the processing plant.

Time Varying EAC

The sound power level of a large source like a processing plant is never constant. Depending on the behaviour of the constituent noise sources the emanated sound power level varies with time. The overall effect of the large complex sound source has been evaluated using the equivalent acoustic centre (EAC) theory as discussed above. The variation of sound power with time was also studied by recording the time series of the sound pressure levels (SPL). The source power model was further developed to enable the user to read time series data from a file and to determine the time series of the sound power level of a complex noise source such as the processing plant. The results of the analysis of Tara data show the variation of EAC over 150 minutes as presented in Table 4.4.

Table 4.4 Variation of the Equivalent Acoustic Centre of the plant during the observation period.

X	Y	Z	L_W, dBA
285044	267870	1578.91	102.882
285041	267874	1578.89	103.185
285049	267882	1578.89	101.918
285046	267890	1578.63	102.110
285044	267853	1579.27	103.217
285033	267865	1578.71	103.835
285044	267886	1578.64	103.628
285043	267885	1578.56	103.729
285048	267894	1578.74	104.070
285047	267877	1578.84	103.436
285056	267885	1578.98	102.488
285043	267898	1578.61	103.913

Maximum displacement of the EAC in X-direction =22.6595m
Maximum displacement of the EAC in Y-direction =45.3031m
Maximum displacement of the EAC in Z-direction =0.71479m
Standard deviation of Sound Power Level s= 0.71525

The EAC was found to be varying with maximum displacement in the Y direction up to 45.3 m. The sound power level generated by the plant, however, was fairly constant, the variation being 2.15 dBA. Therefore, for situations where the instantaneous sound pressure level is required, this can be calculated from the experimentally determined time series at the EAC definer locations. The present experimental results show that the noise sources located in the Y direction were subject to wider variation. During the

observation period a cement pump was working for some time near the northern wall of the mill. This explains the wider range of movement of EAC in the Y co-ordinate direction.

The correlation coefficient of the measured and predicted data shown in Figure 4.9 was found to be 0.963894. This shows that the method of EAC is applicable for representing the sound power level of large and complex sources comprising of a number of noise generators.

4.3.2 Acoustic Database Technique (ADT)

The Acoustic Database Technique was developed for predicting environmental noise levels for surface mines and quarries during the design and planning stage of operations. This method (ADT) of determination of sound power level of noise sources also uses the scheme of noise zoning mentioned in the EMT.

The short coming of the EMT is in its inability to predict noise levels at the planning stage. The Acoustic Database Technique can provide information of probable environmental noise impact due to new mines and quarries. It considers the planned equipment complexes and their deployment strategy within the quarry/mine. The work zones are represented by EACs and their sound power levels are calculated on the basis of the surface plans of the proposed quarry and acoustic data of the equipment. The source power model described in Section 4.3.1 was further developed to enable the user to enter equipment and field specific noise data from a database for the prediction of the location and sound power level of EAC at the design stage. The flow diagram of the model incorporating the acoustic database is shown in Figure 4.11.

Reliability of this technique depends on the data stored in the acoustic database. This database is developed by studying the noise levels of different equipment deployed in the mine. Such noise levels can also be available from the manufacturers' test reports. However, *in situ* verification of these levels is also necessary. Once the database is developed it gives the sound pressure level at standard distances from the machine in different directions. The database should be able to provide such noise levels for various

categories of equipment classified on the basis of machine weight, installed power capacity and production rate. British Standard (BS: 5228) gives such data for some construction equipment. For different types of surface mining and quarrying operation such a database is yet to be established. Table 4.5 shows some typical data for certain commonly used surface mining and quarrying machinery.

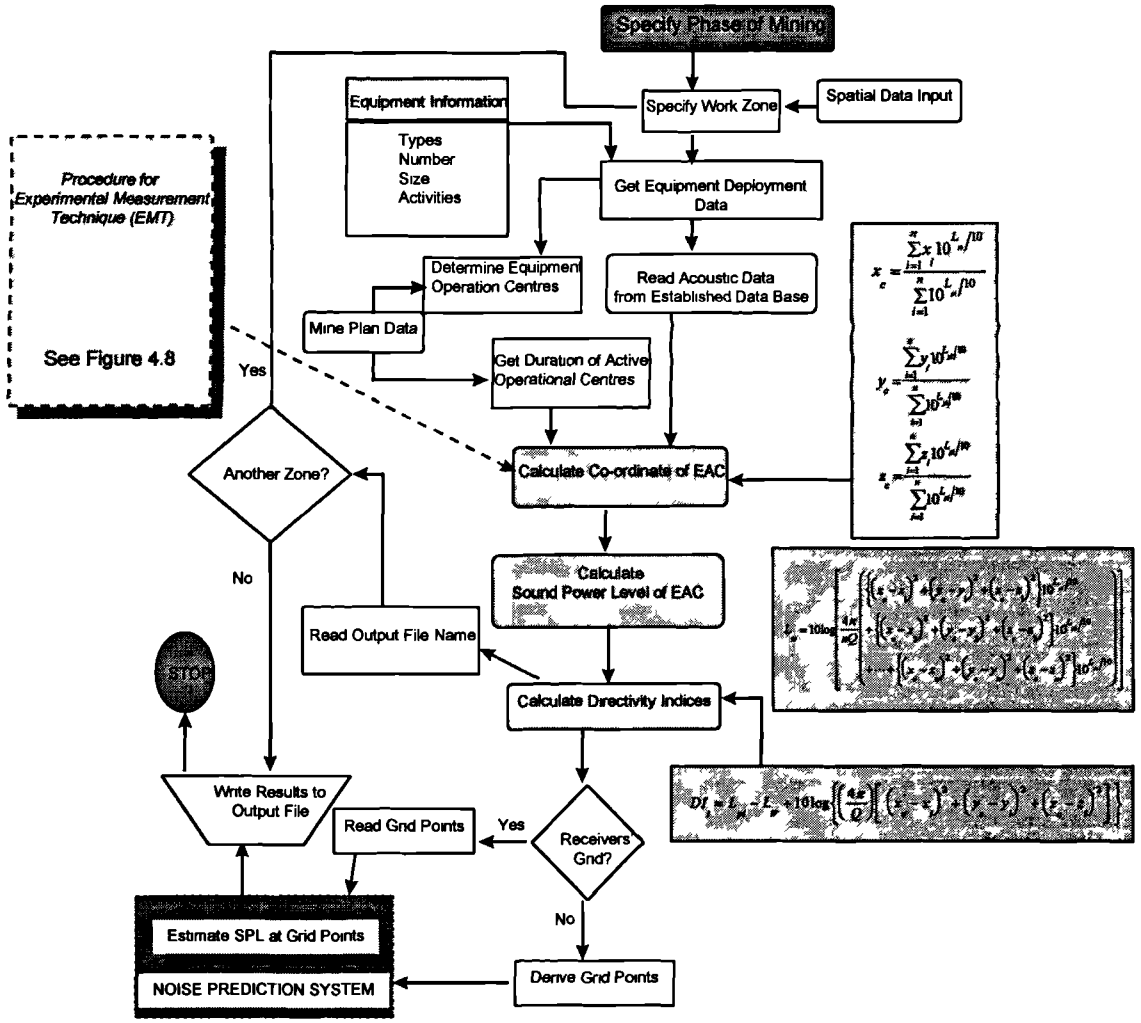


Figure 4.11 The flow diagram of the source power model after the implementation of the Acoustic Database Technique -Stage 2 (EAC.CPP).

Table 4.5 Noise levels of different machinery (after Bartholomae and Parker, 1983).

Typical Noise Exposure Level for Operators and Bystanders (dBA)				
Name of Machinery	**Without Noise Treatment**		**With Noise Treatment**	
	Lower limit	**Upper Limit**	**Lower Limit**	**Upper Limit**
Diesel Powered Rotary Drills	85	100	75	90
Electrically Driven Rotary Drill	76	95	76	85
Machine Mounted Percussion Drills	100	118	80	114
Crawler Tractor	95	105	85	95
Electric Shovel and Dragline	---	---	72	89
Diesel Powered Dragline, Cranes, Shovels, Hydraulic Excavator	85	98	80	88
Haulage Trucks	85	110	80	90
Scrapers	85	100	85	90
Front End Loader	94	100	82	90
Graders	85	98	80	88
Coal Augers	90	100	86	90

4.3.3 Activity Accounting Technique (AAT)

This technique has been developed for the purpose of detailed noise analysis in surface mines. Different types of equipment are deployed in mining or quarrying operations for performing a specific operation. These operations are completed as a sequence of definite activities. Each of these activities generate specific types of noise, characterised by their frequency spectrum. The noise quality in the far field of a working zone of a surface mine depends on this spectrum.

The AAT depends on identifying different activities in the quarry and determining their duration and frequency spectra. The number of such activities increases with the increase of the size of the quarry or mine and in many situations may require a large amount of data processing. Therefore, if noise quality prediction is not necessary this technique with frequency analysis may not be suggested. However, small mines or construction sites near residential areas may need to analyse noise quality. Such operations do not have a large number of work zones. Therefore, analysis by Activity

Accounting Technique would be very useful for noise assessment and prediction purposes in such cases. This technique may be used without frequency analysis to determine the broad band noise levels. For a specific case, based on available noise data, sound pressure levels at specified locations within work-zones can be calculated. To evaluate the noise sources in that work zone these sound pressure levels are provided as input data to the source power model developed, and the sound power level of the representative equivalent acoustic centre of the zone is determined. Figure 4.12 shows the procedures involved in this technique. The implementation of the AAT is discussed in detail in the following sections.

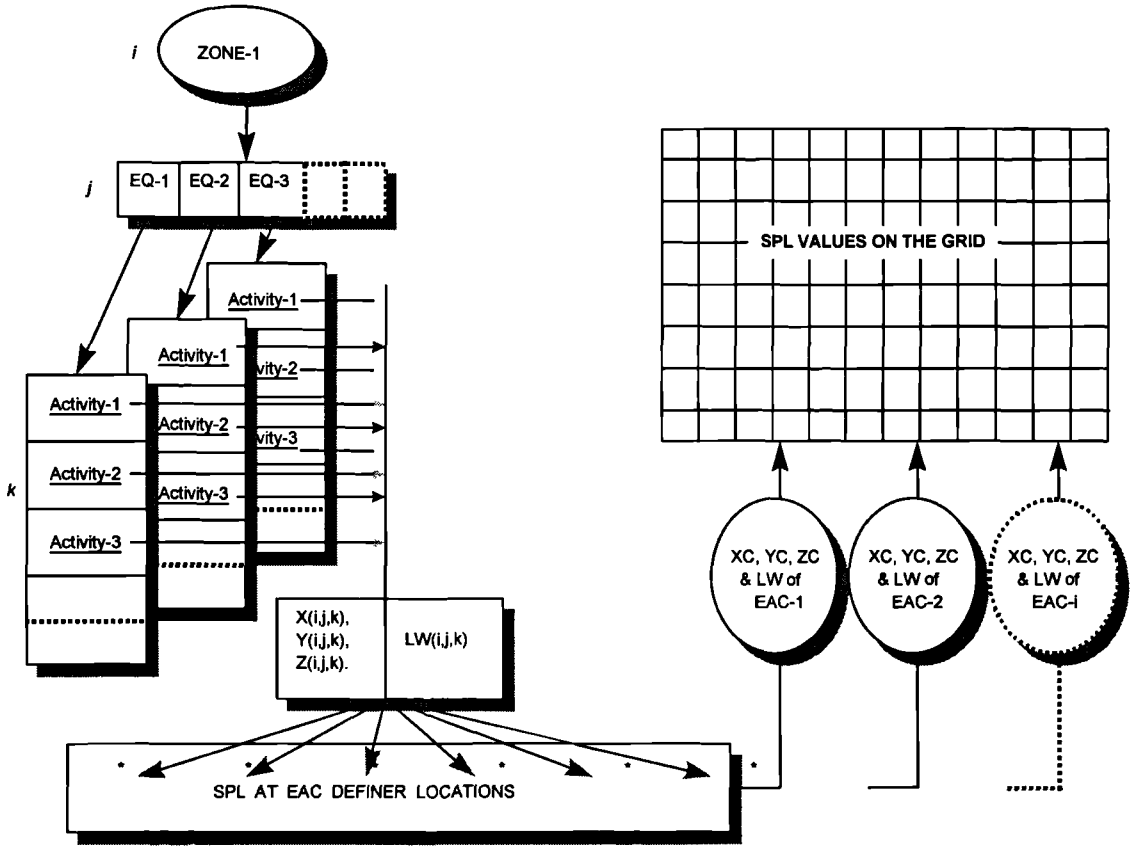


Figure 4.12 Activity Accounting Technique of evaluating sound power levels of the noise sources in a work zone within a surface mine.

4.3.3.1 Work Study of Equipment Complex

The study of noise levels of an equipment complex can be carried out at the site under consideration or in any site where similar equipment are deployed. Except for a few cases, the suppliers of the equipment in consideration also may conduct this type of work study and supply the data on request. The purpose of the work study is to identify the various compositional activities involved in the working of a machine or group of machines. Through such study the duration of each activity is determined and the total cycle time of all the activities involved in a particular operation are determined. The total number of such activities for a given production target or work duration is also determined. Statistical analysis of the data acquired during the work study gives the necessary information of the noise field near the surface mines. In the present work, such a study was conducted in a limestone quarry in the Republic of Ireland. Results of this experimental study are discussed in Section 4.3.3.4.

4.3.3.2 Establishment of Noise Signature

Depending on the type, age, maintenance level and operation scheme a machine or a group of machines generate noise of different qualities characterised by a specific spectrum of sound pressure level. The Activity Accounting Technique has been developed to use such specific a spectrum for each activity. Noise signature of an activity can be established based on large number of *in situ* noise measurements. For example, Planned Preventive Maintenance (PPM) management prepares the noise signature of certain components of some machinery. Associating the environmental noise prediction program with such systems, the noise signatures for various activities can be established. However, the best method to establish such signature is by conducting a large number of noise spectrum measurements and statistical decision making. In the present work the noise signature for front end loader and dump truck operation in a quarry was established. However, since the main objective of this research was the development of an environmental noise prediction model, very limited experimental work was carried out to establish the noise signature of activities in surface mines.

4.3.3.3 The Assessment of Activity Sound Power Levels

The assessment of sound pressure level at a far field location requires the determination of sound power level of the source. Determination of the sound power level of an activity is carried out by measuring sound pressure levels. Such measurements must be carried out within the area of influence of that activity. The sound pressure levels are either experimentally determined or taken from the specific acoustic signature of the activity. The noise signature of an activity is the sound pressure levels at different frequencies given at a specific distance from the source of the activity.

The sound power level of an activity is determined from the noise signature at a specified distance. The governing equation as discussed in Chapter 3 is:

$$L_W = L_p + 10\log R + D \tag{4.15}$$

where,

L_W : sound power level, dBA
L_p : sound pressure level, dBA
R : distance from source to the measurement location, m
D : corrections due to source-receiver location, dBA

Once the sound power levels of the activities for different frequencies are determined the corresponding sound pressure levels at any grid point around the source can be calculated. For this purpose the distances of the grid point from the source are evaluated. The next important parameter influencing the acoustic environment is the duration of the activities. From the production target and cycle time of operation the duration of different activities over a base period is determined. In some cases the measuring instrument may give readings in dB. Such values should be A-weighted. In the present work the frequency-wise sound power levels of different activities were determined experimentally. The results of these experiments are shown in Section 4.3.3.4.

The source characterisation model described in Section 4.3.1 and 4.3.2 was further developed to include the option of using the AAT for predicting the noise spectra from the sound pressure signature of the activities of the mining machinery within a zone. Figure 4.13 shows the structure of the model after the implementation of the AAT. The

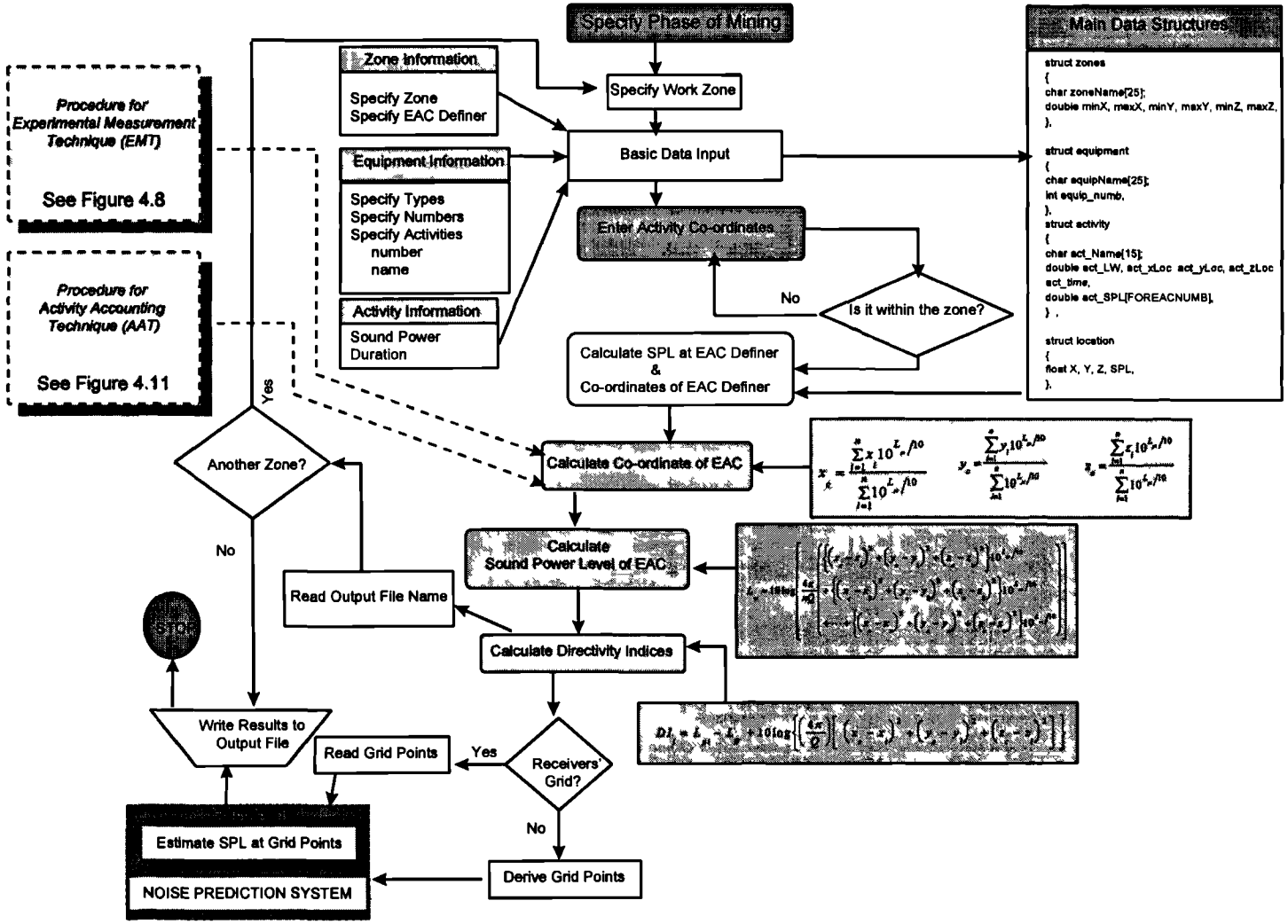


Figure 4.13 The flow diagram of the source power model after the implementation of the Activity Accounting Technique -Stage 3 (EAC.CPP).

output of the model is used to predict the sound pressure level in the far field. The model developed for this purpose will be discussed in Chapter 6.

The prerequisite of this technique is to have an experimentally verified acoustic database for various activities involved in surface mining. To evaluate the equivalent acoustic centre (EAC) of a work zone in a quarry from such a database the following procedures are followed:

- Identify the work zone.
- Determine the types of equipment working in this zone.
- Determine the number of equipment in each zone.
- Identify the activities performed by each equipment.
- Evaluate the duration of each activity during the base period.
- Determine the location of the activities.
- Evaluate the activity sound power level.
- Find out sufficient locations within each zone to determine the equivalent continuous sound pressure levels from each activity in the zone and determine their resultant sound pressure levels at these locations. These locations will be the definers for the EAC.
- Determine the EAC and its directivity of each zone from the above sound pressure levels and locations.
- Determine the sound pressure levels at the grid points from each EAC without any attenuation.
- Determine the resultant effects of all zones.

To validate the AAT, experiments were conducted to determine the activity location and duration of the activities involved in excavation by a front end loader and dump truck. The experimental results were then analysed using the model developed to determine the sound pressure level at a location near the operating quarry. The result of this estimated noise spectrum was compared with the measured noise spectrum.

4.3.3.4 Experimental Verification of the AAT

The experiment was conducted in a limestone quarry in Ireland. The floor of the quarry was dipping towards the north at a gradient of 1 in 10. The face was similar to a box cut with an advancing face of 105 m. The resultant sound field is a semi-reverberant field formed by the direct, reflected and scattered sound energies. There were four main operating zones in the quarry. To validate the activity accounting technique the work

zone at the deep face was selected. The main operating machinery in this zone were the Front End Loader (FEL) and dump trucks. The objective of the experiment was to determine the sound power levels of the activities in this zone. Table 4.6 presents the atmospheric conditions during noise monitoring in the quarry in November 1994. Figure 4.14 illustrates the surface plan of the limestone quarry and Plate 4.1 shows the working conditions in the quarry during the experiments.

Table 4.6 The atmospheric conditions during noise monitoring at the limestone quarry.

Particulars	Values
Ambient Temperature	7^0 — 10^0 C
Cloud coverage	4 — 8
Maximum wind velocity	4.2 — 8.5 ms^{-1}
Wind direction	W — WSW
Rain	none
Relative humidity	90%

Table 4.7 Octave band analysis of RMS sound pressure levels for various activities with FEL and Dump Trucks (from 2900 RTA).

Freq. Hz	FEL loading	FEL moving (loaded)	FEL moving (empty)	Truck moving (loaded)	Truck moving (empty)	FEL face dressing	FEL bucket filling
16.0	65.9	60.9	76.6	73.5	79.5	62.9	66.0
31.5	76.1	82.6	77.7	74.9	78.1	81.6	78.8
63.0	84.2	82.9	79.5	82.4	96.3	87.7	82.6
125.0	77.7	88.3	84.9	93.7	99.4	87.9	92.4
250.0	76.1	78.6	80.8	86.9	89.8	81.7	86.8
500.0	75.2	75.0	77.9	82.6	85.7	92.6	76.4
1000.0	74.6	76.3	76.8	81.7	83.1	94.3	77.4
2000.0	73.1	70.3	73.3	80.7	80.6	91.7	92.4
4000.0	65.2	65.2	70.2	76.8	76.9	78.3	67.8
8000.0	52.3	54.6	62.3	76.1	69.3	62.4	58.5
16000.0	39.9	43.8	53.7	57.0	61.7	49.6	50.2
dBA	79.2	80.1	81.6	87.8	89.8	97.4	83.2

A Larson Davis Real Time Analyser, Model-2900 RTA was used to record the RMS sound pressure levels at different frequencies. The analyser was also used to measure the A-weighted level over the total band for various activities of the machines at the face. Table 4.7 provides the octave band analysis of noise generated during different

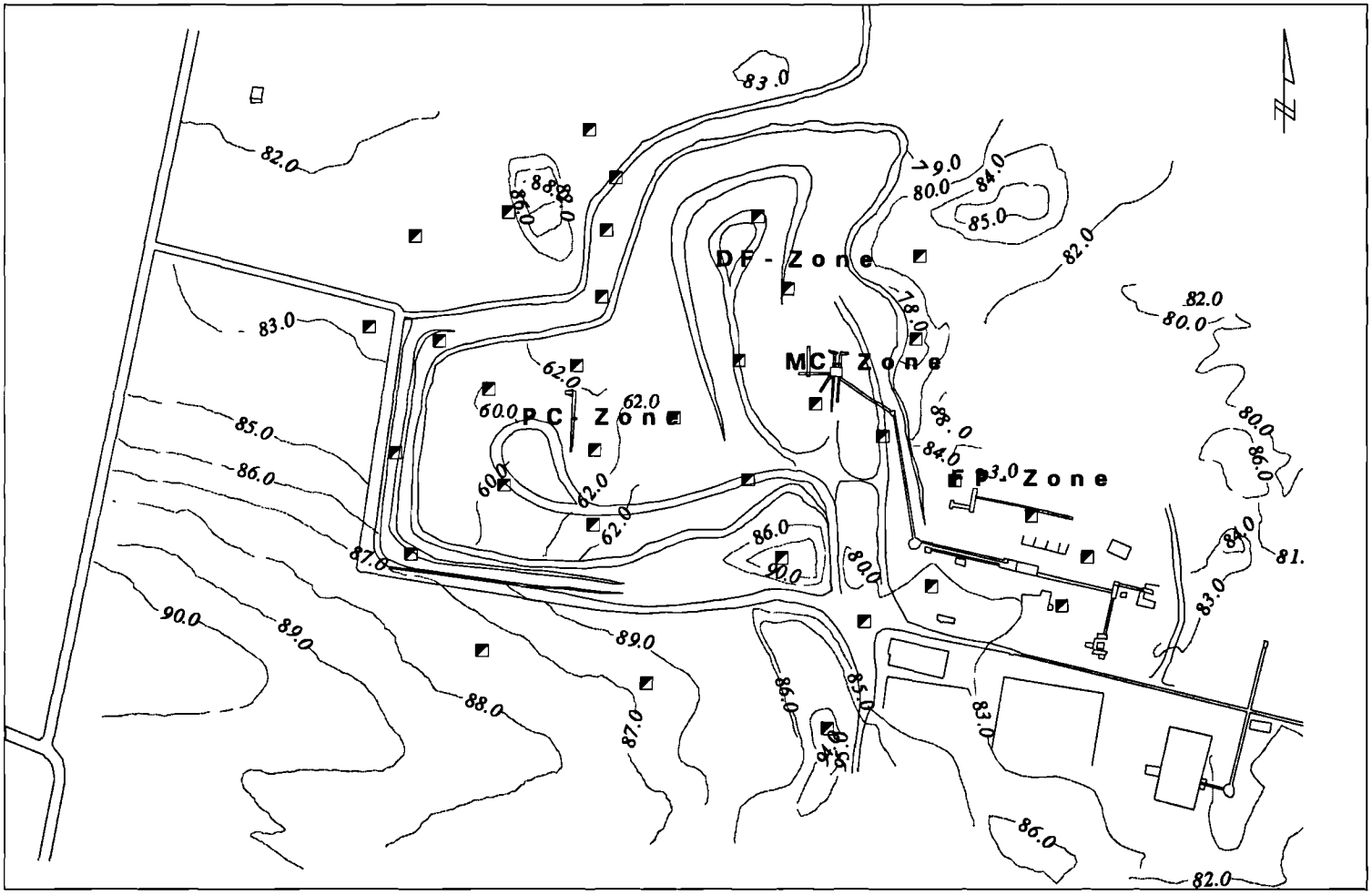


Figure 4.14 Surface plan of the limestone quarry.



Plate4.1 Working conditions at the limestone quarry



Plate 4.2 View of the surface plants of the limestone quarry.

activities measured at a distance of 10 m from the source. Figure 4.15 shows examples of SPL spectrum recorded for a 35 T dump truck by the instrument. Continuous monitoring of sound pressure levels in the quarry revealed that:

- The highest sound pressure levels were at a frequency of 125 kHz for all the activities.
- The movements of FEL without load and the trucks gave the highest sound pressure levels at low frequencies. FEL moving with empty bucket yields a sound pressure level of 66.7 decibels whereas a loaded truck causes 62.2 decibels at a frequency of 8 Hz.
- The highest A-weighted noise levels were obtained during dressing of the face with the FEL.

The internationally favoured descriptor of environmental noise is the A-weighted equivalent continuous sound pressure level expressed as dBA. It is the steady-state sound that has the same A-weighted level as that of the time-varying sound energy over the specified time interval and is calculated as:

$$L_{eq} = 10\log\left(\frac{1}{T}\int_0^T 10^{0.1L_{pi}}\,dt\right) \tag{4.16}$$

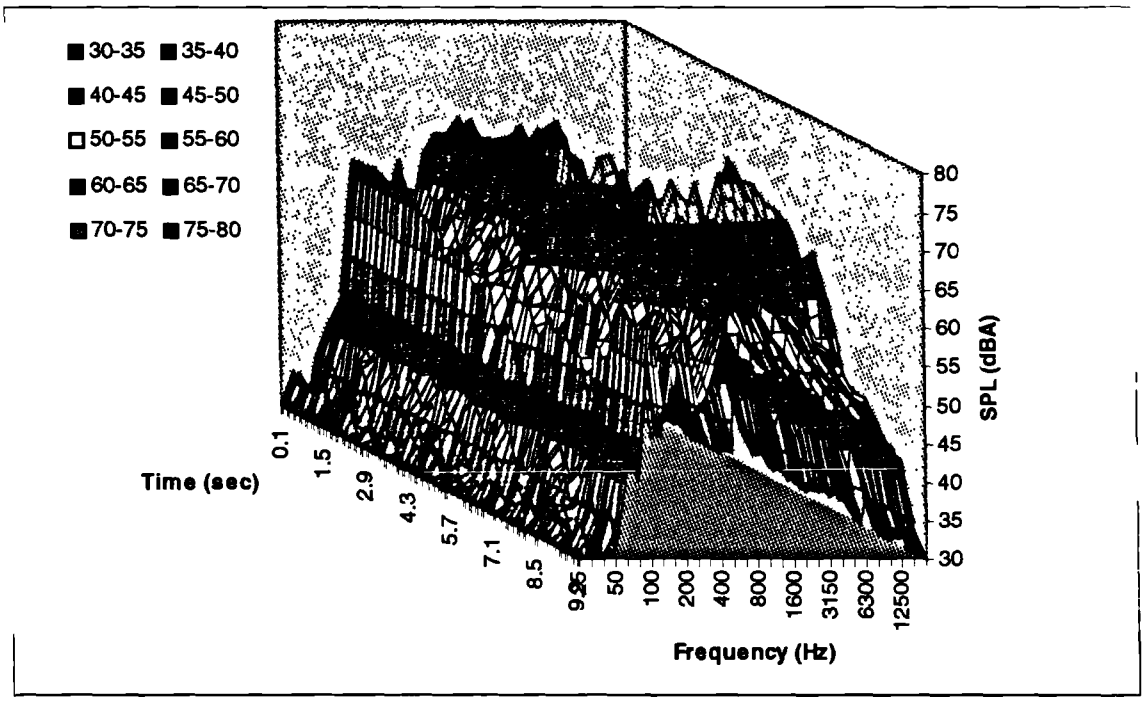
Where,

L_{pi}: sound pressure level of ith duration of length dt, dBA
T : total duration of noise exposure, min

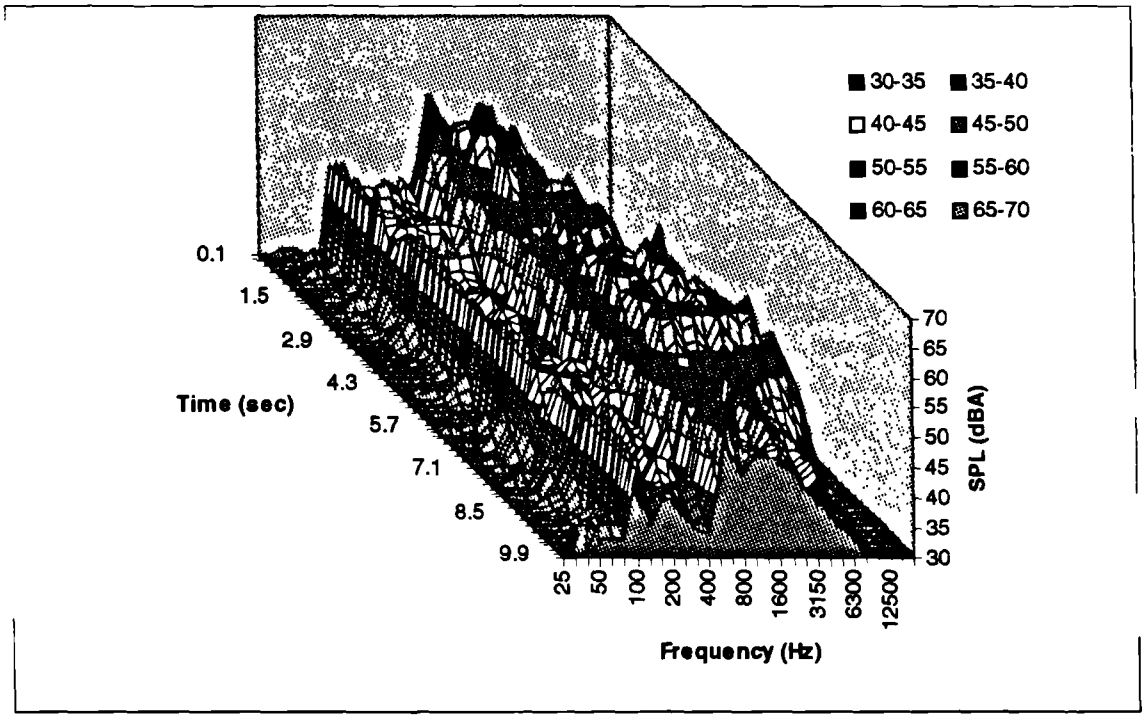
The experimental measurements provided the noise levels for various activities associated with an hour of steady state operation of the FEL-dump truck combination. Table 4.8 shows the A-weighted sound pressure levels of these activities and their corresponding duration.

Table 4.8 A-weighted sound pressure levels and the duration of various activities of FEL and dump truck.

Id	Activity	Duration (min)	SPL (dBA)
Act:1	FEL loading on to the truck	13.3	79.2
Act:2	FEL moving with load	13.3	80.1
Act:3	FEL moving with empty bucket	10.0	81.6
Act:4	Truck moving in the work zone with load	1.2	87.8
Act:5	Truck moving in the work zone without load	0.8	89.8
Act:6	FEL dressing the face	5.3	97.4
Act:7	FEL filling its bucket	6.7	83.2
Act:8	Truck is idling in the work zone	9.4	82.4



(a)



(b)

Figure 4.15 SPL spectrum of 35T RD dump truck (a) being loaded by hydraulic shovel (b) moving with load on level ground (recorded by Larson Davis RTA 2900).

The operating parameters associated with the above observations were:

- The length of haul road between the face and the main in-pit-crusher is 500 m.
- The average speed of the truck is 20 $kmhr^{-1}$.
- The number of trucks working is 2 and serving FEL is 1.
- The Cat 988B wheel loader is of heaped capacity 5.0 m^3.
- The blasting is of average quality and the bucket fill factor is 0.85.
- The production rate is 125 m^3hr^{-1}.

The working face of the quarry was in an isolated area. Therefore, the monitored sound pressure level for an activity represents the sound pressure level due to that particular activity at any point within the working zone. The production requirement and haulage specifications determine the average number of trucks loaded per hour in the work site. In the test quarry the FEL had to load eight trucks per hour. The number of passes to fill a truck was 5. These figures prescribe the duration of different activities. Thus, Equation 4.16 can calculate the noise level in the near field of the quarry. The value will be the noise level for one hour steady state operation of the quarry expressed as equivalent continuous sound pressure level. This was measured as 87.97 dBA in the test quarry.

Sound Power Levels of Activities

In the Activity Accounting Technique it is necessary to determine the sound power level of the activities within a work zone. If the frequency spectra of the generated noise is known then the frequency content of the noise at a receiver location can also be determined. The locations of various activities of the working zone during the steady state operation are necessary for determining the SPL spectra due to them. Table 4.9 presents the activity centres of the FEL and dump truck operation zone of the quarry during the study. The table also shows the locations of the monitoring stations for these activities. The equation to determine the sound power level at the activity centre is:

$$L_W = L_p + 20\log r + 11 \tag{4.17}$$

Where,

L_W : sound power level at a particular frequency

L_p : sound pressure level at a distance r in the free field distance

Table 4.9 Locations of activities and their monitoring stations.

Activities	Activity Centres			Monitoring Stations		
	X	Y	Z	X	Y	Z
FEL Loading on to the truck	586.78	192.46	48	596	192.46	46
FEL moving with load	596.17	164.30	47	606	164.30	46
FEL moving with empty bucket	600.86	164.30	47	610	164.30	46
Truck moving in the work zone with load	633.72	211.24	51	643	211.24	48
Truck moving in the work zone without load	591.47	211.24	51	601	211.24	48
FEL dressing the face	647.80	154.91	46	657	154.91	46
FEL filling its bucket	657.19	154.91	46	667	154.91	46
Truck is idling in the work zone	610.25	197.16	51	620	197.16	48

Table 4.10 shows the sound power levels at different frequencies for the various activities. Determination of the sound power spectra was based on the measured SPL spectra. Figure 4.16 shows the example of calculated sound power level spectra based on the SPL spectra measured by using the real time analyser (Larson Davis RTA 2900).

Table 4.10 Sound power levels (dB) of different activities for the octave frequencies.

Frequency	Act: 1	Act: 2	Act: 3	Act: 4	Act: 5	Act: 6	Act: 7	Act: 8
31.5	59.47	63.44	59.34	65.57	72.67	60.8	63.0	61.27
63.0	61.47	64.94	73.54	61.97	72.67	62.7	62.3	61.27
125.0	63.07	59.94	82.24	77.77	74.47	59.3	71.2	72.67
250.0	71.37	62.24	97.74	93.57	89.07	80.6	68.1	87.57
500.0	97.07	91.94	107.64	104.87	110.87	93.9	97.0	89.57
1000.0	107.27	113.64	108.74	106.27	109.47	112.6	109.8	110.37
2000.0	115.37	113.94	110.54	113.77	127.67	118.7	113.6	111.17
4000.0	108.87	119.34	115.94	125.07	130.77	118.9	123.4	121.57
8000.0	107.27	109.64	111.84	118.27	121.17	112.7	117.8	109.97

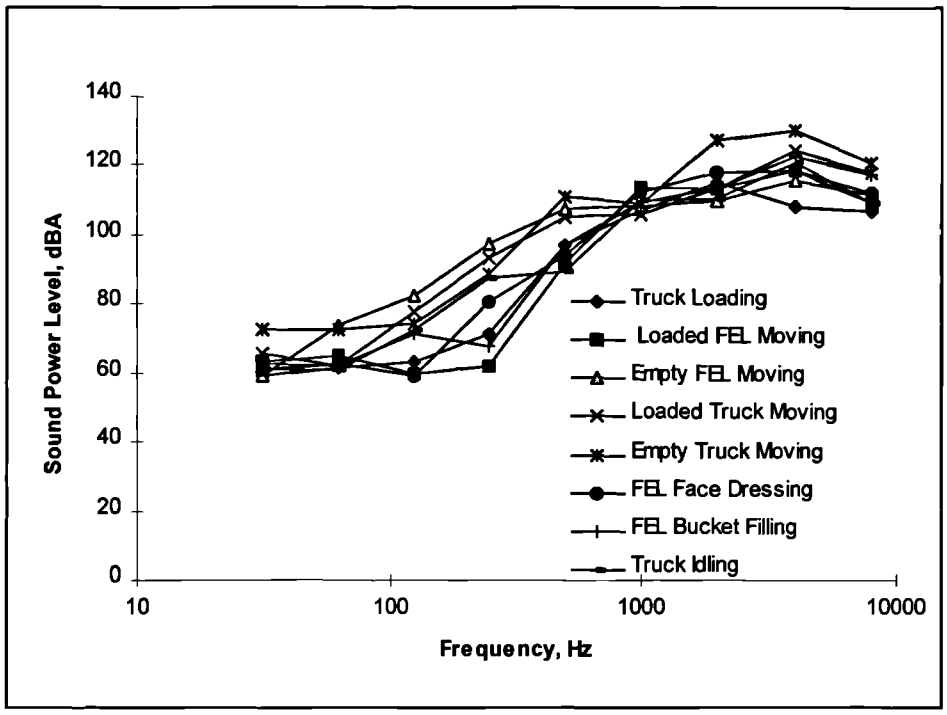


Figure 4.16 Sound power spectra of the activities of FEL and dump truck operation.

4.4 Conclusion

A new environmental noise prediction system has been developed for use in surface mining and quarrying operations. The system consists of four main models. The first of these, the source power model, has been developed using the principle of Equivalent Acoustic Centre. The surface mining and quarrying operations are grouped into work zones and the equivalent acoustic centre of each zone is determined. The source power model determines the location, sound power level and directivity of the EAC. Three complementary techniques have been developed and implemented in the development of the source power model for this purpose, namely the Experimental Measurement Technique (EMT), the Acoustic Database Technique (ADT) and the Activity Accounting Technique (AAT). The experimental technique was developed and tested by experiments conducted at the processing plant of Tara Mines in the Republic of Ireland. The results show that this concept is applicable for determining the sound power level of complex noise zones comprising of number of noise generating operations. The techniques have been coded in C++. The Acoustic Database Technique was developed for use in mining in the design and planning stage of mine operation. However, in the

absence of an established and reliable database this has not been tested experimentally. It is envisaged that future work for designing and the development of a database will make use of this technique more widespread. Limited experiments were carried out to test the Activity Accounting Technique and sound power level of the quarrying activities involving operations of Front End Loader and Dump Trucks were established. Noise signatures of various activities in the pit were studied during these experiments (see Appendix 2). These were not used in the present modelling as these signatures will have to be further verified with more experiments The results of the experimental measurement techniques of the noise source characterisation model will be used to test the prediction model and will be further discussed in Chapter 8.

The noise prediction system needs to consider various attenuation of the noise energy during propagation for estimating far field noise levels near surface mines and quarries. Absorption of sound energy by ground and air, and noise reducing effects of the pit-walls are the important factors affecting the far field noise levels. These factors are discussed in the following Chapter.

Chapter 5

The Development of a Ground Attenuation Model

5.1 Introduction

The development of a model to determine the sound power level of a work zone in a quarry or a surface mine was described in the last chapter. The second important element in a noise prediction system is the attenuation model. The objective of this model is to determine the loss of sound energy during propagation so that the sound pressure level at a location near the mine can be evaluated. As described in Chapter 3, ground absorption, air absorption and barrier effects of pit walls are the major causes of attenuation to the noise level in a surface mining environment.

Sound waves generated by the noise sources are modified during propagation from the source to the receiver. The nature of this modification is influenced by acoustic phenomenon such as reflection, refraction and scattering over the underlying ground and

behaviour of the air medium under the prevailing meteorological conditions. Moreover, the noise received by a receiver at any location depends on the effects of on site constructions acting as a noise barrier. In the case of surface mines and quarries, the noise sources are normally located within the pit. Therefore, the pit walls act as a barrier between the source and the receiver. This induces a reduction of sound energy during propagation. The attenuation models developed for the noise prediction system in this research have considered the ground effects, the atmospheric effects and pit-wall effects.

Sound propagation over ground surfaces has been studied theoretically and experimentally by number of researchers (De Jong *et al*, 1983; Rasmussen, 1982a, 1982b). However, these studies were not directed to implement in mining conditions. Moreover, mine planning and design had hardly considered environmental noise prediction as a necessity in the past. As a result, not much work on the effects of the ground surface on the propagation of mining noise is available. A theoretical model to account for ground attenuation over mining terrain can be developed based on the available acoustic principles. However, such a model requires site specific input data such as the flow resistivity of the ground surface near mining area. Unfortunately, sufficient information is not available in this respect. Therefore, to validate any theoretical model of ground attenuation the flow resistivity of the prevailing ground surface must be determined by experiments.

This chapter describes the model developed in the present research to evaluate the attenuation of sound energy due to ground effects. The development of the model was carried out in two phases. First, the theories of acoustics describing this phenomenon were studied. Based on the general theory, software was developed to evaluate the attenuation. One of the input parameters of this model is the flow resistivity of the ground surface. Due to the absence of sufficient knowledge, the flow resistivity of mining terrain had to be determined experimentally in the present research. The second phase of the model development was to carry out field experiments to test the validity of the theoretically evaluated attenuation, implementing if necessary the required changes to the models. The results obtained are then provided to the noise prediction system that

will be discussed in Chapter 8. Attenuation due to air absorption and pit-walls will be described in Chapters 6 and 7 respectively.

5.2 Attenuation due to the Ground Surface

Ingard (1953) observed that the measured sound pressure levels within a certain distance from the source are less than the values predicted considering the geometric spreading and molecular absorption. This excess attenuation was attributed to turbulence. However, Delaney and Bazley (1970a) and Jonasson (1972a) proved that there is a significant influence of the nature of the ground surface on this excess attenuation. The ground surface behaves like an interface between air and ground media for the propagating sound wave. The sound absorbing properties of the ground surface were experimentally investigated by Dickinson and Doak (1970) and expressed in terms of normal acoustic impedance of the ground surface. They concluded from their experimental results that a granulated inorganic material behaves as a better sound absorbent in the presence of moisture. On the other hand, organic materials absorb more acoustic energy in the absence of moisture. This was proved that for a grass-covered area the normal absorption coefficient varies within 0.45 - 0.10 as frequency changes from 1 kHz to 200 Hz. Frost increases this range to 0.28 - 0.2 and rain causes a reduction from 0.28 to 0.04. The degree of sound-field modification near the ground-atmosphere boundary depends on the acoustic impedance and propagation constant. When both the source and the receiver are located near to the ground the influence of ground impedance becomes more significant. Under this condition the reflection of acoustic waves from the ground results in a specific interference pattern in the total sound field depending on the specific characteristics of the ground (Hess *et al*, 1989). The characteristics of the absorbent materials and their effects on sound attenuation were studied by Delaney and Bazley (1970b), considering plane waves and a point source. Chessel (1976) analysed these for spherical waves from a point source. All these studies characterised acoustical properties of the ground in terms of the single parameter, the effective flow resistivity (σ). Flow resistivity of the ground surface is defined as the flow resistance per unit thickness, i.e. the ratio of the pressure drop across a sample of material to the linear air velocity through it. Attenborough (1982, 1988)

developed a multi-parameter model to account for the ground effects. The four parameters used for characterising acoustical properties of a homogeneous rigid framed porous medium are:

- Porosity of the air filled pores connected with soil surfaces, Ω.
- Pore factor, *sp*
- Flow resistivity, σ
- Tortuosity, T of the pores defined as:

$$T = \Omega^{-n} \tag{5.1}$$

Where,
n: grain shape factor

This four-parameter approach of determining acoustic impedance of a material for evaluating absorption of sound energy is more suitable for the design of noise control systems. In the present work however, the single parameter model specified by flow resistivity of ground surface was used. This method was chosen as it was seen from the work of Isei *et al* (1980) that such an approach achieved a good correlation between the theoretical and experimental results in analysing the performance of noise barriers together with the effects of the ground surface.

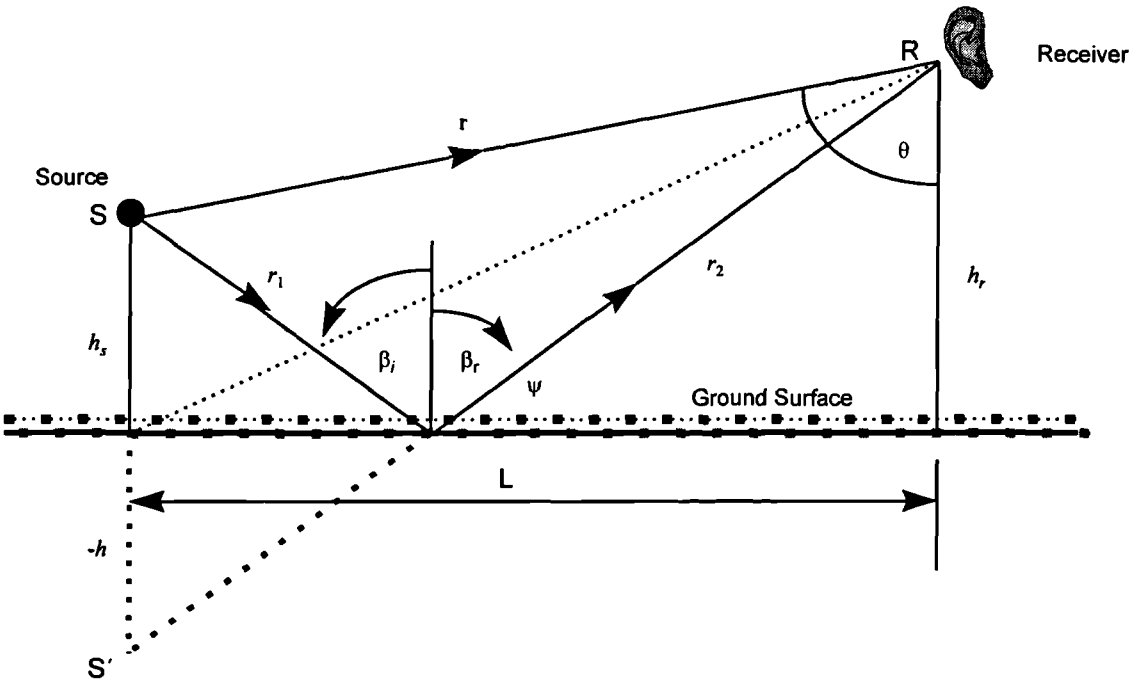


Figure 5.1 Combination of reflected and direct sounds at the receiver's location.

5.2.1 Acoustic Phenomena over the Ground Surface

Figure 5.1 shows the simplest phenomena that occur when there is a noise source at a height of h_s from the ground surface. The receiver is located at a horizontal distance of L from the source and it is at a height of h_r from the ground surface. The direct distance of separation of the source and the receiver is r as shown in the figure. The total sound level at the receiver is the combination of sounds from the direct source, S and the reflections from an image source, S'.

The ratios of h, r and h_s are important for estimating the effects of the phenomena at the interface. The sound level at the receiver will be an incoherent combination of the direct and reflected levels. The direct and the reflected sound appears at random phases. The direct source and its image source are incoherent sources by definition. They combine together on a linear energy (pressure square) basis. Let L_{pd} and L_{pr} be the sound pressure levels in decibels due to direct and reflected waves respectively. The corresponding root-mean square pressures in Pascals are:

$$\begin{aligned} \langle p_d^2 \rangle &= p_{ref}^2 10^{0.1 L_{pd}} \\ \langle p_r^2 \rangle &= p_{ref}^2 10^{0.1 L_{pr}} \end{aligned} \tag{5.2}$$

where,

p_d : root-mean square pressure due to the direct wave
P_r : root-mean square pressure due to the reflected wave
P_{ref} : reference pressure, 2×10^{-5} Pa

Total mean square sound pressure, p_t is given as:

$$\langle p_t^2 \rangle = \langle p_d^2 \rangle + \langle p_r^2 \rangle \tag{5.3}$$

This gives,

$$L_{pt} = 10 \log \left(\frac{\langle p_t^2 \rangle}{p_{ref}^2} \right) \tag{5.4}$$

where,

L_{pt}: total sound pressure level at the receiver's location, dB

The direct and the reflected sound waves having complex pressure amplitudes P_d and P_r give the following reflection coefficient, R:

$$R = \frac{P_r}{P_d} \tag{5.5}$$

This reflection coefficient depends on the *angle of incidence*, β and the *characteristic acoustic impedance* of air and the ground. Transmission of an incident sound wave into the solid medium determines the nature of the reflected wave in the case of air-to-solid incidence. The nature of the transmitted wave depends on the *porosity* and *internal elastic structure* of the solid. These two material properties vary widely with the rock types. Within the same rock type, their values change with the change of physical state at different phases of mining. Therefore, in a surface mining site the nature of the acoustic wave transmitted into the rock mass will vary widely.

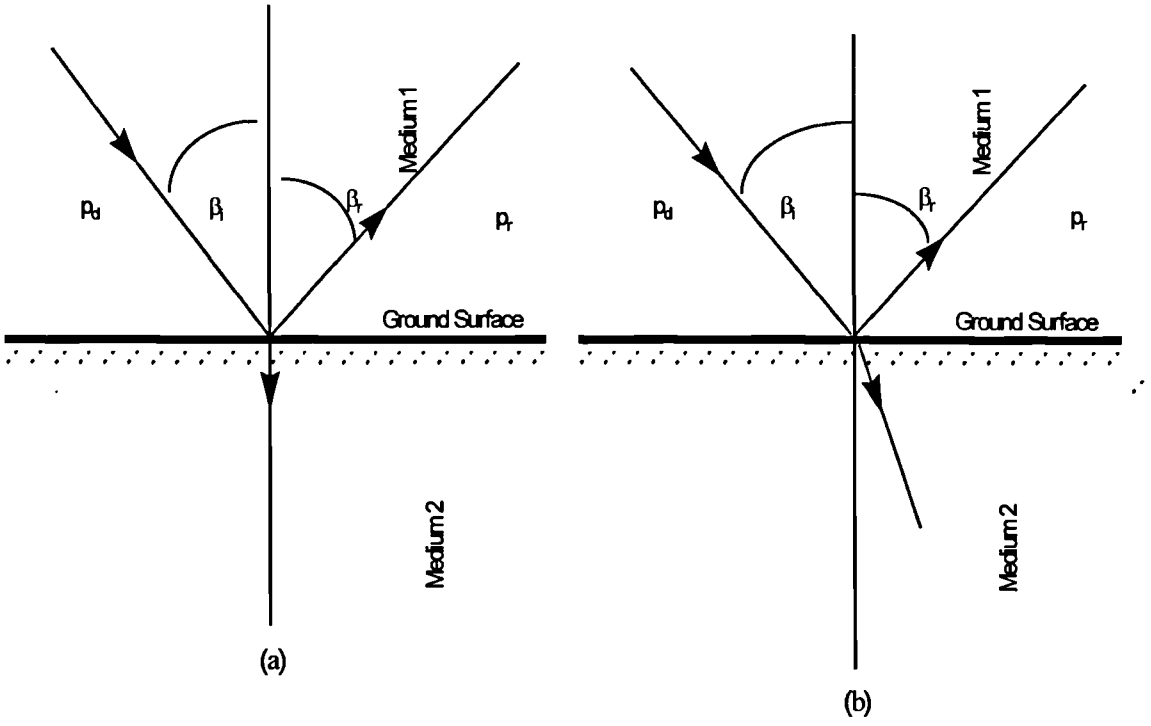


Figure 5.2 Reflection of an acoustic wave.

The wave transmission into the rock may take place in two ways. Firstly, it may propagate effectively only in a direction perpendicular to the surface (Figure 5.2a). Secondly, it may make an angle with the normal similar to a plane wave entering into a second fluid (Figure 5.2b). In the case of refraction in rigid elastic solids the wave splits into two waves. One is the longitudinal bulk wave travelling in one direction and the other is the transverse shear wave travelling at a lower speed and in a different direction.

There are two types of surfaces of anisotropic solids: normally reacting and locally acting. Acoustic waves propagating parallel to such surfaces travel with a much lower speed than those propagating perpendicular to the surface. This is typical of solids having a honeycomb structure. Such solids contain fluids in the capillary pores within the structure. The orientation of some capillary pores is at a right angle to the surface. The speed of compression waves passing through the fluids of such pores is much higher. The other path of propagation of compression waves is through the pore walls. In this case, the speed of propagation through the solid material of the structure is much lower.

5.2.2 Reflected Acoustic Waves on an Air-Solid Interface

Ground surface can be assumed to be a locally reactive medium (Malecki, 1969). This infers that the wave in the ground medium can propagate only in the direction normal to the boundary surface (Figure 5.3a). In such surfaces the refracted rays travel nearly perpendicularly to the surface, irrespective of the particular angle of incidence. The ratio of acoustic pressures to the normal component of air particle velocity is independent of the angle of incidence, i.e. it does not depend on the direction of the incident wave.

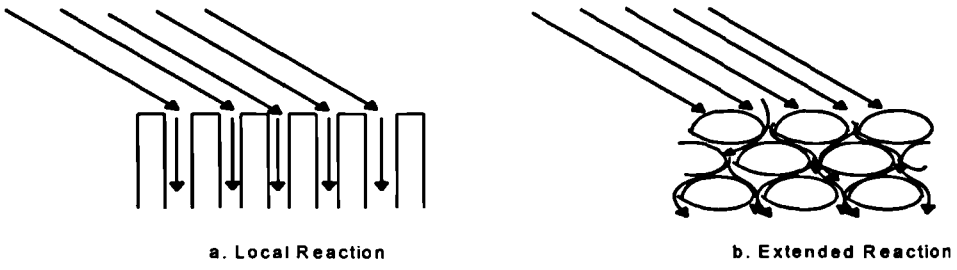


Figure 5.3 Behaviour of acoustic waves at ground surface: a. Local reaction, b. Extended reaction.

The behaviour of an acoustic wave in the fluid media is expressed in terms of specific normal acoustic impedance, Z_n. This is defined as the complex ratio of the acoustic pressure at the ground surface to the resulting normal component of particle velocity into the ground. Mathematically:

$$Z_n = \frac{p}{\vec{u}.\hat{n}} \tag{5.6}$$

where,

p : acoustic pressure
$\vec{u}$: particle velocity
$\hat{n}$: unit vector perpendicular to the interface

The acoustic pressure is not always in phase with the particle velocity at the solid-surface. Therefore, the normal specific acoustic impedance becomes a complex quantity. One can express it as:

$$Z_n = r_n + jx_n \tag{5.7}$$

Here,

r_n : the resistive component
x_n : the reactive component

For the reflection phenomenon at the air-solid boundary the following boundary conditions are important:

- The acoustic pressures on both sides of the boundary are equal. This condition of continuity of pressure means that there can be no net force on the plane separating the two media.
- The particle velocities normal to the boundary are equal. This condition of the continuity of the normal velocity requires that the fluid remains in contact.

Thus, the pressure and normal particle velocity in medium 1 are ($p_i + p_r$) and $(u_i + u_r)\hat{x}$ so that the two boundary conditions are:

$$\begin{gathered} p_i + p_r = p_t, \text{ at } x = 0 \\ \text{and} \\ u_i + u_r = u_t, \text{ at } x = 0 \end{gathered} \tag{5.8}$$

where,

u_i : particle velocity due to the incident ray
u_r : particle velocity due to the reflected ray

The above equation gives the condition of continuity for normal specific acoustic impedance across the boundary as:

$$\frac{p_i + p_r}{u_i + u_r} = \frac{p_t}{p_u} \tag{5.9}$$

Figure 5.4 shows the other case of oblique incidence shown in Figure 2b. Highly porous ground behaves like this. The condition that the normal component of the particle velocity at the boundary should be continuous can be expressed as:

$$u_i \cos\beta_i + u_r \cos\beta_r = u_t \tag{5.10}$$

where,

β_i : incident angle
β_r : reflected angle

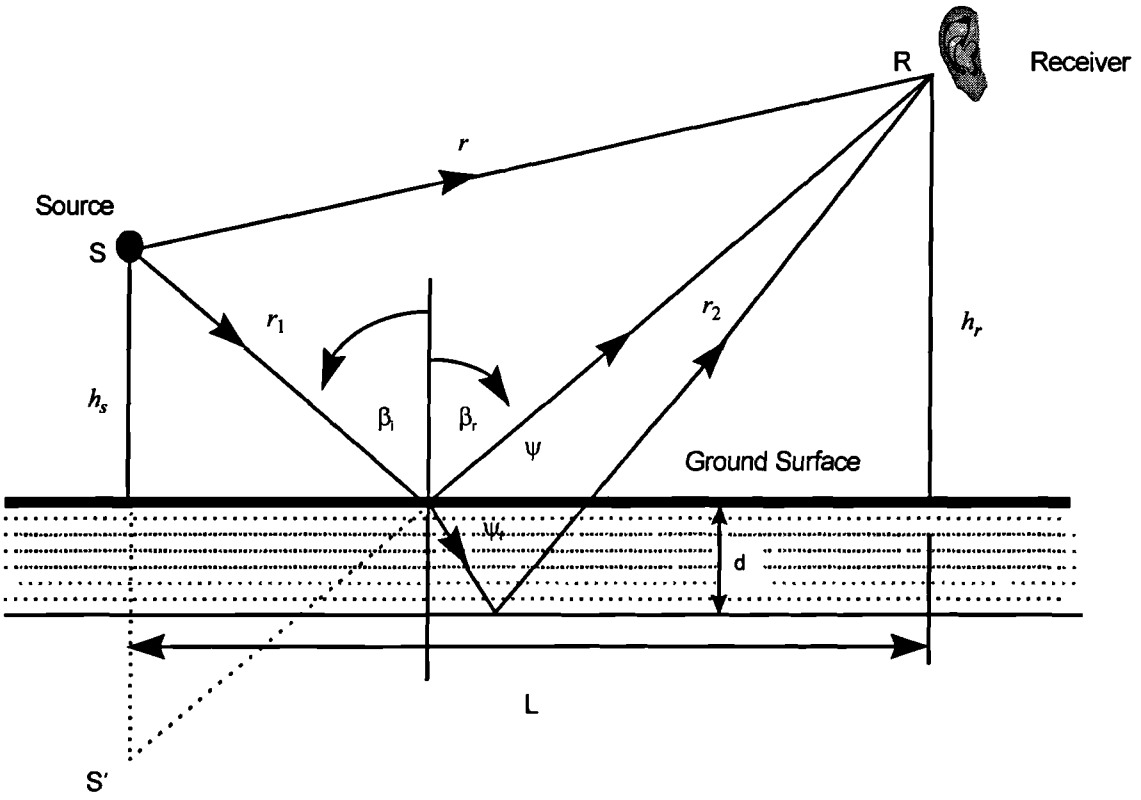


Figure 5.4 Refraction of a sound ray at the interface of ground and the atmosphere.

Therefore, the condition of continuity of the normal specific impedance applied at the ground surface is:

$$Z_n = \frac{p_i + p_r}{u_i \cos\beta_i + u_r \cos\beta_r} \tag{5.11}$$

Now, the characteristic acoustic impedance of the fluid media, Z is:

$$Z = \frac{p_i}{u_i} = \frac{p_r}{u_r} \tag{5.12}$$

Considering the direction of u_i and u_r to be opposite, it is derived that:

$$Z\frac{p_i + p_r}{p_i - p_r} = Z_n \cos\beta_i \tag{5.13}$$

The coefficient of reflection, R is:

$$R = \frac{p_r}{p_i} \tag{5.14}$$

Thus,

$$\begin{aligned} Z\frac{1+R}{1-R} &= Z_n \cos\beta_i \\ \Rightarrow R &= \frac{Z_n \cos\beta - Z}{Z_n \cos\beta + Z} \end{aligned} \tag{5.15}$$

where, $Z = \rho_o c$ is the specific acoustic impedance of air.

Considering grazing angle, ψ, one determines R for the case of local reaction (Ingard, 1951) as:

$$R = \frac{\sin\psi - \dfrac{Z}{Z_n}}{\sin\psi + \dfrac{Z}{Z_n}} \tag{5.16}$$

The density of air, ρ_o at 20° C is 1.21 kgm^{-3} and the speed of sound, c, at that temperature is 344 ms^{-1}. Thus, it is essential to evaluate the reflection coefficient R to

determine the normal specific acoustic impedance or characteristic impedance of the ground. For a perfectly reflecting hard surface R is equal to 1. This will be the case when Z_n is infinity or very large and thus the ratio of Z and Z_n is negligible. On the other hand, if the grazing angle ψ is very small such that ($\sin\psi$) is much less than Z/Z_n, then the coefficient of reflection R will be -1. This means a phase change of 180° after reflection and a cancellation of incident and reflected waves takes place.

If the refracted ray makes an angle ψ_t with the horizontal ground surface as shown in Figure 5.4, the pressure reflection coefficient R_p is given as (Chessel, 1976):

$$R_p = \frac{Z_2 \sin\psi - Z_1 \sin\psi_t}{Z_2 \sin\psi + Z_1 \sin\psi_t} \tag{5.17}$$

The relation between the incident angle ψ and refracted angle ψ_t is:

$$k_2 \cos\psi_t = k_1 \cos\psi \tag{5.18}$$

Where k_1 and k_2 are the propagation coefficients in the two media. Therefore,

$$\sin\psi_t = (1-\cos^2\psi_t)^{0.5} = \left(1-\frac{k_1^2}{k_2^2}\cos^2\psi\right)^{0.5} \tag{5.19}$$

Then the reflection coefficient for plane wave is:

$$R_p = \frac{\sin\psi - \frac{Z_1}{Z_2}\left(1-\frac{k_1^2}{k_2^2}\cos^2\psi\right)^{0.5}}{\sin\psi + \frac{Z_1}{Z_2}\left(1-\frac{k_1^2}{k_2^2}\cos^2\psi\right)^{0.5}} \tag{5.20}$$

Rudnick (1947) used this equation for semi-infinite or extended media and obtained good correlation between experimental and theoretical results.

Let the refracted ray meet a harder surface at a depth of d (Figure 5.4). The acoustic impedance for this situation is different from Z_2. The thickness of the porous layer

influences the impedance. The following equation gives the new impedance in such cases (Nicolas and Berry, 1984):

$$R_p = \frac{\sin\psi - Z_1/Z_2(d)}{\sin\psi + Z_1/Z_2(d)} \tag{5.21}$$

$$Z(d) = \frac{Z_1}{\cos\psi_t}\coth\left(-ik_2 d\cos\psi_t\right) \tag{5.22}$$

where,

$$\cos\psi_t = \left(1-\left(\frac{k_1}{k_2}\right)^2\cos^2\psi\right)^{0.5} \tag{5.23}$$

Figures 5.1 and 5.4 show sound propagating over flat ground. It is assumed that the atmosphere is non-refracting. However, in real-life there may be situations of curvature of the ray path due to meteorological conditions and the ground surface may not be flat. In surface mining, there may be occasions of a receiver being located at up- or down-gradient. These probable cases of outdoor propagation of noise over ground surfaces are shown in Figure 5.5.

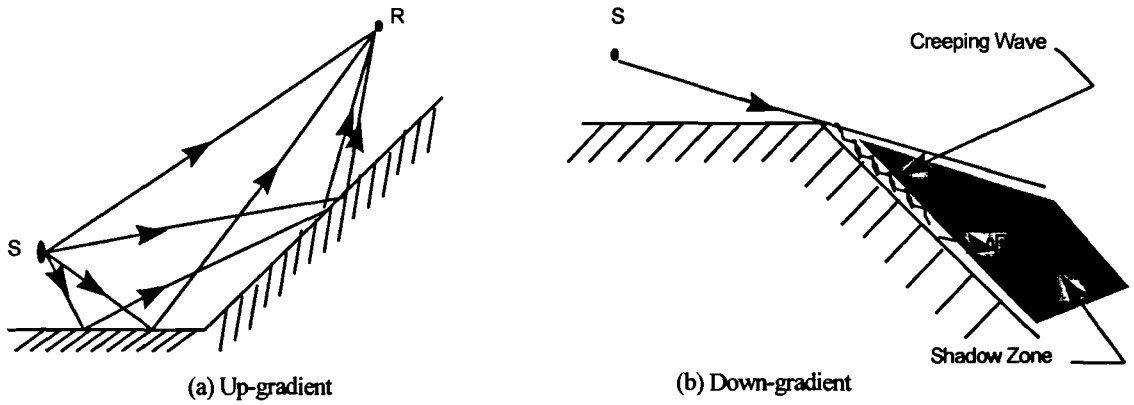


Figure 5.5 Effect of terrain conditions over outdoor noise propagation.

The down-gradient case will have to be considered while developing a model for noise propagation in hilltop mining. This aspect is not studied in the present research. The up-

gradient case is considered while determining the effect of pit walls as noise barriers in surface mining operations. This is described Chapter 7.

5.2.3 Characteristic Impedance of the Ground

Equations 5.20 and 5.21 show that the coefficient of reflection depends on the characteristic acoustic impedance of the ground. However, there is no simple method to determine the characteristic acoustic impedance of the ground surface. The elaborate experiments conducted by Delaney and Bazely (1970b) to measure the acoustic properties of various fibrous absorbent materials had indicated that the characteristic impedance of a porous solid depends on the *frequency* of the sound wave and *flow resistivity* of the material.

A bulk porous material can be considered to be of open cell structure. A constant differential pressure across such a material induces a steady flow of gas through it. The flow resistance, R_f(MKS rayls) of a material is the ratio of differential pressure (Pa) to the normal velocity (ms^{-1}). Flow resistivity of the materials of uniform composition is the flow resistance per unit material thickness. It is a characteristic property with units of MKS rayls per metre. Established values of flow resistivity of typical ground surfaces are shown in Table 5.1 (Bies and Hansen, 1980, Embleton *et al*, 1983).

Table 5.1 Values of flow resistivity for typical ground surfaces (after Embleton *et al*, 1983).

Ground Surface	Flow Resistivity MKS rayls m^{-1}(Min.)	Flow Resistivity MKS rayls m^{-1} (Max.)
Forest area; pine or hemlock	2×10^4	8×10^4
Grass	1.5×10^5	3×10^5
Roadside dirt, small rocks (<0.1 m mesh)	3×10^5	8×10^5
Sandy silt, hard packed by vehicles	8×10^5	2.5×10^6
Thick layer of limestone chips (0.01m-0.025m mesh)	1.5×10^6	4×10^6
Earth, exposed and rain packed	4×10^6	8×10^6
Quarry dust, fine and hard packed by vehicles	5×10^6	2×10^7

The characteristic acoustic impedance, Z, and propagation constant, k, are two complex quantities affecting the coefficient of reflection. They are expressed as:

$$Z = R + iX \tag{5.24}$$

$$k = a + ib \tag{5.25}$$

The experimentally determined power-law relations give the terms of the above equations. These terms are functions of the ratio of frequency and specific flow resistance per unit thickness. The established relations are (Isei, 1980):

$$\begin{aligned} \frac{R}{\rho_1 c_1} &= 1 + 9.08\left(\frac{f}{\sigma}\right)^{-0.75} \\ \frac{X}{\rho_1 c_1} &= 11.90\left(\frac{f}{\sigma}\right)^{-0.73} \end{aligned} \tag{5.26}$$

and

$$\begin{aligned} \frac{\alpha}{\omega/c_1} &= 1 + 10.8\left(\frac{f}{\sigma}\right)^{-0.70} \\ \frac{\beta}{\omega/c_1} &= 10.3\left(\frac{f}{\sigma}\right)^{-0.59} \end{aligned} \tag{5.27}$$

Thus, Equations 5.24, 5.25, 5.26 and 5.27 give an indirect method for the determination of the acoustic impedance and propagation constant of ground surface.

Bies and Hansen (1988) developed a procedure for the calculation of the complex characteristic impedance of the ground, Z_n. Following the Delaney-Bazely model they defined a parameter X as the ratio of the product of density of air, ρ_o, and speed of sound, c to the flow resistivity of ground. Mathematically,

$$X = \frac{\rho_o f}{R_l} \tag{5.28}$$

The resulting expression, validated for the flow resistivity range of 10^3 to 5×10^4 is:

$$Z_n = \rho_o c\left[1 + 0.057X^{-0.754} - i0.087X^{-0.732}\right] \tag{5.29}$$

Sutherland (1994) suggested the following equations for the determination of the characteristic acoustic impedance, Z_c, of porous media:

$$Z_c = \left[1 + a\left(f/\sigma\right)^b\right] + i.\left[c\left(f/\sigma\right)^d\right] \tag{5.30}$$

$$ik = -\frac{2\pi f}{c}\left[\left[p\left(f/\sigma\right)^r\right] + i.\left[q\left(f/\sigma\right)^s\right]\right] \tag{5.31}$$

The values of the constants in the above equations are reported by various authors as shown in Table 5.2.

Sutherland (1994) suggested the following relations amongst the constants:

$$b = d, \qquad c = a\tan\left[b.p/2\right], \qquad -1 < b < 0 \tag{5.32}$$

$$r = s, \quad p = -q\tan\left[r.p/2\right] \tag{5.33}$$

Table 5.2 Acoustic impedance and propagation constants to be used in Equations 5.30 and 5.31.

Author	a	b	c	d	p	q	r	s
Delaney and Bazley (1970)	0.0511	-0.750	0.0768	-0.730	0.175	0.0858	-0.590	-0.700
Miki (1990)	0.0700	-0.632	0.1070	-0.632	0.160	0.0858	-0.618	-0.618
Sutherland (1994)	0.1340	-0.553	0.0453	-0.836				

Bies and Hansen (1988) calculated the complex propagation constant, k:

$$k = \left(\frac{\omega}{c}\right)\left[1 + 0.0978X^{-0.700} - i0.189X^{-0.595}\right] \tag{5.34}$$

Chessel (1976), Isei (1980), Hasabe and Kaneyasu (1987) considered the ratio of propagation constants in the two media under consideration as:

$$\frac{k_2}{k_1} = \left\{1 + 10.8\left(\frac{f}{s}\right)^{-0.70}\right\} + i10.3\left(\frac{f}{s}\right)^{-0.59} \tag{5.35}$$

The acoustic impedance of a ground surface can be determined experimentally either by the Close Impedance Tube Method (Embelton *et al*, 1976) or by Microphone Arrays. In the first method, ground impedance is measured directly by using a closed impedance tube over the ground surface. In the second method the vertical, horizontal or inclined arrays of microphones are used to measure the sound pressure levels of the sound wave reflected by the ground surface. Readers may refer to Dickinson and Doak, (1970) for the method of calculating acoustic impedance directly from the standing wave ratios or to Daigle and Stinson (1987) for a phase difference technique to determine ground impedance by sound measurements. The latter method needs elaborate experimentation and therefore it is only justified to apply this method where critical evaluation of the ground absorption is necessary. For the purpose of environmental impact prediction of mining noise the author has followed the method of acoustical measurements (Isei, 1980; Embelton *et al*, 1983; Hess *et al*, 1989). Readers may refer to Attenborough (1985) for a similar method of indirect assessment of ground impedance.

For the ground surfaces available in the mining environment the values of ground impedance have not yet been established. The present work has applied the indirect method to determine excess attenuation of ground absorption by determining acoustic impedance in the field and by evaluating the theoretical and experimental curves obtained.

5.2.4 Evaluation of the Sound Field over a Ground Surface

Referring to Figure 5.4 the acoustic field at the receiver can be expressed as:

$$\phi_R = \phi_d + \phi_r + \phi_g \tag{5.36}$$

Here, ϕ_d, ϕ_r and ϕ_g are the contributions from the direct, reflected and diffracted field respectively.

As shown in the figure, the receiver receives a portion of the diffracted wave. This is the contribution of the so-called ground wave. The acoustic field at a distance from the source can be expressed as the summation of waves originating from the source and an

image source with specific source strengths. The source strength is a function of the reflection coefficient and an additional parameter. This additional parameter is called the numerical distance. This parameter is a function of normal impedance and the position of the receiver and it varies with frequency.

Thus the sound field at the location of the receiver is expressed as:

$$\phi_R = \frac{Ae^{ikSR}}{SR} + R\frac{Ae^{ikTR}}{TR} + (1-R)F(w)\frac{Ae^{ikTR}}{TR} \tag{5.37}$$

where,

k : phase constant, $k = \frac{2\pi f}{c}$
R : reflection constant
SR : distances of the receiver from the source
TR : distances of the receiver from the image source
w : numerical distance
$F(w)$: function that takes the ground wave into account

Numerical distance, w is evaluated as a function of the propagation constants of the interfacing media, angle of incidence, specific acoustic impedance of the medium, and the locations of the source and receiver with respect to the surface of interface. Table 5.3 presents a number of relationships proposed for the numerical distance.

The value of the function $F(w)$ is evaluated for two conditions. Without qualifying the term "small" Rudnick evaluated $F(w)$ for smaller w values as:

$$F(w) = 1 + i(\pi w)^{0.5} e^{-w} \times \left[w - \frac{w^2}{3 \cdot 1!} + \frac{w^3}{5 \cdot 2!} - \cdots \right] \tag{5.38}$$

For large values of w, $F(w)$ is expressed as:

$$F(w) = -\left[\frac{1}{2w} + \frac{1 \cdot 3}{(2w)^2} + \frac{1 \cdot 3 \cdot 5}{(2w)^3} \cdots \right] \tag{5.39}$$

Jonasson (1972a) pointed out that the last expression can be used for $|w| \geq 7$. However, for smaller absolute values of $F(w)$:

$$F(w) = 1 - ie^{-w}\sqrt{\pi w} - 2e^{-w}w\left(1 + \frac{w}{1!3} + \frac{w^2}{2!5} + \cdots\right) \tag{5.40}$$

Isei (1980) used a cut-off point of 10 for w to decide "small". In his work $F(w)$ was reported as:

1. For $|w| \leq 10$:

$$F(w) = 1 + i(\pi w)^{0.5}e^{-w} - 2we^{-w}\left[1 + \frac{w}{1!3} + \frac{w^2}{2!5} + \cdots\right] \tag{5.41}$$

2. For $|w| > 10$: Same as Rudnick's equation (5.49).

Table 5.3 The numerical relationship proposed for calculating the numerical distance.

Author	Expression for Numerical Distance, w
1. Rudnick (1947)	$w = i\frac{4kTR}{(1-R)^2}\left(\frac{Z_1}{Z_2}\right)^2\left(1 - \cos^2\phi_c\left(\frac{k_1}{k_2}\right)^2\right)$
2. Ingard (1957), Jonasson(1972)	$w = \frac{ikTR\left(\sin\phi_c + \frac{Z_1}{Z_2}\right)^2}{2\left(1 + \sin\phi_c\frac{Z_1}{Z_2}\right)}$
3. Brekhovskikh (1960)	$w^2 = ikTR\left(1 - \frac{\frac{k_2}{k_1}\cos\phi_c - \sin\phi_c}{\left(\frac{k_2^2}{k_1^2} + 1\right)^{0.5}}\right)$
4. Isei (1980)	$w = \frac{ik_1SR}{(1-R)^2\cos^2\phi_c}\left(\frac{Z_1}{Z_2}\right)^2\left\{1 - \left(\frac{k_1}{k_2}\right)^2\cos^{2c}\phi_c\right\}$

5.2.5 Excess Attenuation by Ground Absorption

Bies and Hansen (1988) determined the reflection loss A_r as:

$$A_r = -20\log|R| \tag{5.42}$$

Reflection from the ground surface reduces the energy level of the reflected wave. Thus, there occurs excess attenuation, A_g, due to the decrease in energy A_r. This excess attenuation is expressed as:

$$A_g = -10\log\left[1+10^{-0.1A_r}\right] \tag{5.43}$$

Noise quality at any location depends on the frequency spectra of sound pressure levels. Ground attenuation of acoustic wave is also a frequency dependent phenomenon. Therefore, to determine the frequency spectrum of the sound wave at a point, one needs to evaluate ground absorption at different frequencies.

The Weyl-Van der Pol solution (Lawland and Rudnick, 1951; Ingard, 1951; Bies and Hansen 1988) uses the value of k to determine sound pressure level, $p(r, r_1, r_2)$, at the receiver's position. The excess attenuation due to ground absorption is then calculated as:

$$A_{gi} = -20\log kr - 10\log\left|p(r,r_1,r_2)\right|^2 \tag{5.44}$$

where,

$$p(r,r_1,r_2) = \frac{e^{-ikr}}{kr} + R\frac{e^{-ik(r_1+r_2)}}{k(r_1+r_2)} + \left(1 - RG(w)\frac{e^{-ik(r_1+r_2)}}{k(r_1+r_2)}\right) \tag{5.45}$$

The amplitude factor $G(w)$ is given as:

$$\begin{aligned} G(w) &= 1 - i\pi^{0.5} w g(w) \\ w &= 0.5(1-i)\left[k(r_1-r_2)\right]^{0.5}\left[\rho c/Z + \sin\theta\right] \end{aligned} \tag{5.46}$$

for small w ($|w|<3$),

$$g(w)=e^{-w^2}-\left[\frac{2iw}{\sqrt{\pi}}\right]\sum_{n=0}^{\infty}\frac{\left(-2w^2\right)^n}{1\times 3\times\cdots\times(2n+1)} \tag{5.47}$$

For both real and imaginary parts of w greater than 6:

$$G(w)=-iw\left[\frac{0.5124242}{w^2-0.275255}+\frac{0.05176536}{w^2-2.724745}\right] \tag{5.48}$$

For values of w where the real part is greater than 3 and the imaginary part is greater than 2,

$$G(w)=-iw\left[\frac{0.4613135}{w^2-0.1901635}+\frac{0.09999216}{w^2-1.7844927}+\frac{0.002883894}{w^2-5.5253437}\right] \tag{5.49}$$

The excess attenuation A_g averaged over a one third or octave band is calculated by combining logarithmically the attenuation calculated at several different frequencies equally spaced throughout the band as:

$$A_g=-10\log_{10}\left[\frac{1}{n}\sum_{j=1}^{n}10^{-0.1A_{gj}}\right] \tag{5.50}$$

However, when compared to the results of specific experiments carried out by Isei *et al* (1980), the excess attenuation obtained by the above method deviated considerably from the experimental values.

5.3 The Development of the Ground Attenuation Model

The ratios of the propagation constants and the acoustic impedance of the interfacing media are to be determined in order to calculate the noise field at the receiver according to the theories mentioned above. In the absence of a direct method of determining these values most of the authors used the semi-empirical relationship given by Delaney and Bazley (1970b). In this method, these ratios are determined in terms of the flow resistivity of ground surface. Although some experimentally determined values of flow resistivity have been accepted for noise level prediction purposes, there is no agreement

between the previous researchers findings as to which values are representative of a mining case. The empirical relationships given by Delaney and Bazley are applicable within the interpolating range $10 \leq {}^{f}/_{\sigma} \leq 1000$, and may not always be valid in many real life situations in mining.

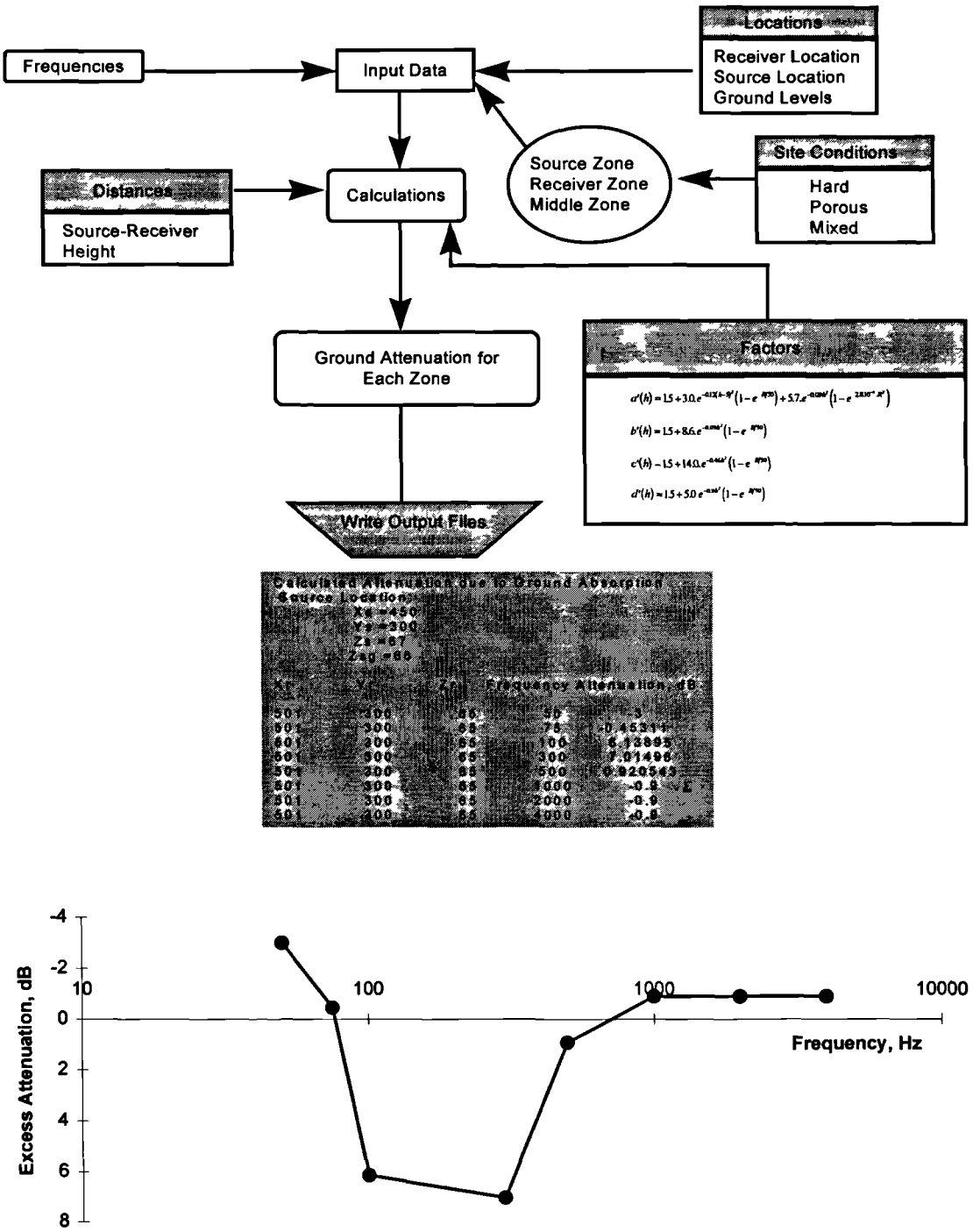


Figure 5.6 Program structure of the ISO method for determining attenuation due to the ground and a program output.

ISO 9613-2.2, 1994 describes a model for evaluation of ground attenuation considering the site conditions. This method depends on the evaluation of site characterising factors. However, to apply this method to mining areas these factors will have to be empirically determined. The author tested the method by developing some software (ATN_GRN.CPP) incorporating this method. Figure 5.6 shows the flow diagram and output of the software. It was found that the output does not match with the experimental findings reported by Isei (1980) and the experimental results obtained by the author.

In the present research, it was assumed that the relationships for numerical distances and flow resistivities hold well for the types of soil that are encountered in surface mining. Under this assumption the attenuation due to the ground was determined according to the theory used by Isei (1980) using the following relationships:

$$\phi_R = \frac{Ae^{ikSR}}{SR} + R\frac{Ae^{ikTR}}{TR} + (1-R)F(w)\frac{Ae^{ikTR}}{TR} \tag{5.46}$$

$$\phi_f = \frac{Ae^{ikSR}}{SR} \tag{5.47}$$

$$ATT_g = -10\log\left|\frac{\phi_R}{\phi_f}\right| \tag{5.48}$$

where,

ATT_g : excess attenuation due to ground absorption.

The above procedures were incorporated in the software developed (GRAB.CPP), which was written in C++. Figure 5.7 illustrates the structure of the model. This model can calculate the excess attenuation due to ground absorption for a specific location and configuration of the source and receiver. As the input data, the model requires user-supplied values of flow resistivity of the ground surface.

Table 5.4 shows an output of the model for a particular source-receiver configuration based on theoretical input values. Figure 5.8 is a graphical representation of the output. The figure illustrates the dependency of the excess attenuation on the frequency and flow resistivity of the ground surface. Thus, this theoretical study has shown that for

Table 5.4 Theoretical excess attenuation for a given source receiver configuration*.

Frequenc	20000	10000	5000	2500	1250	650	300	150	75	40
63	-6.0	-6.0	-6.0	-5.9	-5.9	-5.9	-5.8	-5.8	-5.6	-5.2
80	-6.0	-6.0	-5.9	-5.9	-5.9	-5.9	-5.8	-5.6	-5.3	-4.8
100	-5.9	-5.9	-5.9	-5.9	-5.9	-5.8	-5.7	-5.4	-5.0	-4.2
125	-5.9	-5.9	-5.9	-5.9	-5.8	-5.7	-5.5	-5.2	-4.5	-3.3
160	-5.9	-5.9	-5.8	-5.8	-5.7	-5.5	-5.2	-4.7	-3.6	-1.8
200	-5.8	-5.8	-5.8	-5.7	-5.6	-5.3	-4.9	-4.1	-2.5	0.1
250	-5.8	-5.7	-5.7	-5.5	-5.4	-5.0	-4.4	-3.2	-0.9	2.5
315	-5.6	-5.6	-5.5	-5.3	-5.0	-4.5	-3.6	-1.8	1.3	5.3
400	-5.4	-5.3	-5.2	-5.0	-4.6	-3.8	-2.4	0.2	4.1	7.3
500	-5.1	-5.0	-4.8	-4.5	-3.9	-2.7	-0.7	2.6	6.4	7.3
630	-4.6	-4.4	-4.1	-3.6	-2.8	-1.1	1.6	5.3	6.6	5.4
800	-3.7	-3.5	-3.0	-2.3	-1.0	1.4	4.8	6.2	4.4	2.7
1000	-2.3	-1.9	-1.3	-0.2	1.7	4.8	6.2	3.9	1.6	0.3
1250	0.2	0.8	1.8	3.6	6.2	6.8	3.6	0.9	-0.8	-1.7
1600	6.7	8.1	10.1	11.0	7.2	2.7	-0.1	-1.8	-2.8	-3.4
2000	14.3	11.0	7.5	4.3	1.4	-0.9	-2.4	-3.3	-3.9	-4.2
2500	0.8	0.3	-0.5	-1.3	-2.2	-2.9	-3.4	-3.7	-3.8	-3.9
3150	-4.1	-4.1	-4.0	-3.8	-3.4	-2.8	-2.2	-1.6	-1.2	-0.9
4000	-5.2	-4.7	-3.9	-2.6	-0.7	1.8	4.4	6.7	8.5	9.5
5000	-0.4	1.0	3.0	5.0	4.6	2.3	0.6	-0.6	-1.3	-1.7
6300	1.8	0.6	-0.6	-1.8	-2.8	-3.4	-3.8	-4.0	-4.2	-4.2
8000	-4.6	-3.7	-2.4	-0.4	2.1	4.9	7.2	8.7	9.5	9.8

*Source Height – 0.375m, Receiver Height = 1.17m, Source-to-Receiver Distance = 10m

estimating noise attenuation due to ground surface the flow resistivity of the ground will have to be determined. As the noise pollution concept is comparatively new in the mining industry, there is no standard practice for evaluation of flow resistivity of the ground surface near mining operations. Therefore, a number of systematic experiments were conducted during the present research to establish a method to evaluate the flow resistivity of the ground surface. These experiments are discussed in the next section.

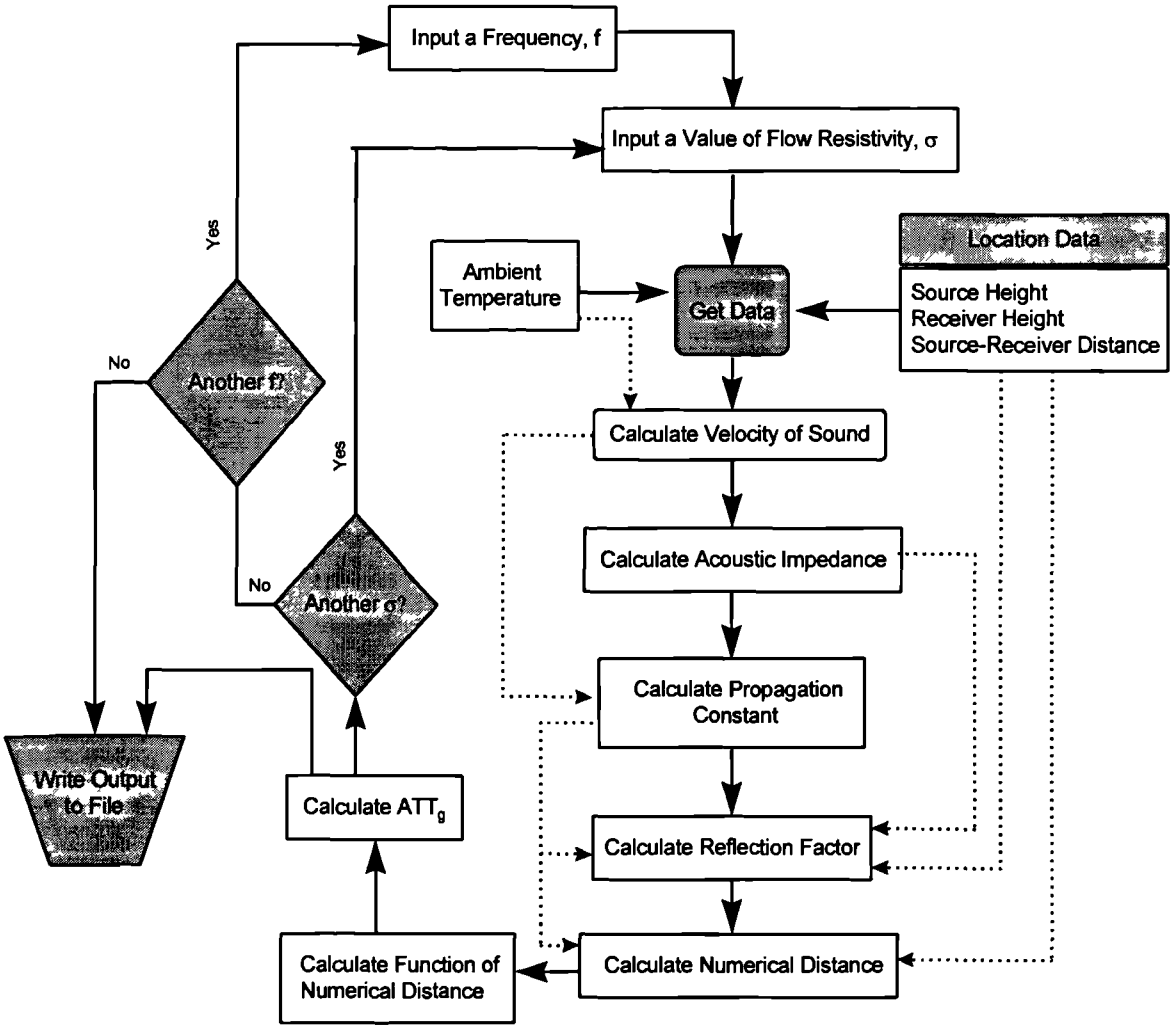


Figure 5.7 The structure of the ground attenuation model developed.

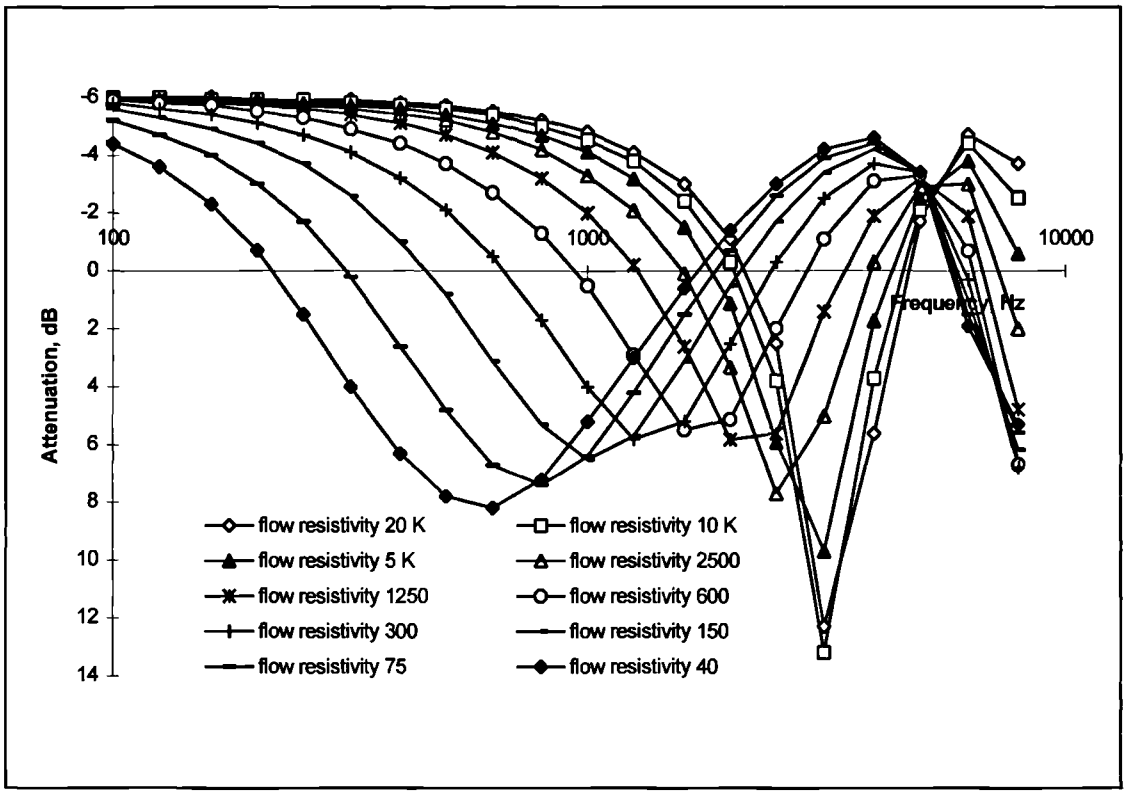


Figure 5.8 Theoretical excess attenuation due to ground absorption for different values of flow resistivity and frequencies.

5.4 Experimental Evaluation of Flow Resistivity

The indirect method of determining the flow resistivity of a particular ground surface is the method of experimental determination of excess attenuation of the ground surface by means of acoustical measurements (Isei *et al* 1980). A reliable noise source capable of generating sound at different frequencies is an essential prerequisite in such experiments. Also, the experimental area should be free from other external noise sources which, in most circumstances, is an impossible task as these sources can seldom be eliminated fully.

The objective of the experiments carried out in this part of the research was to determine the flow resistivity of different types of soil normally available near surface mines and quarries. This was achieved by determining experimentally the excess attenuation of sound energy over these ground surfaces.

The experiments were carried out at and around the tailings dam of Tara Mines. The site is far from other human disturbances, therefore this helped in minimising the external noises. However, flying birds, aeroplanes etc. were contributing to the background noise. The design of the experiments, observations made and the analysis of the results are discussed below.

5.4.1 Experimental Design

The experimental layout is illustrated in Figure 5.9. The noise generator and the instruments for measuring the wind velocity and the reference sound level meters were located at R. Stations 1, 2, 3, 4,...., n are the positions of the sound level meters for measuring sound pressure levels at different distances from the source. The measurements were carried out in all the sectors.

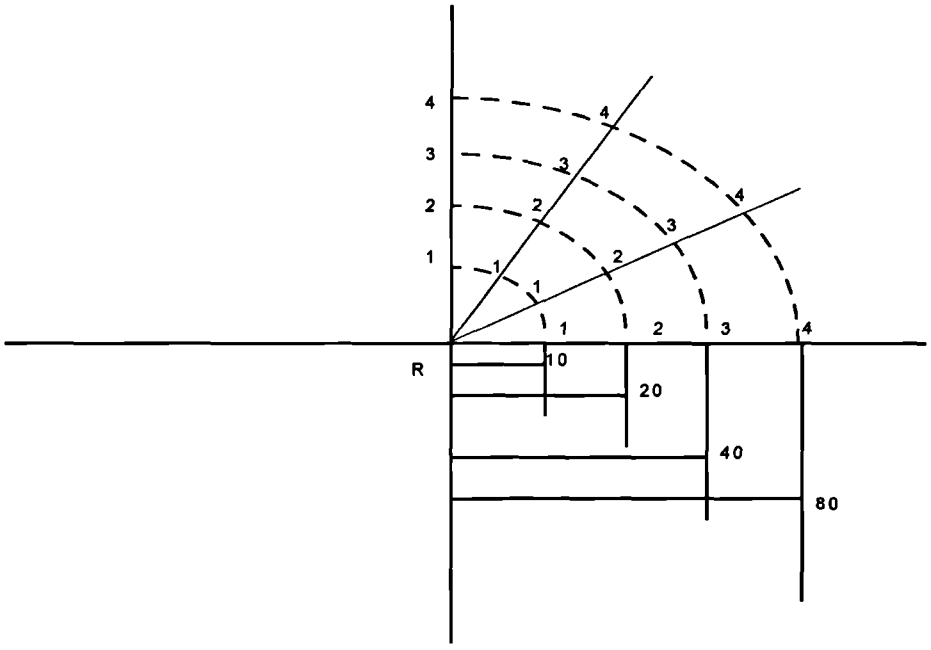


Figure 5.9 Scheme of the field experiments.

Measurements taken in different sectors under constant temperature and humidity were used to determine the effect of wind direction on noise propagation. If carried out over a long period of time covering a range of climatic conditions, these measurements can also be used to evaluate the effects of temperature and humidity on noise propagation.

However, due to limited resources and time the effects of humidity and temperature were not studied experimentally.

A sine wave generator capable of generating sound at different frequencies was used as the noise source. The output of this generator was broadcast by the DML-1152 speaker system manufactured by Electro Voice Inc. The specifications of the generator and the speaker were as follows:

Sine Wave Generator

Frequency range	0.02 Hz to MHz in 7 ranges with tuning range 1000:1 frequency control
Outputs	Sine, triangle, square-wave, pulse, ramp etc.
Temperature range	0 to 50 °C

Speaker

Make	Electro Voice Inc., Michigan.
Model	DML-1152 series Deltamax
Speaker Height	76 cm
Speaker width	45.2 cm
Speaker Depth	41.4 cm
Directivity	Higher directivity over 1 kHz

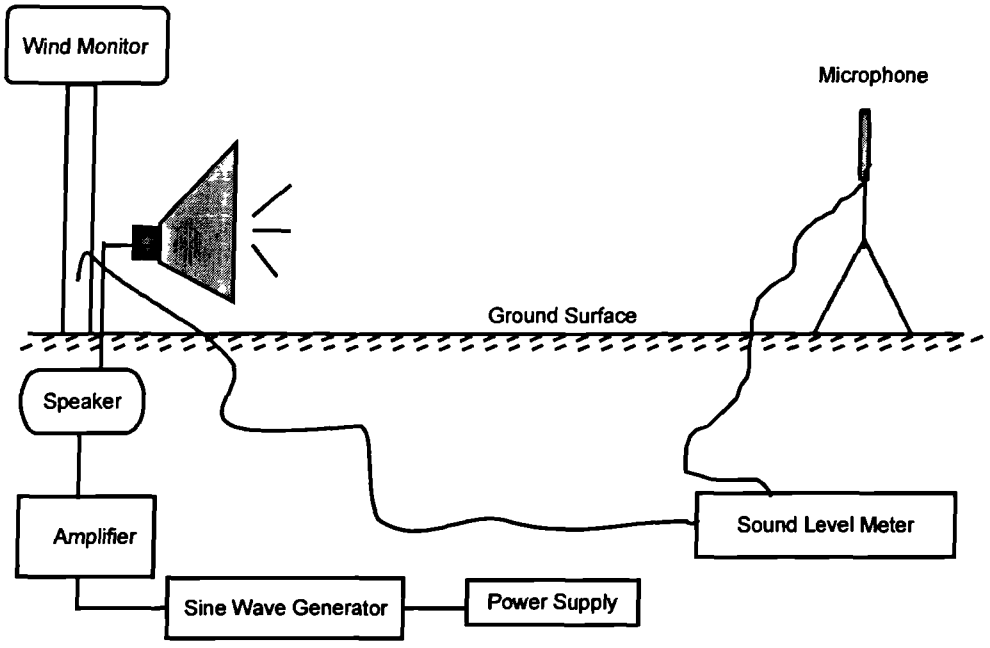


Figure 5.10 Experimental set-up used in determining the excess attenuation due to ground absorption.

Figure 5.10 illustrates this experimental set-up. Continuous sound level meters (Larson Davis SLM 820 and 870) were used to record the noise levels at distances of 10 m, 20 m, and 40 m from the source. A Larson Davis wind velocity monitor (Model 2400) was used to collect the wind data during the experiments. Another sound level meter was used to record the reference levels at a distance of 1 m in front of the speaker. The sound energy was generated by the speaker at different frequencies and the sound level meters recorded the A-weighted sound pressure levels and 1 minute L_{eq} simultaneously at each of the measurement stations. The climatic conditions observed during this experiments were:

Cloud level[1] = 0 - 0.3
Ambient temperature = 15-20 °C
Average wind velocity = 0.1-3.7 ms^{-1} NW

Figure 5.11 shows schematically the arrangement of the speaker, the reference SLM and SLM at a distance of 10 m. The location of the equivalent point source for the speaker, P was determined according to the principle of rectangular plate source and was found to be at a distance of b/π m in front of the plane[2] of the speaker.

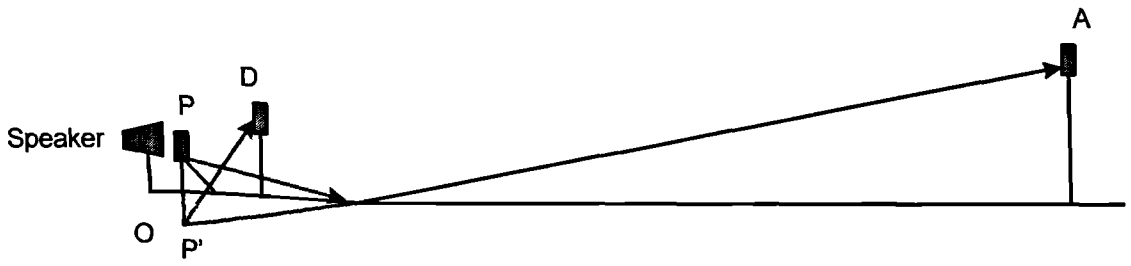


Figure 5.11 Arrangement of speaker and sound level meters. O: Position of speaker, D: Reference sound level meter at a distance of 1 m from O. A: Recording sound level meter at a distance of 10 m from O. P: Equivalent point source at a distance of 0.239 m from O. P': Image source.

[1] Cloud coverage values are given as 0 for the clear sky and 8 for the sky totally covered by cloud.

[2] Technology and law for pollution prediction.
Committee of Editors for Technology and law for pollution prediction. Publications, Japan (In Japanese).

The sound pressure level at the equivalent point source location is obtained by the following equation:

$$L_0 = L_1 - 20\log\frac{b}{\pi} \tag{5.53}$$

where,

b : width of the rectangular source

This value changes with frequencies, *FREQ*[*I*], where *I* changes from 1 to 22 for the 1/3 octave frequencies starting from 63 Hz. The value is also dependent on the flow resistivities, *FRES*[*J*], of the soil. The theoretical flow resistivities tested were 40, 75 150, 300, 600, 1250, 2500, 5000, 10000 and 20000. Thus the size, *J* of the array of flow resistivity was 10. The theoretical calculation of excess attenuation considers sound power level of the source as constant. In the experiment the sound power level could be varied at different frequencies. Therefore, the sound power level of the source producing 63 Hz sound was taken as the reference value. With reference to Figure 5.11 the following variables were defined:

DD : horizontal distance between the equivalent source (P) to the reference station
DD = (1 - *b*/π) =0.873 m
HS : height of source = height of the center of the speaker = 0.3 m
HRD : height of the receiver sound level meter located at a distance of 1m in front of the speaker =0.67 m

The reference sound pressure level, L_0, can be determined at P by adding theoretical excess attenuation at D to the measured sound pressure level at D. Theoretical excess attenuation, *TEXATTD*[*I, J*], under a constant power source is a function of frequencies, *FREQ*[*I*], and flow resistivities, *FRES*[*J*], of the ground. Thus, the sound pressure levels at P for different frequencies and flow resistivities can be calculated. However, measured sound pressure levels at D need correcting. This correction is due to the deviation of the sound pressure level at a particular frequency from the sound pressure level at a base frequency. The base frequency in the present case is 63 Hz and the following relationships allow the calculation of the sound pressure levels at point P:

$$
\begin{aligned}
SPLS[I,J] &= SPLDM[I] + TEXATTD[I,J] \\
CORR[I,J] &= SPLS[I,J] - SPLS[1,J] \\
CORSPLS[I,J] &= SPLS[I,J] - CORR[I,J]
\end{aligned}
\tag{5.54}
$$

where,

SPLS[I, J] : reference sound pressure level at P at *I*th frequency and *J*th flow resistivity
SPLDM[I] : measured sound pressure level at D for the *I*th frequency
TEXATTD[I, J] : theoretical excess attenuation at D for *I*th frequency and *J*th flow resistivity
CORR[I, J] : correction for referring to the base frequency
CORSPLS[I, J] : corrected sound pressure level at P for *I*th frequency and *J*th flow resistivity

The measured sound pressure levels at different distances in front of the source provide the sound power level of the equivalent point source. From this sound power level one can calculate the sound pressure levels at the measuring stations, and excess attenuation due to ground absorption at that point is determined by accounting for the attenuation due to spreading.

These normalised sound pressure levels at the equivalent source point determine the expected sound pressure levels at the second measuring point (A in Figure 5.11). The excess attenuation due to ground absorption are the differences between the expected values and the corrected measured values of sound pressure level. To compare these measured excess attenuation with the theoretical values a program EXPEXATT.FOR was developed. From the outputs of this program the flow resistivity of the soil was determined for use as input for the ground attenuation model (GRAB.CPP). The theoretical curves are drawn for a wide range of values of flow resistivity. The flow resistivity of the ground is selected on the basis of the best correlation of the measured and theoretical values.

5.4.2 Analysis of Results and Discussion

A number of experiments were conducted on various types of soil. The recorded A-weighted decibel levels were converted to sound pressure level (dB) with reference to the sound pressure level observed at a distance of one metre in front of the source. The

frequency spectrum of the excess attenuation due to ground absorption was calculated for different assumed flow resistivities of soil. The coefficient of correlation of the calculated or theoretical excess attenuation and experimental results were determined for all possible cases. The flow resistivity of soil was then considered to be equal to the value that gives the best correlation. The results of these experiments are discussed below:

5.4.2.1 Experiments over Grass Covered Soft Soil

Plate 5.1 shows the site of the experiments. The experiments were carried out at different direction of propagation of sound with respect to wind direction. Sections A3.1, A3.2 and A3.3 of Appendix 3 gives the experimental results. These results were utilised to determine the flow resistivity of the grass-covered soft soil under consideration. Coefficients of correlation between the measured and theoretical values for all the experiments were evaluated. Measurement at 40 m distances were more sensitive to other unavoidable noise in the site. Moreover, the sound pressure levels of noise were near threshold values. Therefore, the measurements at 40 m distances were disregarded in further analysis. Table 5.5 shows the coefficient of correlation for the measured values at 10 m for the three different directions of propagation.

Thus, it is obvious that the measured excess attenuation corresponds to the theoretical excess attenuation with a flow resistivity of 150 raylsm^{-1}. Therefore, for noise prediction purposes over this type of soil one can use the theoretical model coded in GRAB.CPP, taking flow resistivity as 150 raylsm^{-1}.

Table 5.5 Coefficients of correlation between the measured and theoretical excess attenuation over grass-covered soft soil at 10 m for measurements at different directions.

Flow Resistivity (raylsm^{-1})	Experiment 14-1	Experiment 14-2	Experiment 14-3
40	0.591057	0.599289	0.447114
75	0.744980	0.757561	0.619779
150	**0.820831**	**0.840906**	**0.717932**
300	0.754923	0.780907	0.661700
600	0.509388	0.565710	0.425639

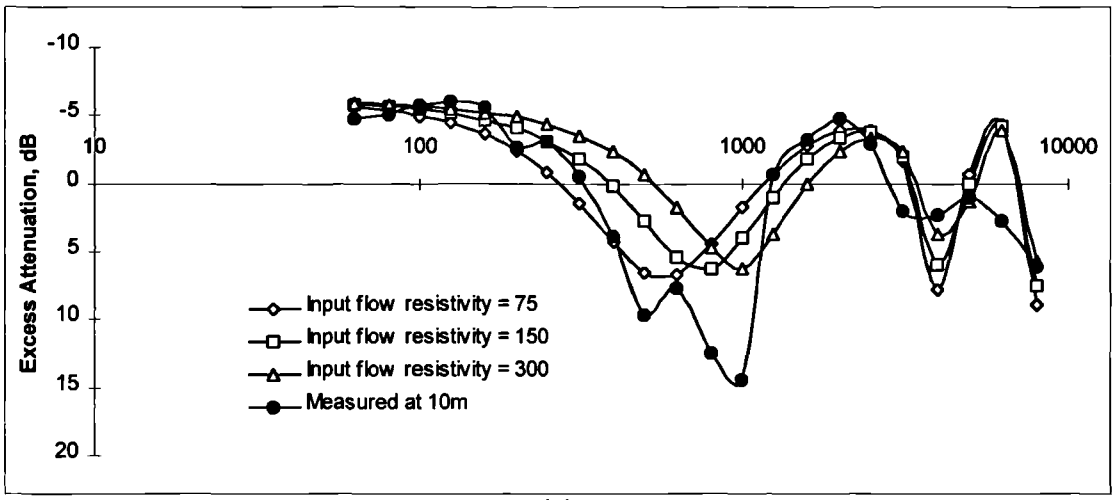


(a)

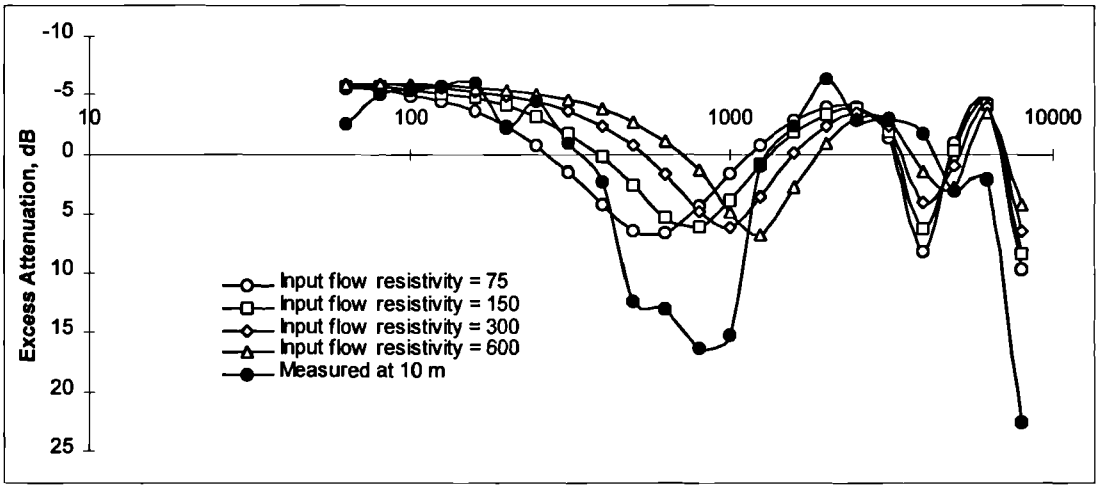


(b)

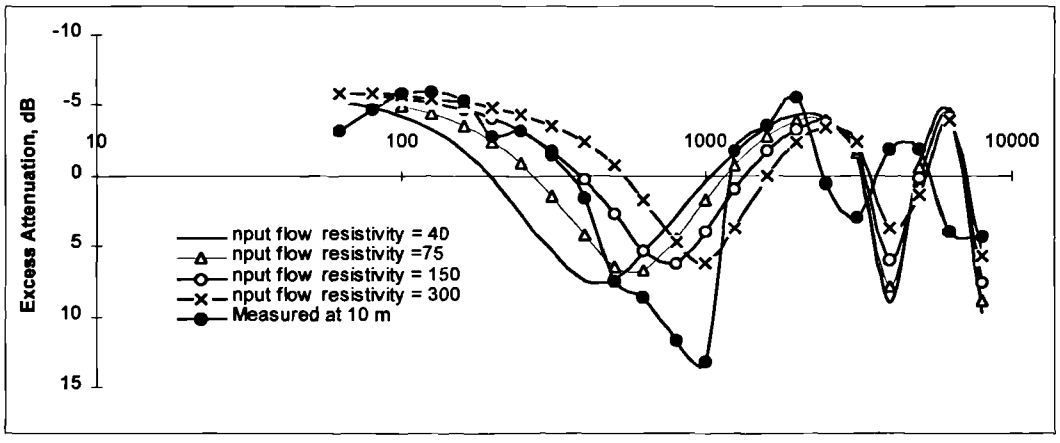
Plate 5.1 Noise attenuation experiments over grass covered soft soil.



(a)



(b)



(c)

Figure 5.12 Experimental and theoretical excess attenuation due to ground absorption over grass covered soft soil. (a). In the direction of wind, (b). Opposite to the wind direction, (c). At 135^{o} to the wind direction.

The curves in Figure 5.12 show the experimental and theoretical excess attenuation due to ground absorption over grass covered soft soil. Appendix 3 presents the plots of the experimental results for all the experimental conditions. These conditions include the experiments with varying distances and wind directions.

5.4.2.2 Experiments over Settled Quicksand

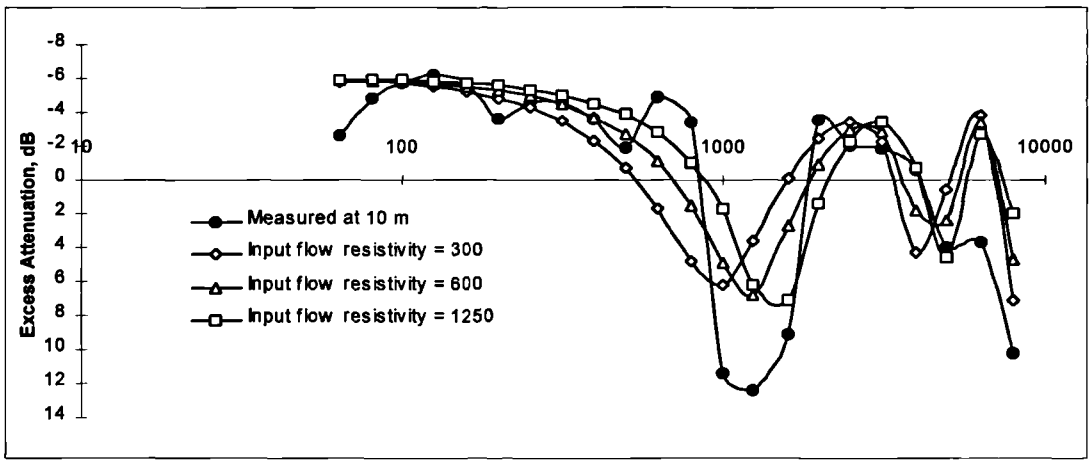
The second set of experiments during this phase of the study were carried out over settled quicksand. These experiments were conducted for four different conditions. The relative angular displacement of the direction of sound propagation was 45°, 90° and 180°. Measurements of sound pressure levels were also carried out at longer distances.

However, these long distance measurements could not provide very clear response to study ground absorption because of the influence of external sounds in the site. Coefficients of correlation were calculated for the measured spectra and theoretical spectra for different values of flow resistivity.

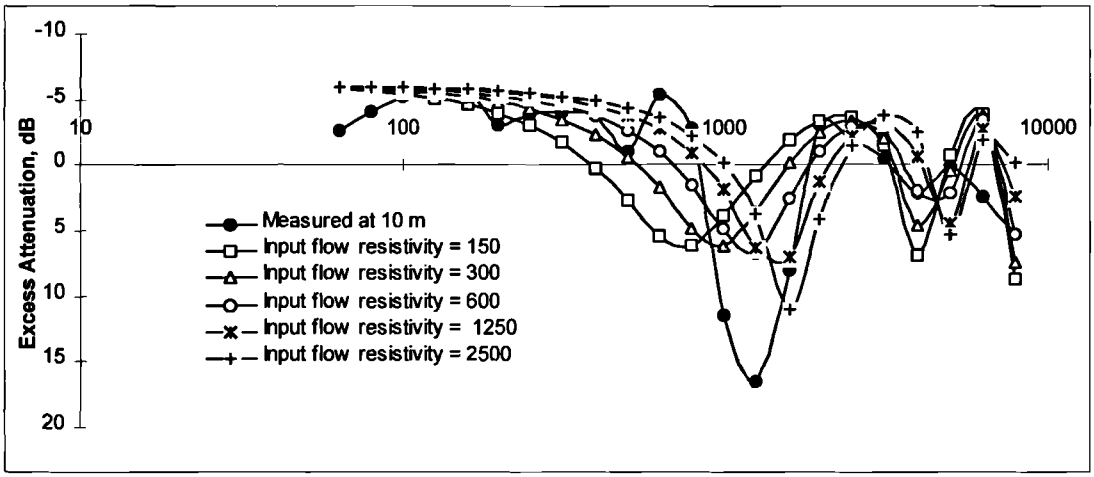
Table 5.6 gives the coefficients of correlation between measured and theoretical excess attenuation at 10 m under different wind directions. Sections B3.1, B3.2 and B3.3 of Appendix 3 present the detailed results of observation including those at 20 m and 40 m distances from the source. Long distance observations were erroneous due to the presence of birds singing near the experimental site. The correlation figures show that the measured excess attenuation corresponds best to the theoretical excess attenuation for a flow resistivity of 600 raylsm^{-1}.

Table 5.6 Coefficients of correlation between measured and theoretical excess attenuation for different wind directions.

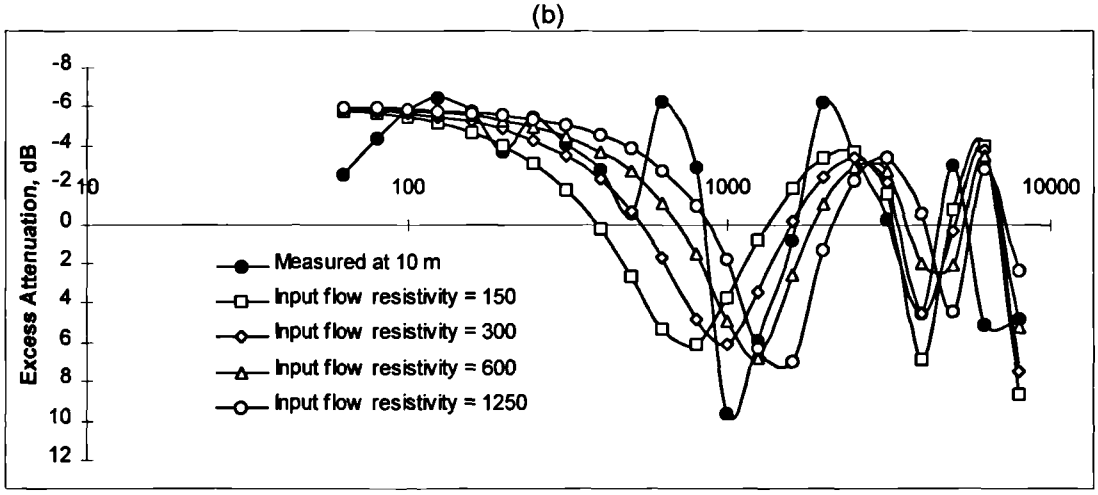
Flow Resistivity (raylsm^{-1})	Experiment 14-4	Experiment 14-5	Experiment 14-6
40	0.051196		
75	0.210540		
150	0.420719	0.383241	0.505364
300	0.678414	0.646768	0.676103
600	**0.852498**	**0.833740**	**0.716050**
1250	0.831247	0.798636	0.561202
2500		0.648431	0.373939



(a)



(b)



(c)

Figure 5.13 Excess attenuation due to ground absorption over settled quicksand, (a) along wind direction, (b) along 45° to wind direction, (c) along 90° to wind direction.

Therefore, for prediction purposes, this value can be considered for similar types of soil. However, such predictions must be corrected by a site factor. As shown in the figures the measured excess attenuation is higher near 1000 Hz. Correction will have to be applied for such behaviour until the theory can be updated to quantify the external influences, or measurement techniques are developed to filter out the unwanted information of environmental noise. Figure 5.13 shows the plot of the experimental and theoretical excess attenuation for different directions of sound propagation with respect to wind velocity.

5.4.2.3 Experiments over the Road Surface

Two sets of experiments were conducted over a gritty road surface simulating the haul roads. The directions of sound propagation were at 15^{o} along and 165^{o} opposite to the wind direction. Plate 5.2 shows the site of these experiments. Sections C3.1 and C3.2 of Appendix 3 present the detailed experimental results for these tests. Coefficients of correlation were calculated for the measured spectra and theoretical spectra for different values of flow resistivity.

Table 5.7 presents the coefficients of correlation between the measured and theoretical excess attenuation at 10 m for the two conditions of direction of wind velocity. In this experiment, the theoretical attenuation for flow resistivity of 600 raylsm^{-1}corresponds well to the measured excess attenuation. Hence, for such soils a flow resistivity of 600 raylsm^{-1} can used in the model. However, such predictions must be corrected by a site factor. Figure 5.14 shows the plot of the theoretical and experimental results. The fluctuations in the amplitudes in the figure were due to the adjustment of amplitudes of the speaker during the experiment.

Table 5.7 Coefficients of correlation between measured and theoretical excess attenuation over gritty road surface at a distance of 10m under different wind directions.

Flow Resistivity (raylsm^{-1})	15^{o} Along	165^{o} Opposite
150	0.538298	0.401372
300	0.726872	0.665037
600	**0.786025**	**0.838097**
1250	0.634120	0.793892
2500	0.424949	0.643900

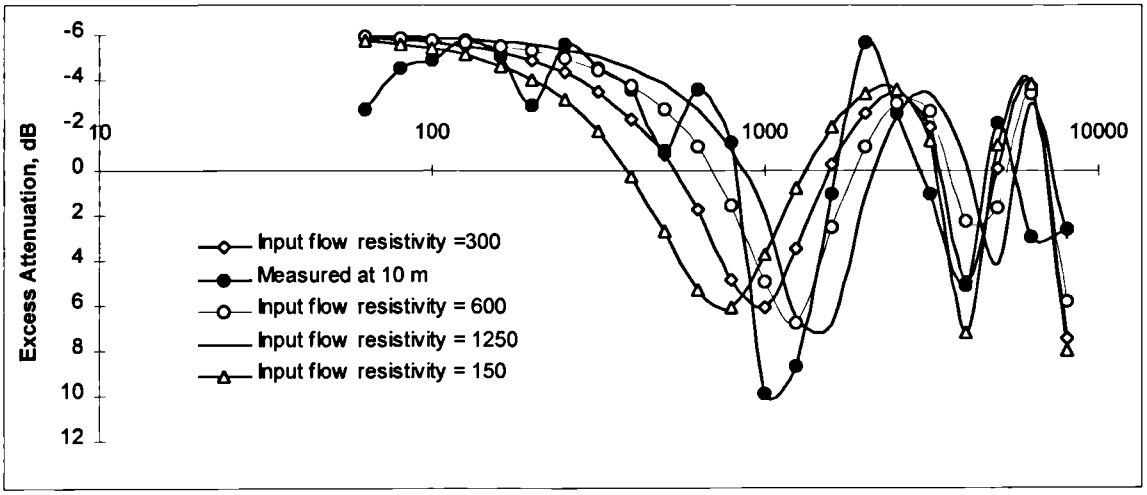


(a)

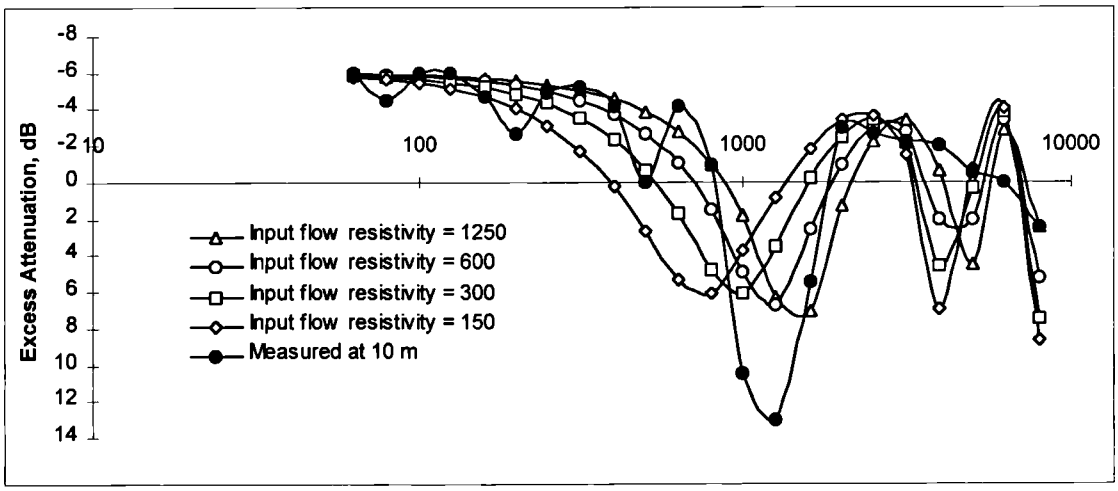


(b)

Plate 5.2 Noise attenuation experiments over gritty road surface.



(a)



(b)

Figure 5.14 Excess attenuation due to ground absorption over gritty road surface, (a) at 15° to the wind direction, (b) at 165° to the wind direction.

5.4.2.4 Effects of Distance on Ground Absorption

The experiments were conducted with measurements taken at 10 m, 20 m and 40 m from the source. Some experiments were also carried out at 80 m, 160 m and 320 m. Due to the presence of external noise sources (birds, aeroplanes, etc.) this data could not be analysed properly. However, the effects of distance from the source in excess

attenuation due to ground absorption could be clearly observed from the 10 m, 20 m and 40 m readings.

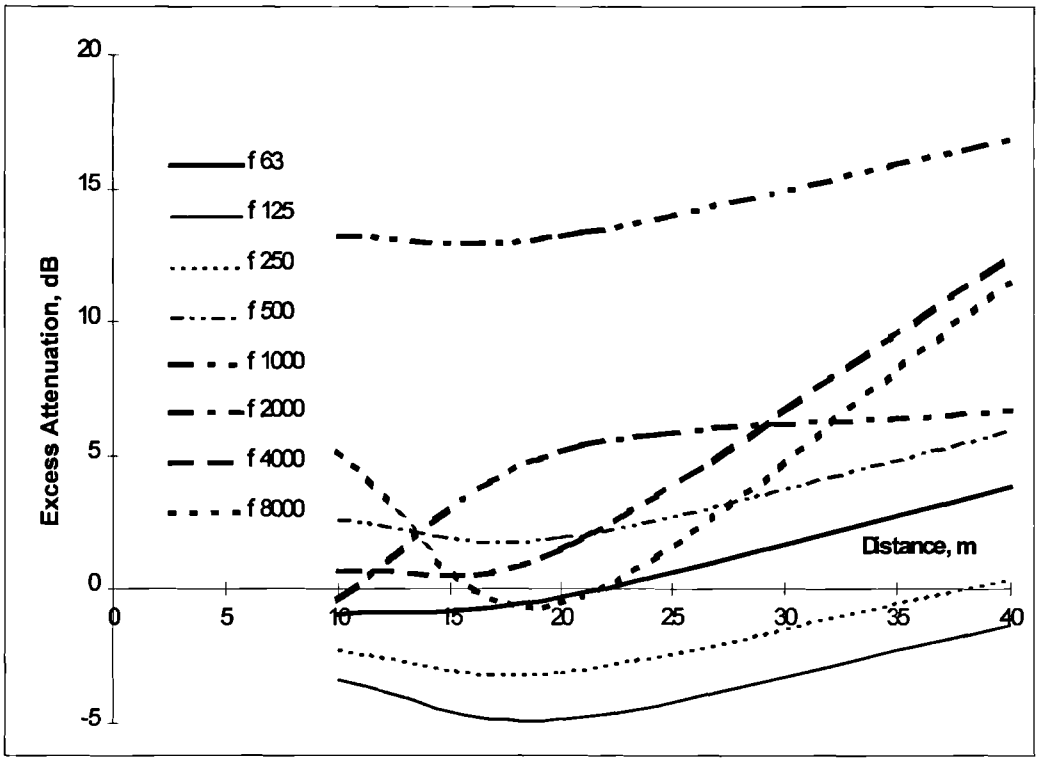
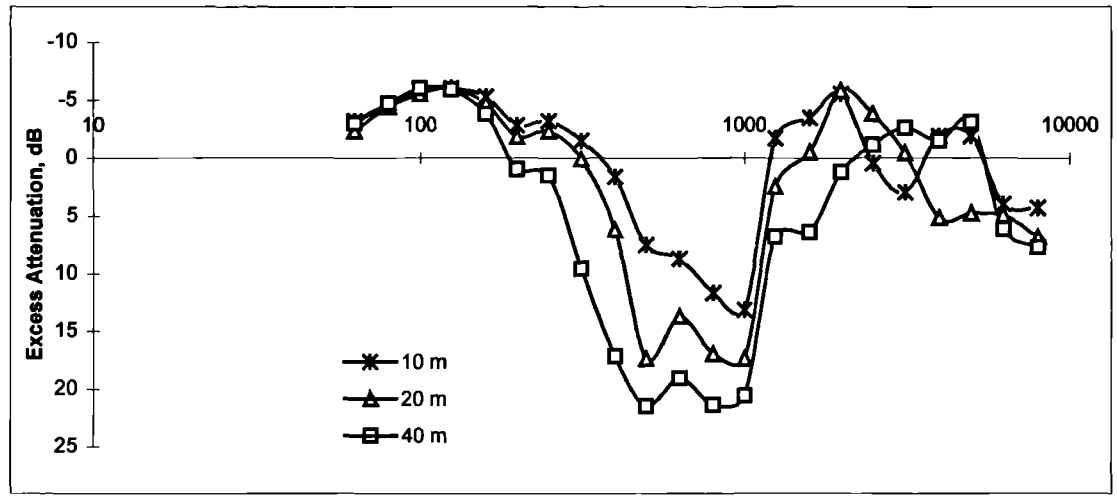


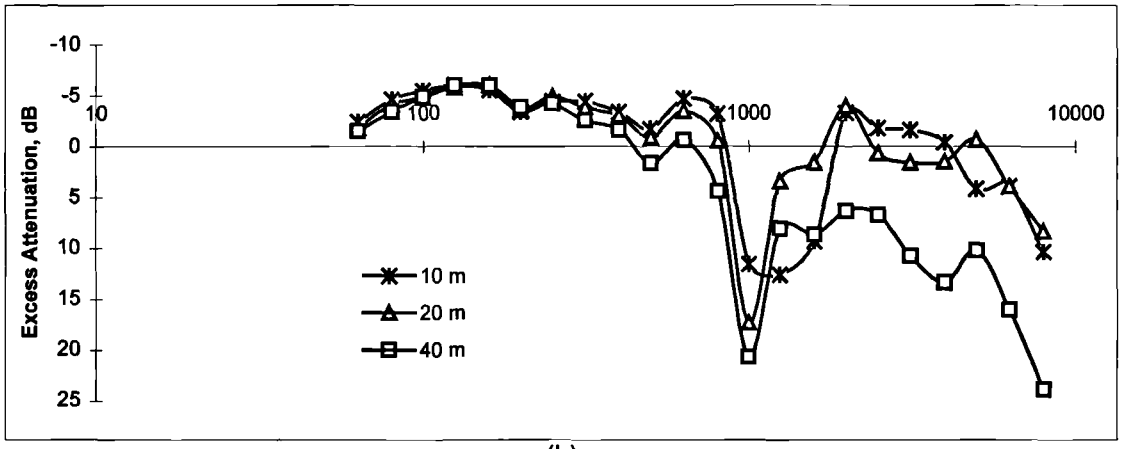
Figure 5.15 Excess attenuation due to ground absorption at different frequencies (f) as a function of distance.

Figure 5.15 shows the results of experiments on excess attenuation due to ground absorption at different distances. It is obvious from the figure that excess attenuation due to ground absorption is maximum for the frequency around 1 kHz. For all frequencies it appears that excess attenuation due to ground absorption is a function of distance.

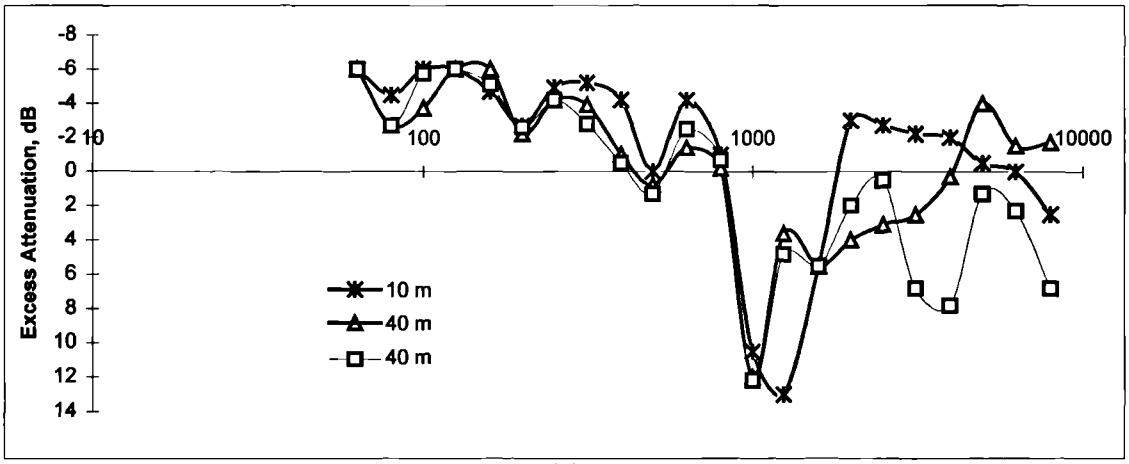
Ground absorption tends to decrease within a short distance from the source. This can be explained by considering the reflected sound energy. The receiver in the experiment received the sound energy reflected from the road surface. As a result measured ground absorption is less within 10 m than those measured at higher distances. Figure 5.16 presents the measured excess attenuation at different distances.



(a)



(b)



(c)

Figure 5.16 Effect of distance on excess attenuation due to ground attenuation over (a) Grass-covered soft soil at 135° to the wind direction, (b) Settled quicksand along the wind direction , (c) Gritty road surface at 165° to the wind direction.

5.4.2.5 Effects of Wind Velocity on Ground Attenuation

The experimental results also revealed the effects of wind direction over the excess attenuation. Figure 5.17 shows the plot of such results for the grass covered soft soil. Curve A in the figure represents the theoretically derived excess attenuation due to ground absorption under still wind conditions for a flow resistivity of 150 raylsm^{-1}. Curve B represents the excess attenuation when the direction of the wind is 45° to the direction of propagation of sound. Curve C represents the propagation of sound in the opposite direction of wind. The Curve D represents the excess attenuation when the sound is propagating along the wind direction. In this research precise wind monitoring was not carried out. However, the observations as shown in Figure 5.17 suggest that more experiments on mining terrain will be necessary in the future to establish a relationship between wind velocity and ground absorption. The theoretical model of ground attenuation has not considered the wind velocity as a parameter. Figure 5.18 shows the change in measured ground attenuation over grass-covered soft soil on 180° change in wind direction.

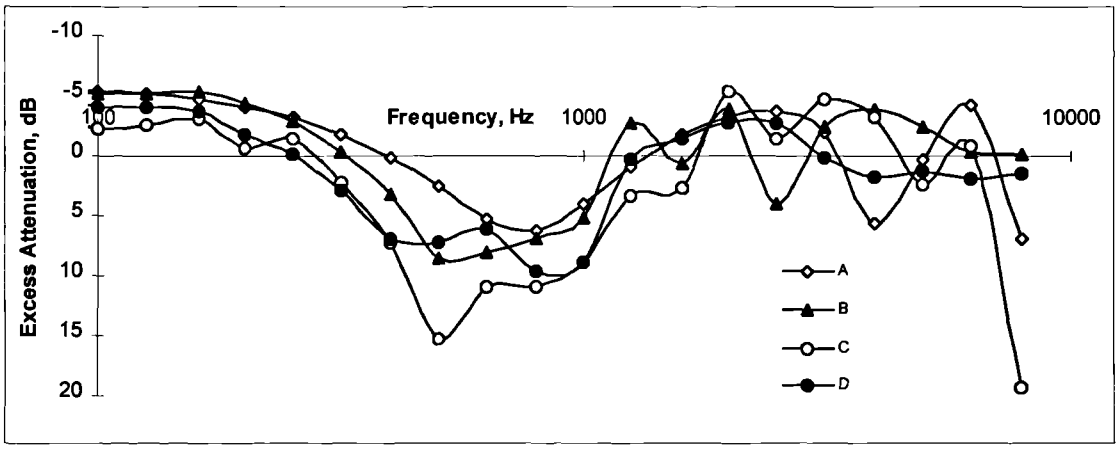


Figure 5.17 Effect of wind direction on ground absorption.

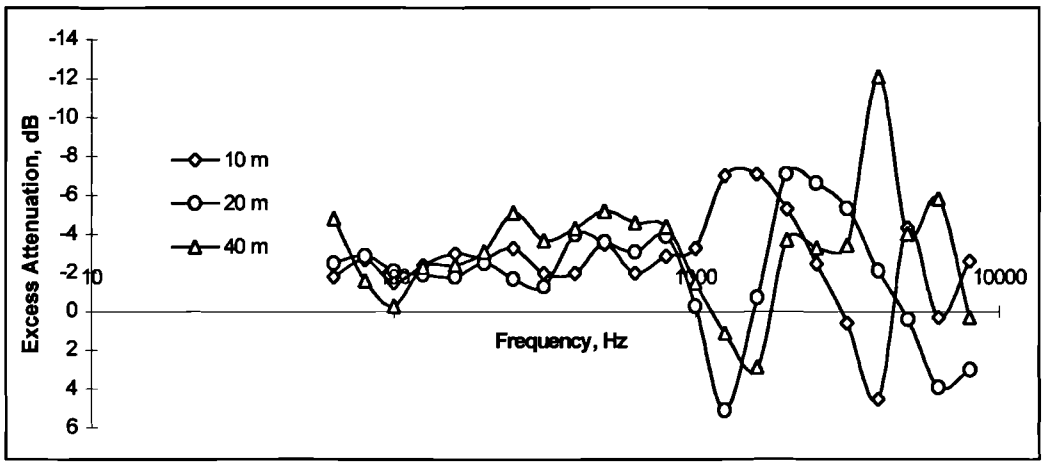


Figure 5.18 Variation of excess attenuation over grass-covered soft soil due to a 180^{0} change in the direction of wind.

5.5 Conclusion

This chapter reviewed the theory of absorption of sound energy by a ground surface and described the ground attenuation model developed in this research. In the model excess attenuation due to ground absorption is derived as a function of the flow resistivity of the ground surface. The flow resistivity of the ground, which is the critical input parameter for the model, was determined through systematic experiments in the field. The acoustic impedance of the ground surface and the propagation factor of acoustic the acoustic wave travelling in the air medium overlying the ground surface are determined as a function of the flow resistivity using the proved well accepted theory of wave propagation. The attenuation due to the ground surface is therefore determined in the developed model as a function of the flow resistivity.

Experimental studies conducted for testing the ground attenuation model have shown that the flow resistivity of the ground can be deduced from the results of systematic experiments conducted to measure sound pressure levels. In this research the flow resistivity of three types of mining terrain were evaluated experimentally. It was found that the grass covered soil has a flow resistivity of 150 raylsm^{-1} whereas the gritty road surface and the settled quicksand have shown a flow resistivity of 600 raylsm^{-1}. These values can be provided as input to the model (GRAB.CPP) for prediction of sound energy while travelling over such types of soil. The method used to determine the flow

resistivity of the ground surface could not be used for other types of mining terrain due to the limited resources and time and it is expected that similar work will be conducted in future for this purpose. The other important attenuation factors are discussed in the next two chapters.

Chapter 6

The Development of an Air Attenuation Model

6.1 Introduction

The behaviour of propagation of acoustic waves through the atmosphere modifies the overall noise field at a specific location. It was mentioned in Chapter 2 that attenuation of propagating sound energy has been studied since Stokes (1845; 1851) published theoretical treatment on the influence of heat radiation and internal friction on the propagation of elastic waves. The attenuation constant of air was first measured by Neklepayev (1911). In dry air with no CO_2 the attenuation constant was found to be greater than that calculated according to the classical theory by 30-200%. The dissipation of energy is a result of transfer of energy due to collisions of molecules having greater energy, which come from the region of compression, with the molecules of a non-perturbed region at rest or with molecules of a region in which the medium is rarefied. Moreover, when a portion of the air media is perturbed during noise generation

a thermal radiation takes place from the perturbed region because of the temperature difference between the region of perturbation and the surrounding medium. This causes attenuation of acoustic energy in air. This attenuation is also affected by fog or rain and the presence of trees and walls.

The atmosphere is neither static nor uniform. It is constantly moving at a random speed. The wind and the temperature gradient in the atmosphere do not follow a precise rule. The density, relative humidity and temperature of any specific volume of air in the atmosphere vary with the time of day and the day of the year. All these variables are modified by other atmospheric and meteorological phenomena. Sound pressure levels at a receiver fluctuate due to these effects. Therefore, noise prediction and control systems need to model the complex behaviour of acoustic waves under atmospheric change. Delaney (1977) and Piercy *et al* (1977) reviewed the previous work in this field. Larsson and Israelsson (1991) conducted a series of studies over more than fifteen years to account for meteorological effects on outdoor sound propagation. These studies have established certain methods to account for these effects in environmental noise prediction. American National Standard (ANSI S1.26 1978) provides procedures for accounting for air attenuation of propagating sound. However, to apply these procedures in surface mining and quarrying environments, an adequate methodology considering the geo-mining and terrain conditions must be developed.

In the present work, a methodology to evaluate atmospheric attenuation of surface mining and quarrying noise based on the available information has been developed. This chapter describes the air attenuation model developed to calculate the reduction of noise levels in the air over a surface mining area.

6.2 Excess Attenuation due to Air

Excess attenuation due to air A_e can be experimentally determined at a particular site by measuring sound pressure levels L_1 and L_2 at distances r_1 and r_2 from a source in its far-field. A_e is expressed as:

$$A_e = L_1 - L_2 + 20\log\left(\frac{r_2}{r_1}\right) \tag{6.1}$$

The above excess attenuation comprises of a number of factors. Attenuation due to atmospheric effects includes absorption of acoustic energy by air and attenuation by fog or rain. Other attenuation includes that due to barrier effects of trees and other hindrances, and absorption by the ground surface modified according to the wind and temperature gradient.

6.3 Theory of Molecular Absorption

Classical theories of wave propagation assumed that no energy losses occur during the collisions of molecules. This is because the molecules are perfectly elastic, and the particles move as a point mass having three external degrees of freedom. Early works in this field disregarded the influence of the possible rotational motions of the molecules (assumed to be spheres) since these molecules have negligible moments of inertia. Both of these assumptions are approximately correct for monatomic gases only. For example, the particles of diatomic gases have three additional degrees of freedom due to rotational motions of the spatial system. Quantum theory suggests that one of the later degrees of freedom has no influence on the possibilities of changes of vibrational and rotational energy levels of its atoms.

According to the kinetic theory of gases, at thermal equilibrium every degree of freedom participating in the process has a precisely determined mean quantity of energy associated with it. However a particle has a certain internal inertia. This means that the energy connected with the internal and rotational degrees of freedom has a smaller value immediately after a rapid condensation than in the steady state. This energy gradually increases to the equilibrium value in the steady state condition.

Suppose a volume dV of a media within a boundary suddenly receives some energy, dE_0. Also suppose that there is no energy exchange across the boundary. This energy will initially increase the velocity of progressive motions of the molecules. This will raise the temperature and pressure of the media. Then it will increase the energy of the

external degrees of freedom of progressive motion, that is the external energy dE_a of the molecules (for t=0, dE_0=dE_a). Division of equilibrium energy into external and internal degree of freedom results in the perturbation of the media. This perturbation gradually subsides.

A state of equilibrium returns after a long time. At the state of equilibrium, the internal energy of particles together with the energy of rotational motions will be equal to E_{ieq}. At a time t, it is equal to $E_i(t)$. Since the term E_{ieq}- $E_i(t)$ is small compared to E_a, higher order terms can be neglected. It also can be assumed that the instantaneous speed of the return of the molecules to the state of energy equilibrium is proportional to the deviation from this state (Malecki, 1969). This gives:

$$\frac{1}{\tau}\left[E_{ieq} - E_i(t)\right] = \frac{\delta E_i}{\delta t} \tag{6.2}$$

The quantity τ is the *relaxation constant* or *relaxation time* for a given medium. The relaxation time is defined as the time during which $E_i(t)$ will increase from zero to the value of $(1\text{-}1/e)E_{ieq}$= 0. $6321E_{ieq}$. The solution of the above differential equation for a sudden change of energy supplied to the region dV yields:

$$E_i(t) = E_{ieq}\left[1 - \exp\left(-\frac{t}{\tau}\right)\right] \tag{6.3}$$

The energy of internal vibrations of the molecules reduces the energy of progressive motions. The total energy, therefore, is given as:

$$E_0 = E_a + E_i \tag{6.4}$$

In the state of equilibrium corresponding to a very slow energy supply, the total energy E_{eq} equals:

$$E_{eq} = E_a + E_{ieq} \tag{6.5}$$

The equalisation of the levels of energy is very fast. As a result, there is no need in the energy balance to consider the heat dissipation outside the perturbed region. The effect of the friction of the medium is also negligible.

By definition, the specific heat of change at constant volume (C_v) is $(\delta E/\delta T)_v$. Therefore, from the above equation:

$$\frac{dE_{eq}}{dT} = \frac{dE_a}{dT} + \frac{dE_{ieq}}{dT} = C_{va} + C_{vi} \tag{6.6}$$

where C_{va} is the specific heat corresponding to the external degrees of freedom, or the so-called external specific heat of the medium, and C_{vi} is the specific heat corresponding to the internal and rotational degrees of freedom or the internal specific heat of the medium.

The quantities C_{va} and C_{vi} have a somewhat different physical significance. The temperature of the medium depends solely and uniquely on E_a as this part of energy is responsible for the increase in velocity of the molecules, and consequently also of pressure. However, E_{ieq} has no direct bearing on the change of pressure and causes only an increase in the general specific heat of the gas. For a change during which the state of energy equilibrium is preserved, this fact does not affect much because E_{ieq}/E_a is a constant quantity for the given conditions. Its effect is shown only by the fact that for a polyatomic media, C_v is slightly greater than the value given by the kinetic theory of gases.

The above explanation does not hold for the dynamic processes. For a system suddenly receiving a supply of energy, the specific heat changes with time:

$$\frac{dE}{dT} = C_v(t) = \frac{dE_a}{dT} + \frac{dE_{ieq}}{dT}\left[1 - \exp\left(-\frac{1}{\tau}\right)\right] \tag{6.7}$$

By definition,

$$\frac{dE_a}{dT} = C_{va}, \quad \frac{dE_{ieq}}{dT} = C_{vi} \tag{6.8}$$

Therefore,

$$C_v(t) = C_{va} + C_{vi}\left[1 - \exp\left(-\frac{t}{\tau}\right)\right] \tag{6.9}$$

The change of the specific heat of the medium C_v, which accompanies a sudden supply of energy, causes $\chi = C_p/C_v$ to vary as C_p remains constant during the change.

Since, $dP/P_0 - \chi(\delta\rho/\rho_0) = 0$, it is concluded that at the first instance after a sudden supply of energy, an increase of the instantaneous value of the apparent volume stiffness of the medium takes place.

From the solution of acoustic wave equation, it is known that $(\delta P/\delta\rho) = c^2$. In adiabatic processes the change of pressure of the medium depends not only on the change of its density but also on the change of the internal energy of the particles. This is the case with an ideal gas. One expresses this in a most general manner as:

$$\left(\frac{\delta P}{\delta\rho}\right)_{\rho_0} = \left(\frac{\delta P}{\delta\rho}\right)_{E_i} + \left(\frac{\delta P}{\delta E_i}\right)_{\rho} \frac{\delta E_i}{\delta\rho} \tag{6.10}$$

For a sinusoidal process the solution of Equation 6.2 takes the form:

$$E_i = \frac{1}{1 - j\omega\tau} E_{ieq} \tag{6.11}$$

After substituting this to Equation 6.10:

$$\left(\frac{\delta P}{\delta\rho}\right)_{\rho_0} = \left(\frac{\delta P}{\delta\rho}\right)_{E_i} + \frac{1}{1 - j\omega\tau}\left(\frac{\delta P}{\delta E_i}\right)_{\rho}\left(\frac{\delta E_{ieq}}{\delta\rho}\right) \tag{6.12}$$

The first term of the above equation determines the perturbation taking place in the medium without the participation of changes in the internal energy level of particles which occur when the vibration frequency is so high that the internal vibrations and rotation of the molecules have no time to develop $(\omega\tau >> 1)$. This term describes the behaviour of an ideal gas having a specific heat C_{va}. The velocity of wave propagation in such a gas will be:

$$\left(\frac{\delta P}{\delta \rho}\right)_{E_i} = c_a^2 \tag{6.13}$$

The second term of the equation gives the influence of the energy absorption by molecules on the propagation velocity of the perturbation. This can be written as:

$$\left(\frac{\delta P}{\delta \rho}\right)_{r_0} = \frac{1}{1 - jwt}\left[\left(\frac{\delta P}{\delta \rho}\right)_{eq} - jwt\left(\frac{\delta P}{\delta \rho}\right)_{Ei}\right] \tag{6.14}$$

The quantity

$$\left(\frac{\delta P}{\delta \rho}\right)_{eq} = \left(\frac{\delta P}{\delta \rho}\right)_{Ei} + \left(\frac{\delta P}{\delta E_i}\right)_{\rho} \frac{\delta E_{eq}}{\delta \rho} \tag{6.15}$$

determines the velocity c_{eq} of the perturbation which is so slow ($\omega\tau << 1$) that the state of equilibrium between the internal and external energy of the molecules is maintained throughout the processes:

$$c_{eq}^2 = \left(\frac{\delta P}{\delta \rho}\right)_{eq} \tag{6.16}$$

This velocity is less than c_a and, since this refers to the processes in which the full value of C_{vi} is appreciable, $C_v = C_{va} + C_{vi.}$

The last term in the Equation 6.14 determines the passage from a very slow process to a very rapid process. It gives the influence of frequency involved in the molecular phenomena on the propagation of the acoustic wave.

Representing dilation (i.e. the relative change in the volume) of the medium as ϑ and separating the real and imaginary parts of Equation 6.14 one obtains:

$$-p = \left[\frac{c_{eq}^2 + (\omega\tau)^2 c_a^2}{1 + (\omega\tau)^2} + j\frac{\left(c_a^2 - c_{eq}^2\right)\omega\tau}{1 + (\omega\tau)^2}\right]\rho_0 \vartheta \tag{6.17}$$

The processes due to wave propagation are approximately adiabatic, hence:

$$c_{eq}^2 = \frac{C_p}{C_{va}+C_{vi}}\frac{P_0}{\rho_0},\quad c_a^2 = \frac{C_p}{C_{va}}\frac{P_0}{\rho_0} \tag{6.18}$$

Since C_p is independent of relaxation phenomena,

$$\left(\frac{c_a}{c_{eq}}\right)^2 = \frac{C_{va}+C_{vi}}{C_{va}} \tag{6.19}$$

After substituting the values of c_{eq} or c_a in to Equation 6.17 one gets:

$$-p = \rho_0 c_{eq}^2\left[\frac{1+\frac{C_{va}+C_{vi}}{C_{va}}(\omega\tau)^2}{1+(\omega\tau)^2} + j\frac{C_{vi}}{C_{va}}\frac{\omega\tau}{1+(\omega\tau)^2}\right]\vartheta \tag{6.20}$$

Thus reduction of pressure is related to the ratio of specific heats. Following this theory the attenuation constant (a_{ml}) and wave propagation velocity (c_{ml}) are given as:

$$\alpha_{ml} = \frac{1}{c_a}\frac{\chi-1}{2\chi}\frac{C_{vi}}{C_{va}}\frac{\omega^2\tau}{1+(\omega\tau)^2},\quad c_{ml} = c_a\left[1+\frac{\chi-1}{2\chi}\frac{C_{vi}}{C_{va}}\frac{\omega^2\tau}{1+(\omega\tau)^2}\right] \tag{6.21}$$

Thus, this theory led to a practical method of determination of the attenuation of acoustic waves by determining the attenuation constant.

6.4 Evaluation of Air Absorption

A propagating sound wave loses energy because of heat conduction, radiation, viscosity and diffusion. According to the classical absorption theory such loss is proportional to the square of frequency and does not depend on humidity. Molecular absorption in still homogeneous air is an exponential effect. It is expressed as proportional to the distance from the source. The constant of proportionality is referred to as the attenuation coefficient, α. Thus,

$$A_a = \alpha\frac{r}{1000} \tag{6.22}$$

where,

A_a : Excess attenuation due to air absorption at a distance r from the source

Kneser (1933) theoretically evaluated the attenuation coefficient due to air absorption as a function of frequency, humidity and temperature. This finding was experimentally verified by Knudsen (1933). Though the theoretical results and the experimental values were closer when these values were near to the peak value when the curves of α/α_{max} versus normalised absolute humidity were plotted, the measured data were generally higher than the theoretical values. Based on these studies, design charts were prepared for engineering estimations of the excess attenuation in still air to account for the molecular absorption (Wiener, 1980).

Effects of the atmosphere are accounted for in the German Standards (VDI 2714/VDI 2720), considering the absorption in air and attenuation over ground surface under different meteorological conditions. In the case of octave bands, α_a is calculated in dB per metre as:

$$\alpha_{a,\ octave} = \left[0.02 + 0.36 f(kHz) + 0.036\left(f(kHz)\right)^2\right] 10^{-2} \qquad (6.23)$$

A method of calculating air absorption is also provided in ISO 3891. It is suggested in the German Standards that for octave bands above 2000 Hz, the attenuation values are to be calculated at a frequency which corresponds to the lower third octave in the relevant octave bands. This takes into account the attenuation within the band itself that causes lower frequencies within each band to predominate.

Figure 6.1 shows the attenuation due to air absorption calculated using Equation 6.23 for different source-receiver distances (R). This equation has taken the effects of humidity and temperature into consideration. However, this method does not allow the selection of the prevailing temperature and relative humidity values to determine the attenuation.

Sutherland *et al* (1974) determined the coefficients of air attenuation for different meteorological conditions and tabulated these as shown in Table 6.1. The air attenuation

model developed by the author uses these values for prediction purposes as it allows to select the most appropriate factor for the prevailing ambient temperature and the relative humidity. Figure 6.2 illustrates the attenuation due to air absorption at 50% relative humidity with an ambient temperature of 20 ^{0}C.

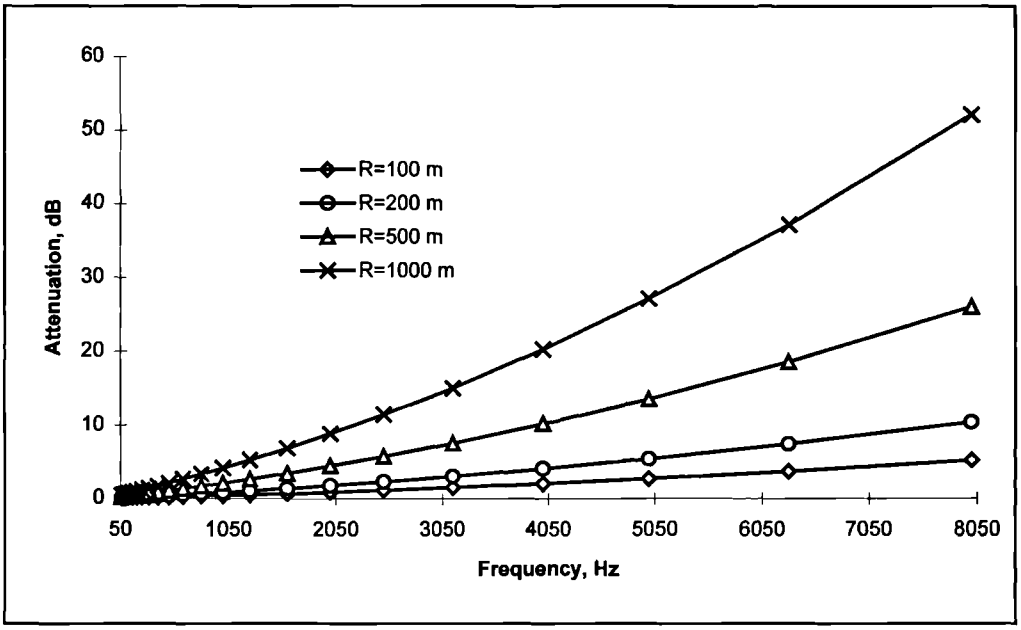


Figure 6.1 Attenuation due to air absorption (derived from the German Standards VDI 2714/VDI 2720).

Table 6.1 Attenuation due to atmospheric absorption (after Sutherland *et al*, 1974).

Humidity	Temp.	a (dB per 1,000m)							
(%)	(^{o}C)	63 Hz	125 Hz	250 Hz	500 Hz	1 kHz	2 kHz	4 kHz	8 kHz
	15	0.2	0.6	1.3	2.4	5.9	19.3	66.9	198.0
25	20	0.2	0.6	1.5	2.6	5.4	15.5	53.7	180.5
	25	0.2	0.6	1.6	3.1	5.6	13.5	43.6	153.4
	30	0.1	0.5	1.7	3.7	6.5	13.0	37.0	128.2
	15	0.1	0.4	1.2	2.4	4.3	10.3	33.2	118.4
50	20	0.1	0.4	1.2	2.8	5.0	10.0	28.1	97.4
	25	0.1	0.3	1.2	3.2	6.2	10.8	25.6	82.2
	30	0.1	0.3	1.1	3.4	7.4	12.8	25.4	72.4
	15	0.1	0.3	1.0	2.4	4.5	8.7	23.7	81.6
75	20	0.1	0.3	0.9	2.7	5.5	9.6	22.0	69.1
	25	0.1	0.2	0.9	2.8	6.5	11.5	22.4	61.5
	30	0.1	0.2	0.8	2.7	7.4	14.2	24.0	58.4

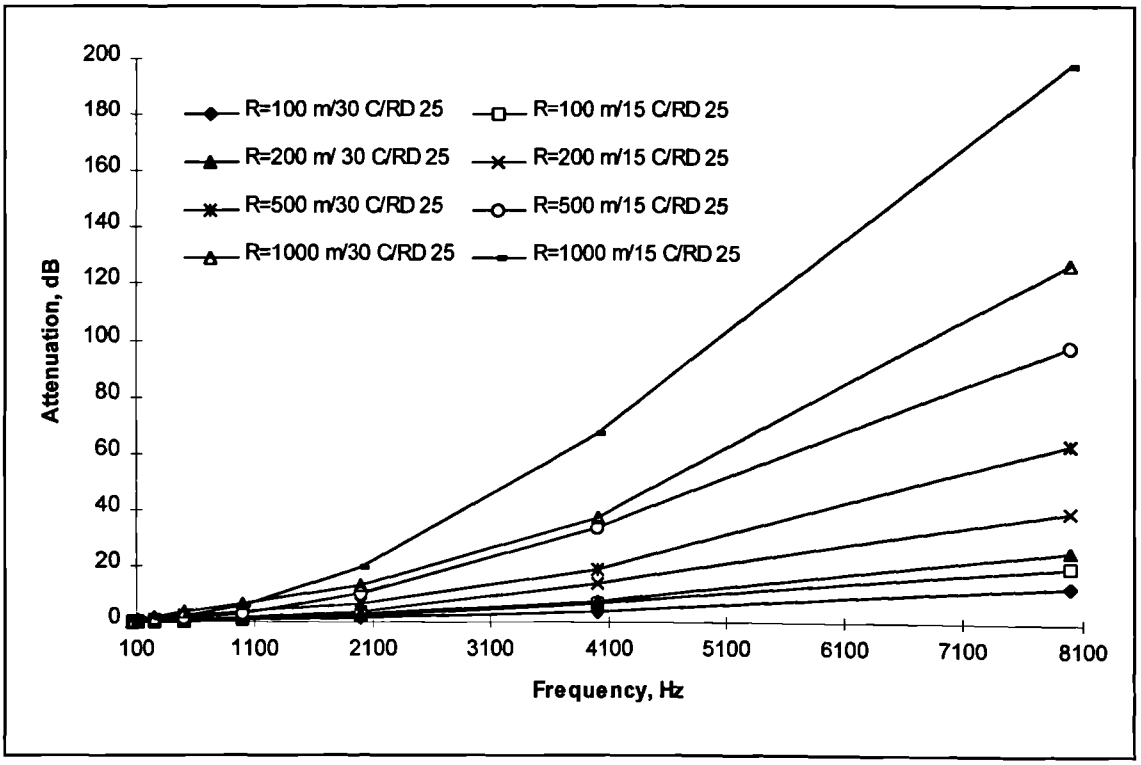
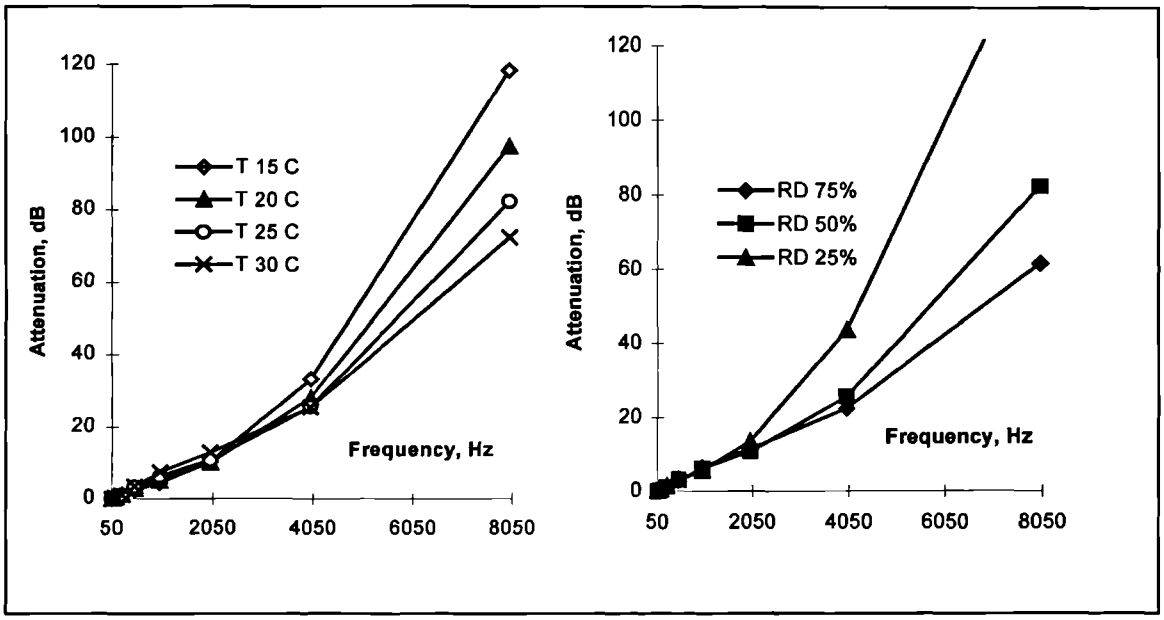


Figure 6.2 Air attenuation at different atmospheric conditions (drawn after Sutherland *et al*, 1974).



(a) (b)

Figure 6.3 Attenuation due to air absorption over a distance of 1000 m, (a) At 25^{o} C, (b) At 50 % relative humidity.

The dependence of the attenuation due to air absorption on the meteorological conditions can be seen from Figure 6.3. It is obvious from these graphs that the air attenuation model must take the atmospheric conditions into account.

6.5 Meteorological Effects on Sound Propagation

The ambient noise level at some distance from a source is a function of the spatial variation of speed of sound. Spatial variation of wind velocity and air temperature induces refraction of acoustic rays. This phenomenon results in a change of ray trajectory. Consequently, the noise level at the receiver changes with the spatial variation of wind velocity and temperature.

Theoretical aspects of meteorological effects of acoustic propagation were studied by many researchers. Chessell (1973) described a method for three-dimensional acoustic-ray tracing in a non-homogeneous anisotropic atmosphere. Daigle *et al* (1983) studied the propagation of sound taking temperature gradient and turbulence into account. Using a method derived from geometrical optics, Raspet *et al* (1985) studied sound propagation in a layered atmosphere bounded by ground surface. Rasmussen (1986) developed a method to account for the influence of wind and temperature gradient.

There were many experimental studies as well. Scholes and Parkin (1967) experimentally studied the effect of wind and temperature gradients on sound propagation. The general approach in environmental noise prediction is to classify the atmospheric conditions and specify the effects. Marsh (1982) used such a classification in developing the CONCAWE model for noise prediction. None of these theories have been specifically tested under the conditions that prevail in surface mines. The effects of the atmosphere on noise propagating from the pit bottom have not yet been established. The present study has not included theoretical analysis of the atmospheric effects. However, in order to account for the effects of meteorological parameters on noise attenuation, a methodology was developed using the accepted theories tested elsewhere. This methodology was incorporated in the air attenuation model in the form of a small software module (METEOK.CPP). The following section describes the theory relevant to the development of this module.

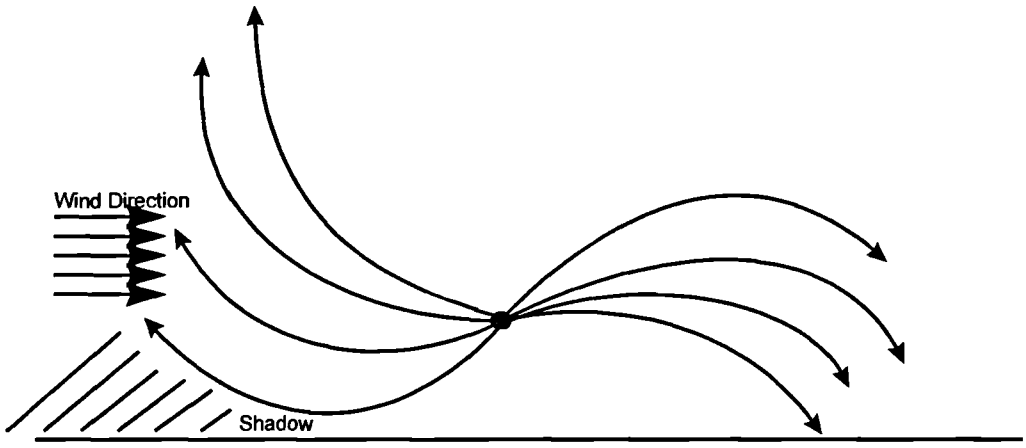


Figure 6.4 Effects of wind direction on sound propagation.

6.5.1 Ray Path Curvature

Atmospheric absorption, refraction and scattering by turbulence are the most significant meteorological effects on sound propagation. Standardised methods apply corrections of atmospheric absorption to take these into account on an average. Change of refractive conditions of the media modifies the radius of curvature of the ray path between a source and a receiver. The bending of rays with wind and temperature gradients can be represented as shown in Figure 6.4. Such bending results in a change in the path length between the source and the receiver. Depending on the phase relationship between the waves intersecting at the receiver, there occurs an amplification or attenuation of some frequencies. Due to the change of the ray path length, noise levels at the receiver vary depending on the meteorological conditions even if the source power is constant. When propagating with wind, the sound waves are convected towards the ground. This can partly or even totally neutralise the effect of a noise barrier constructed for noise control. Therefore, consideration of the wind pattern at a particular area is very important for noise control purposes. The wind velocity gradient changes with location, time of the day and the elevation. This leads to strong local and temporal fluctuations of the sound level that especially occurs at great distances from small localised sound sources. A pronounced directivity characteristic of the sound sources can augment this effect. Ray bending also occurs due to temperature gradients as shown in Figure 6.5.

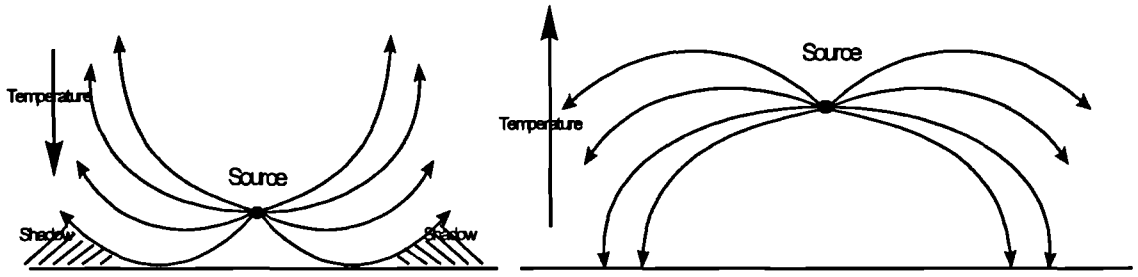


Figure 6.5 Effect of temperature gradient on acoustic propagation.

Turbulent scattering induces fluctuations of the phase and amplitude of the propagating sound waves. These cancel the interference between different rays arriving at the receiver. As a result of this phenomenon, sound levels higher than those expected are found for the frequencies with maximum ground effects. Moreover, due to turbulence, there is always some scattered sound in the shadow zone as well.

The weather's effect on sound pressure level is based on refraction. Upward bending of sound rays gives lower noise levels and downward bending offers higher noise levels. The parameter for characterising the curvature of near-horizontal sound rays due to refraction is given as (Gutenberg, 1942):

$$\frac{1}{R} = \frac{\dfrac{10}{\sqrt{T}}\dfrac{\delta T}{\delta z} + \dfrac{\delta u}{\delta z}}{c\left(1+\dfrac{u}{c}\right)^2} \tag{6.23}$$

where,

R : radius of curvature
T : temperature (K)
c : velocity of sound (m/s)
u : component of the wind vector (ms^{-1}) in the direction of the ray

Increase in the values of $1/R$ shows an increase in the sound level. The normalised curvature is taken as:

$$k \cong {(0.6 + \Delta T + \Delta u)}/{3.2} \tag{6.24}$$

where ΔT is the temperature difference in °C or K. Δu is the difference in the wind velocity component (ms^{-1}) at a height of 0.5 m and 10 m (the meteorological standard height for measurement of wind velocity). In the case where there is no profile measurement available from a meteorological mast, a method for estimating the radius of curvature without a profile measurement can be used (Larsson, 1992b).

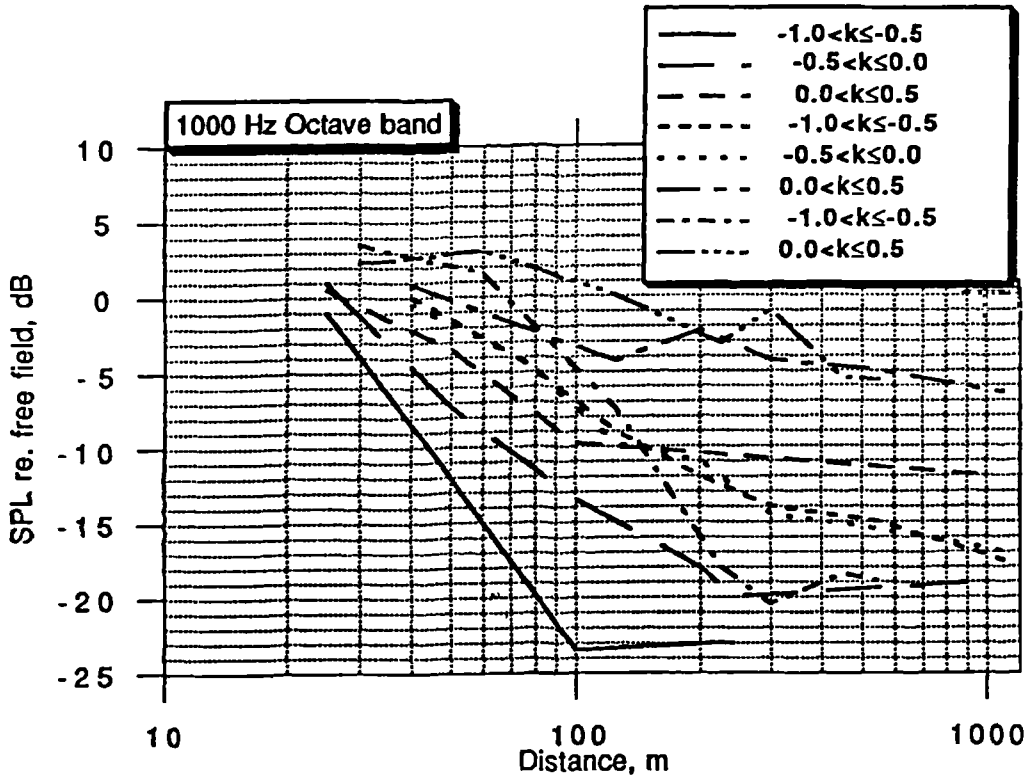


Figure 6.6 Sound pressure level and distance of propagation under different values of *k* under different values of source and receiver height (After Larson, 1992b).

The values of *k* vary during the day and throughout the year. Determining hourly values of *k* for a period of two years will provide a clear picture of how the propagation of noise changes over time due to meteorological changes. Negative values of *k* mean upward bending of the sound ray. This is usually expected during the summer when the temperature decreases with height. Upwind conditions in winter are compensated with a temperature increase with height. This phenomenon is more pronounced in aircraft noise. In mining noise, the vertical gradient is less important as the level difference between the source and the receiver is rarely very large. Figure 6.6 shows that when the

curvature is negative (-1.0 <k -0.5) the decrease in sound pressure level is about 15 dB per doubling of the distance. This rate continues to 100 to 300 metres when it attains a value of 6 dB per doubling the distance. For positive curvature (0<k<0.5), peak sound level is at 300-400 m. The distribution of k depends on the climate, and must be determined for individual sites.

6.5.2 Meteorological Considerations

Discarding some of the observational data is useful for calculating k in statistical noise estimation for practical purposes (Larsson, 1992b). If the minimum value of the hourly k on some days is less than -3.0, measurements from those days are rejected. The ground attenuation is much higher when the noise is generated near ground and the level difference of source and receiver is less. If a mine is very deep and spread over a large area, the determination of k is essential.

If one wishes to use the statistical method of analysing the meteorological data for noise prediction purposes, continuous monitoring for a long period is necessary as one requires at least seven days of significant data after rejecting the less significant data sets. Meteorological data for a longer period provide the distribution of the sound propagation conditions. To account for the meteorological effects on noise propagation at any specific site, one needs to determine the meteorological parameters of the site from the measured data over the area or collect it from the nearest meteorological test station. Such data may need careful analysis and structuring to represent the real site conditions. Along with the meteorological data source-receiver position is very important for noise prediction. A prediction model needs to include all possible alternative situations. From the meteorological and source-receiver location data the radius of curvature of the sound ray ($1/R$) can be calculated and the distribution of $1/R$ over a longer period can be evaluated.

The L_{eqA} and $L_{\max}$ should be calculated for different days. The overestimation of noise levels because of above rejection is avoided by calculating the expected level as the arithmetic mean values instead of the energy mean value from the seven days.

6.5.3 Estimation without Wind Profile Measurements

In the method stated above for calculating k, wind velocity and temperature profiles both near the source and the receivers are necessary as the input data. In the absence of such a measured and statistically processed database the following alternative method is useful.

Table 6.2 Aerodynamic roughness length for some typical terrain types (after Stull, 1988 and Oke, 1987).

Surface	Aerodynamic Roughness Length, z_0 (m)
Ice, mud flats	1 x 10-5
Snow: flat ground to farmland	0.1-11 x 10-4
Water: Calm to open sea	1-10 x 10-4
Sand, desert	5 x 10-4
Grass: cut or short (»0.02-0.1m)	0.003-0.02
Grass; long(»0.1-1m)	0.02-0.1
Farmland: open to hedged	0.02-0.1
European average	0.09
Wooded country	0.1-0.5
Dense woodland	0.3-1
Urban areas	04-3
Mountains	2-80

There is a relationship between wind velocity and temperature profiles. Neglecting the change in the wind profile due to the temperature profile, the wind speed, v, at height z is given as:

$$v(z) = \frac{u_*}{\kappa} \ln \frac{z}{z_0} \tag{6.25}$$

where,

κ : von Karman constant 0.4
z_0 : roughness length

z_0 is determined from Table 6.2. Friction velocity u_* is given as:

$$u_* = \frac{\kappa v(z_m)}{\ln \frac{z_m}{z_0}} \tag{6.26}$$

The friction velocity is determined from the measured values of wind speeds at different heights, z_m. For a wind speed difference between a receiver height of 10 m and 0.5 m, Δv is given by:

$$\Delta v = v(10) - v(0.5) = \frac{u_*}{\kappa}\left(\ln \frac{10}{z_0} - \ln \frac{0.5}{z_0}\right) \tag{6.27}$$

Δu for calculation of radius of curvature k can be calculated from the measurement of the angle ϕ_u between the direction of wind velocity and the line joining the source and the receiver using the equation:

$$\Delta = \Delta v \cos(\phi_u) \tag{6.28}$$

Δt for 0.5-10 m height can be determined from the elevation of the sun and wind velocity. In the past, this technique was applied to airport noise analysis and gave good results for positive values of k. Δt is evaluated by using the method of Turner (1964) as applied by Larsson (1992). Elevation of the sun is characterised by the net solar index (NSI). The values of NSI are selected using the following method (Turner, 1964): For given values of NSI Δt is calculated from Table 6.3.

- 1. If the cloud cover is 8/8 octas and the cloud base is less than 2500 m NSI is equal to 0 for day or night.
- 2. During the period between sunset and sunrise
  - a) If the total cloud coverage is less than or equal to 3/8, NSI = -2.
  - b) If the total cloud coverage is greater than 3/8, NSI= -1.
- 3.a During the daytime for cloud coverage less than or equal to 4/8:
  - a) If the solar altitude is less than or equal to 150 NSI = 1.
  - b) If the solar altitude is between 150 and 350, NSI = 2.
  - c) If the solar altitude is between 350 and 600, NSI = 3.
  - d) If the solar altitude is greater than 600, NSI = 4.
- 3.b During the daytime for cloud coverage greater than 4/8:
  - a) If the cloud base is less than 2500 m subtract 2 from NSI.
  - b) If the cloud base is higher than 2500 m subtract 1 from NSI.
  - c) If NSI comes to be less than 1 it is considered as 1.

Table 6.3 Values of Δt under different conditions.

Wind Speed, ms^{-1}	NSI=4	NSI=3	NSI=2	NSI=1	NSI=0	NSI=-1	NSI=-2
<0.8	-2.5	-2.5	-1.3	-0.2	-0.1	1.0	4.1
0.8—1.8	-2.5	-1.3	-1.3	-0.2	-0.1	1.0	4.1
1.8—2.9	-2.5	-1.3	-1.3	-0.2	-0.1	1.0	4.1
2.9—3.3	-1.3	-1.3	-0.2	-0.1	-0.1	0.0	1.0
3.4—3.9	-1.3	-1.3	-0.2	-0.1	-0.1	-0.1	0.0
4.O—4.9	-1.3	-0.2	-0.2	-0.1	-0.1	-0.1	0.0
5.0—5.4	-0.2	-0.2	-0.1	-0.1	-0.1	-0.1	0.0
5.5—5.9	-0.2	-0.2	-0.1	-0.1	-0.1	-0.1	-0.1
>5.9	-0.2	-0.1	-0.1	-0.1	-0.1	-0.1	-0.1

6.5.4 The Sound Propagation Parameter

As an alternative to the above method Larsson and Israelsson, (1991) defined a sound propagation parameter which is used to describe the noise level as a function of W:

$$W = \frac{k\left(z_s + z_r\right)^2}{d} \tag{6.29}$$

where,

k : normalised radius of curvature
z_S : source height
z_r : receiver height
d : distance between source and receiver

In a situation where W is nearly equal to zero, the sound pressure level of that area will be very sensitive to the weather conditions. Therefore, this method can be used to characterise the site in terms of noise level prediction.

6.6 The Development of the Air Attenuation Model

To apply the present theoretical knowledge for acoustic prediction in surface mining operations, one needs to develop an easy-to-use application module. Zouboff *et al* (1994) discussed an approach for qualitative assessment. However, such an approach needs further modification to provide the attenuation due to air absorption on a grid

around the mining area. Also, the mine planner needs to know how the prevailing weather conditions are influencing the noise field for evolving and updating their noise control measures.

The author has developed a model to predict the attenuation due to absorption by air and to determine the radius of curvature of the ray path for any location of the receiver around a mine or a quarry. The model can be used to obtain the cumulative distribution of k over a longer period for general mine planning purposes.

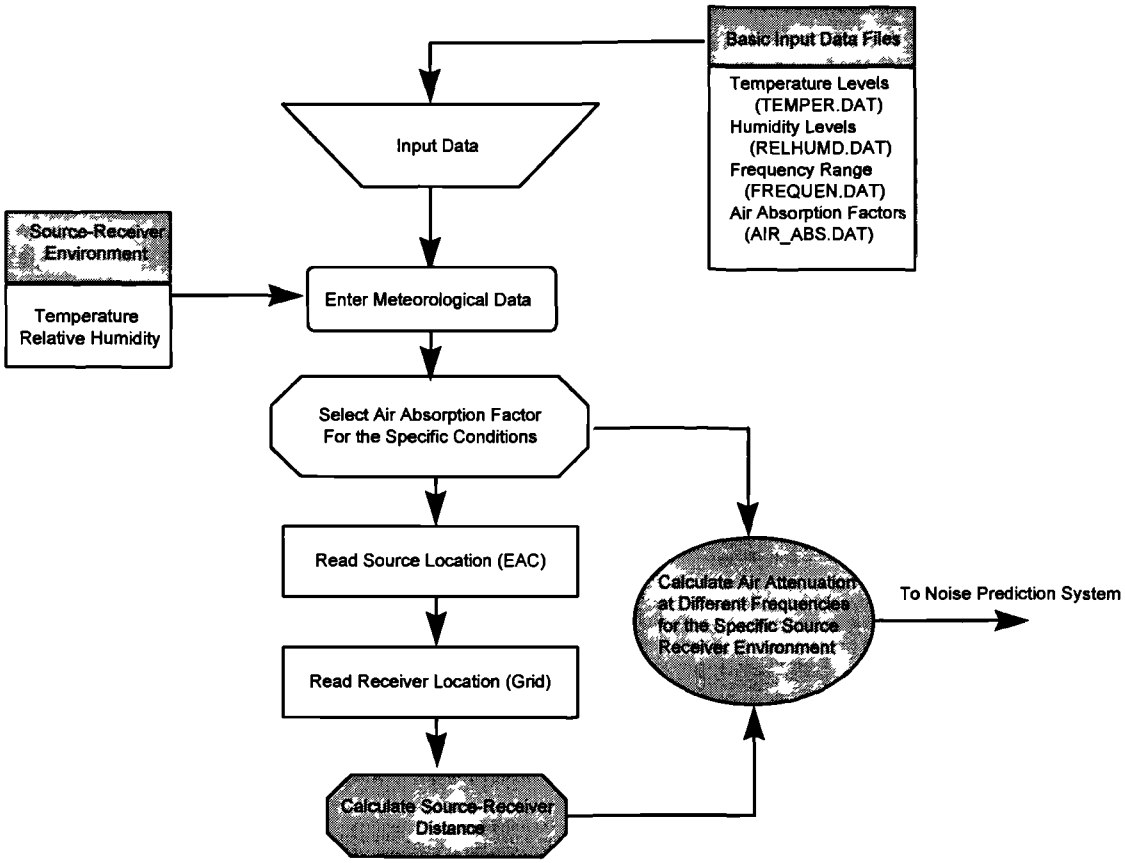


Figure 6.7 Air attenuation model.

The principles and theory discussed in Section 6.4 were used in developing the air attenuation model for use in the mining and quarrying environment. Figure 6.7 shows the structure of the air attenuation model. Using the values of absorption rate m the air absorption (A_a) at a distance X can be determined by the equation:

$$A_a = mX \tag{6.22}$$

In the model application the distance X to the receiver point is measured from the co-ordinates of the EAC. Values of air absorption factor for different relative humidities (RH) and temperatures (T) are retrieved from the input data files provided by the user (Figure 6.7). In the absence of precise values of coefficient of air attenuation for different temperatures and relative humidities, ambient temperature is categorised in four levels as 0, 1, 2 and 3. The air absorption values of 15°, 20°, 25° and 30° are then selected for these categories respectively. Similarly relative humidity is categorised into 3 categories: 0, 1, 2. The temperature and relative humidity values provided by the user are assigned a category value and the corresponding air absorption coefficient is selected from the source table. Table 6.4 shows the assumed categories.

The model (AIRABFIN.CPP) was developed to determine the value of A_a for any location of the EAC and receiver, based on Sutherland *et al* (1974) and German Standard. This is used in the noise prediction models described in Chapter 8.

Table 6.4 Assumptions in development of the air attenuation module.

Parameter	Category	Range	Value for Air Attenuation
Temperature, °C	0	<17.5	15
	1	17.5-22.5	20
	2	22.5-27.5	25
	3	>27.5	30
Relative Humidity, %	0	<0.35	25
	1	0.35-0.65	50
	2	>0.65	75

In a large and deep surface mine the meteorological parameters are more predominant factors in affecting the pit-to-surface propagation of noise. The ray path of noise propagation in such cases cannot be assumed to be straight and therefore the determination of the radius of curvature of the ray path is necessary. In the air attenuation model, the effects of the meteorological parameters were incorporated using the theory discussed in Section 6.5. A small module (METEOK.CPP) was developed for this purpose. Figure 6.8 shows the basic steps involved in the module and Figure 6.9 is a

sample output of the module for a four hourly logging of temperature and wind velocity data. As noted in

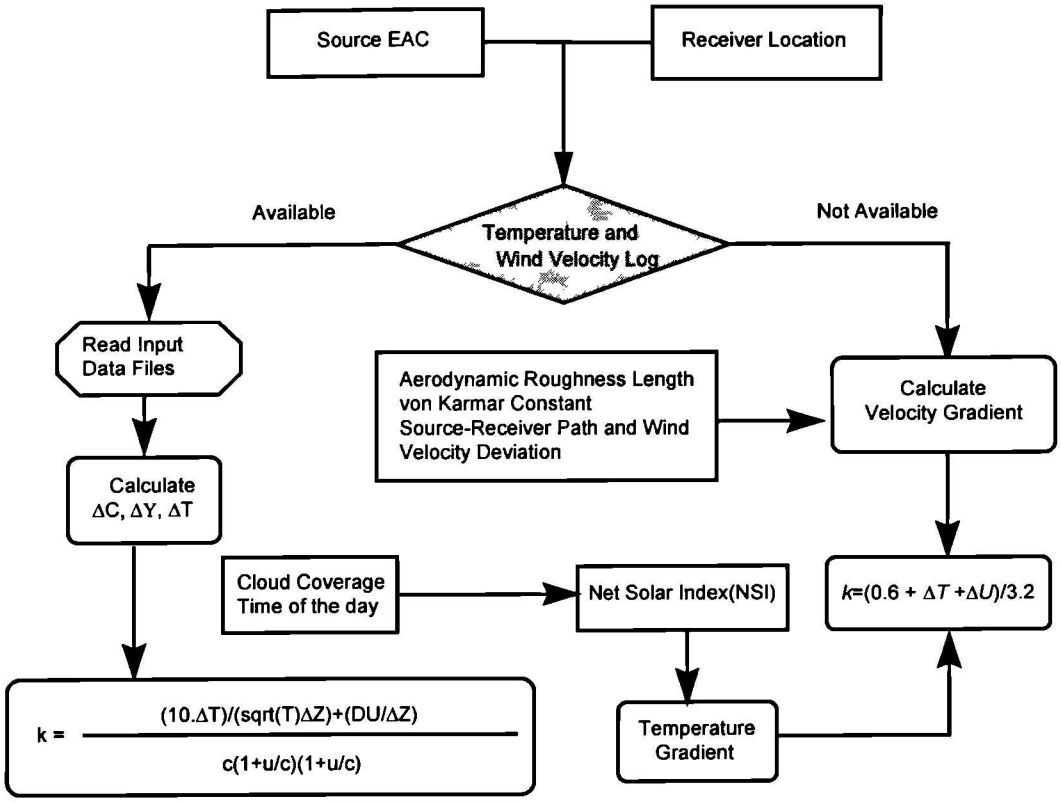


Figure 6.8 Steps to determine the radius of curvature of acoustic path from source to receiver.

```
**********OUT PUT OF METEOK.CPP**************

Input data files are:

        1. qbottemp.dat : Temperature at pit bottom.
        2. qsurtemp.dat : Temperature at pit top.
        3. temgrad.dat  : Temperature gradients.
        4. qsurwin.dat  : Wind velocity at pit top.
        5. qbotwin.dat  : Wind velocity at pit top.
        6. wingrad.dat  : Wind velocity gradients.


Pit surface level : 200
Pit bottom level : 65

Number of intervals of daily data record : 6

        Hour        Radius of Curvature

          1          -0.876605
          2          -0.854019
          3          -0.865109
          4          -1.4456
          5          -1.94428
          6          -2.25397
```

Figure 6.9 Sample output of module METEOK.CPP.

the output file the module reads the input data from a number of files. These files store the processed meteorological data. The temperatures and the wind velocity are monitored continuously by the commercially available data acquisition systems. These data are processed to provide the best statistical information for the *base period* of noise prediction. The base period of noise prediction is the duration of measurement of equivalent continuous sound pressure level. The sample output shows the ray path curvature to determine four hourly L_{eq}. Therefore, in this case the input data files provided the most significant and representative values of the temperatures and wind velocities of the surface mine at the pit top and pit bottom. In the absence of such statistically measured data the module determines the values of k by using the theory discussed in Section 6.5.3 and the Table 6.3. Figure 6.10 shows a sample output of this procedure of the module.

```
**********OUT PUT OF METEOK.CPP**********
        Without measurement of Wind Profile

Pit surface level :200
Pit bottom level :60
Terrain Type : Farm Land
Net Solar Index :2

Number of intervals of daily data record :6

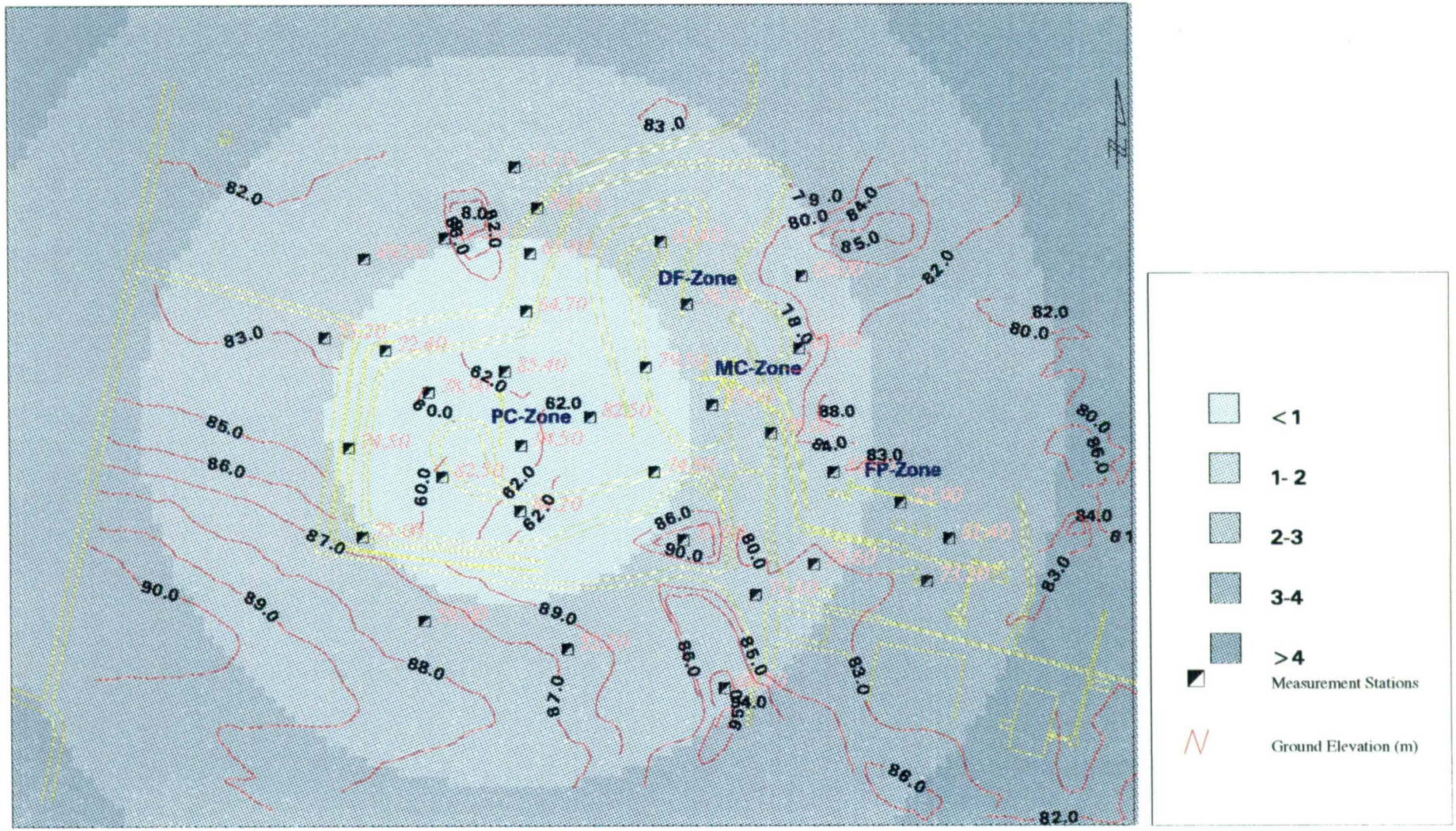
        Hour            Radius of Curvature

          1                 0.180914
          2                 0.17927
          3                 0.182559
          4                 0.182559
          5                 0.184203
          6                 0.181737
```

Figure 6.10 Sample output of METEOK.CPP determining radius of curvature of sound propagation path without wind profile measurement.

For shallow depth quarries and surface mines the ray path curvature is not very important since the height differences of the source and the receiver are not very large. However, for long distance propagation of noise, attenuation due to air must take the ray path curvature into account. As illustrated in Figure 6.7, values of k influence the sound pressure level in the free field.

Figure 6.11 Attenuation due to air of the noise generated in the Primary Crusher Zone of the test quarry.


DF-Zone
MC-Zone
PC-Zone
FP-Zone
< 1
1- 2
2-3
3-4
> 4
Measurement Stations
Ground Elevation (m)

The model developed (AIRABFIN.CPP) has been used to predict the air attenuation over the quarry described in Chapter 4. The predicted values are presented in a shaded grid by using the GIS. Figure 6.11 presents the attenuation due to air around the test quarry.

6.7 Conclusion

Attenuation of acoustic energy due to molecular absorption in air has been formulated by different researchers. The author has adopted the values obtained by Sutherland *et al* (1974) and developed a model to predict attenuation due to absorption in air considering temperature and relative humidity (AIRABFIN.CPP). A procedure has been developed to determine the ray path curvature due to temperature and wind velocity gradient between the source at the pit bottom and the receiver positions outside the mine. The program METEOK.CPP can be used to determine the radii of curvature of ray paths in a surface mining site, provided that the necessary meteorological input data are available. However, in the present work no experimental verification of the temperature and velocity gradient within a surface mine was possible. In the present model straight line propagation of acoustic waves has been assumed. Chapter 8 describes a case study of environmental noise level prediction near a quarry which uses the air attenuation model described in this chapter.

In surface mining and quarrying the pit walls act as an important noise-reducing barrier. The theory of noise attenuation due to the pit wall and the prediction model developed for this purpose will be discussed in the next chapter.

Chapter 7

The Development of a Pit-Wall Attenuation Model

7.1 Introduction

Chapters 5 and 6 described the attenuation of sound energy due to ground absorption and air absorption. The noise level at any location is also attenuated by the presence of a barrier between the source and the receiver. In this thesis, any physical obstruction that interferes with the direct line of sight between a source of sound and a receiver is referred to as a *barrier*. Concrete blocks, asbestos, sheet metal, fibre glass panels and high density plastic are used for constructing such barriers for noise control purposes. The concept of noise barriers was developed from the use of partial enclosures for noisy equipment in studying room acoustics. The diffraction of acoustic waves at the edge and around the end of the barriers determines the extent of attenuation due to a barrier. With non-porous barriers of sufficient surface density the receiver will be subjected to sound energy due to the diffraction of sound waves around the boundaries of the barrier. Many theoretical and experimental studies on barriers suggested that a barrier of superficial

weight equal to 10 kgm^{-2} can provide a transmission loss of 20 dB (Kurze, 1974). Redfearn (1940) developed a practical method to use the theory of acoustic wave diffraction for the design of acoustic barriers. Maekawa (1965) experimentally developed a design chart for barrier attenuation. Rathe (1969) obtained barrier attenuation by the integral equation of Fresnel. Kurze and Anderson (1970) considered the case of oblique incidence and derived an equation for determining attenuation due to a barrier. This equation conforms with the findings of Rathe and the experimental results of Maekawa (1962). Jonassion (1972b) studied the barrier effect of depressed roads. De Jong *et al* (1976) modified the theory for barrier loss (Maekawa, 1968), and included the wind and temperature effects in this analysis. Elizabeth and Russel (1977) studied attenuation of sound by wide barriers. The Department of Transport, UK, prepared guidelines for calculating barrier loss for depressed roads (HMSO, 1988). These procedures provide the basic theories and methodologies for determining the attenuation of sound energy during propagation from a source located at the pit bottom. However, careful consideration of the geo-mining conditions is necessary when applying these procedures for predicting environmental noise levels near surface mining and quarrying operations.

The study of the propagation of acoustic waves from sources located at the floor of a surface mine necessitates the development of a methodology using the theories of acoustic barriers. A generalised methodology is difficult to establish as the site conditions vary widely from one site to another. Even a single site may offer number of different solutions. In surface mining the pit-walls behave like noise barriers between the noise sources such as the mining machinery and the receivers. They intercept the direct source-to-receiver propagation path. Isei *et al* (1980) developed a theory for analysing ground absorption during sound propagation over a barrier. Hasabe and Kaneyasu (1987) extensively worked with the theory of barrier effects of walls of depressed roads. Earlier studies on barrier attenuation were mainly aimed at designing acoustic barriers to control noise. One main objective of this research has been to incorporate barrier attenuation in the noise prediction system developed.

In surface mining one needs to consider a number of different types of noise barrier:

1. Screen-type barrier
    a. Semi-infinite rigid screen
    b. Absorbing screen
    c. Screen on a rigid ground
    d. Screen on an absorptive ground
    e. Screen of finite length
2. Wedge shaped barrier
3. Wide barrier
4. Buildings as barrier
5. Trees as barrier

The performance of these barriers depends on the angle of incidence of the sound waves, materials of construction of the barrier, acoustic properties of the ground, barrier geometry, location of the sound source with respect to the barrier, the type of source, atmospheric conditions, etc. The analysis of all these factors is beyond the scope of this research. The author considers the pit-walls as the main cause of noise attenuation due to barrier effects in surface mining. This chapter discusses the theories relevant to barrier attenuation and describes the model developed by the author to predict the attenuation due to the barrier effect of pit-walls in surface mining operations.

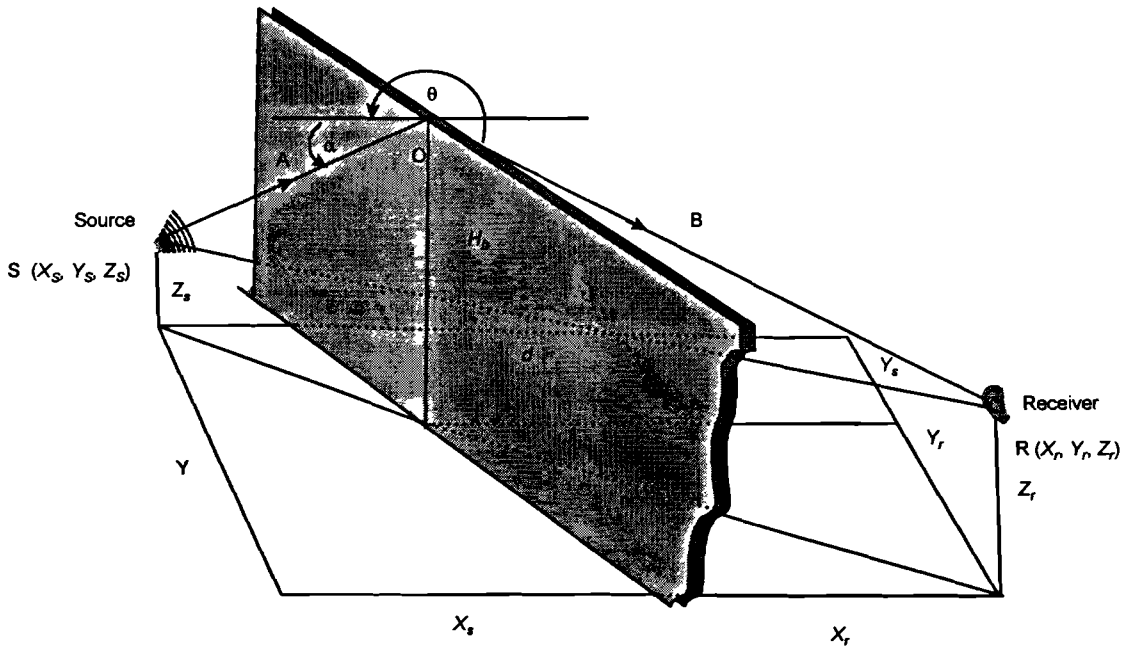


Figure 7.1 The geometry of the sound propagation path over a barrier wall.

7.2 The Basic Theory of Barrier Attenuation

Acoustic rays are diffracted over the edge of a barrier. Figure 7.1 illustrates the geometry of sound propagation over a thin barrier between the source and the receiver. In order to determine the attenuation caused by a barrier the difference between the diffracted path and the direct path in the absence of the barrier is calculated. On the basis of this path difference (δ) the Fresnel number (N) is defined as:

$$N = \pm \frac{\text{path length difference}}{\left(\frac{\lambda}{2}\right)} = \pm \frac{A + B - d}{\left(\frac{\lambda}{2}\right)} \tag{7.1}$$

$$N = \frac{2\delta}{\lambda} \tag{7.2}$$

where,

λ : wavelength
A : distance from the source to the edge of diffraction
B : distance from the edge of diffraction to the receiver
d : distance from the source to the receiver in the absence of the barrier
δ : path difference

Rathe (1969) considered attenuation due to a barrier, A_b, to be equal to 5 dB for cases where the Fresnel number is 0. That is, if the source, point of diffraction and the receiver lie on the same line then the barrier attenuation is 5 dB. For Fresnel number greater than or equal to 1, barrier attenuation was given as:

$$A_b = 13 + 10\log(N) \qquad for \quad N \geq 1 \tag{7.3}$$

Rathe (1969) also developed a table for barrier attenuation in terms of a characteristic frequency, f_1. In this method, the maximum attenuation by a barrier was considered to be 24 dB. Characteristic frequency f_1 was defined as:

$$f_1 = \frac{c}{4\delta} \tag{7.4}$$

Table 7.1 gives the values of attenuation due to a thin barrier as suggested by Rathe (1969). Kurze and Anderson (1970) have suggested the following equation for barrier attenuation:

$$A_b = 5 + 20\log\frac{(2\pi N)^{1/2}}{\tanh(2\pi N)^{1/2}} \tag{7.5}$$

Table 7.1 Attenuation by thin barriers (after Rathe, 1969).

Freq (Hz)	$< \frac{f_1}{64}$	$\frac{f_1}{64}$	$\frac{f_1}{32}$	$\frac{f_1}{16}$	$\frac{f_1}{8}$	$\frac{f_1}{4}$	$\frac{f_1}{2}$	f_1	$2f_1$	$4f_1$	$8f_1$	$16f_1$	$32f_1$	$64f_1$
A_b (dB)	5	5	6	6	7	8	9	11	13	16	19	22	24	24

The difference between these two approaches can be seen from Figure 7.2.

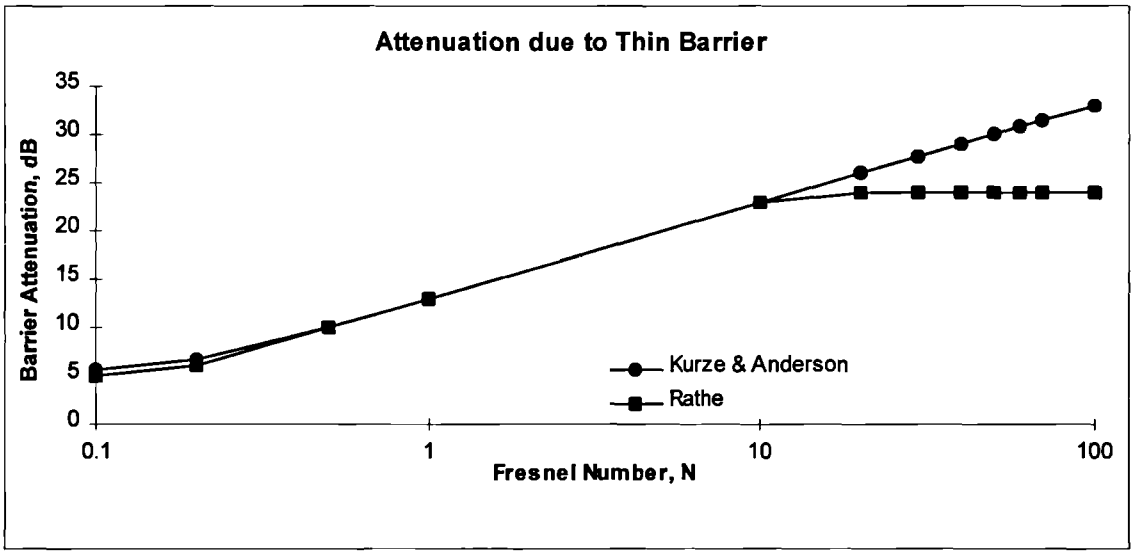


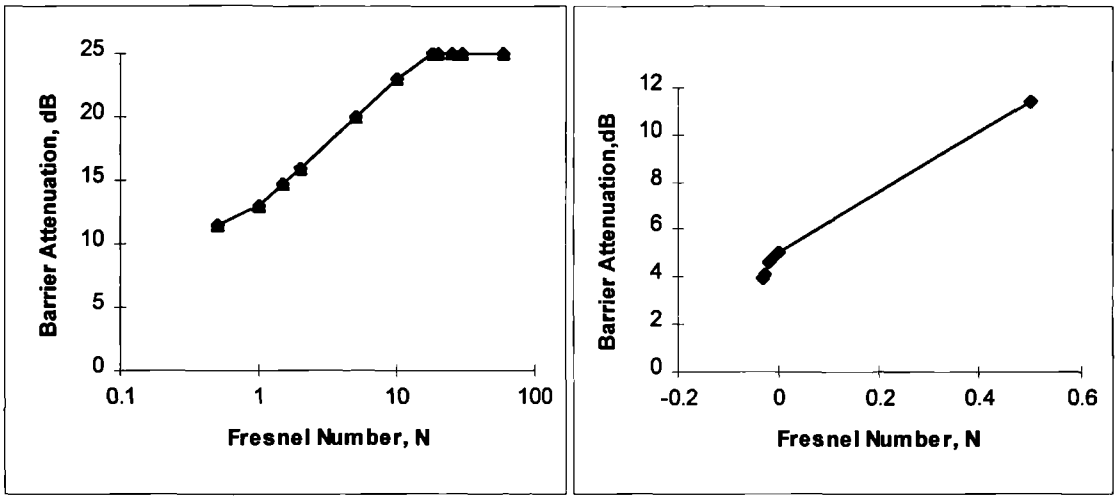
Figure 7.2 Attenuation due to a thin barrier (after Kurze and Anderson, 1970; Rathe, 1969).

The CONCAWE[1] model calculates the barrier attenuation, A_b as (Marsh, 1982):

[1] The Oil Company's International study group for Conservation of Clean Air and Water

$$\begin{aligned} -0.3 \le N < -0.02 \quad & A_b = 5.65 + 66N + 244N^2 + 287N^3 \\ -0.02 \le N < 1.0 \quad & A_b = 5.02 + 21.1N - 19.9N^2 + 6.69N^3 \\ 1.0 \le N < 18.0 \quad & A_b = 10\log N + 13 \\ N \ge 18.0 \quad & A_b = 25 \end{aligned} \tag{7.6}$$

Figure 7.3 illustrates these values graphically for the lower and higher regions of Fresnel Number.



(a) (b)

Figure 7.3 Barrier attenuation calculated using CONCAWE model for (a) higher values of Fresnel Number and (b) Lower values of Fresnel Number (after Marsh, 1962).

For a semi-infinite rigid screen one can determine the barrier loss of the sound energy radiated by a point source by the following equation (Kurze, 1974):

$$\Delta L = 10\log 4\pi^2 \frac{\delta}{\lambda} - 20\log\frac{d}{A+B} + 10\log\left(1+\frac{d}{A+B}\right) - 20\log\left(1+\frac{\sin\varphi/2}{\sin\left(\theta+\varphi/2\right)}\right) \tag{7.7}$$

where,

ΔL: loss due to the barrier
λ : wavelength
A : distance from the source to the edge of diffraction
B : distance from the edge of diffraction to the receiver
d : distance from the source to the receiver in the absence of the barrier
δ : path difference
θ : angle between the diffraction plane and a line joining diffraction point and the receiver
φ : deviation angle of the direct ray path to arrive at the receiver

7.2.1 Wind Effect on Barrier Attenuation

In long distance propagation of sound, atmospheric bending and scattering of acoustic waves into the shadow zones reduce the effectiveness of barriers. The effects of wind, temperature and humidity was not accounted for in the above methods of barrier attenuation calculations. Therefore, the theoretically predicted barrier attenuation is usually higher than the measured values. Various experimental results have shown that maximum barrier attenuation lies within 25-30 dB.

The atmospheric effects of sound propagation were discussed in Chapter 6. A wind gradient is caused by the friction between a moving mass of air and the ground surface, and also by the temperature gradient. Under the conditions of temperature inversion sound waves bend towards the ground surface. This tends to reduce the shielding effect of a barrier. It was observed that at a wind velocity of 16 kmh^{-1}, the reduction at 200 Hz is 0. However, at 6400 Hz the reduction is 13 dB (Scholes *et al*, 1971).

The BBN/EEI noise model[1] considers that the wind and atmospheric conditions reduce the effect of the barrier by a factor of (1-*d*/3000) whenever the combined distance of the source to the barrier and of the receiver to the barrier exceeds 600 m. Here, *d* is the direct distance from the source to the receiver.

If the wind direction is within ±22.5° of the source-receiver line and if the wind speed exceeds 5 ms^{-1} the barrier attenuation is assumed to be zero (no barrier) for predicting noise by considering long-term energy average conditions. Beyond the above downwind[2] angle the effects of the barrier start to develop again. This is because the sound waves bend over the top of the barrier as if it was not there. For the adjacent wind sectors (22.5°), the barrier attenuation is multiplied by a factor that follows a sinusoidal

[1] This noise prediction system was developed by Edition Electric Institute by Bolt Beranek and Newman Inc. in 1978.

[2] Wind from source to receiver

variation from zero at 22.5° to unity at 45°. In the case of upwind[1] noise propagation at any angle, the barrier attenuation is considered to be independent of the wind speed. For upwind and crosswind noise propagation conditions barrier attenuation is unchanged from the neutral conditions.

7.3 Barrier Attenuation of Surface Mining and Quarrying Noise

In surface mining and quarrying operations the predominant noise sources are located within the pit. The pit-walls behave as thick barriers and the noise propagating from these sources to the neighbourhood on the surface is attenuated. There are also some safety berms constructed on the pit top. This reduces the noise level for any receiver located outside the pit boundaries.

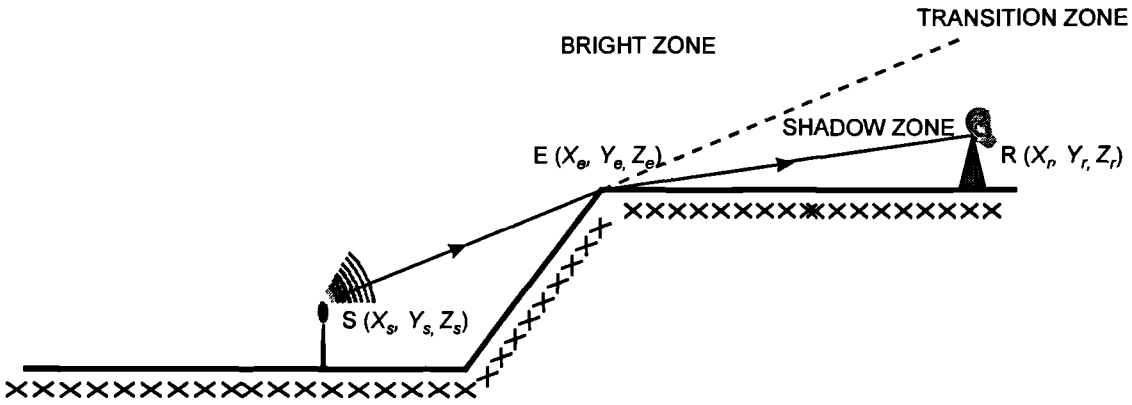


Figure 7.4 Diffraction of sound waves at the edge of pit-walls.

The Fresnel number for the diffraction of sound waves at the edge of the pit can be determined using Equation 7.1. The input parameters are calculated using the location of the source, receiver and the diffraction edge as shown in Figure 7.4.

The Fresnel number is positive if the pit-wall is in the line of sight. For this condition the slope of the line SE must be greater than or equal to that of the line ER. The region with positive Fresnel number is called the *shadow zone*. If the line joining the source and the receiver is not interrupted by the pit-wall the Fresnel Number is assigned a

[1] Wind from receiver to source

negative sign. The effect of the slope is observed very close to the edge of the barrier. The region near the line SE above the pit surface is known as the *transition zone*. Sound pressure level increases as one moves higher above the pit surface. The extent of the transition zone depends on the frequency content of the sound. The region with a negative Fresnel number is not affected by the barrier effect of the pit-walls. This region is called the *bright zone*. The depth of the pit and location of the source is important in determining the effects of the pit-walls on the sound pressure level exposure of the receiver. Alternatively, for a given pit geometry, the optimum location of the noise source within the pit can be determined for noise control purposes.

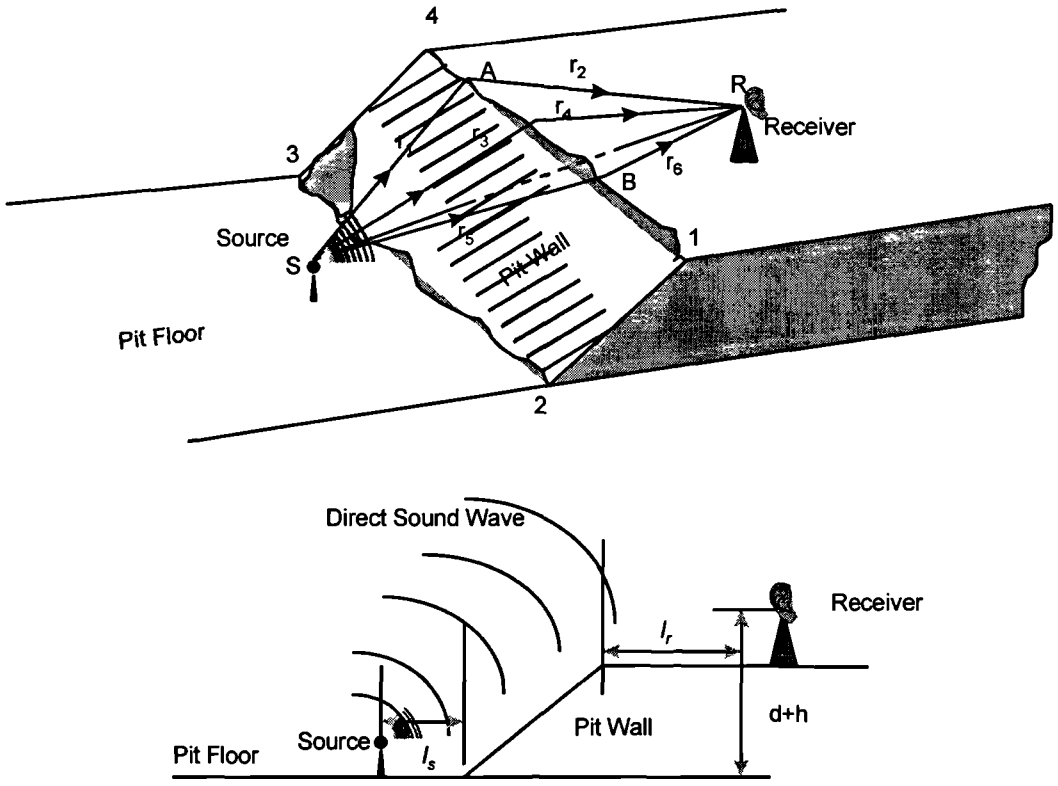


Figure 7.5 Pit-wall as a noise barrier.

7.3.1 Attenuation by the Pit-walls

Figure 7.5 illustrates a typical case of pit-wall as a noise barrier. The situation within a surface mine can be assumed to be similar to a semi-reverberant noise field where the noise source is surrounded by a number of reflecting surfaces. Let the mean square pressure at the receiver (R) in the absence of the barrier be represented as p_o^2. This

represents the situation when there is no obstruction between the source (S) and the receiver (R). Let the sound pressure level corresponding to this mean square pressure be L_{po}.

Let us define that L_W (dBA) is the sound power level of the source and Q_θ is the directivity factor at an angle in the direction of the receiver. r (m) is the distance between the source and the receiver. This is the shortest distance between S(X_S, Y_S, Z_S) and R(X_R, Y_R, Z_R).

If the soil or rock on the sloping surface 1234 (with a surface area A) has an average sound absorption coefficient α then the *site constant,* R_c, will be given by the following relationship assuming that the absorption in air is negligible:

$$R_c = \frac{S\alpha}{1-\alpha} \tag{7.8}$$

Thus, this constant depends on the average sound absorption coefficient of the surfaces present between the source and the receiver.

To develop a method for evaluating the sound energy loss due to the pit-wall (SL) the absorbing surface needs to be considered. Figure 7.5 shows that this area, subtended by the ray paths, comprises three parts. These include a triangular portion at the pit floor, another triangular portion at the pit-top surface and a trapezoidal inclined surface at the pit-wall. Area A is calculated using the co-ordinates of the source and receiver locations. The sound pressure level (without pit-wall loss) at a distance R from the source can be expressed as (Norton, 1989):

$$L_{\text{po}} = Lw + 10\log\left\{\frac{Q_\theta}{4\pi R^2} + \frac{4}{R_c}\right\} + D \tag{7.9}$$

Where,

L_{po}: sound pressure level
L_W: sound power level
Q_q : directivity factor
R : source to receiver distance
R_c : site constant
D : corrections accounting for the effects of various attenuation

Neglecting the corrections at this stage, Equation 7.9 can be expressed as:

$$L_{po} = L_W + 10\log\left(\frac{Q_\theta}{4\pi R^2} + \frac{4}{R_c}\right) \tag{7.10}$$

Now, let the mean square pressure at distance R with the pit-wall present be represented by p_2^2. The square of the pressure due to the diffracted field beyond the barrier (say, p_{b2}^2) can be taken as:

$$p_2^2 = p_{b2}^2 + \text{ Other Corrections}$$

$$\therefore L_{p2} = L_{b2} \qquad \text{(Neglecting the other contribution)}$$

The sound pressure loss due to the pit-wall (SL) is then given by:

$$SL = L_{po} - L_{p2} = 10\log\left(\frac{p_o^2}{p_2^2}\right) \tag{7.11}$$

This attenuation will be felt within the shadow zone as shown in Figure 7.6. The receiver is exposed to two types of noise fields, the *direct field* and the *diffracted field.*

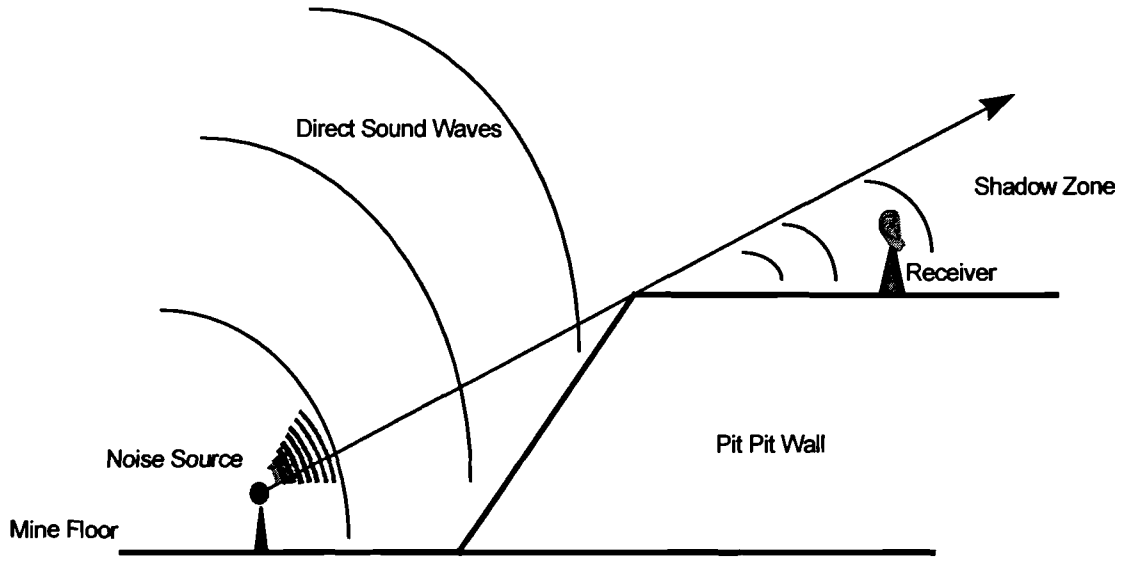


Figure 7.6 Sound fields for a noise source at the mine floor.

Sound energy will be diffracted from all the points along the line of the pit-wall. However, it can be assumed that the maximum effect will be along the line of shortest distance as shown in Figure 7.5. The receiver at R will be exposed to some direct wave as well as to the reflected sound waves from the opposite pit-wall. The correction for reflection from the opposite walls will be discussed in the next section.

The height of the shadow zone above the surface level is a function of the position of the noise source in the pit and on the depth and slope of the pit-walls. The height of the shadow zone above the surface level is a function of the location of the noise source in the pit and the depth and slope of the pit. The maximum height of influence, H will be given in terms of the co-ordinates of the source, receiver and the edge of the pit-wall by the equation:

$$H = X_r\left(\frac{d}{\sqrt{(X-X_s)^2+(Y-Ys)^2}}\right) \tag{7.12}$$

where,

d : depth pit-wall
H : maximum height of the shadow zone
X_r : x coordinate of the receiver
X_s : x coordinate of the source
Y_s : y coordinate of the source
X : x coordinate of the edge of pit-wall
Y : y coordinate of the edge of pit-wall

Thus, for a particular pit geometry, the attenuation will depend on the relative positions of the source and the receiver.

According to the Fresnel diffraction theory, only the portion of the energy that is incident upon the edges of a barrier contribute to the wave field that is diffracted beyond the barrier. Let the mean square pressure due to the direct field without the pit-wall be represented by p_{do}^2. The mean square pressure in the diffracted field can be written as:

$$p_{b2}^2 = p_{do}^2 \sum_{i=1}^{n}\left(\frac{1}{3+10N_i}\right) \tag{7.13}$$

The Fresnel number, N_i, is evaluated as:

$$N_i = \frac{2\delta_i}{\lambda} \tag{7.14}$$

where,

λ : wavelength of the sound frequency being considered
δ_i : difference between the *i*th diffracted path and the direct path between the source and the receiver without the barrier

If the lengths of the direct and indirect paths (r_i) are known the values of δ_i are calculated as:

$$\begin{aligned} \delta_1 &= (r_1 + r_2) - (r_3 + r_4) \\ \delta_2 &= (r_5 + r_6) - (r_3 + r_4) \\ \delta_3 &= (r_7 + r_8) - (r_3 + r_4) \end{aligned} \tag{7.15}$$

Considering a monopole source:

$$p_{do}^2 = \frac{W\rho_o c Q_\theta}{4\pi r^2} \tag{7.16}$$

Where,

W : radiated sound power of the source
ρ_o : mean density of the medium
c : speed of sound
Q_θ: directivity factor of the source

The distance between source and receiver (without the pit-wall) is given as:

$$r = \sqrt{\{(Xs - Xr)^2 + (Ys - Yr)^2 + (Zs - Zr)^2\}} \tag{7.17}$$

From Equations 7.15, 7.16 and 7.17 the diffracted mean square pressure can be obtained as:

$$p_{b2}^2 = p_{do}^2 \sum_{i=1}^{n} \left(\frac{1}{3 + 10N_i} \right) \tag{7.18}$$

$$p_{b2}^2 = \frac{W\rho_o c Q_\theta}{4\pi\left(\frac{\left(l_S^2 + l_R^2\right)}{\left(l_S^2 + l_R^2 - h^2\right)}\right)} \sum_{i=1}^{n}\left(\frac{1}{3+10N_i}\right) \tag{7.19}$$

In Equation (7.19) a term Q_B is defined as effective directivity, according to the following equation:

$$Q_B = Q_\theta \sum_{i=1}^{n}\left(\frac{1}{3+10N_i}\right) \tag{7.20}$$

In the present research only the path of maximum influence has been considered, therefore:

$$Q_B = Q_\theta\left(\frac{1}{3+10N_1}\right) = Q_\theta\left[\left(\frac{\lambda}{3\lambda+20\delta_1}\right)+\left(\frac{\lambda}{3\lambda+20\delta_2}\right)\right] \tag{7.21}$$

where d_1 and d_2 are the path differences, i.e. the difference between the diffracted and direct path of sound rays. In the present sound field:

$$p_2^2 = p_r^2 + p_{b2}^2 \tag{7.22}$$

where $p_r^2 = \frac{4W\rho_o c}{R}$.

Therefore, the total mean square sound pressure at the receiver position with the pit-wall present can be represented as:

$$p_2^2 = W\rho_o c\left(\frac{Q_B}{4\pi R^2} + \frac{4}{R_c}\right) \tag{7.23}$$

The sound power level at the receiver is then found as:

$$L_{p2} = L_W + 10\log\left(\frac{Q_B}{4\pi R^2} + \frac{4}{R_c}\right) \tag{7.24}$$

Thus applying the correction from the reflecting pit-wall one obtains:

$$L_{p2} = L_W + 10\log\left(\frac{Q_B}{4\pi R^2} + \frac{4}{R_c}\right) + D \tag{7.25}$$

The loss of sound pressure level of noise due to the pit-wall, *SL*, is thus determined to be:

$$SL = L_{po} - L_{p2} = 10\log\left[\left\{\left(\frac{Q_\theta}{4\pi R^2}\right) + \frac{4}{R_c}\right\} \Big/ \left\{\left(\frac{Q_B}{4\pi R^2}\right) + \frac{4}{R_c}\right\}\right] \tag{7.26}$$

The value of SL depends on the position of the receiver and the source and the Fresnel number dependent term Q_B. It must be emphasised that the loss will be different at different frequencies, since diffraction is a frequency dependent phenomenon.

The development of a methodology to determine the attenuation of mining noise due to barrier effects of the pit-walls considering the influence of reflections from the opposite walls are discussed in the remaining sections of this chapter.

7.3.2 Correction for Pit-wall Reflection

The prediction of surface mining and quarrying noise should also consider the reflection of acoustic energy from the pit-walls. For this purpose, a correction factor which is referred to as the *Reflection Correction* (*RC*) is added to the predicted noise level to account for the extra sound energy received at the receiver position. The author has adopted the method established for similar geometry in evaluating the road traffic noise (HMSO, 1988). Referring to Figure 7.7, the reflection correction can be evaluated using the following equation:

$$RC = [1.5 + (E_2 - E_3)\{1 + E_5(E_1 - 1)\}]E_4 \tag{7.27}$$

The values of the correcting factors E_i (i=1, 2,···, 5) depend on the geometry of the pit, measured as the height of the nearer wall (d), height of the far end or the reflecting wall (D_r) and the height of the receiver (Z_r). The rule to determine E_1 is given as:

if D_r is greater than or equal to d and Z_r is greater than or equal to d, then $E_1 = d$;
if D_r is greater than or equal to d and Z_r is less than d, then $E_1 = Z_r$; *for* $Z_r < 1$, $E_1 = 1$;
if D_r less than d and Z_r is greater than or equal to D_r, then $E_1 = D_r$;
if D_r is less than d and Z_r is less than D_r then E1= Z_r, for Z_r r <1, E1=1.

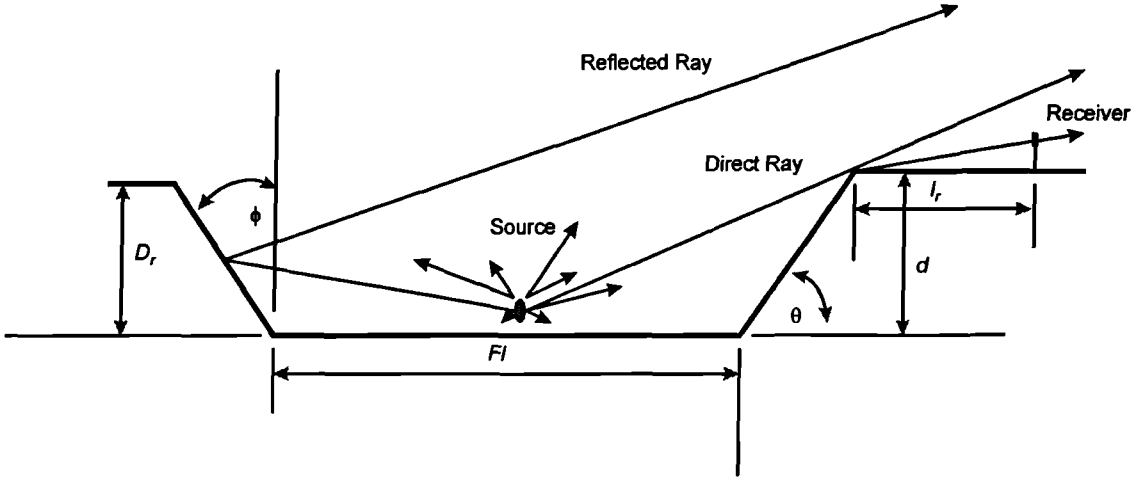


Figure 7.7 A simple geometric model for a surface mine or a quarry.

E_2 is calculated as:

$$E_2 = \left[8.2 - 3\log\left(Z_r + 10\right)\right]\log\left(Z_r + 10\right) - 5 \tag{7.28}$$

If Z_r is less than 0, E_2 is taken as 0.2 and if Z_r is greater than 30, E_2 is taken as 0.44. E_3 is determined as:

$$\begin{aligned} E_3 &= \left[1 - 0.6\log\left(35 + \frac{l_r}{2}\right)\right]\log\left(35 + \frac{l_r}{2}\right) \\ l_r < 10 &\Rightarrow E_3 = 0.06 \\ l_r > 80 &\Rightarrow E_3 = -0.23 \end{aligned} \tag{7.29}$$

Where,

l_r: distance from the diffraction edge to the receiver

If the distance between the facing walls is Fl, E_4 is calculated as:

$$\begin{aligned} E_4 &= \log\left(1 + (270 / Fl)\right) \\ Fl < 30 &\Rightarrow E_4 = 1 \\ Fl > 70 &\Rightarrow E_4 = 0.69 \end{aligned} \tag{7.30}$$

If the reflecting wall has an angle ϕ with the vertical, E_5 is given as:

$$E_5 = \exp(-0.019\phi^2) \tag{7.31}$$

7.4 The Development and Evaluation of a Model for the Assessment of Pit-wall Attenuation

The theoretical and experimental work carried out on barrier attenuation was formulated in the form of a predictive software (SLXPAR.CPP) coded in C++ as part of the noise prediction system. The model structure is shown in Figure 7.8. This model was further tested, together with the other elements of the prediction system, by conducting the final experiments at a quarry in the Republic of Ireland. A detailed description of these experiments and the relevant discussions are presented in Chapter 8. Therefore, only the elements relevant to the pit-wall attenuation model will be discussed in this section. An example output from the pit-wall attenuation model is shown in Figure 7.9.

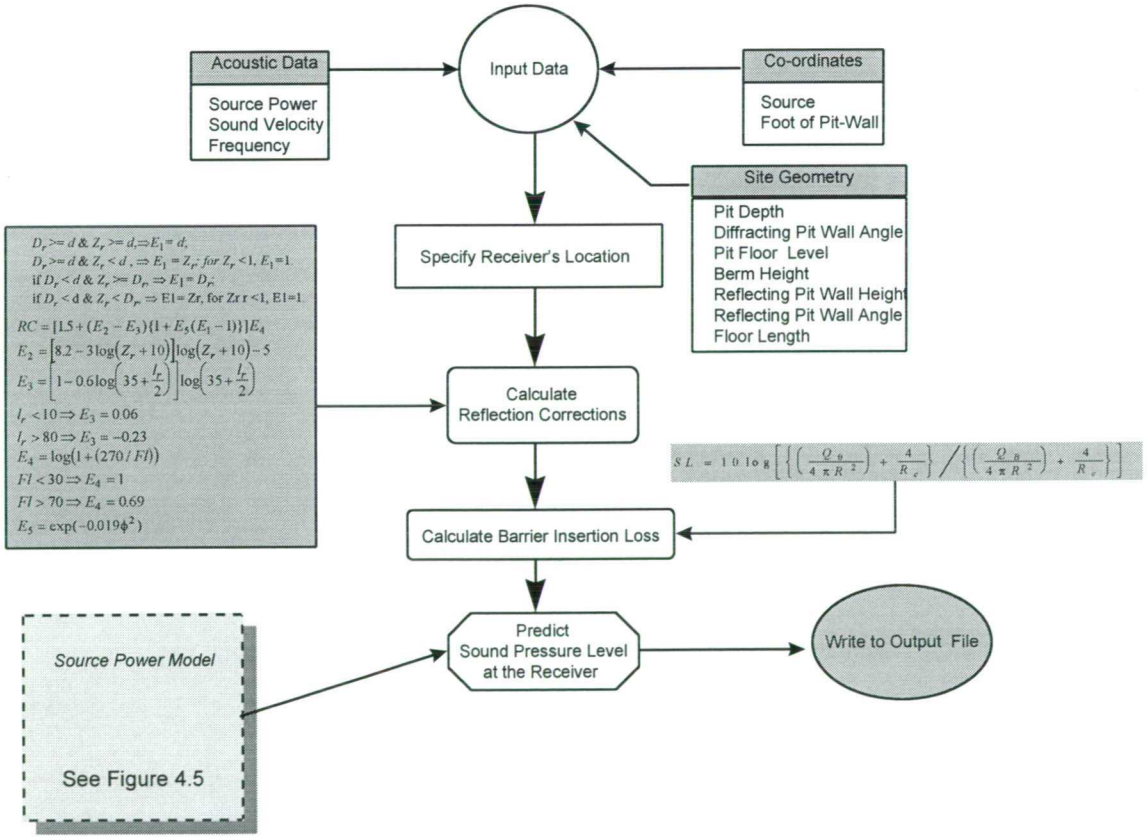


Figure 7.8 Model structure for evaluating attenuation due to pit-wall.

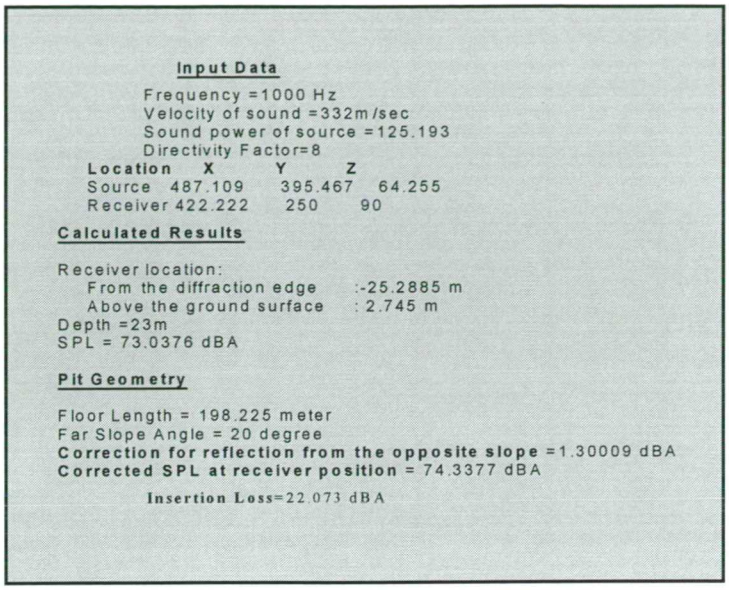


Figure 7.9 An example output from the pit-wall attenuation model.

A plan of the limestone quarry where the final validation was carried out was presented in Figure 4.14 in Chapter 4. In order to study the effect of the quarry walls, the sound pressure levels at different stations at the quarry top near the Portable Crusher Zone (PC-Zone) were monitored during a period of steady state operation of the crusher. Using the model developed, sound pressure levels were predicted at the same stations. Table 7.2 presents the predicted and measured values at these stations. The coefficient of correlation of the measured and predicted values was found to be 0.998154. This high degree of correlation is observed because the verification stations were close to the quarry and the other sources of attenuation were insignificant. Figure 7.10 presents the comparison of the measured values with the values predicted by the model. This shows that the model at its present stage gives satisfactory results provided that the sound (and the site) is free from scattering, complex barriers, highly reflecting surfaces, wind velocity and temperature gradient. The model can also be used to evaluate the effects of the pit geometry on the attenuation of noise levels.

Table 7.2 Predicted and measured values at different locations near the quarry.

Measuring Station No.	X	Y	Z	Predicted SPL, dBA	Measured SPL, dBA	Error dBA
1	177.003	344.311	54.8816	48.444	47.5	0.9440
2	85.303	122.248	49.9201	49.263	51.2	-1.9370
3	353.643	304.713	74.2249	49.9201	51.0	-1.0799
4	347.541	345.932	74.9518	51.2587	53.0	-1.7413
5	352.704	403.958	75.7506	51.6141	52.5	-0.8859
6	359.746	441.792	75.6976	54.7356	54.5	0.2356
7	418.284	475.000	63.8505	54.8816	55.3	-0.4284
8	375.016	525.000	51.2587	63.8505	65.0	-1.1495
9	349.055	555.000	48.4440	74.2249	75.0	-0.7751
10	423.664	468.783	78.4657	74.9518	76.0	-1.0482
11	220.000	492.622	54.7356	75.7506	75.4	0.3506
12	120.000	528.994	51.6141	78.4657	78.0	0.4657
13	485.000	395.600	90.4505	90.4505	91.0	-0.5495

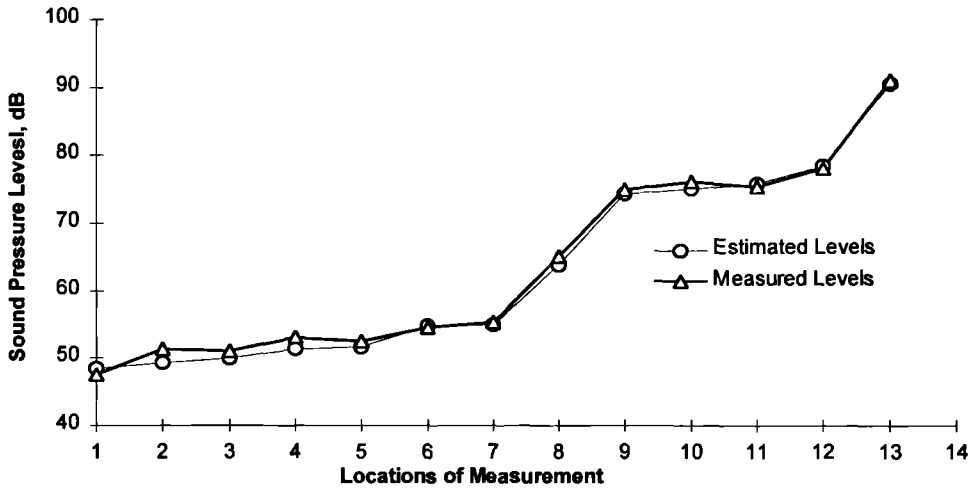


Figure 7.10 Comparison of measured and predicted values.

7.4.1 The Effects of Pit Geometry

The experimental data were also analysed to study the effects of pit geometry on the predicted noise levels. The distance of the pit-walls from the source influences the attenuation during propagation. Figure 7.11 shows the results of this study. This analysis suggests that the highest noise attenuation will be obtained when the source is closest to the pit walls. This fact can be utilised during the design of surface mines and quarries by placing the permanent installations closer to the pit walls.

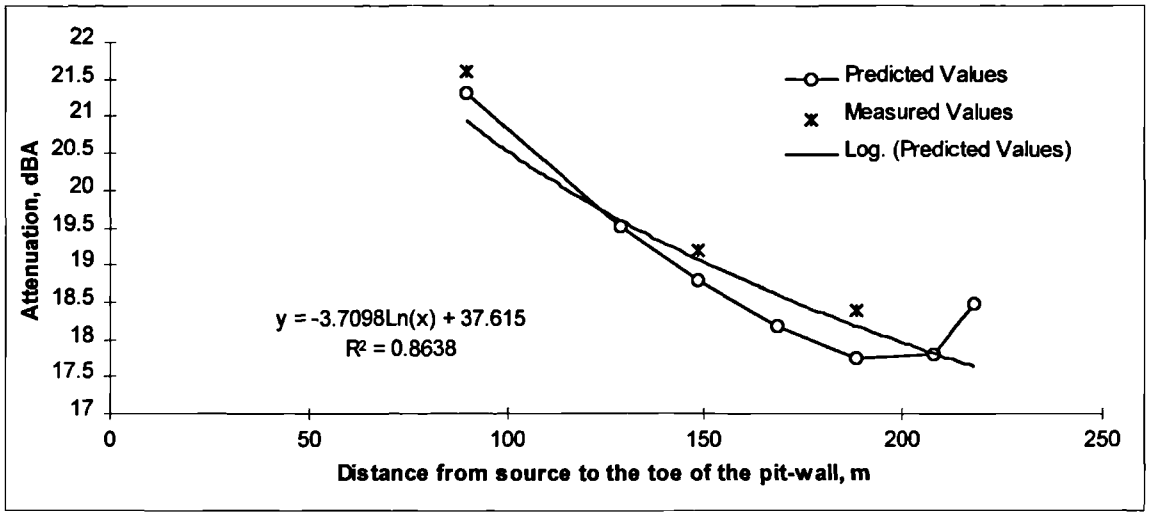


Figure 7.11 The effect of distance between noise source and pit-wall on noise attenuation.

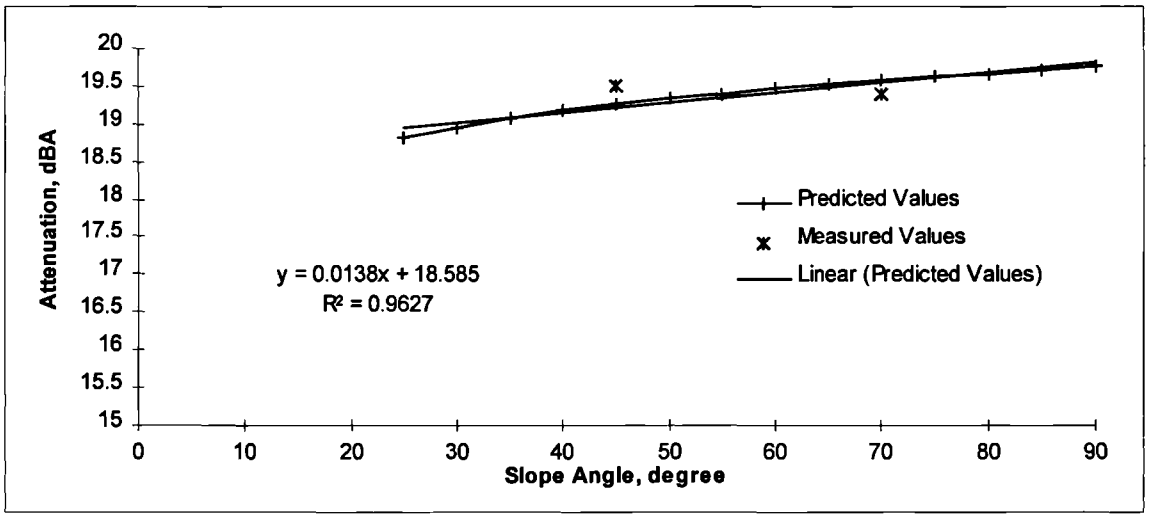


Figure 7.12 The effect of slope angle of pit-wall on attenuation.

Similarly, Figure 7.12 shows the effect of the pit-slope angle in attenuating noise levels near the pit top. The role of safety berms on the pit top for noise attenuation purposes was also studied using the results of the experimental work. Figure 7.13 presents the effects of berm height on the attenuation.

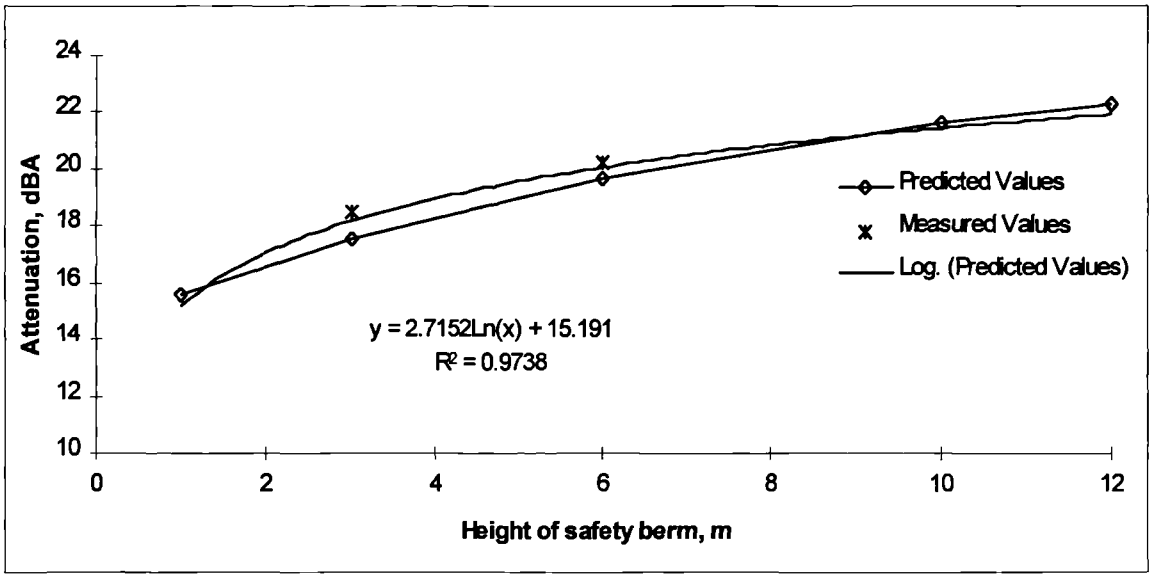


Figure 7.13 The effect of safety berm height on noise attenuation.

In this final experiment, steady state noise levels from the portable crusher zone of the quarry were used to determine the equivalent acoustic centre (EAC) of the zone, and the predicted values were calculated from the sound power level and the location of the EAC. The theoretical attenuation for different pit slope angles, source to toe distance and berm heights were calculated using the model developed based on the theory described in Section 7.3.1. For the verification of the theoretical values there were not many experimental results, as these parameters could not be varied in the field. However, the experimental and predicted values under the existing mining parameters were compared and presented in Figures 7.11, 7.12, 7.13. The difference between the predicted and measured values may be due to the experimental errors as the influence of other factors could not be filtered out. It is concluded that more controlled experiments will be necessary to improve upon the existing relationships between noise attenuation and pit geometry characterised by the slope angle, distance of source from the pit-wall and the berm height. These relationships will help in designing surface mines and quarries for environmental noise control. An example of such an application is presented in the next section.

7.4.2 A Study of Environmental Noise Control in Surface Mines

The model described in this Chapter can be used to determine the source-zone within an open pit of given geometry so that a receiver outside the mine will not receive direct sound energy from the noise source working in the pit. Figure 7.14 illustrates this problem where R represents the location of the receiver.

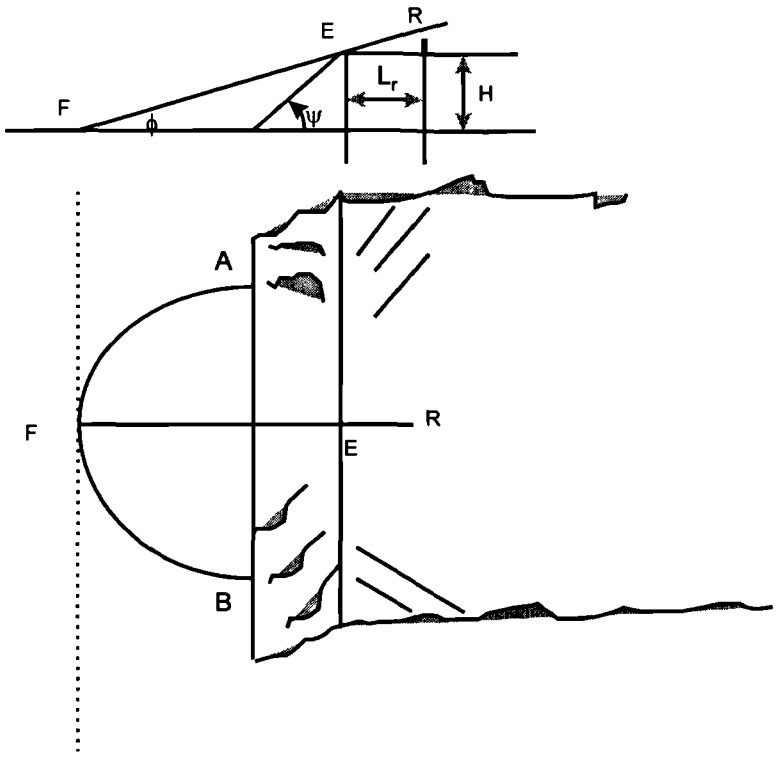


Figure 7.14 Geometric position of the receiver with respect to the pit-wall.

The receiver at this position will receive direct sound energy from a source located anywhere where which is external to the zone defined by the arc AFB. Let the following assumptions be made:

- The floor and the surface at the pit top are horizontal.
- The slope height is H and the slope angle is ψ.

For the above situation one needs to determine the space covered by the conical surface generated by EF, the pit floor and the pit-wall. Let the positions of the reference points be given by the following co-ordinates:

R: (X_r, Y_r, Z_r)

F: (X_f, Y_f, Z_f)
E: (X_e, Y_e, Z_e)

The distance from the receiver to a point on the pit floor, FR is:

$$FR = \sqrt{\left(X_r - X_f\right)^2 + \left(Y_r - Y_f\right)^2 + \left(Z_r - Z_f\right)^2} \tag{7.32}$$

The optimum source location within a pit would transmit minimum direct sound energy to a receiver location. One can geometrically determine such a zone within the pit for every observer's position. Figure 7.14 shows such a zone bounded by the line FR, the pit floor and the pit-wall.

Let us determine the co-ordinates of a source position for no direct sound energy at the receiver's position. Let the observer to pit-wall-edge distance along the X-axis be $\pm L_r$. The sign depends on the position of the observer. A negative sign is used for an observer to the right of the edge. The co-ordinates of the point of contact of the edge and FR will be:

$$\begin{aligned} X_e &= X_r \pm L_r \\ Y_e &= Y_r \\ Z_r &= gZ_r \end{aligned} \tag{7.33}$$

where, gZ_r is the ground surface at the receiver. The angle made by FR with the pit floor is:

$$\phi = \text{atan}\left(\frac{Z_r - gZ_r}{L_r}\right) \tag{7.34}$$

The radius of the base circle of the generator cone is:

$$R = FR\cos\phi \tag{7.35}$$

Thus, the boundary of the source zone will be an arc of a circle. The equation of the circle is:

$$\left(x - X_r\right)^2 + \left(y - Y_r\right)^2 = R^2 \tag{7.36}$$

Under the conditions:

a) $X_e - \frac{H}{\tan q} > x > X_f$, if the observer is to the right of the source and the edge.

b) $X_e + \frac{H}{\tan q} < x < X_f$, if the observer is to the left of the source and the edge.

the co-ordinate on the vertical axis would be within the following limit:

$$Z_f < z < \left(Z_f + h\left(\frac{X_e - X_f \pm H/\tan\theta}{X_e - X_f} \right) \right) \tag{7.37}$$

Thus for the given situation one can determine the zone for locating the source. In real life situations the noise source should be placed as near as possible to the pit-wall considering other safety factors like slope stability, working environment and the technological requirements. The above discussion confirms that a higher value of H will provide more room for locating the noise source that will send minimum direct energy to an observer outside the pit-wall. In other words, there will be maximum attenuation due to ground absorption and barrier effects in the case of the deeper mines.

7.5 Conclusion

This chapter presented the theory adopted in developing a model to account for the effects of pit-wall as a noise barrier in predicting the far field noise levels near surface mines. The pit walls of a surface mine modify the noise field on the surface as diffraction of acoustic waves occurs over the edge of the walls between the source and the receiver. At the same time, the opposite walls reflect back a certain amount of sound energy. The geometry of the mine plays an important role in determining the resultant sound field. It was observed that the attenuation by the pit-walls depends significantly on the slope angle, on the height of the safety berms and on the location of the source.

Experiments were conducted at a limestone quarry in the Republic of Ireland and the sound pressure levels were monitored at a large number of stations outside the quarry. The geometric and acoustic data were used as the input data in the model to calculate

the barrier loss. The barrier loss was evaluated for specific conditions of pit slope angle, berm height and source location. These were compared with the values obtained by direct measurements. The coefficient of correlation between the predicted and measured sound pressure levels was found to be 0.960372. Based on the results of the experimental work it was decided to incorporate the pit-wall attenuation model within the noise prediction system developed.

The overall sound energy received by a receiver at a location on the pit surface is also influenced by the sound absorbing property of the surface of the benches on the pit-walls. This effect was not discussed in this chapter. Barrier effects of noise can be analytically determined over the frequencies by using the theory proposed by Hasabe and Kaneyasu (1987). This theory was developed and validated for acoustic wave propagation over a depressed road with a finite impedance. The author has conducted field experiments to study the relevance of this theory in mining conditions. These experiments and the theories of combining the barrier effects with the ground absorption characteristics of the pit-walls will be discussed in the next chapter. This is done within the context of overall integration of the models developed into the final noise prediction system.

Chapter 8

System Integration and Final Field Validation

8.1 Introduction

The objective of this research was to develop a noise prediction system with four components, namely the source power model, the ground attenuation model, the air attenuation model and the pit-wall attenuation model. The source power model predicts the sound power level of the noise sources based on the theory of Equivalent Acoustic Centres. The development of this model was discussed in Chapter 4. The attenuation models provide the attenuation of sound energy under the prevailing mining and environmental conditions. Attenuation models developed to account for ground absorption, air absorption and the effects of pit-walls as barriers were described in Chapters 5, 6 and 7. These models were integrated to formulate the noise prediction system which is used to determine the noise levels at any location around the mining area. Experiments were conducted during the development of these models to test their validity. The results of these experiments together with the principles underpinning the

integration of the individual models are presented using the example of ground absorption and pit-wall attenuation models in this chapter.

8.2 The Integration of the Source Power and Attenuation Models for Noise Prediction

The prediction of the noise levels around surface mines requires a number of sequential steps. Figure 8.1 illustrates this procedure in terms of equivalent continuous sound pressure levels based on the methodology developed by the author as discussed in Chapter 4. This procedure is applied to determine the noise levels over a grid surrounding the mining area.

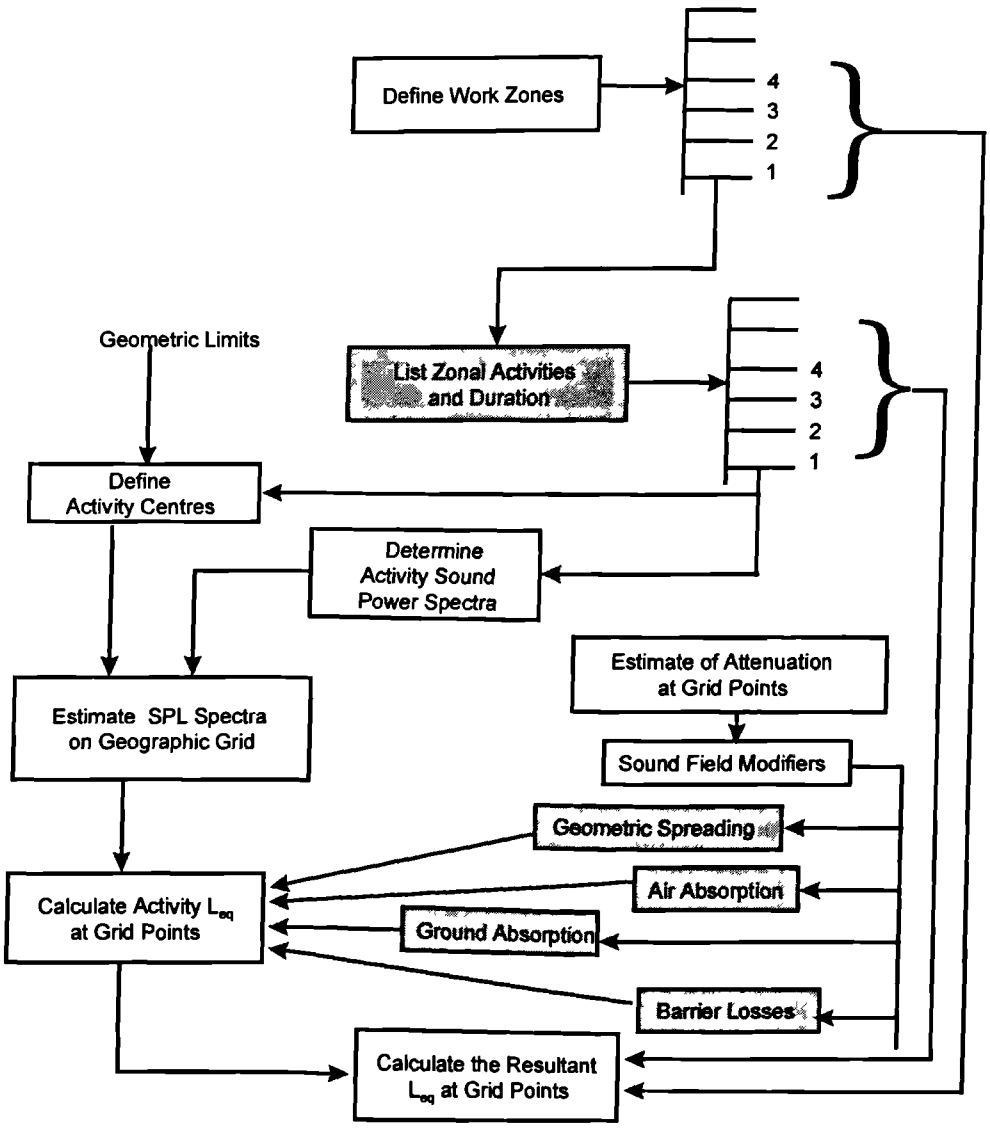


Figure 8.1 Steps involved in predicting the noise levels around surface mines and quarries.

The noise sources in a working zone of a surface mine or quarry may be stationary, semi-mobile or mobile. Figure 8.2 illustrates the possible sources and operating conditions of noise generating sources in the working zones. The noise sources in mining seldom exist alone. Therefore, the noise prediction must be capable of evaluating the sound power levels of machines operating in combination. Alternatively, each activity in each working zone must be reduced to a point source of definite sound power level. These equivalent sources are the equivalent acoustic centres (EAC) of all the activities in each working zone. By defining the duration of each activity in these zones under different stages of production one can predict the equivalent continuous sound pressure level for any period of interest by following the Activity Accounting Technique (AAT) of sound power modelling as discussed in Chapter 4.

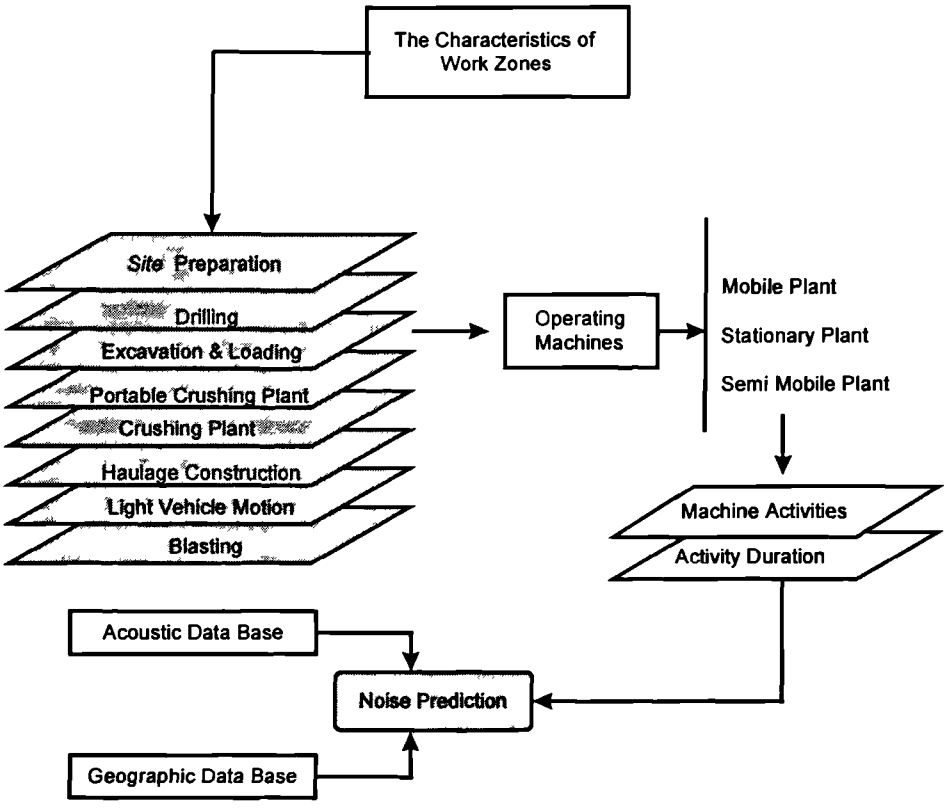


Figure 8.2 The characteristics of working zones relevant to noise prediction in surface mining and quarrying.

The noise prediction system developed in this research integrates the source power model and the attenuation models such that:

$$L_p = L_w - A_s - A_g - A_a - A_b + D_c + R_c \tag{8.1}$$

Where,

L_p : sound pressure level at the receiver's location
L_w : sound power level of the equivalent acoustic centre of the work zone
A_s : attenuation due to spreading
A_g : attenuation due to ground absorption
A_a : attenuation due to air absorption
A_b : attenuation due to slope as noise barrier
D_c : directivity corrections
R_c : reflection correction

In its current format the model does not consider the following aspects of surface mining noise:

- Reflection and scattering of noise by structures and buildings within the mining area,
- Haulage noise,
- Blasting noise.

Surface mines and quarries are comprised of spatially distributed work zones. Each work zone has its own set of machinery generating various types of noise. The resultant noise levels vary with time, depending on the sequence of operations in these zones. Consequently, the amplitude and the frequency of acoustic waves in the neighbourhood vary with time. Therefore, the equivalent continuous sound pressure level (L_{eq}) is accepted as an index to measure environmental noise levels. In order to predict the L_{eq} in dBA due to various operations in a work zone, the author has developed a methodology based on the Equivalent Acoustic Centre concept.

In this method, the noise sources within a geographically delineated space are modelled as an equivalent point source. This is referred to as the EAC, and was discussed in detail in Chapter 4. An EAC is characterised by its broad-band sound power level and location and is based on the total impacts of all the noise sources present within a zone. The sound power level of the EAC is based on measured sound pressure levels at the EAC

definer locations in the work zone and represents the overall effects of interference and reflections within the zone. In the present work it was assumed that the directivities of the EAC remain constant within its far field. The sound pressure level at any location in the same direction but external to the zone will be influenced by these directivities. Depending on the behaviour of the noise sources the sound power level and location of the EAC may change with time. Therefore, the L_{eq} in the neighbourhood depends on this time-dependent behaviour.

In order to apply the developed noise prediction system, the surface mine or the quarry is divided into a number of work zones. The EAC is determined for all these zones for the steady state operations of all the noise sources within the zone. Sound pressure levels at the grid points over the surface mining area are then calculated based on the EAC of each zone. The worst noise situation is represented by considering the simultaneous operations of all the work zones. This scheme is incorporated in the noise prediction system developed. Figure 8.3 presents the overall noise prediction system concept and the way the individual models developed in this research were integrated.

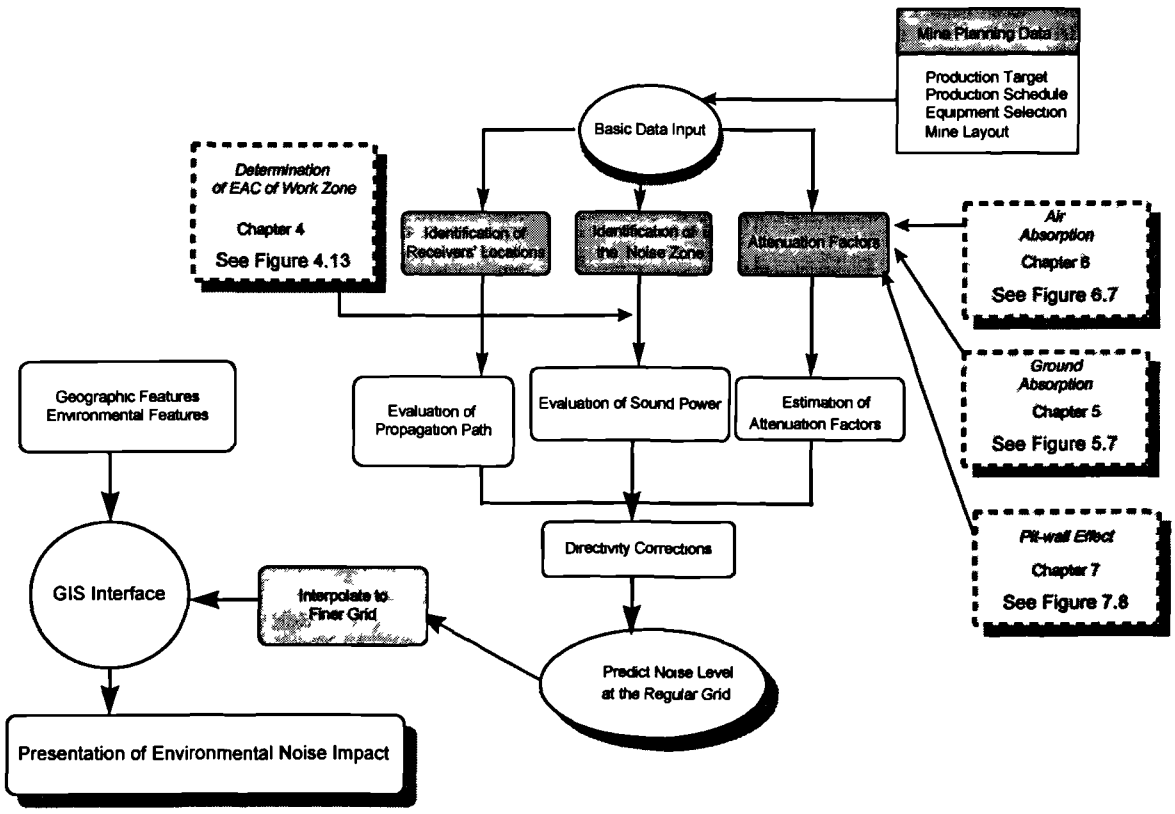


Figure 8.3 The noise prediction system developed for surface mines and quarries.

Out of a number of noise propagation and attenuation corrections referred to in Equation 8.1, the integration of the ground absorption and pit-wall attenuation effects have proved to be the most theoretically challenging elements in this model integration process. The next section will discuss this element in detail and will present examples of field experiments used to validate the integration approach adopted.

8.2.1 Ground Absorption and Barrier Attenuation

The attenuation effect of a pit-wall is mainly due to its performance as an barrier and an absorbent. The nature of the ground surface on the pit-wall and on adjoining plains influences the overall loss of acoustic energy propagating from the pit to the surface. The concept suggested by Hasabe and Kaneyasu (1987) can be used for determining the attenuation during pit-to-surface propagation of noise. However, the method involves a large number of calculations and uses considerable computer time.

Sound propagating from the pit bottom undergoes absorption by the ground surface and attenuation by the pit-wall acting as a barrier between the receiver and the sound source. Jonasson (1972) studied the sound attenuation due to combined effects of ground absorption and barrier attenuation. The pattern of sound propagation over ground varies with the type of ground. This variation is more pronounced in the frequency range of 250 to 1000 hertz. A small change in acoustic impedance of the ground may cause a significant change in the propagation pattern. Following Hasabe and Kaneyasu (1987) a pit-wall can be represented as shown in Figure 8.4. According to the theory of image sources the receiver will receive sound energy from an infinite number of ray paths. Reflections will take place on all the surfaces. Under these conditions the following assumptions will hold:

a. there is no noise transmission through the pit-walls to the receiver,
b. absorption of sound energy occurs on all three surfaces,
c. refraction of acoustic waves occurs at the edge of the pit-wall.

Since refraction is a frequency dependent phenomenon, frequency analysis of the noise source is necessary for the analysis of the effects of the pit-walls. In the absence of

frequency analysis of the noise source, the effects of pit-walls may be approximated for the predominant frequency.

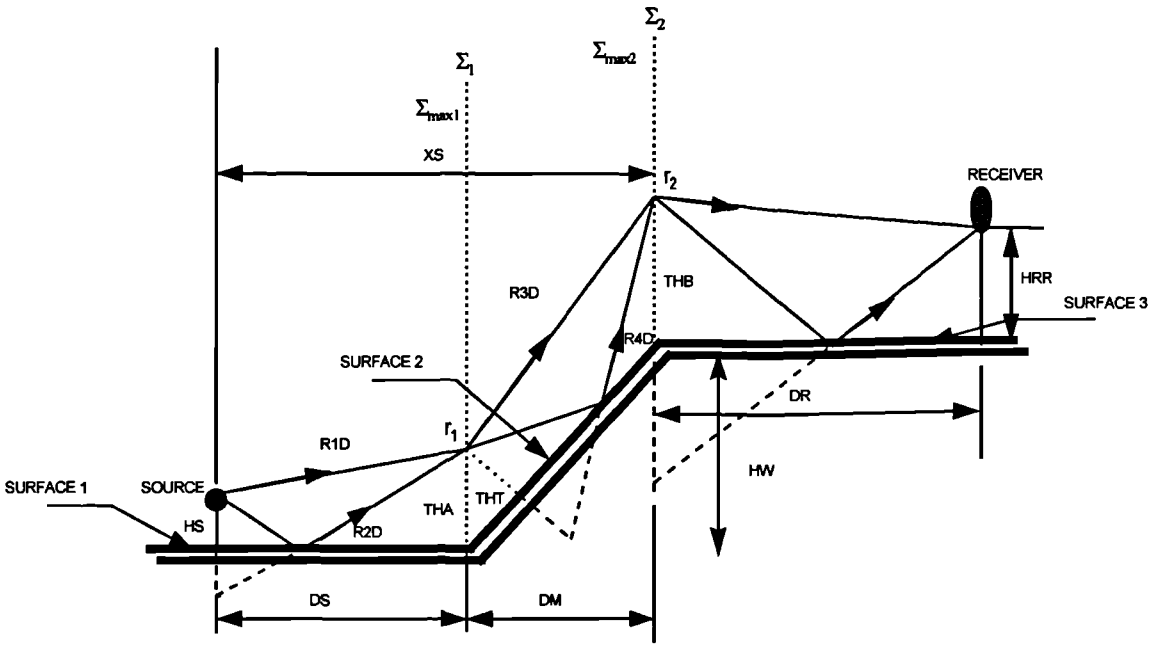


Figure 8.4 Pit geometry affecting the attenuation of sound from a pit-bottom source to a pit-top receiver.

In surface mining it may be assumed that the acoustic rays travel over three types of surface during propagation from the source to a receiver. The surface of the pit floor can be represented as Surface 1, the inclined surface of the slope as Surface 2 and the surface at the pit top as Surface 3. The acoustic phenomena occur mainly on two segments. The first part of the terrain is the flat surface of the pit floor. The second part of the terrain is the wedge shaped area including the sloping surface and the pit top.

8.2.1.1 The Acoustic Phenomena at the Pit Bottom

The velocity potential at a receiver with a direct atmospheric distance of separation R_1 is expressed as:

$$\phi(R_1) = \frac{e^{ikR_1}}{4\pi R_1} + Q\frac{e^{ikR_2}}{4\pi R_2} \tag{8.2}$$

where,

R_2 : distance of the receiver from the image source
k : the propagation constant
Q : plane wave reflection factor

The reflection factor, Q, is determined as a function of the plane wave reflection coefficient at an angle θ, $R(\theta)$, and the numerical distance, ω, as:

$$Q = R(\theta) + [1 - R(\theta)]F(\omega) \tag{8.3}$$

$R(\theta)$ and $F(\omega)$ are expressed in terms of specific acoustic impedance Z as:

$$R(\theta) = \frac{(Z\cos\theta - 1)}{(Z\cos\theta + 1)} \tag{8.4}$$

$$F(\omega) = 1 + i\sqrt{\pi}e^{-\omega^2}\,\mathrm{erfc}(-i\omega) \tag{8.5}$$

The numerical distance is a measure of the effect of distance and is calculated as:

$$\omega = \left(ikR_2\right)^{0.5} \times \left(\beta + \cos\theta\right) \tag{8.6}$$

β is the specific acoustic admittance of the surface and erfc(-iω) represents the complementary error function. Admittance, propagation constant and acoustic impedance of the ground surface are determined for different frequencies and flow resistivities of the ground surface following the methods developed by Isei *et al* (1980) as discussed in detail in Chapter 5.

8.2.1.2 The Acoustic Phenomena at the Pit Walls

The pit-walls can be considered as wedge-shaped barriers. The wedge angle between Surfaces 2 and 3 in Figure 8.4 is taken as the supplementary angle of the angle of the pit-wall. The reflected rays over Surfaces 1 and 2 result in the formation of image sources over surfaces Σ_1 and Σ_2.

Ambient sound propagation is described by the Helmholtz wave:

$$\left(\Delta + k^2\right)\phi(r) = -\delta(r - r') \tag{8.7}$$

where,

ϕ : velocity potential
k : wave number

The source at r' is represented by the Dirac's delta-function $\delta(r-r')$.

The velocity potential in the presence of a reflecting ground surface is given by Equation 8.2. Performing extensive acoustic analysis of the effects of pit-walls. Hasabe and Kaneyasu (1987) derived the resultant field at the receiver's position at R in Figure 8.4 as:

$$\phi(R) = -ik\frac{XM.XR}{8\pi^2}\int_0^\infty\int_0^\infty\sum_{i=1}^{2}\sum_{j=3}^{4}\sum_{k=5}^{6}Q_{i2}Q_{j4}Q_{k6}.\varepsilon \times \left[\frac{e^{ik\left(R_i+R_j+R_k\right)}}{\left\{R_j^2.R_k^3\left(R_j+R_k\right).\left(R_i.R_j+As.R_j.R_k+Am.R_k.R_i\right)\right\}^{0.5}}\right]dz_1.dz_2 \tag{8.8}$$

A_S and A_m in the above expression are defined as:

$$As = \left(\frac{DS}{DS+DM}\right)^2, \quad Am = \left(\frac{DM}{DS+DM}\right)^2 \tag{8.9}$$

Considering the limit for practical purposes the above equation can be written as:

$$\phi(R) = -ik\frac{DS.DM}{8\pi^2}\sum_{l=1}^{l_{max}}\sum_{m=1}^{m_{max}}\sum_{i=1}^{2}\sum_{j=3}^{4}\sum_{k=5}^{6}Q_{i2}Q_{j4}Q_{k6}.\varepsilon \times \left[\frac{e^{ik\left(R_i+R_j+R_k\right)}}{\left\{R_j^2.R_k^3\left(R_j+R_k\right).\left(R_i.R_j+As.R_j.R_k+Am.R_k.R_i\right)\right\}^{0.5}}\right]\Delta z_1.\Delta z_2 \tag{8.10}$$

The effective reflective coefficients of ground surfaces can be determined as complex functions of the following parameters:

- horizontal distance between the source and the receiver (D),
- perpendicular distance from the source to the reflecting surface (TH),
- perpendicular distance from the receiver to the reflecting surface (RH),
- frequency of the wave (f),
- acoustic impedance of the ground surface (Z),
- velocity of the propagation of the sound wave (c).

The complex reflection coefficient (R) is expressed as a function of the angle of incidence (θ_i) and the admittance (β) of the ground surface. The angle of incidence is determined by the specific dimensions of the site as:

$$\tan\theta_i = \frac{DS}{RH + THA} \tag{8.11}$$

R is expressed as:

$$R = \frac{\cos\theta_i - \beta}{\cos\theta_i + \beta} = R(\theta) \tag{8.12}$$

Representing acoustic impedance of air as Z_o and that of the reflecting surface as Z_i the above equation can be re-written as:

$$R = \frac{\cos\theta_i - Z_o/Z_1}{\cos\theta_i + Z_o/Z_1} \tag{8.13}$$

The reflection factor of a surface is expressed in terms of the reflection coefficient R(θ) as:

$$R = R(\theta) + (1 - R(\theta))F(\omega) \tag{8.14}$$

In the above equation the parameter numerical distance, ω and the function, $F(\omega)$ are calculated by Equations 8.6 and 8.5 respectively. The error function erfc(x) in Equation 8.5 is defined as:

$$\text{erfc}(x) = \int_x^\infty e^{-t^2} dt, \quad x = -i\sqrt{\omega} \tag{8.15}$$

The acoustic impedance of the ground is calculated as a function of the following:

- frequency of the sound wave (f),
- flow resistivity of the ground surface material (s),
- velocity of sound level (c),
- thickness of the upper porous layer (Th).

From the surface reflection the impedance of the ground can be determined using the semi empirical relationship given by Delaney and Bazley (1970) as:

$$Z_2 = 1 + \frac{9.08}{\left(\frac{f}{\sigma}\right)^{0.75}} + i\frac{11.9}{\left(\frac{f}{\sigma}\right)^{0.73}} \tag{8.16}$$

The propagation factor (AK_2) is calculated as:

$$AK_2 = k_o\left(1 + \frac{10.8}{\left(f/\sigma\right)^{0.7}} + i\frac{10.3}{\left(f/\sigma\right)^{0.59}}\right) \tag{8.17}$$

where, k_o is the propagation factor in air given as $\frac{2\pi f}{c}$. For a ground surface with a porous upper layer of thickness *Th* backed by a hard surface the acoustic impedance is given as:

$$Z_2 = k\frac{i\cos(k.Th)}{\sin(k.Th)} \tag{8.18}$$

Determining the reflection factors and acoustic impedance the velocity potential at the receiver location is determined. The excess attenuation due to the pit-wall incorporating the ground absorption and barrier effects is determined as:

$$A_b = 20\log\left|\frac{\phi(R)}{\phi(R)_{free}}\right| \tag{8.19}$$

where $\phi(R)_{free}$ is the velocity potential at the receiver in the absence of the pit-wall. This procedure has been programmed to calculate the resultant theoretical excess attenuation. Figure 8.5 presents the structure of the combined pit-wall-ground absorption prediction model BARLOS.FOR. Figure 8.6 shows an example output for a specific pit-wall geometry.

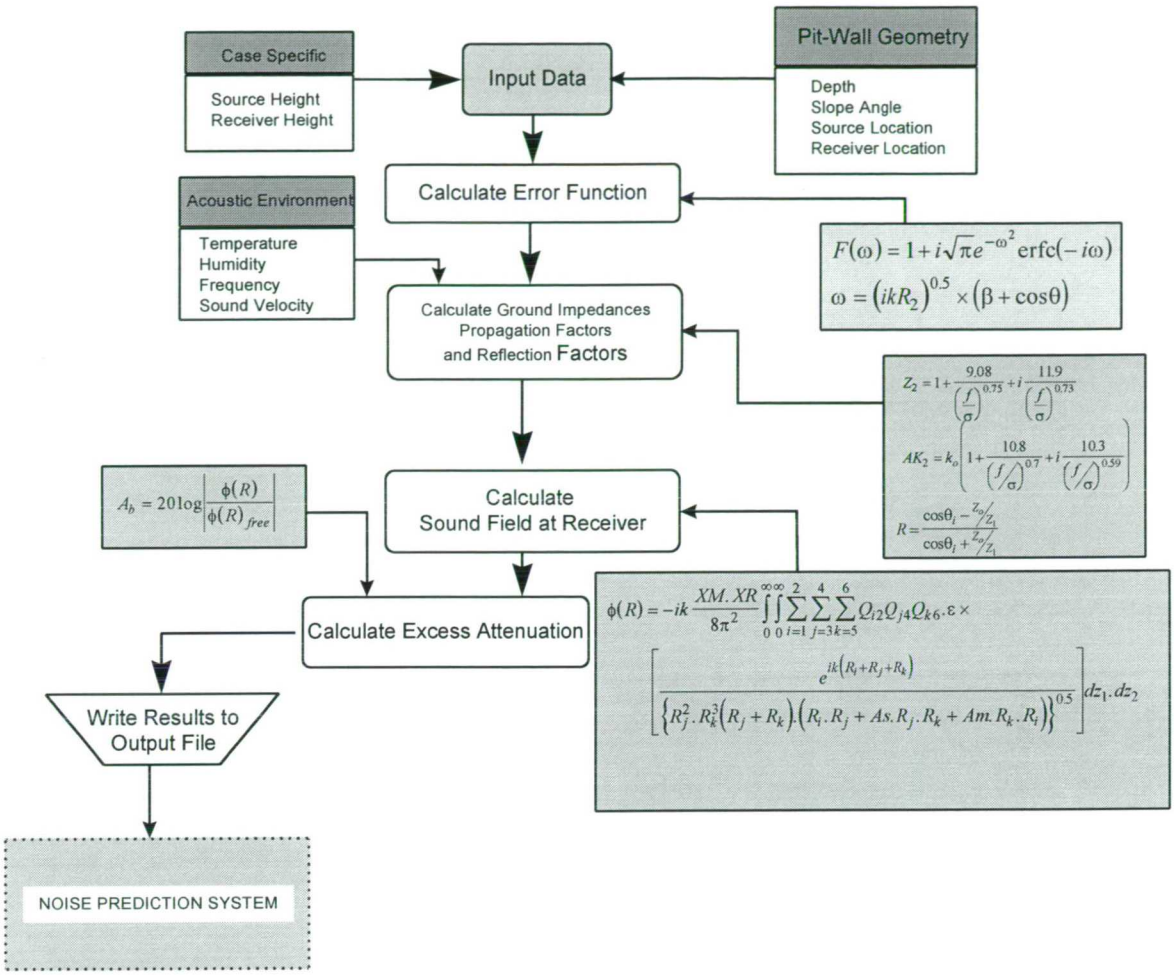


Figure 8.5 The structure of the combined pit-wall-ground absorption prediction model.

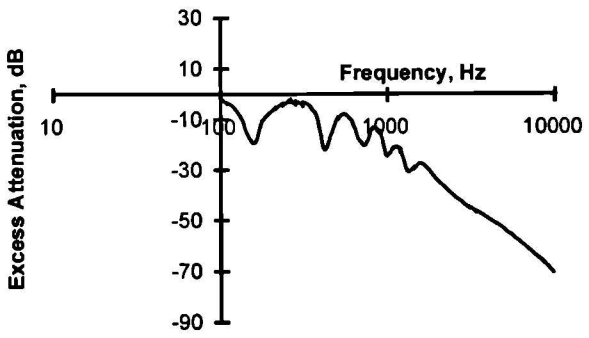


Figure 8.6 Theoretical excess attenuation due to the combined effects of pit-walls and ground attenuation.

8.2.2 Experimental Validation of the Combined Pit-wall and Ground Attenuation Model

To verify the applicability of the above theory in a mining situation field experiments were conducted on a controlled site near the tailing dam of Tara Mines. The same equipment described in Section 5.4.1 in Chapter 5 was used to generate and continuously record the noise levels during the experiments (Plate 8.1).

Figure 8.7 presents a schematic diagram of the experimental conditions used validating the theory of attenuation by the combined effects of ground absorption and the barrier.

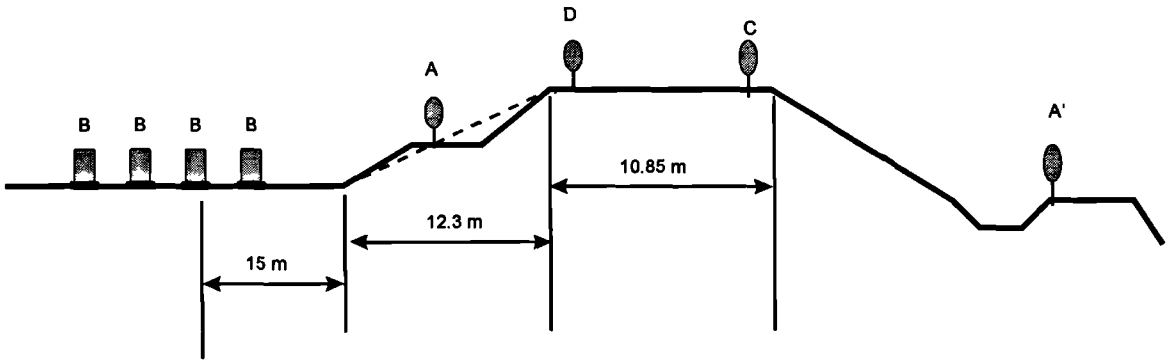


Figure 8.7 Schematic diagram of the pit-wall attenuation experiments carried out.

In Figure 8.6 A, D, C and A′ represent the positions of the sound level meters. B represents the location of the speaker, which was varied during the experiments and for each position, and each location, the sound pressure level was continuously measured and stored by the sound level meters. The source was operated to emit sound at 1/3 octave frequencies. The reference sound level meter was positioned one metre in front of the source and the other sound level meters positioned downstream of the source enabled the evaluation of attenuation due to the site geometry. The meteorological and other site conditions during the experiments were as follows:

a. cloud level : 0 to 0.3
b. atmospheric temperature : 15-20 °C
c. average wind velocity : 0.1-3.7 ms^{-1} predominantly in the NW direction

The experimental site was satisfactorily away from the other sources. However, noise due to birds and machines working at a distance of 750 m was present. Records of A' could not be used.

Figure 8.8 presents the measured data along with the predicted values of the excess attenuation due to the barrier effects of the mound walls.

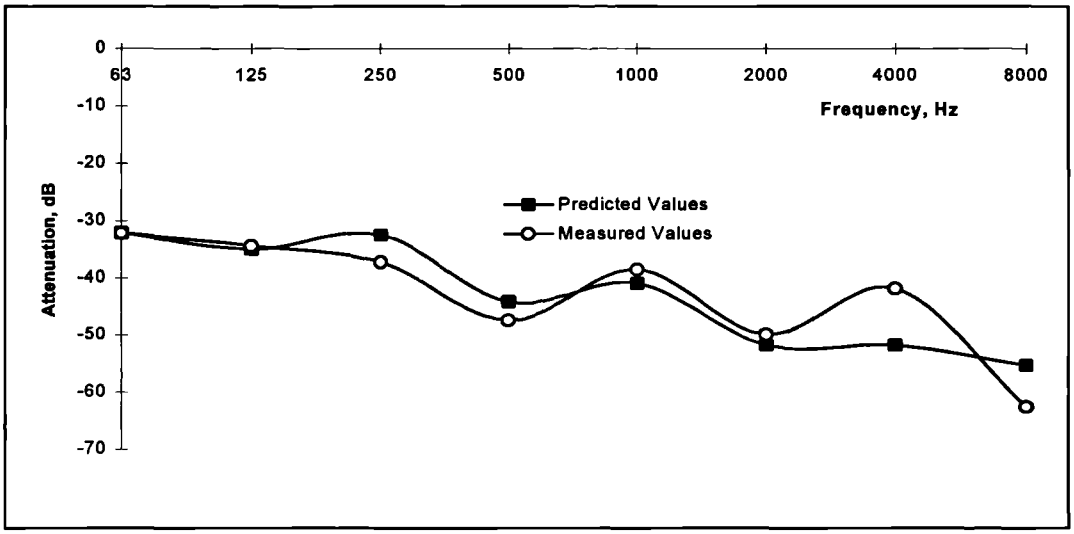


Figure 8.8 Theoretical and measured attenuation due to mound walls.

As shown in the figure, the experimental values matched the predicted results closely. The correlation coefficient of the measured and theoretically derived values is 0.853084. However, it must be stated that the measured values will include some experimental error and they could not exclusively account for the attenuation by the pit-walls alone. The effect of wind or other atmospheric sound has not been separately accounted for. Attempts to minimise the errors were made by taking the measurements simultaneously at different stations and considering the relative values to represent the barrier effects.

8.3 Final Field Validation of the Noise Prediction System

The study of environmental noise under controlled experimental conditions is very difficult because of the plethora of influencing parameters involved. A model without experimental testing will seldom be realistic. While developing a model, therefore, it is essential to test the validity of various mathematical formulations.

Field experiments were designed and carried out during this research into mining acoustics for the development of a prediction system to asses the impacts on environmental noise near mechanised surface mines and quarries. The experiments carried out during this research included the following:

- Field experiments to test the applicability of the Equivalent Acoustic Centre (EAC) concept for large distributed noise sources (described in Chapter 4).
- Field experiments to determine the sound power levels of various activities of mining equipment (described in Chapter 4).
- Field experiments to determine the attenuation by ground absorption (described in Chapter 5).
- Field experiments to determine the effects of wind velocity over ground absorption (described in Chapter 5).
- Field experiments to determine the attenuation due to combined effects of pit-walls and ground absorption (described above)
- Field experiments to determine the EAC of work zones of a quarry for the prediction of noise levels outside the quarry boundaries.

The last experiment in the above list was carried out to validate the whole noise prediction system which was developed incrementally during this research. This experiment was designed to determine the equivalent acoustic centres of the various work zones of a limestone quarry. Besides the quarrying operation, noise is generated in this quarry by the processing of the run-off-quarry products. The processing involves crushing and screening to various sizes. Also, at the top of the quarry, there is a plant producing ready-mix concrete. The surface layout includes a storage yard and a maintenance yard. The quarry is surrounded by agricultural land and a number of farm houses. Quarry production is achieved using a number of Front-End-Loaders (FEL) of 6.5 cubic yards bucket capacity and 50 tonne rear discharge dumper. Other moving noise sources working in the quarry are the road trucks and drills and rock breakers working intermittently. The plan of the quarry and the four work zones identified during the period of the experiments was presented in Chapter 4, Figure 4.14. Plate 8.1 shows the general view of the quarry.

A careful investigation of the deployed equipment and study of work plans revealed that the quarry has four noise-generating zones. These are:

- Portable Crusher Zone (PC)
- Deep Face Zone (DF)
- Main Crusher Zone (MC)
- Fixed Plant Zone (FP)

The Portable Crusher Zone is located towards the western side of the quarry. Positioned on the pit floor at a level of 62 m, the portable crusher is comprised of a primary jaw crusher, secondary cone crusher and a vibrating screen. Materials are conveyed by 1.2 m wide conveyor belts. The main generators of noise are the crushers, screen and the conveyor drive. The crusher is fed by a front end loader of 6 m^3 bucket capacity. The finished product is transported by road trucks. On average two trucks are moving in the work zone while another one is loaded by a 4.6 m^3 hydraulic shovel. The zone is surrounded by benches with an overall slope angle of 60 to 70 degrees on three sides. The average height of the quarry walls was 23 m. On one side there were loose soil heaps separating the zone from the main crusher zone. The sound field of this zone is characterised by the reflected sound from the side walls. In order to determine the sound power level of this work zone under steady state operating conditions seven monitoring stations were selected within the zone and the sound pressure levels were measured.

The Deep Face Zone (DF) is at a level of 45 m towards the northern end of the quarry. The main noise source in this zone is the front-end-loader loading the 50 tonne capacity dump trucks. At the time of the experiments the excavator was operating very close to the quarry wall. In order to determine the EAC of this zone six stations were selected for sound pressure level measurements.

The Main Crusher Zone (MC) is composed of an in-pit crusher. The crushers and the conveyor drive are the main noise generators in this zone. The dump trucks also contribute to the noise in the zone. Eight monitoring stations were selected to determine the EAC of this zone.

The fixed plants (FP) are located on the surface of the eastern side of the quarry. A rotary breaker, conveyor belts and a front-end-loader loading road trucks are the main noise generating activities in this zone. This zone covers a larger area compared to the other zones. Twelve monitoring stations were selected for noise measurements in this zone.



Plate 8.1 General view of the quarrying operations.

The Equivalent Acoustic Centres of these work zones were determined on the basis of simultaneous measurements of sound pressure levels at the monitoring stations. The locations of the monitoring stations were determined by surveying and marked on the plan.

During the field experiments the meteorological conditions were as follows:

- Cloud level = 5 to 8.
- Atmospheric temperature = 5-10 ^{o}C.
- Average wind velocity = 3-9 ms^{-1}predominantly in the E and ENE direction.

A reference monitoring station was selected towards the north western side of the quarry. The sound level meter at this station was coupled with wind monitors to determine the effect of wind velocity on noise propagation.

Table 8.1 shows the general features of the two different models of Larson Davis Noise Level Meters used during the field experiment. The frequency analysis of the mining machinery was carried out using the real time analyser, Larson Davis Model-2800. The technical features of this analyser are:

- Measuring Range: -10 to 200 dB SPL with appropriate transducer.
- A- and C-weight filters in accordance with ANSI S1.4-1983 Type), IEC 651 Type 0 and IEC 804 Type 0.
- 1/1 and 1/3 octave real-time digital filters with frequency range 1 Hz to 20 kHz.
- 4 modes of working: Sound Level Meter Mode, Standard Analysis Mode, Intensity Analysis Mode and Cross Channel Analysis Mode.
- Operating temperature: -10 to 50^{0} C.

The effects of wind velocity on sound propagation were determined using a Larson Davis Model-2140 Wind Speed and Direction Monitor coupled with the Larson Davis Model-870 Noise Level Meter. The wind speed sensor is a four-blade propeller that induces a sinusoidal ac voltage with frequency proportional to wind speed. To define the wind direction, the vane position is translated into a voltage by a precision potentiometer, the reference voltage of which is provided by the Model 870 Noise Level Meter. The specifications of Model-2140 Wind Monitor are:

- Wind speed : 0 to 60 $msec^{-1}$
- Gust speed : 80 $msec^{-1}$
- Propeller threshold speed : 0.6 $msec^{-1}$

Table 8.1 General features and the functions of the Larson Davis Noise Level Meters used.

MODEL-870	MODEL-820
115 dB dynamic range for error free measurement.	110 dB dynamic range for error free measurement.
Impulse measuring range greater than 118 dB.	Impulse measuring range greater than 80 dB.
Measurement range is 15-130 (dBA).	Measurement range is 30-140 (dBA).
A and C weighting plus 16 user selectable bandwidth.	Selectable A and C weighting for RMS.
256 kilobytes standard memory.	Complete data logging capabilities with 256 kilobytes standard memory.
Sampling periods are user selectable from 32 samples per second for 42 minutes with memory capacity up to 64000 samples (standard) or 250,000 samples (optional).	Time history sampling periods are user selectable from 32 samples per second to one sample every 255 minute.
Direct interfaces for printers, digital data recorders, analog tape recorders, computers, modems, and optional floppy disk drives.	RS-232 computer and modem interface standard. All functions fully programmable. Software available for IBM-PC™ compatible computers. Direct printer interface to print and graph all measurement results.
Interfaces with optional Model 2100 weather proof outdoor microphone system for use in harsh environment and permanent installation. Interfaces with optional Model 900 series preamplifiers and accessories.	Interfaces with optional Model 2100 weather-proof outdoor microphone system for use in harsh environments and permanent installation.
Size: 5.08 x 22.88 x 15.18 cm (H x W x D). Weight: 1.701 kg.	Size: 15 x 7.5 x 2.5 cm (H x W x D) Weight: 393 g

8.3.1 Prediction of Sound Pressure Level Spectra

The Activity Accounting Technique (AAT) developed to determine the sound power level spectra for different activities of mining machinery operating in a surface mine was discussed in Chapter 4. Based on these sound power levels, sound pressure levels can be predicted at any location outside the mine provided that the attenuation at different frequencies is evaluated. In order to validate the integrated noise prediction system, sound pressure level spectra experiments were conducted at the Deep Face Zone of the test quarry deploying a front-end-loader and dump trucks as the production machinery. This section presents the results of the validation work carried out to predict the sound pressure spectra at a selected location as part of the final system validation.

The noise field near a working shovel and dumper is mainly due to the various activities of the machines. The equivalent continuous sound pressure levels (L_{eq}) at a location in the far field depend on the noise generated by the activities. The duration of the activities is an important parameter influencing the L_{eq} level. There is a definite working time cycle for each of the activities involved in a work zone deploying an excavator and a dump truck. This results in a cyclic variation of the noise field. Various activities contributing to noise, their duration per cycle and their sound pressure levels are represented as shown in Table 8.2. The other parameters affecting the noise level in the system are:

q_t : capacity of the truck, tonnes
q_e : bucket capacity of the excavator, tonnes
D : hauling distance, km
V : truck speed, kmh^{-1}
t_r : truck running time, min (=120D/V)
t_{in} : time between loading two trucks, min
t_c : cycle time of the shovel, min

Table 8.2 Acoustic emissions of mining activities.

Activities	Duration per cycle (min)	Sound Pressure Level (dBA)
Crowding	t_{cr}	L_{cr}
Excavating	t_e	L_e
Swinging with load	t_{sl}	L_{sl}
Loading	t_l	L_l
Swinging empty	t_{se}	L_{se}
Spotting and positioning	t_{sp}	L_{sp}
Propelling	t_p	L_p
Interchanging	t_{in}	L_{in}
Dumper idling	t_D (= t_c +t_{in})	L_D

The cycle time of a shovel can be represented as:

$$t_c = t_{cr} + t_e + t_{sl} + t_l + t_{se} + t_{sp} \tag{8.20}$$

Where,

t_{cr} : crowding time
t_e : excavation time
t_{sl} : slewing time with load
t_l : bucket discharge time
t_{se} : slewing time with empty bucket
t_{sp} : time for spotting and positioning

The truck loading time is given as:

$$\text{Truck loading time} = t_c\left(\frac{q_t}{q_e}\right) \tag{8.21}$$

Thus, the number of dump trucks (n) for the rated hourly production capacity is determined as:

$$n = \frac{t_c \cdot \left(\frac{q_t}{q_e}\right) + t_{in} + \frac{60D}{V}}{t_c \cdot \left(\frac{q_t}{q_e}\right) + t_{in}} \tag{8.22}$$

Number of cycles for loading a truck:

$$n_1 = \frac{Heaped\ Capcity\ (truck)}{Bucket\ Capacity\ (excavator) \times b.f.f} \tag{8.23}$$

where,

$b.f.f$: bucket fill factor

Durations of different activities for a given hourly production can be represented as shown in Table 8.3. The duration of each of the noise generating activities per shift is obtained by multiplying the duration per hour by the effective working hours during the 8 hourly shift. Let these times be represented as T_i, i=1, 2, ..., 9. It is assumed here that the engines of dumpers near the shovel are put off during the period other than the effective working hour.

Table 8.3 Activities in the excavator-truck operating zone and their hourly duration.

Activity	Duration per hour (min)
Crowding	$t_{cr} \times n \times n_1$
Excavating	$t_e \times n \times n_1$
Swinging with load	$t_{sl} \times n \times n_1$
Loading	$t_l \times n \times n_1$
Swinging empty	$t_{se} \times n \times n_1$
Spotting and positioning	$t_{sp} \times n \times n_1$
Propelling	$t_p \times n \times n_1$
Interchanging truck loading	$t_{in} \times n_1 \times (n-1)$
Dumper idling near shovel	$t_D \times n \times n_1$

Thus, the 8 hourly L_{eq} for the shovel dumper operation can be expressed as:

$$L_{eq} = 10 \log \left[\frac{1}{8} \sum_{i=1}^{9} T_i \times 10^{L_i/10} \right] \tag{8.24}$$

The activity accounting technique was used to predict the sound power level of a loader-truck operation in the test quarry as discussed in Chapter 4 (Figure 4.16). The routines coded in C++ for the prediction of sound pressure spectra at a selected location in the far field of a work zone deploying mining machinery are shown in Figure 8.9. The predicted sound pressure levels are then corrected for combined ground absorption, pit-wall effects and air absorption. The sound pressure levels at different frequencies for the activities of the loader and dump trucks in the deep face zone were predicted at a station on the eastern bank of the quarry as shown in Figure 8.10. These predicted values are plotted in Figure 8.11. The predicted L_{eq} at this station for the duration of the experiment was 81.62 dBA. This value was found to be 2.4 dBA less than the directly measured value. The prediction has not taken the noise due to the operation of the fixed plants near the measurement station and the passage of aeroplanes during the experiment into account. Thus, it was concluded that AAT can be used for noise level prediction provided that a database of the sound power levels of activities is available and the reliability of the prediction depends on the accuracy of this database.

```
class airab
{
private:
float freqXc[acts], freqYc[acts], freqZc[acts], freqx[acts],freqy[acts],freqz[acts],measDist[acts] ;
 float Xr,Yr,Zr,A_weight[octs];

                    float freq[octs];
                    float SPL[octs][acts];
                    float sourc_Pow[octs][acts]; // power levels of the source activities at different freq
                    float pred_SPL[octs][acts];  // predicted SPL at reciever's location

                    float dist[acts] ;
                    float predAwt[octs][acts];
                    float actDba[acts],act_time[acts],Leq;
public:
                    void get_XYZc() ;
                    void get_XYZdef();
                    void get_LPdef();
                    void get_OctFreq();
                    void cal_measDist(); //distances from the monitoring
                                         //point to the activity centere
                    void cal_PowCent();
                    void showReslt();
                    void get_RecLoc();
                    void cal_dist();       //distances from the activity
                                           // centre to the receiver's location
                    void cal_predSPL();
                    void get_Aweight(); // getting the data for a-weighting at diferent freq
                    void cal_predAwt();
                    void cal_actDba();
                    void get_Times();
                    float cal_Leq();
                    };
```

Figure 8.9 The software code written to predict sound pressure level spectra based on the Activity Accounting Technique.

Predicted A-weighted SPL
At an observer Location of (650,350,79) due to different activities at the deep face of the quarry

Freq	Crowding	Excavating	Swinging (L)	Swinging (E)	Propelling	Spotting	Truck Loading	Truck Idling
31.5	51.5316	56.7992	59.1736	52.1986	54.7702	55.6722	52.8671	55.2709
63.0	53.1488	62.5188	55.1515	71.0128	76.0855	61.9920	66.4869	66.4869
125.0	51.6179	52.8972	52.4852	64.2698	66.5468	55.8712	60.9660	54.9511
250.0	50.9249	49.5324	51.7747	60.1408	62.6306	67.0086	50.8036	53.5435
500.0	50.6700	51.2243	48.8200	59.5258	60.3370	69.1044	52.1996	55.1643
1000.0	49.6532	45.7730	46.9858	58.9248	58.2659	67.0584	67.7540	51.9134
2000.0	42.8748	41.9469	43.7595	55.9510	55.5616	54.9446	44.4409	45.9559
4.0000	34.1163	36.0503	52.9197	58.6707	51.6379	43.7936	39.8927	39.8052
8000.0	37.4536	43.1232	52.9197	52.5658	58.0079	49.0396	49.6496	38.3325

Activity wise Band dBA
At observer Location of (650,350,79)

Act 1 : 78.93
Act 2 : 81.43
Act 3 : 79.52
Act 4 : 84.30
Act 5 : 89.61
Act 6 : 83.67
Act 7 : 82.28
Act 8 : 81.91

Leq: 81.62 dBA

Figure 8.10 Program output for noise level prediction based on the Activity Accounting Technique.

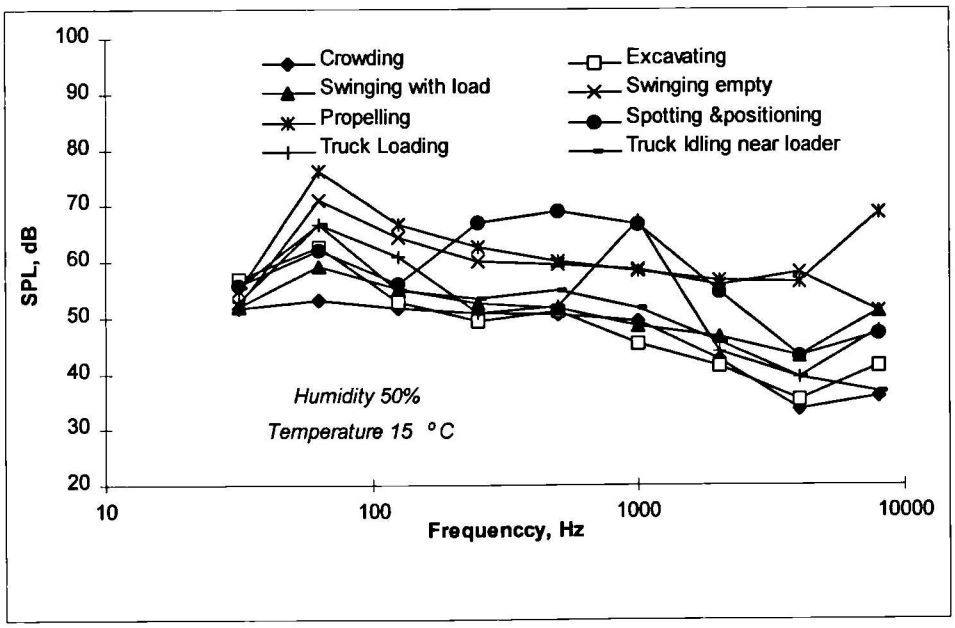


Figure 8.11 Estimated spectra due to various activities at a selected location under specific atmospheric conditions.

8.3.2 Experimental Noise Measurements at the Test Quarry

To test the validity of the noise prediction system developed the Experimental Measurement Technique discussed in Chapter 4 was applied to evaluate the sound power levels of the work zones in the test quarry. The attenuation due to air absorption,

Table 8.4 A sample of data recorded by the sound level meter.

Model 870 Serial Number: A0319

Station: BHUN9.870 Thu 10Nov1994 Period = 00:05 (hh:mm)

Time	Duration	L_{eq} dBA	L_{min} dBA	L_{max} dBA	*L1* dBA	*L5* dBA	*L10* dBA	*L33* dBA	*L50* dBA	*L90* dBA	Wind Avg ms^{-1}	Wind Dir @ Max
12:54:49	00:10.40	71.9	67.2	75.7	75.7	75.2	74.4	72.0	71.2	69.4	8.9	SSW
12:55:00	05:00.00	73.7	63.7	98.5	80.0	77.0	75.9	73.2	71.7	68.5	8.1	SW
13:00:00	05:00.00	70.2	52.8	80.5	77.7	75.4	74.2	70.7	68.2	57.7	6.7	SE
13:05:00	05:00.00	65.2	50.7	79.5	75.5	72.5	69.7	61.6	58.2	54.0	7.0	ENE
13:10:00	05:00.00	66.7	51.6	80.9	75.9	73.0	71.2	64.7	61.5	55.3	7.5	ESE
13:15:00	02:57.87	69.4	52.3	84.9	80.0	75.7	73.7	66.0	62.2	55.1	8.1	E
10:54:59	00:00.93	63.5	62.8	64.0	64.0	64.0	63.8	63.7	63.5	63.0	0.0	N
10:55:00	05:00.00	72.0	57.7	90.0	84.0	78.2	74.5	68.4	66.4	61.0	1.1	ENE
11:00:00	05:00.00	74.4	66.4	84.2	80.5	78.0	77.0	74.7	73.5	68.7	2.8	E
11:05:00	05:00.00	75.0	68.9	81.2	79.4	77.9	77.2	75.5	74.7	72.2	3.0	ENE
11:10:00	05:00.00	74.7	68.0	84.5	80.2	77.5	76.5	75.0	74.2	71.2	2.7	ENE
11:15:00	05:00.00	75.0	70.4	82.9	79.5	77.7	77.0	75.5	74.7	72.7	2.0	ENE
11:20:00	05:00.00	74.7	68.0	81.2	79.2	77.4	76.5	75.2	74.5	72.2	1.8	ENE
11:25:00	05:00.00	75.5	70.5	82.4	78.9	77.9	77.2	75.9	75.2	73.2	2.1	ESE
11:30:00	05:00.00	74.2	67.0	84.5	80.5	77.5	76.5	74.2	73.4	70.5	3.8	ESE
11:35:00	05:00.00	74.0	67.0	79.7	78.2	76.9	76.0	74.5	73.5	70.7	3.2	E

ground absorption and the barrier effects of the pit-walls were evaluated by using the models developed.

Noise levels in dBA were continuously monitored at each of the monitoring stations for each work zone. Noise measurements were also carried out with a hand held sound level meter at different locations around the quarry for the verification of predicted values. Measurements were also taken at a number of relevant locations to record the effect of berms on noise propagation. The data stored on the sound level meters was down-loaded to a PC and time series of the observation period were obtained. Table 8.4 shows a sample of the recorded data at a particular monitoring station.

Table 8.5 The co-ordinates and sound pressure levels at the monitoring stations.

Location	X	Y	Z	SPL (dBA)
Portable Crusher zone.				
1	488.568	448.406	63.5	85.4
2	506.214	423.966	68.0	87.2
3	500.684	399.643	64.0	102.5
4	503.892	375.474	67.0	94.5
5	482.203	359.429	64.0	93.9
6	465.443	380.360	64.0	95.2
7	471.286	401.505	64.0	101.2
8	462.760	422.601	64.0	84.5
Deep Face zone				
1	646.061	600.372	48	79.2
2	660.873	574.701	47	77.4
3	631.231	588.031	47	80.2
4	643.253	576.486	47	83.4
5	610.504	548.066	51.5	79.5
6	637.114	532.634	52.5	78.6
Main Crusher zone				
1	694.307	497.729	64	72.4
2	703.895	473.222	64	73.2
3	724.25	470.691	64	76.7
4	739.699	451.795	65	86.5
5	746.411	422.324	68	84.2
6	710.945	407.585	71	78.9
7	692.713	415.404	69	77.5
8	659.001	431.641	70	75
9	678.031	454.374	65	82.7
Fixed Plant zone				
1	811.994	348.862	84	83.4
2	849.401	324.014	83	83.2
3	877.577	318.577	83	75.9
4	905.435	311.691	83	69.5
5	925.451	283.168	83	81.4
7	903.464	241.42	85	73.2
8	924.63	235.878	85	72.5
9	951.887	226.989	85	75.2
10	957.452	203.382	85	72
11	791.893	258.036	85	74.6
12	726.463	275.143	88	74.5

From the measured L_{eq} values for the steady state operating conditions of the work zones input data for the prediction models were prepared. A regular grid with the south-east corner of the quarry boundary as the origin was selected. The noise monitoring system was validated in an area of 1100x800 m^2 around the quarry. The position of the monitoring stations were determined with respect to the origin of the selected grid. Table 8.5 presents the co-ordinates and the steady state sound pressure levels measured at the monitoring stations.

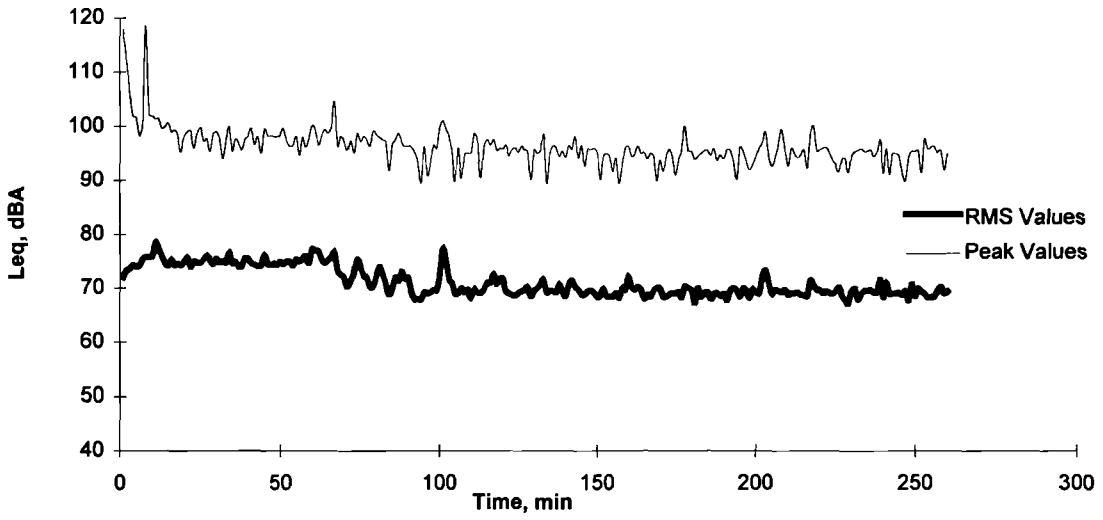


Figure 8.12 Measured time series at one of the noise monitoring stations in the test quarry during the experiment.

8.3.3 Directivity Corrections

An example of the time series recorded by the Larson Davis SLM 870 is shown in Figure 8.12. Input data files as shown in Table 8.5 were prepared from such observed time series recorded by the sound level meters. These were used to determine the EAC's of the four work zones following the theory discussed in Chapter 4. Table 8.6 summarises the output obtained by using the source power model described in Chapter 4. The equivalent acoustic centre data was then used to determine the directivities of the noise zones and the predicted noise levels at the receivers' locations around the quarry. Attenuation due to ground absorption, air absorption and the pit-wall was determined using the attenuation models described in Chapters 5, 6, and 7. The EAC based

prediction of sound pressure levels at a particular location in the far field needs to be corrected for the directivity indices. The following section discusses the technique developed by the author for directivity corrections to the EAC based predicted values.

Table 8.6 The co-ordinates and the predicted sound power levels of the four Equivalent Acoustic Centres at the test quarry.

Noise Zones	X	Y	Z	L_W
Portable Crusher	487.109	395.467	64.2550	125.193
Production Face	637.764	572.294	48.4168	109.943
Main Crusher	722.774	441.976	66.3545	113.507
Fixed Plant	861.931	305.410	83.7938	116.950

The directivity indices of the EAC at the position of the EAC definer are given as the deviations of the measured sound pressure levels from the values predicted from the sound power level of the EAC. The directivity corrections are considered as vector quantities since their values depend on the direction with respect to the EAC. In Figure 8.13, S is the location of the EAC of a large area source determined on the basis of measurements at *n* stations with co-ordinates (x_i, y_i), where i=1, 2, 3,..., *n*. Let there be a position (x, y) of a receiver, R, in the far field of a noise source S. It is assumed that the directivity correction at the position of a receiver would be the combined effect of the directivity indices obtained at the nearby measurement stations. Therefore, one needs to consider only those directivity indices which are directed towards this position. The directivity indices of the measurement stations that do not influence the predicted levels at the particular position of a receiver can be eliminated as follows:

Draw a perpendicular PP to the line RS joining (x, y) and the EAC (x_c, y_c). The slope of the line RS is given as:

$$\tan\theta = \frac{y - y_c}{x - x_c} \tag{8.25}$$

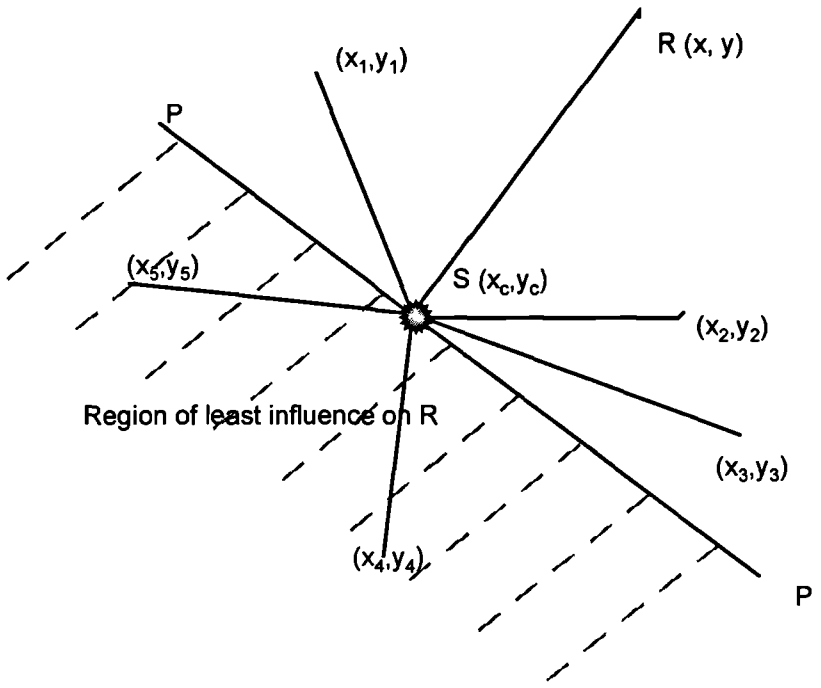


Figure 8.13 The directivity corrections for the EAC based sound pressure levels.

Therefore, the slope of the perpendicular is given as:

$$\tan\theta' = -\frac{x - x_c}{y - y_c} \tag{8.26}$$

The slopes of the lines joining the EAC and the measurement stations are given as:

$$\tan\alpha_i = \frac{y_i - y_c}{x_i - x_c} \tag{8.27}$$

The condition *if* $\alpha_i > \theta'$ or $\alpha_i > \theta' + 180^0$ is used for discarding the measurement station of least influence.

Now the problem is reduced to calculate the influence of the significant directivity indices. If there is no station of significant directivity index, the position of the receiver does not require directivity correction. If there is only one significant station then the directivity index of that measurement station will be assigned to the receiver position. If more than one measurement station remains after the above elimination of least significant measurement station their combined effects will have to be evaluated.

The directivity indices of these points are combined together by taking the resultant effects of these stations. Figure 8.14 shows R_1 as the resultant directivity for directivities P and Q at measurement stations 1 and 2 respectively. Similarly, R_2 is the resultant of R_1 and S is the directivity of location 3. Knowing the slopes of the lines joining the locations with the EAC, the resultant can be obtained as:

$$R_1^2 = P^2 + Q^2 + 2PQ\cos|\alpha_2 - \alpha_1| \tag{8.28}$$

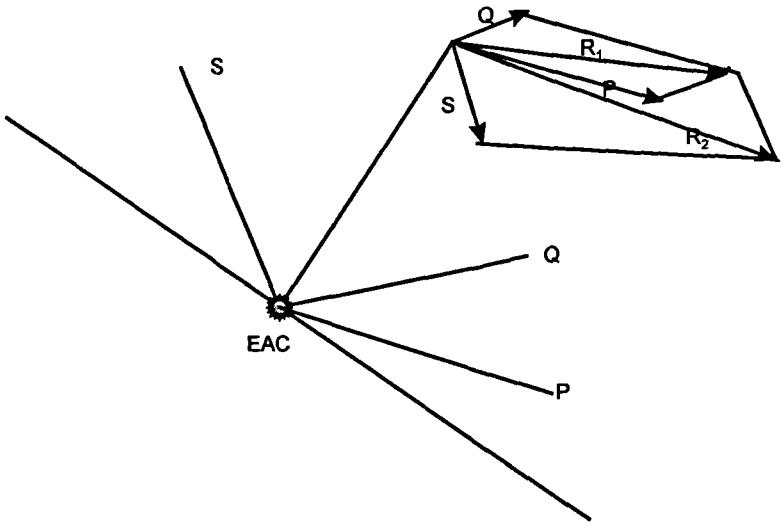


Figure 8.14 Combining the significant directivities.

The slope of the direction of this correction is given as:

$$\tan\gamma = \frac{P\sin|\alpha_2 - \alpha_1|}{Q + P\cos|\alpha_2 - \alpha_1|} \tag{8.29}$$

R_2, the resultant of R_1 and S, is determined in a similar way. In cases where the values of the directivities are less than 6 dB another assumption has been used. In this assumption the shortest distance from the receiver location to the lines joining the EAC and the EAC definer stations are determined. The directivity of the measuring station for which this perpendicular distance is minimum is considered as the directivity of the receiver location. In the system developed, the second procedure for directivity corrections was incorporated using a small module (DIRCOR.CPP). The first method has not been tested in this research. The directivity indices for the test case in the quarry were calculated for each EAC at each node of a 50x50 m^2 grid over the mining area.

8.3.4 Far Field Noise Prediction Results

The predicted and measured sound pressure levels at different monitoring stations within and around the quarry are given in Table 8.7. This shows that the overall coefficient of correlation of the measured and predicted values at the selected verification locations is 0.998154. This high degree of correlation is observed because the verification stations were close to the quarry and therefore the other noise effects were minimised.

Table 8.7 Predicted and measured sound pressure levels at different locations near the quarry.

Station No.	X	Y	Z	Predicted SPL, dBA	Measured SPL, dBA	Error, dBA
1	177.003	344.311	54.8816	48.4440	47.5	0.9440
2	85.303	122.248	49.9201	49.2630	51.2	-1.9370
3	353.643	304.713	74.2249	49.9201	51.0	-1.0799
4	347.541	345.932	74.9518	51.2587	53.0	-1.7413
5	352.704	403.958	75.7506	51.6141	52.5	-0.8859
6	359.746	441.792	75.6976	54.7356	54.5	0.2356
7	418.284	475.000	63.8505	54.8816	55.3	-0.4184
8	375.016	525.000	51.2587	63.8505	65.0	-1.1495
9	349.055	555.000	48.4440	74.2249	75.0	-0.7751
10	423.664	468.783	78.4657	74.9518	76.0	-1.0482
11	220.000	492.622	54.7356	75.7506	75.4	0.3506
12	120.000	528.994	51.6141	78.4657	78.0	0.4657
13	485.000	395.600	90.4505	90.4505	91.0	-0.5495

Figure 8.15 shows the comparison of the measured values near the portable crusher zone with the values predicted by the prediction system developed. This shows that the system at its present stage gives satisfactory results provided that the selected prediction points are not affected by external noise sources. The environment should also be free from scattering, complex barriers, highly reflecting surfaces, high wind speed and temperature gradients.

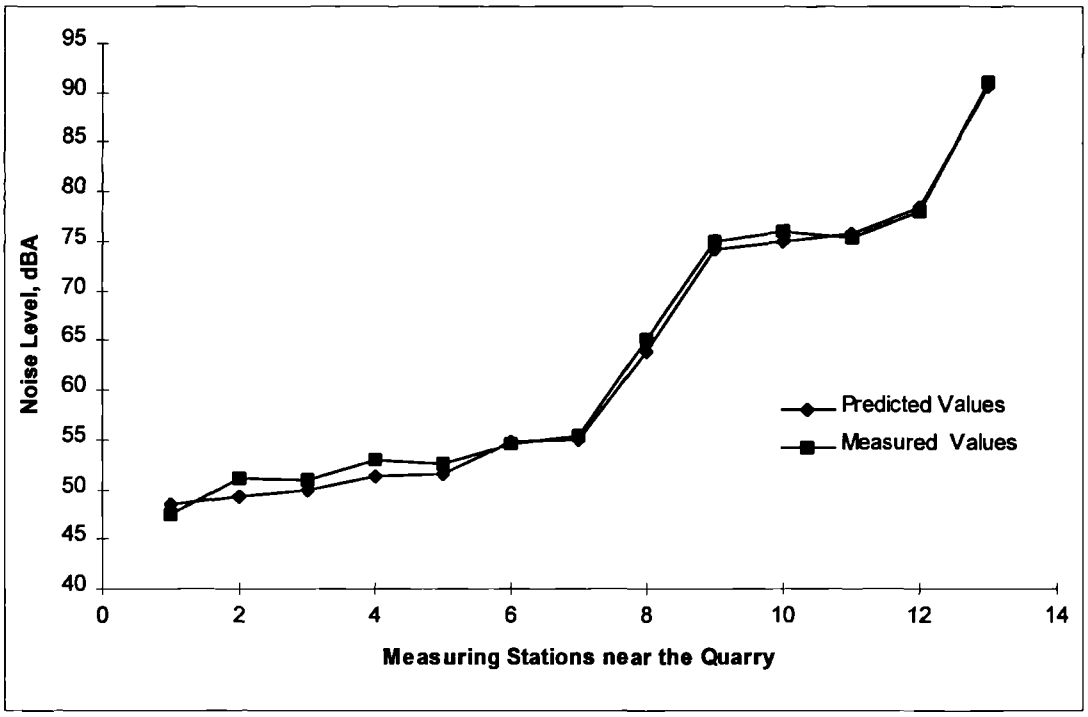


Figure 8.15 Comparison of measured and predicted sound pressure levels near the test quarry.

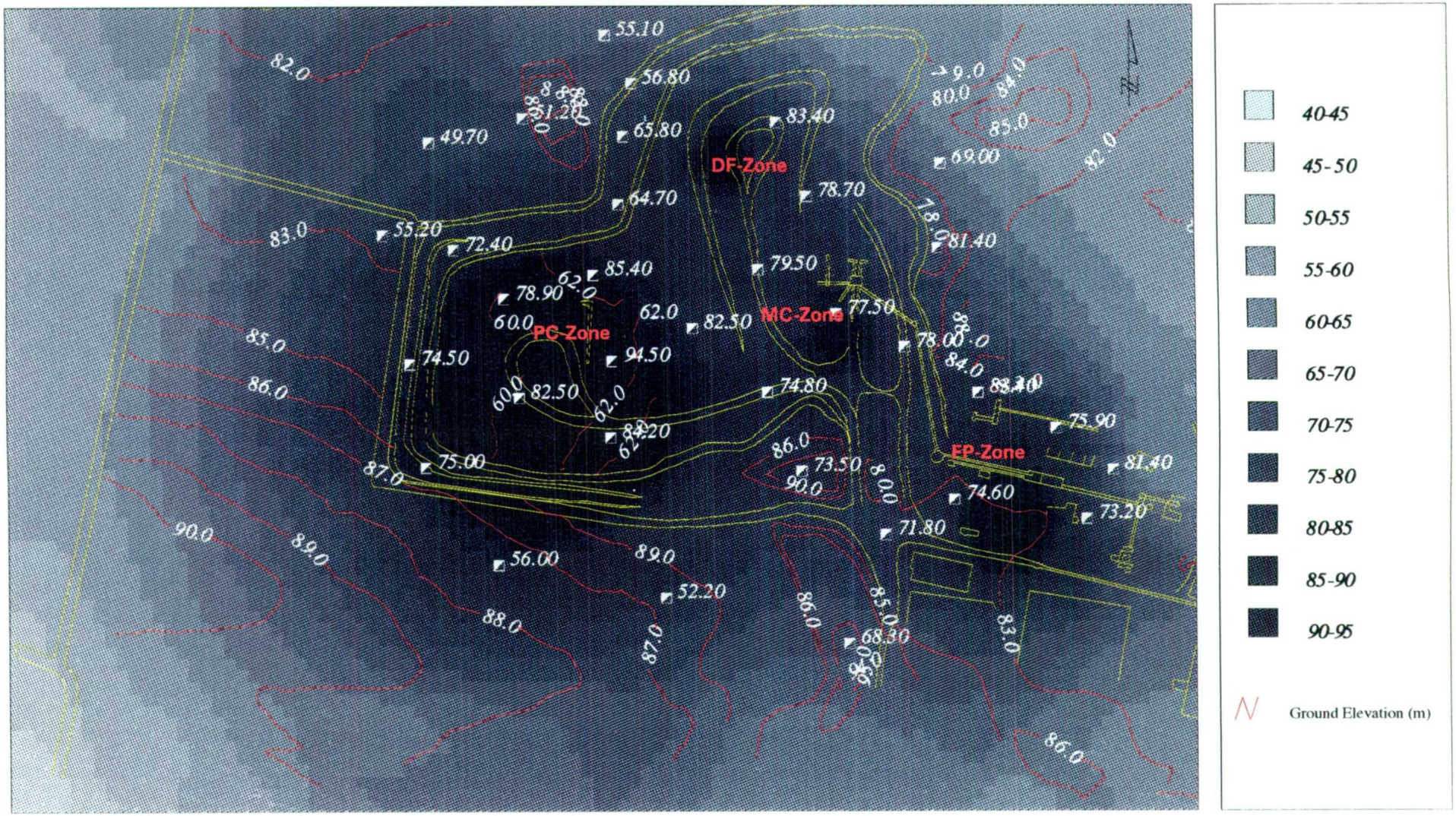
Following the initial validation experiments using a number of monitoring stations close to the quarry the next step was to carry out noise predictions for a regular grid in a large area around the quarry. The predicted sound pressure levels were then interpolated using UNIMAP to obtain a sound pressure level distribution over a finer grid size of 10x10 m^2 for GIS interpretation. Figure 8.16 presents the GIS output showing the quarry topography, surface structures and geographic features together with the measured and predicted noise levels around the quarry. The predicted noise levels shown in grey-scale GRID format include the corrections for directivity and the attenuation due to spreading, ground absorption, air absorption and pit-wall barrier effects.

8.4 Conclusion

This chapter presented the methodology used to integrate the source power model and the three attenuation models developed under a noise prediction system. The model was validated by conducting a comprehensive field measurement/prediction exercise at a limestone quarry in the Republic of Ireland.

Figure 8.16 A GRID overlay of predicted noise levels over the topography, surface structures and geographic features around the test quarry.

Predicted Noise Levels (dB) due to all zones



The noise prediction system developed works with user provided input data. The data format depends on the type and purpose of the application that the system intends to serve. For the determination of noise quality in detail at a given location the system uses the Activity Accounting Technique developed and discussed in Chapter 4. To use this technique the system must be provided with detailed information regarding the activities involved in a particular working complex. Unfortunately, such acoustic databases are rarely available. Therefore, a method of evaluating the basic input data based on the production capacity, equipment specifications and equipment deployment strategy has been suggested. This suggested technique has been validated with acoustic information derived experimentally in the field research. Thus it could be concluded that the theoretical calculations involving the activity pattern and geometric location of the activity centre based on the production target and equipment selection can lead to accurate predictions of the sound power levels. Future developments in accounting for complex reflection, scattering and attenuation of sound energy in the quarry environment will improve this method of noise level prediction and will contribute to the acoustic design of surface mines and quarries.

In cases where detailed noise quality is not important, the environmental noise can be predicted in terms of equivalent continuous sound pressure levels. The equivalent continuous sound pressure level is determined by evaluating the sound power level of different work zones represented by the Equivalent Acoustic Centres of each zone. Attenuation due to air and ground absorption including the effects of pit-walls are theoretically calculated, based on the prevailing meteorological and terrain conditions using the models described in Chapters 5, 6 and 7.

The limestone quarry used for the validation work had four definite work zones. The measured values confirmed the predicted values. The validation area was deliberately selected closer to the quarry to eliminate the effects of external factors on the noise level.

Chapter 9

Conclusions and Recommendations for Future Research

9.1 Introduction

This thesis has presented the results of experimental and theoretical research into environmental noise levels near surface mining and quarrying operations conducted by the author during 1994-96, and proposes a system for modelling and predicting such noise.

The noise fields around a surface mining area are varied in nature depending on the mining system deployed and the prevailing terrain conditions. During the execution of this research, various aspects of noise prediction in large and complex industrial operations have been critically studied. Field experiments were designed and carried out under varied field and operational conditions. The findings of the current theoretical and experimental research led to the development of surface mining noise assessment techniques, and a prediction system such that acoustically designed surface mines and

quarries can be achieved in the future. Current mine planning and design procedures do not quantitatively test the alternative designs of surface operations for possible environmental noise impact as no reliable method for such quantification exists. Therefore, it is believed that the Acoustic Database Technique and the Activity Accounting Technique developed in this research will find wide applications as mine planning tools for quantifying possible environmental noise impact. The proposed techniques, and the models developed, have been validated through field experiments. Through critical analysis of its findings the present study revealed a number of critical areas demanding careful research for further development and refinement of the present methods of modelling and prediction.

This chapter summarises the main conclusions of the research. The recommendations for future research necessary in the area of mining noise and acoustic mine design are also discussed in the following sections.

9.2 Conclusions

The noise field near surface mining areas results from activities distributed over the working zones of the mine. The impact of noise in the mining environment depends upon the sound power level of the noise generators, the prevailing geo-mining conditions and the meteorological parameters of the working site. To assess the noise level in terms of daily noise exposure in such areas is challenging as the sound energy is generated by a number of noise sources simultaneously, or singly in a random pattern. Therefore, mere studies of the sound power levels of the machinery deployed will not provide a useful method for noise level prediction near surface mines. Rather, the noise levels will have to be studied as an integrated effect of various activities, their working environments and the prevailing geographic and meteorological parameters.

The method of wave acoustics was adopted in this research, as the alternative, the energy accounting technique known as 'statistical energy analysis' (SEA), necessitates more experimental details of all the machinery to determine the sound power level within a surface mine. In mining conditions the equipment locations and working

environment continuously change as the mining activities progress. Therefore, it was decided that the SEA method will not always be feasible and simple to carry out. The ray acoustic technique may be used as an alternative method, and could be rather useful in areas where very high levels of noise propagate over a long distance.

The International Standards Organisation has suggested a generalised method for estimating noise levels near construction sites deploying a number of earth moving machinery. The Standards suggest the values of sound power levels of various machinery working in such operations and propose a method to calculate the noise levels based on these values. However, this information does not account for the variation of the noise levels with age, maintenance level, working strategy and loading conditions. In this research, the noise level due to the steady state operations of a group of machinery working at a normal production rate has been determined on the basis of the *sound power levels of the working zones* of a mine or quarry where different machines may work under different conditions. Attenuation of noise due to ground absorption, air absorption and the effects of the pit-wall on sound propagation from the working zone was considered in this estimation.

However, the most difficult and critical problem in predicting noise levels near mining operations on the basis of the sound power levels of working zones in a quarry was the evaluation of the sound power level. The methods available in the Standards were reviewed. The L_{eq} method prescribed by the Standards considers barrier corrections of 5 dB or 10 dB in the noise prediction model. In a mining application the barrier effects of the pit-wall cannot be approximated with such ease, and must be evaluated from the geo-mining conditions. The plant sound power method described in the Standards does not provide detailed method of determining the directivities of the distributed sources. The mining and quarrying operations involve a number of machines of different categories distributed over different areas within the mine. Depending on their placement, the overall noise emanating from the mine varies in quality and level. The mining operation is also characterised by a number of machines working simultaneously. Each of these has their own cycle of activities. Sound power levels recommended by the manufacturers often neglect this aspect. Moreover, depending on

the placement of the machines in the mine, the noise levels in certain directions may be higher than those in the other directions. This effect is not attributed to a particular machine alone, rather a number of machines working together in the area. Because of this, the calculation of sound power in a mine simply on the basis of the type and the number of a particular machinery will not be of much benefit. Therefore, the challenge was to develop and establish a technical approach to express the sound power level of the mine so that the directivities could be accounted for. The method of the Equivalent Acoustic Centre (EAC) was applied to address this problem. Thus, for environmental noise prediction purposes, it is useful to represent each of the work zones within a mine as an equivalent noise source. The present work developed the Equivalent Acoustic Centre (EAC) method for such purposes. In this method a large noise source comprised of a number of distributed sources is represented by a point source, characterised by its specific location and sound power level. It was proved in the field that measuring the sound pressure levels and the co-ordinates at a number of EAC definer locations will enable the determination of the sound power level and co-ordinates of the equivalent acoustic centre of a complex noise source.

The preliminary validation experiments to determine the EAC's were conducted at the processing plant of Tara Mines in the Republic of Ireland. The sound power level of the whole plant was represented by the EAC determined by these experiments for predicting the noise level in the surrounding area. When compared with the measured sound pressure levels, the predicted values yielded a correlation coefficient of 0.96. These early results encouraged further research into this concept. Moreover, it was observed at Tara that the EAC is not a static location. In order to predict a time series of the sound pressure levels at a particular location the time dependent behaviour of the EAC can also be determined. The study at the Tara Plant showed that the EAC of the processing plant was varying with a maximum displacement of 45.3 m in the Y co-ordinate direction during the 150 minute experimental period. The sound power generation had a standard deviation of 0.715. By determining the location and the sound power level of the EAC over a period of time, the periodic change of sound pressure level at a selected location can be easily determined. These findings of the preliminary validation tests led

to further studies on the applicability of the method in surface mining and quarrying environments.

The research resulted in the incremental development of a source power model incorporating three complementary techniques referred to in this research as the Experimental Measurement Technique (EMT), the Acoustic Database Technique (ADT) and the Activity Assessment Technique (AAT). The EMT was developed for application in existing mines and works with input data from planned experiments. The ADT was developed for use at the design stage of a mine and would work with input data from an acoustic database. Both these techniques can predict the equivalent continuous sound pressure level in the surrounding area. However, they do not reveal the noise quality, as the sound pressure level spectra are not obtained in these techniques. If noise quality assessment is of primary concern the Activity Accounting Technique (AAT) can be used for any mine at its working or design stage. This technique generates the noise level spectra for various activities performed by a group of machinery taking the input information from the equipment deployment strategy, equipment specifications and production targets. All these modules were coded in C++ to evolve the Source Power Model which became the core of the noise prediction system developed.

The AAT depends on identifying different activities in the quarry and determining their duration and frequency spectra. The number of such activities increases with an increase in size of the mine and in many situations may require a large amount of data processing. Therefore, if precise noise quality prediction is not necessary this technique may not be suggested. However small mines or construction sites near residential areas may need to analyse noise quality and the AAT will be useful for that purpose. A reliable database to support the AAT is rarely available and therefore a method of evaluating the minimum input data, based on the production capacity, equipment specifications and deployment strategy has been developed. Limited studies were carried out at the deep face of a limestone quarry in the Republic of Ireland to test the validity of the developed technique. The noise signatures of Front End Loader (FEL) and Dump Truck operations were experimentally derived. The studies on the activities

of FEL's and dump trucks revealed that high level noise was generated by these machines whilst travelling empty. The predominant frequency was found to be 125 Hz. Since low frequency noise propagates longer distances, activities with such machinery needs closer attention during the design of the face layout. Based on the experimentally determined frequency spectra of sound power levels of different activities in a work zone the sound pressure level spectra at selected locations were predicted. The broad band sound pressure level so predicted was found to be 2.4 dBA less than the directly measured value. This deviation could be attributed to the fact that the prediction model does not consider external noise sources. During the field experiments, the presence of a crushing plant and aeroplanes flying overhead affected the noise field.

The Experimental Measurement Technique was used to determine the sound power levels of the EAC's of the test quarry during the final validation of the noise prediction system, incorporating the attenuation of noise by ground absorption, air absorption and effects of the pit-walls. To determine the EAC of a work zone the locations of EAC definers were fixed and sound pressure levels at these locations were monitored. In this research, these EAC definer locations were determined by subjective on-site decision-making on site. The following assumptions were made:

- The work zones operate simultaneously in a steady state,
- External noise sources are negligible,
- The EAC is stationery,
- Haulage noise is considered as part of the work zones.

The data obtained in experimental measurements were processed by the model developed and four equivalent acoustic centres representing the overall sound power level of the test were determined. Each of the EAC's was characterised by their co-ordinates, sound power levels and directivity patterns. A method of vector addition was developed to account for the effects of the directivity indices of the EAC's in predicting far field noise levels.

Following the development of the source power model, ground absorption, air absorption and the effects of pit-walls were studied as the major causes of noise attenuation. ISO 9613, 1994 suggests a method to calculate ground attenuation. This

procedure was tested in the field and the margin of error was found to be unacceptable. Therefore, the experimental and theoretical method of determining ground attenuation by indirect assessment of the acoustic impedance and propagation constant (following Isei, 1980) was used in developing the ground attenuation model. The developed ground attenuation model calculates the excess attenuation due to ground absorption for a specific location and configuration of the source and receiver. This single parameter model predicting ground attenuation was adopted for its simplicity and accuracy.

Environmental noise pollution research is comparatively new to the mining industry. Therefore, there is no standard practice for evaluating ground attenuation by the mining terrain. The model developed in this research needs site specific input data such as the flow resistivity of the ground surface. Although some experimentally determined values of flow resistivity have been used in the past, there is no clear indication that these values are representative of the mining environment. A simple and easy way of determining flow resistivity by carrying out *in situ* experiments with noise measurements was designed and tested on three different types of mining terrain. These were : grass covered soft soil, a gritty road surface simulating the haul road conditions and settled quicksand simulating the reclaimed areas near overburden dumps. However, further research is required to standardise the flow resistivities of mining terrain for practical use in noise prediction.

In this research, the meteorological effects on ground attenuation of sound energy were not fully studied. The experiments designed may be conducted for a longer period of time, covering a wide range of climatic conditions, to reveal the effects of temperature and humidity on ground attenuation.

The air attenuation model was developed based on the theoretical work carried out in this research. The model considers the user-defined meteorological parameters such as temperature and humidity, and calculates the attenuation due to air for the source receiver configurations. Since sound waves are convected towards the ground when propagating with the wind this may neutralise the effects of noise barriers. Therefore, a study of the wind pattern in a mining area is important for noise control purposes. To

evaluate meteorological effects at a particular site at least two years of monitoring of meteorological data is necessary. These aspects were not studied in this research. However, the air attenuation model developed has the provision of analysing weather data for such purposes. The model has also incorporated the evaluation of ray path curvature indirectly in terms of the Net Solar Index and wind velocity. However, these are not tested in the final validation tests.

Experimental studies under different wind conditions have proved that both the direction and speed of wind have significant influence on the noise level at the receiver's location. Values predicted using available norms were found reasonable. However, the predicted data are specific to selected meteorological information such as temperature and humidity. The developed program to evaluate atmospheric attenuation has been found effective.

The important feature of mining noise is that the main noise sources are located within the pit. The pit-walls act as a noise barrier and provide a good control on environmental noise levels. The author was unable to find much reference to the performance of pit-walls as noise barriers in the literature. The performance of a noise barrier depends, *inter alia*, on the incident angle of sound waves, construction materials of the barriers, acoustic properties of the ground, barrier geometry, location of the sound sources with respect to the barrier, type of noise sources, and atmospheric conditions. Analysis of all these factors was beyond the scope of this research. However, the pit-wall of a surface mine or quarry was considered as a barrier, and the loss of energy radiated from the in-pit sources due to this was evaluated using the theory of image sources and ground absorption considering that the barrier effect is independent of the wind speed.

On considering the acoustic principles, an expression for loss of sound pressure level due to pit-walls was derived and used in predicting their barrier effects. The reflection from the opposite pit-walls was also considered and a reflection correction to the predicted noise levels was introduced. These reflection corrections were adopted from the procedure of calculating traffic noise from depressed roads. In the validation tests a very high correlation (0.99) of predicted and measured values was obtained. It was

shown that the developed model at its present stage yields very good results provided that the site is free from scattering, complex barriers, highly reflecting surfaces and high wind velocity and temperature gradient.

The attenuation of noise levels (dA) was found to be varying logarithmically with distance from the source to the toe of the pit-wall (D):

$$dA = -3.7098 \ln(D) + 3.7615 \tag{9.1}$$

The effect of slope angle θ on the attenuation was found to be linear, represented by:

$$dA = 0.0138\theta + 18.585 \tag{9.2}$$

The effects of the height of a safety berm (B_h) under the prevailing geometric configuration of the test quarry were studied and the following relationship was obtained to relate the berm height to attenuation:

$$dA = 2.7152 \ln(Bh) + 15.91 \tag{9.3}$$

These relationships are, however, not yet ready to use for the purposes of acoustic design of surface mines. Further experiments establishing a correlation with other geo-mining factors, equipment density, production schedules and site characteristics will have to be carried out.

The noise prediction system was developed from an integration of the above-mentioned four models, namely the source power model, the ground attenuation model, the air attenuation model and the pit-wall attenuation model. In this system, the noise sources within a geographically delineated space are modelled as an equivalent point source referred to as the EAC, characterised by its broad band sound power level and location.

The observed dependence of attenuation on the pit geometry and source location implies that acoustically sound mine planning can help to assess the impact of noise pollution in the neighbourhood of surface mining operations.

Apart from the design and manufacturing, noise levels generated by a machine vary with the level of maintenance and the operational skill. Prediction of the time weighted

noise level due to various mining activities is achievable by breaking down all possible activities and determining the sound pressure level of these activities at a known distance. The noise levels at a location can be estimated by determining the sound power levels of the equivalent acoustic centre. The following factors affect realistic assessment or prediction of noise due to surface mining and quarrying operation:

- Acoustic absorption and reflection characteristics of the ground,
- Effects of wind velocity on the sound wave propagation from a depth upward,
- Sound power levels for the equipment complex with all possible operating systems,
- Noise sources at different phases of opencast mining operation,
- Impact of haul road profiles on the noise field,
- Effects of pit geometry on noise field,
- Ageing and maintenance of mining machinery.

Acoustical impedance of the ground surface varies depending on the other physical properties of the ground. The nature of the ground surface influences the sound field over it. The sound field is modified according to the specific normal acoustic impedance, especially when both the source and receiver are located near to the ground. In the mining and quarrying environment all the noise sources and receivers are near to the ground. This calls for more attention to the nature of excess attenuation of the propagating acoustic wave. Experimental determination of the flow resistivity of the ground surface is a prerequisite for applying the noise prediction system.

The noise data are spatio-temporal. However, in the present study the attempts were made to predict the equivalent continuous sound pressure level, and decay of sound with time was not considered. The prediction system has been developed assuming steady state operation of the mining activities.

9.3 Recommendations for Future Research

The new technique of representing sound power of a work zone in terms of its EAC has not been subjected to systematic error analysis. A method for estimating reliability and risk of the noise prediction system will have to be conducted for this purpose.

The EAC definer locations in this research were decided by subjective decision making on site. To make the noise prediction system more commercially applicable, further

research is needed to determine the EAC definer location based on the equipment type and movement, bench design, face layout and number of significant noise generating activities in a work zone. The development of the database necessary for the Acoustic Database Technique will also require a considerable amount of experimental noise research in the future.

In determining the EAC one source of error is the assumption that the directivity factor, Q was taken to be constant for all the measurement stations. The value of Q was considered as 8 (Norton, 1989) because the work zones are within a quarry. The theory will have to be further developed to determine the EAC's for varying Q. Moreover, in certain work zones the assumptions of equivalent-to-point source may not be valid. There is, however, scope for developing a line source equivalent of work zones. This area will have to be considered in future research in this field.

Hohenwarter (1990) proposed the method of sound event level of event wise energy accounting for the study of noise fields. Considering the large number of randomly excited spatially distributed non-coherent events involved in production scheduling and equipment deployment in surface mining, this method may provide a realistic alternative in evaluating surface mining noise. Further research is required in this field.

The incidence of sound waves over the mining terrain results in the transmission of some energy through the rock, depending on the porosity and the internal elastic structure of the rock. These two rock properties vary widely with rock type and the values change with physical state at different stages of mining. The current research into mining noise has not considered the nature of acoustic transmission into the rock-mass. Future research in this field could establish the relationship between the behaviour of different types of rock under varied mining conditions and their impact on the absorption of the sound energy propagating over them. It may be possible to find a correlation between the acoustic impedance of the ground surface and other geo-technical properties of soil. This will help in determining the attenuation of noise generated within the mining areas. This information would be one of the basic inputs to the design or performance analysis of any noise barriers near mining areas. The

technique developed for evaluating the flow resistivity of the ground surface will have to be further investigated. The procedure to determine the ground attenuation by this method will have to be compared with the methods given in the Standards to verify their relative merits and applicability to evaluating the mining terrain.

This research has considered the noise sources located inside the pit and ground reflections for a case of up-gradient propagation of noise. To apply these methods for the down-gradient propagation of noise, further research will be necessary. This will help to develop a method to predict environmental noise levels in hill-top mining conditions.

The effects of the atmosphere on noise propagating from the pit bottom have not yet been established. The atmospheric effects were determined on the basis of available information on the coefficient of atmospheric attenuation (Sutherland *et al,* 1974). It is recommended that further study should be conducted to correlate atmospheric attenuation of noise with changes of wind pattern as a result of the progress of mining activities. More experiments will be necessary to establish the relationship between the wind velocity and ground absorption near mining terrain under different mining conditions.

Acoustic analysis of mining operations is one of the prerequisites for the development of environmentally friendly mining practice. Feedback of such analysis to the noise prediction systems would definitely improve the reliability of the latter. Hence, further research is needed to incorporate acoustic analysis into the management information systems (MIS) and maintenance management systems.

Haul roads in a surface mine are one of the major noise sources. Further research is necessary to compare the noise generation of various modes of transportation. It is also necessary to evaluate haul road profiles in terms of their impact on the noise field. Research is needed to determine the height of safety berms on a haul road so that they can also perform as noise barriers. Such work will lead to an acoustically designed haulage system.

Present work has not considered the impact noise produced in surface mining and quarrying. The impacts of blasts and other impact noise within a mine needs to be investigated considering, their spatio-temporal behaviour.

The Equivalent Acoustic Centre approach has modelled the work zone of a quarry as a point source. It is assumed that the noise generating activities are constant and prediction is carried out for steady state operations. Future research will have to consider modelling the work zone as a fluctuating spherical noise source, so that the effects of inclusion and omission of a particular noise source can be closely examined.

In the present work the impact of dynamic behaviour of mining has not been modelled. The change of configuration of mine requires the determination of sound power level and location of new EAC's of the work zones. Research is needed to model the dynamic behaviour of the resultant noise field. One of the objectives of such study will be to determine the noise history at the receiver location as a function of the locus of the noise source within the mine.

Research into the development of techniques to acoustically design surface mines and quarries is essential. Research is also needed to determine the possible locations of the machinery within a quarry for maintaining the L_{eq} level at a receiver location within a predetermined limit. Alternative designs of equipment deployment and face layouts need to be tested for their impact on environmental noise. The models developed in this research can be used as a starting point for such innovative work.

In order to model noise fields near residential areas adjacent to the mining activities, one needs to consider the scattering of acoustic waves by buildings. Sound levels in the residential areas near mining can be estimated macroscopically by considering repeated scattering of the sound energy by the buildings (Kuttruff, 1982). These aspects, though not covered in the present model, would be of much importance for designing residential areas and civil constructions near surface mining and quarrying activities.

REFERENCES

Alster, M., 1982. *An Improved Method for Determination of Radiated Sound Power and Sound* Transmission From Large Sources, J. of Snd & Vib., Vol. 82, No 2, pp. 261-274.

Anderson, T. D., 1971. Hearing damage can cost up to $40,000.00!, CMJ., Vol. 92, No. 9, Sept'71, pp. 44-45

ANSI S1.26 1978. *Method for the Calculation of the Absorption of Sound by the Atmosphere*, American National Standard, New York.

Attenborough, K.,1982. *Predicted Ground Effects for Highway Noise,* J. Snd & Vib., Vol. 81, No 3, pp 413-424.

Attenborough, K., 1985. *Acoustical Impedance Models for Outdoor Ground Surfaces,* J. Snd & Vib., Vol. 99, No 4, pp 521-544.

Attenborough, K.,1988. *Review of Ground Effects on Outdoor Sound Propagation from Continuous Broadband Sources,* Applied Acoust., Vol. 24, pp 289-319.

Bar, T., 1886. Proceedings of Glasgow Phil. Society, 17, 223-37, 1886.

Bartholomae, R. C., Parker, R. P., 1983. *Mining Machinery Noise Control Guidelines*, A Bureau of Mines Handbook, United States Department of Interior, 1983.

Beckenbauer, Th., 1992. *Living with Leq in Germany,* Proceedings of 'euro noise'92, Imperial College, London, 14-18 Sept,1992, I.O.A., Vol. 14, Part 4 (1992), pp. 33-40.

Beranek, L. L, 1954. *Acoustics,* McGraw Hill, New York

Beranek, L. L., Blazier, W. E. and Figwer, J. J, 1971. *Preferred Noise Criterion (PNC) Curves and Their Application to Rooms,* J. of Acoust. Soc. of Am., Vol. 50, pp1223-1228.

Bies, D. A., 1976. *Uses of Anechoic and Reverberant Rooms*, Noise Control Engineering J., Vol. 7, pp. 154-63.

Bies, D. A.; Hansen, C.H.; 1980. *Flow Resistance Information for Acoustical Design*, Bulletin of the Australian Acoustic Society, 7, pp 17-22.

Bies, D. A. and Hansen, C. H., 1988. *Engineering Noise Control, Theory and Practice*, Unwin Hyman, London.

Brüel and Kjær, 1982. Noise Control, Principles and Practice, Denmark.

BS 4196. *Sound Power Levels of Noise Sources.*

BS 5228, 1975. *Code of Practice for Noise Control on Construction and Demolition Sites.*

BS 5228, Part 1, 1984 (ISBN 0 580 13738 4). *Noise Control at Construction and Open Site.*

BS 4142, 1990. *Method of Rating Industrial Noise in Mixed Residential and Industrial Areas.*

BS 7445, 1992. *Acoustics- Description and measurement of Environmental Noise.*

Carter, N. L., Ingham, P. and Tran, K, 1994. *A Field Study of the Effects of Traffic Noise on Heart Rate and Cardiac Arrhythmia During Sleep,* J. of Snd. and Vib., Vol. 169, No. 2, pp. 211-227.

Chakravarti, J. L., 1973. *Noise- Its Limits in Fan Selection,* CMJ., Vol. 94, No. 3, Sept'73, pp.65-68.

Chaldni, E. F. F., 1821. *Die Akustik, Leipzig.*

Chapman, C. J. and Glending, A. G., 1990. *A Theoretical Analysis of Compressed Air Loudspeaker,* J. Snd & Vib., Vol.138, 1990, p.493.

Chessell, C. I., 1973. *Three Dimensional Acoustic-ray tracing in an inhomogeneous anisotropic atmosphere using Hamilton's equation,* J. of Acoust. Soc. Am., Vol. 53, No. 1, pp. 83-87.

Chessell, C. I., 1976. *The Propagation of Noise along a Finite Impedance Boundary,* Department of Defence, Australian Defence Scientific Service Weapons Research Establishment, WRE Technical Note-1724 (AP)

Daigle, G. A., Embleton, T. and Piercy, J. E., 1983. *Line-of-sight propagation through Atmospheric Turbulence near the Ground,* J. Acoust. Soc. Am., Vol. 74, No. 2, pp. 62-68.

Daigle, G. A. and Stinson, M. R., 1987. *Impedance of Grass Covered Ground at Low Frequencies Measured Using a Phase Difference Technique,* J. Acoust. Soc. Am., Vol. 81, pp. 62-68.

Davies, H.G., 1978. *Multiple-Reflection Diffuse-Scattering Model for noise propagation in streets,* J. Acoust. Soc. Am., Vol. 64, No.2, pp. 517-521.

De Jong, R. and Stusnik, E., 1976. *Scale Model Studies of the Effects of Wind on Acoustic Barrier Performance,* Nose Control Engg., Vol. 6, No. 3, pp. 101.

De Jong, B. A., Moerkerken, A. and van der Toorn, J. D., 1983. *Propagation of Sound over Grassland and over an Earth Barrier,* J. Acoust. Soc. Am., Vol. 86, pp. 23-46.

Delany, M. E. and Bazley, E. N., 1970a. *Monopole Radiation in the Presence of an Absorbing Plane,* J. Snd & Vib., Vol. 13, pp. 269-279.

Delany, M. E. and Bazley, E. N., 1970b. *Acoustical Properties of Fibrous Absorbent Materials,* Applied Acoustics, Vol. 3, pp. 105-116.

Delany, M. E., Harland, D. J., Hood, R. A. and Scholes, W. E., 1975. *The Prediction of Noise Levels L_{10} due to Road Traffic,* J. Snd & Vib., 38, (3), 305-316.

Delany, M. E., 1977. *Sound Propagation in Atmosphere: a Historical Review,* Acoustica, Vol. 38, pp. 201-23.

Delany, M. E., Rennie, A. J. and Collins, K. M., 1978. *A Scale Model Technique for Investigating Traffic Noise Propagation*, J. Snd & Vib, Vol. 56, No. , pp. 325-340, 1978.

Derazay, R., 1972. *Hearing Conservation for the Mineral Industry,* USBM, IC No. 8564, 1972.

Dickinson, P. J. and Doak, P. E., 1970. *Measurements of the Normal Acoustic Impedance of Ground Surfaces,* J. Snd & Vib., Vol. 13, No 3, pp 309-322.

ECC Directive 85/337, 1985. *On the Evaluation of Environmental Impact of Some Public and Private Projects*, 27 June.

ECC Directive 86/188, 1986. *On the Protection of Workers from the Risk Related to Exposure to Noise at Work*, 16 May.

Ellison, A. J., Moore, C. J. and Yang, S. J., 1969. *Methods of Measurement of Acoustic Noise Radiated by an Electric Machines*, Proc. IEE, No 116, pp. 1419-1431.

Elizabeth, S. I. and Russel, G. A., 1977. *Acoustical Scale Model Study of Attenuation of sound by Wide Barriers*, J. Acoust. Soc. Am., Vol. 62, No. 3, pp. 601-606.

Embleton, T. F. W., Piercy, J. E. and Olson, N., 1976. *Outdoor Sound Propagation Over Ground of Finite Impedance,* J. Acoust. Soc. Am. Vol. 59, No. 2, pp. 267-277.

Embleton, T. F. W., Piercy, J. E. and Daigle, G. A.; 1983. *Effective Flow Resistivity of Ground Surfaces Determined by Acoustical Measurements,* J. of the Acoustical Society of America, Vol. 74, pp 1239-44

Fehr, R. O., 1951. *The Reduction of Industrial Machine Noise*, Proc. Second Annual National Noise Abatement Symposium, pp. 93-103.

Franke, S. J., Raspet, R and Liu, C.H.; 1988. *A Numerical Prediction of Atmospheric Sound Pressure Levels in Shadow Zones*, J. Acoust. Soc. Am., Vol 83, pp 816-820.

Fujiawara, K., Ando, Y. and Maekawa Z., 1976. *Noise Reduction by an Absorptive Barrier*, J. Acoust. Soc. Jp., Vol. 32, pp. 430-435.

Glaretas, C., 1981. *A New Method for Measuring the Acoustic Impedance of the Ground*, Ph.D. thesis, Pennsylvania State University.

Green, G. S., 1986. *Noise Propagation in Mine Roadways and Longwall Faces*, Ph.D. Thesis, University of Nottingham

Griefahn, B. and Nishi, D., 1992. *Mood and Cardiovascular Functions During Noise, Related to Sensitivity, Type of Noise and Sound Pressure Level*, J. of Snd. & Vib, Vol. 155, N0 1, pp. 111-123.

Gutenberg, B, 1942. *Propagation of Sound Waves in the Atmosphere*, J. Acoust. Soc. Am., Vol. 13, pp. 151-155.

Güdsen, A., 1990. *Application of the SAFARI model to Sound Propagation in the Atmosphere*, J. of Acoust. Soc. Am., Vol. 87, No. 5, pp. 1968-1974.

Hasabe, M. and Kaneyasu, K., 1987. *Acoustic Wave Propagation over a Depressed Road Having Finite Impedance*, J. Acoust. Soc. Jp. (E), Vol. 8, No. 3, pp. 77-84.

Hassal, J. R. and Zaveri, K, 1979. *Acoustic Noise Measurement*, Brüel and Kajer.

Hess, H.M., Attenborough and Heap, N. W., 1989. *Ground Characterisation by Short Range Propagation Measurement*, J. Acoust. Soc. Am, Vol. 87, No. 5, pp 1975-1985.

HMSO, 1975. *Code of Practice for Reducing the Exposure of Employed Persons to Noise*, Department of Employment, HMSO, *London. Prepared by W. Burns and D.W. Ronbinson of British Medical Research Council and National Physical Laboratory respectively.*

HMSO, 1978. *A Guide to Measurement and Prediction of the Equivalent Continuous Sound Level, L_{eq}*, the Department of the Environment.

HMSO, 1990 (ISBN 0 11 752338 0). *The Control of Noise at Surface Mineral Workings, WS Atkins Engineering Sciences*, the Department of the Environment.

HMSO, 1988 (ISBN 0 11 5508473). *Calculation of Road Traffic Noise*, the Department of Transport.

Hohenwarter, D, 1990. *Railway Noise Propagation Model*, J. of Snd. and Vib., Vol. 141, No. 3, pp. 17-41.

Holmer, C. I., 1977. *Investigation for Procedures for Estimation of Sound Power in the Free Field Above a Reflecting Plane*, J. Acoust. Soc. Am., Vol. 61, No 2.

Hughes, A., 1989. *Noise and the Law*, Colliery Guardian, Vol. 237, No. 11, pp 356-358

Hübner, G., 1977. *Qualification Procedures for Free Field Conditions for Sound Power Determination of the Appropriate Environmental Correction*, J. Acoust. Soc. Am., Vol. 61, No 2.

Hutchin, S. M. and Cherqui, J., 1991. *Active Exhaust Noise Cancellation,* J. of Env. Engg, Vol. 4, No.. 3, Sept'91, pp. 12-17.

Ingard, U., 1951. *On the Reflection of a Spherical Sound Wave from an Infinite Plane*, J. Acoust. Soc. of Am., Vol. 23, pp 329-335.

Ingard, U., 1953. *A Review of the Influence of Meteorological Conditions on Sound Propagation*, J. Acoust. Soc. Am., Vol. 25, pp. 405-411.

Isei, T, 1980. *Absorptive Noise Barrier on Finite Impedance Ground*, J. Acoust. Soc. Jpn(E), No 1, pp 3-10.

Isei T., Embleton, T. F. W. and Piercy, J. E., 1980. *Noise Reduction by Barriers on Finite Impedance Ground,* J. Acoust. Soc. Am, Vol. 67, No.1, pp. 46-58, 1980.

Isei, T., Shikada, N., Suzuki, T. and Kinoshita, M., 1982. *Meterological Effects of Sound Propagation Outdoors*, Private collection from Dr T. Isei, National Research Institute for Pollution and Resources, Kyushu, Japan.

ISO 3740 to 3747. *Acoustics— Determination of Sound Power Levels of Noise Sources.*

ISO 4872, 1978. *Acoustics — Measurement of Airborne Noise Emitted by Construction Equipment Intended for Outdoor Use — Method for Determining Compliance with Noise Limits.*

ISO 6081, 1986 *Acoustics— Noise Emitted by Machinery and Equipment — Guidelines for Preparation of Test Codes of Engineering Grade Requiring Noise Measurements at the Operator's or Bystander's Position.*

ISO 1996/1, 1982. *Acoustics- Description and Measurement of Environmental Noise. Basic Quantities and Procedures.*

ISO 1996/2, 1987. *Acoustics- Description and Measurement of Environmental Noise. Acquisition of Data Pertinent to Land Use.*

ISO/DIS 9613-2.2, 1994. *Acoustics-Attenuation of Sound During Propagation Outdoors, Part 2: General Method of Calculation.*

Izumi, K. and Osada, Y., 1988. *Research on Effects and Control of Noise in Japan,* J. of Snd & Vib., Vol. 127, No 3, pp. 401-404.

Jonasson, H. G., 1972a. *Sound Reduction by Barriers on the Ground,* J. Snd & Vib., Vol. 22, No. 1, pp. 113-126.

Jonasson, H. G., 1972b. *Diffraction by Wedges of Finite Acoustic Impedance with Application to Depressed Roads,* J. Snd & Vib., Vol. 25, No. 4, pp. 577-585.

Kinsler, L. E., Frey, A. R., Coppens, A. B. and Sanders, V., 1982. *Fundamentals of Acoustics,* John Wielly & Sons, New York.

Kneser, H. O., 1933. *Interpretation of the Anomalous sound Absorption in Air and Oxygen in Terms of Molecular Collisions,* J. Acoust. Soc. Am., Vol. 5, p.122.

Knudsen, V. O., 1933. *The Absorption of Sound in Air, in Oxygen and in Nitrogen,* J. Acoust. Soc. Am., Vol. 5, p.112.

Kragh, J., 1981. *Road Traffic Noise Attenuation by Belts of Trees,* J. of Snd & Vib, Vol. 74, No. 2, pp. 235-241, 1981.

Kryter, K. D., 1970. *The Effects of Noise on Man,* Academic Press, New York.

Kuttruff, H., 1982. *A mathematical Model for Noise propagation Between Buildings,* J. of Sound and Vibration, Vol.85, No.1, 1982, pp. 115-128.

Kurze, U. J. and Anderson, G. S., 1971. *Sound Attenuation by Barriers,* Appl. Acoust., Vol. 4, pp. 35-53.

Land, W. W., 1973. *Noise Measurements Standards for Machinery in Situ,* J. Acoust. Soc. Am., Vol. 54, No 4.

Larsson, C. and Israelsson, S., 1991. *Effects of Meteorological Conditions and Source Height on Sound Propagation near the Ground,* Applied Acoustics, Vol. 33, pp. 109-121.

Larsson, C.,1992a. *Weather Effects on Sound Propagation near the ground,* 2nd Int. Cong. on Recent Development in air and Structure Borne Sound and Vibration, Auburn University, Alabama, USA

Larsson, C., 1992b. *Meteorological Effects on Long Range Sound Propagation- some Experimental Results---,* Fifth International Symposium on Long range Sound Propagation, Milton Keynes, England.

Lawland, R. B.; Rudnick, I, 1951. *Acoustic Wave Propagation along a Constant Normal Impedance Boundary,* J. of the Acoust. Soc. of Am., Vol. 23, pp 546-549.

Li, Y.L., Franke, S.J. and Liu, C. H., 1991. *Numerical Implementation of an Adaptive Fast-Field Program for Sound Propagation in Layered Media Using the Chrisp Z Transform,* J. Acoust. Soc. Am., Vol. 89, pp 2068-2075

Li, Y. L., White, M. J. and Franke, S. J., 1994. *New Fast Field Programs for Anisotropic Sound Propagation Through an Atmosphere with a Wind Velocity Profile,* J. Acoust. Soc. Am., Vol. 95, No 2, pp. 718-726.

Lord, H. W., Willium, S. G.and Harold, A. E., 1980. *Noise Control for Engineers,* Malabar: Robert E Krieger.

Maekawa, Z, 1962. *Experimental Study on Acoustical Designing of a Screen for Noise Reduction,* J. Acoust. Soc. Jp., Vol. 18, pp. 187-196.

Maekawa, Z, 1965. *Noise Reduction by Screens,* Proc. 5th International Congress on Acoustics, Liege, Paper F13.

Maekawa, Z, 1968. *Noise Reductions by Screen,* Appl. Acoust., Vol. 1, pp. 157-173.

Malecki, I, 1969. *Physical Foundation of Technical Acoustics,* Perganon Press, Oxford.

Marsh, K. J., 1982. *The CONCAWE Model for Calculating the Propagation of Noise from Open Air Industrial Plants,* Applied Acoustics, Vol. 15, p. 411.

Miki, Y, 1990. *Acoustical Properties of Porous Materials-Modifications of Delany - Bazely Models,* J. Acoust. Soc. Jp., No. 1, pp. 19-23.

Neklepayev, N., 1911. *Uber die Absorption kurzer akusticher Wellen in Luft,* Ann.Phys., No. 35, Vol. 175.

Newton, I., 1687. *Philosophiae Naturalis Principia Mathematica,* London.

Nicolas, J. and Berry, J. Luc., 1984. *Propagation du son et effet de sol.(in French),* Revue d'Acoustique, No. 71-4/4, pp. 191-200.

Nijs, L. and Wapenaar, C. P. A., 1990. *The Influence of Wind and Temperature Gradients on Sound Propagation, Calculated with Two-Way Wave Equation,* J. Acoust. Soc. Am., Vol. 87, pp. 1987-1998.

Nijs, L. and Wapenaar, C. P. A.,1992. *Reply to :"Comments on the influence of Wind and Temperature Gradients on Sound Propagation, Calculated with the Two-Way Wave Equation.",* J. Acoust. Soc. Am. Vol. 91, No.. 1, January- 1992, pp. 498-504.

Norton, M. P, 1989. *Fundamentals of Noise and Vibration Analysis for Engineers,* Cambridge University Press, Cambridge.

Öhrström, E. and Rylander, R., 1982. *Traffic Noise Sleep Disturbance Effects,* J. of Snd & Vib., Vol. 84, No 1, pp. 87-103.

Osada, Y., 1988. *An Overview of Health Effects of Noise,* J. of Snd. & Vib, Vol. 127, No 3, pp. 407-410.

Parkin, P. H. and Scholes, W. E., 1954. *Air to Ground Sound Propagation,* J. Acoust. Soc. Am. Vol. 26, pp. 1021-1023.

Peterson, A. P. G. and Gross, E. E., 1977. *Handbook of Noise Measurement,* Massachusetts, General Radio 1977.

Piercy, J. E., Embleton, T. F. W. and Sutherland, L. C., 1977. *Review of Noise Propagation in the Atmosphere,* J. Acoust. Soc. Am. Vol. 61, No. 6, pp. 1403-18.

Piercy, J. E. and Isei, T., 1980. *Noise Reduction by Barriers on Ground with Finite Impedance,* Proc. of International Conference, Inter-Noise, Miami, Florida, USA, 8-10 Dec'1980, pp. 579-584.

Pinder, N, 1995. *Specification for Plant Noise Prediction Programs,* Handout of ISVR Consultancy Services, ISVR, Southampton.

Ramazzini, 1713. De Morbis, Artificium.

Rasmussen, K. B., 1982a. *Propagation of Road Traffic Noise over Level Terrain,* J. Snd. &Vib., Vol. 82, pp. 51-61.

Rasmussen, K. B., 1982b. *Sound Propagation over Non-Flat Terrain,* Technical Report No. 35, Danish Acoustical Laboratory.

Rasmussen, K. B., 1986. *Outdoor Sound Propagation under the Influence of Wind and Temperature Gradient,* J. Snd. &Vib., Vol. 104, No. 2, pp. 321-335.

Raspet, R., Lee, S. W., Kuester, E., Chang, D. C., Richards, W.F., Gilbert, R. and Bong, N., 1985. *A Fast Field Program for Sound Propagation in a Layered Atmosphere Above an Impedance Ground,* J. Acoust. Soc. Am., Vol. 77, pp. 345-352.

Raspet, R, Yao, L., Franke, S. L. and White, M. J., 1990. *Comments on "The influence of Wind and Temperature Gradients on Sound Propagation, Calculated with the Two-Way Wave Equation.",* J. Acoust. Soc. Am. Vol. 87, No. 5, pp. 1987-1998.

Raspet, R, Yao, L., Franke, S. L. and White, M. J., 1992. *Comments on "The influence of Wind and Temperature Gradients on Sound Propagation, Calculated with the Two-Way Wave Equation.",* J. Acoust. Soc. Am. Vol. 91, No. 1, pp. 498-500.

Rathe, E. J., 1969. *Note on Two Common Problems of Sound Attenuation,* J. Snd. and Vib., Vol. 10, No. 3, pp. 472-479.

Rathe, E., J., 1977. *Railway Noise Propagation,* J. of Snd. and Vib., Vol. 51, pp.371-388.

Raymond Derzay, 1972. *Hearing Conservation for the Mineral Industry,* USBM IC 8564, 1972.

Redfearn, S. W., 1940. *Some Acoustical Source-Observer Problems,* Philos. Mag. J. Sci., Vol. 30, pp. 223-236.

Rosenhouse, G. and Peled, N., 1990. *Computer Simulation of the Sound Field Created by Moving Sound Sources in Space with* Reflecting Surfaces, Computational Acoustics Seismo-Ocean Acoustic and Modelling. Published by Elsevier Science Publishers B. V., 1990.

Rudnick, I, 1947. *The Propagation of an Acoustic Wave along a Boundary,* J. Acoust. Soc. of Am., Vol. 19, pp 348-356.

Rylander, R, Anderson, K and Torsmark, U, 1988. *Research on Effects and Control of Noise in Sweden,* J. of Snd & Vib., Vol. 127, No 3.

Rzhevsky. V. V., 1985. *Opencast Mining Unit Operations,* Mir Publications, Moscow.

Rzhevsky. V. V., 1987. *Opencast Mining :Technology and Integrated Mechanization,* Mir Publications, Moscow.

Scholes, W. E. and Parkin, P. H., 1967. *The Effect of Small Changes in Sound Height on the Propagation of Sound over Grassland,* J. Snd & Vib., Vol. 6, No. 3, pp 424-442.

Scholes, W. E. and Salvidge, A. C., 1973. *Statistical Analysis from a Sound Level Meter,* Appl. Acoust.,1973, 6, 111-117.

Schultz, T. J., 1986. *Outlook for the In-Situ Measurement of Noise from Machines,* J. Acoust. Soc. Am., Vol. 54, No. 4.

Smith, B. J., 1971. *Acoustics*, Environmental Physics Series, Longman Group Ltd., London.

Stimpson, G. J., Sun, J. C., and Richards, E. J., 1986. *Predicting Sound Power Radiation from Built-up Structures Using Statistical Energy Analysis,* J. of Snd.. and Vib., Vol. 107, No. 1, pp. 107-120.

Stokes, G.G., 1845. *On the Theories of the Internal Friction of Fluids in Motion and of the Equilibrium and Motion of Elastic Solids,* Trans. Camb. Phil. Soc. 8, p. 287.

Stokes, G. G., 1851. *An Examination of the Possible Effect of the Radiation of Heat on the Propagation of Sound.* Phil. Mag. 1, p.305.

Stubbs, W. and Tate, J. D., 1992. *The Use of L_{Aeq} in Mineral Extraction Noise Assesment,* Procedings of 'euro noise'92, Imperial College, London, 14-18 Sept,1992, I.O.A., Vol. 14, Part 4 (1992), pp. 49-57.

Stull, R. B., 1988. *An Introduction to Boundary Layer Meteorology*, Kluwer Academic Publishers, Dordrecht.

Sutherland, L. C., Piercy, J. F., Bass, H. E. and Evans, L. B., 1974. *Method for Calculating the Absorption of Sound by the Atmosphere,* J. of Acoust. Soc. Am., Vol 56, Suppliment 1 (Abstr.)

Sutherland, L. C., 1994. *Review of Ground Impedance for Grass Surfaces–Delany and Bazley Revisited*, Proc. of the 6th International Symposium on Long Range Sound Propagation, 12-14 June, 19994, Ottawa, Canada.

Thompson, R. J., 1972. *Ray Theory for Inhomogeneous Moving Medium*, J. Acoust. Soc. Am., Vol. 51, No. 5, pp. 1675-1682.

Tonin, R, 1993. *Environmental Noise Modelling,* Environmental Modeling, Vol. 1 in Computer Methods and Software for Simulating Environmental Pollution and Its Averse Effects, P. Zannetti (Ed), Computational Mechanics Publication, Elsvier Applied Science, London.

Tompsett, K. R., 1992. Site noise- an Improved Method of Predicting Noise From Open Sites, *Proceedings of "euro noise", Imperial College, London, 14- 18 September 1992, Book 2, pp. 453-461.*

Turner, D. B., 1964. *A Diffusion Model for an Urban Area*, J. of Applied Meteorology, Vol.3, pp 83-91.

Ver, I. L. and Holmer, C. I., . Interactions of Sound Waves with Solid Structures, *Chapter 11 in the Noise and Vibration Control edited by L.L. Beranek, Mc-Graw-Hill*

Von Gierke, H. E., Robinson, D. W. and Karmy, S. J., 1982. *Results of Workshop on Impulse Noise and Auditory Hazards,* J. of Snd & Vib, Vol. 83, No. 4, pp. 579-584

Walker, J. G., 1977. *Factors Affecting Railway Noise in Residential Areas,* J. Snd & Vib, 1977, 51, (3), 393-398.

Walker, J. G., 1992. *The Application of L_{aeq} to Railway Noise*, Proc. of Euro-Noise 1992, Imperial College, London, 14-18September 1992, Vol. 14, Part 4, pp 49-57.

Weglo, J. K., 1973. *Audiograms -Keep the Level Down,* CMJ., Vol. 94, No. 3, Sept'73, pp.64-65.

West, M., Sack, R. A. and Walkden, F., 1991. *The Fast Field Program (FFP). A second tutorial : Application to Long Range Sound Propagation in the Atmosphere,* Appl. Acoust., Vol. 33, pp 199-228

White, F. A., 1975. *Our Acoustic Environment*, John Willy & Sons, New York.

Wiener, F. M., 1980. *Sound Propagation Outdoors, Fundamentals Underlying Noise Control, Section 2 of Noise Reduction*, Ed. Beranek, L. L, McGraw Hill Book Co., Inc., New York.

Woodhouse, J., 1981. *An Introduction to Statistical Energy Analysis of Structural Vibrations*, Applied Acoustics, No 14, pp. 455-69.

Wilson, C. E., 1989. Noise Control, Harper and Row, New York, pp 10.

Yamanaka, K., Nakagawa, T., Kobayashi, F., Kanada, S., Tanahashi, M., Muramatsu, T., and Yamada, S., 1982. *Criteria for Acceptable Levels of the Shinkansen Super Express Train Noise and Vibration in Residential Areas*, J. of Snd.. and Vib., Vol. 84, No. 4, pp. 586-591.

Yang, S. J. and Elision, A. J., 1985. *Machinery Noise Measurement*, Claredon Press, Oxford, pp. 26-55.

Yuzawa, M, 1977. *Sound Attenuation by Absorptive Barriers*, J. Acoust. Soc. Jp., Vol. 33, pp. 664- 666.

Zouboff, V., Brunet, Y., Berengier, M. and Sechet, E., 1994. *A Qualitative approach of Atmospherical Effects on Long Range Sound Propagation*, Proc. Sixth International Symposium on Long Range Sound Propagation, 12-14 June 1994, Ottawa, Canada

APPENDIX 1

Standards and Guidelines

A1 List of Important Standards and Guidelines on Noise

British Standard BS 5330. Method of Test for Estimating Risk of Hearing Handicap due to Noise Exposure.

International Organisation for Standardisation ISO 3891: 1978. Procedure for Describing Aircraft Noise on the Ground.

British Standard BS 4197: 1967. Specification for a Precision Sound Level Meter.

ISO / DP 9612: 1988. Acoustic — Guidelines for the Measurements and Assessment of Exposure to Noise in the Working Environment.

BS 7025:1988. British Standard Method for Preparation of Test Codes of Engineering Grade for Measurement at the Operator's or Bystander's Position of Noise Emitted by Machinery.

ISO 6081:1986. Acoustics— Noise Emitted by Machinery and Equipment — Guidelines for Preparation of Test Codes of Engineering Grade Requiring Noise Measurements at the Operator's or Bystander's Position.

ISO 3740 to 3747. Acoustics— Determination of Sound Power Levels of Noise Sources.

BS 4196. Sound Power Levels of Noise Sources. (para 0-7)

ISO 4872: 1978. Acoustics — measurement of Airborne noise Emitted by Construction Equipment intended for outdoor use — method for Determining Compliance With noise limits.

BS 5228:1975. Code of Practice for Noise Control on Construction and Demolition Sites

Dept. of the Environment and Mineral Planning Guidance Note MPG 11. The Control of Noise at Surface Mineral Workings (1991)(HMSO -1990)

BS 5228. Part 1:1984 (ISBN 0 580 13738 4)Noise Control at Construction and Open Site

Part2: Guide to Noise Control Legislation for Construction and Demolition, Including Road Construction and Maintenance.

Part3: Code of Practices for Noise Control Application to Surface Coal Extraction by Opencast Methods.

ISO 1996/1. Acoustics- Description and Measurement of Environmental Noise. Basic Quantities and Procedures, 1982.

ISO 1996/2. Acoustics- Description and Measurement of Environmental Noise. Acquisition of Data Pertinent to Land Use, 1987.

ECC Directive 85/337. On the Evaluation of Environmental Impact of Some Public and Private Projects, 27 June 1985.

ECC Directive 86/188. On the Protection of Workers from the Risk Related to Exposure to Noise at Work, 16 May 1986.

BS 4142: 1990. Method of Rating Industrial Noise in Mixed Residential and Industrial Areas.

BS 7445: 1992. Acoustics- Description and Measurement of Environmental Noise.

HMSO Publications

- Aircraft Noise: Flight Routing Near Airport, HMSO, 1971.
- Neighbourhood Noise, HMSO, 1971
- Aircraft Noise: Should the Noise and Number Index be Revised, HMSO, 1973.
- Traffic Noise: The Vehicle Regulations and Their Enforcement, HMSO, 1973.
- Aircraft Noise: Selection of Runway Sites for Maplin, HMSO, 1972.
- Noise in Public Places, HMSO, 1973.
- A Guide to Noise Units, Dept. of the Environment, 1973.
- Noise in the Next 10 Years, HMSO, 1974.
- Aircraft Engine Noise Research, HMSO, 1974.
- Aircraft Noise: Review of Aircraft Department Routing Policy, HMSO, 1974.
- Noise Limits, HMSO, 1975.
- Bothered by Noise ? How the Law Can Help You. Noise Advisory Council, 1975.
- Concord Noise Levels, HMSO, 1977.
- Hearing Hazards and Recreation, Dept of the Env., 1977
- Helicopter Noise in the London Area, HMSO, 1777.

- A Guide to Measurement and Prediction of the Equivalent Continuous Sound Level, Leq, (Dept of the Env. Pub.), HMSO, 1978
- The Noise Implications of the Transfer of Freight from Road to Rail. HMSO.
- The Control of Noise at Surface Mineral Workings, WS Atkins Engineering Sciences, Department of Environment., HMSO 1990 ISBN 0 11 752338 0
- Calculation of Road Traffic Noise, Department of Transport, HMSO 1988 ISBN 0 11 5508473
- Procedural Specification for Limitation of Noise and Equipment for Use in the Petroleum Industry, Oil Companies Materials Association, Specification No. NWG1.

APPENDIX 2

Noise signature of specific activities in surface mining and quarrying

A2 Noise Signature of Shovel Dumper Operation

Shovel dumper operations were studied at Tara Mines, Republic of Ireland. The studies were conducted with a 35 t rear discharge dump truck and a 4.6 m^3 Hydraulic shovel. Figures A2.1-A2.12 illustrates the noise signatures determined from the data recorded by Larson Davis RTA-2900. Plate A2.1 shows the experimental conditions.

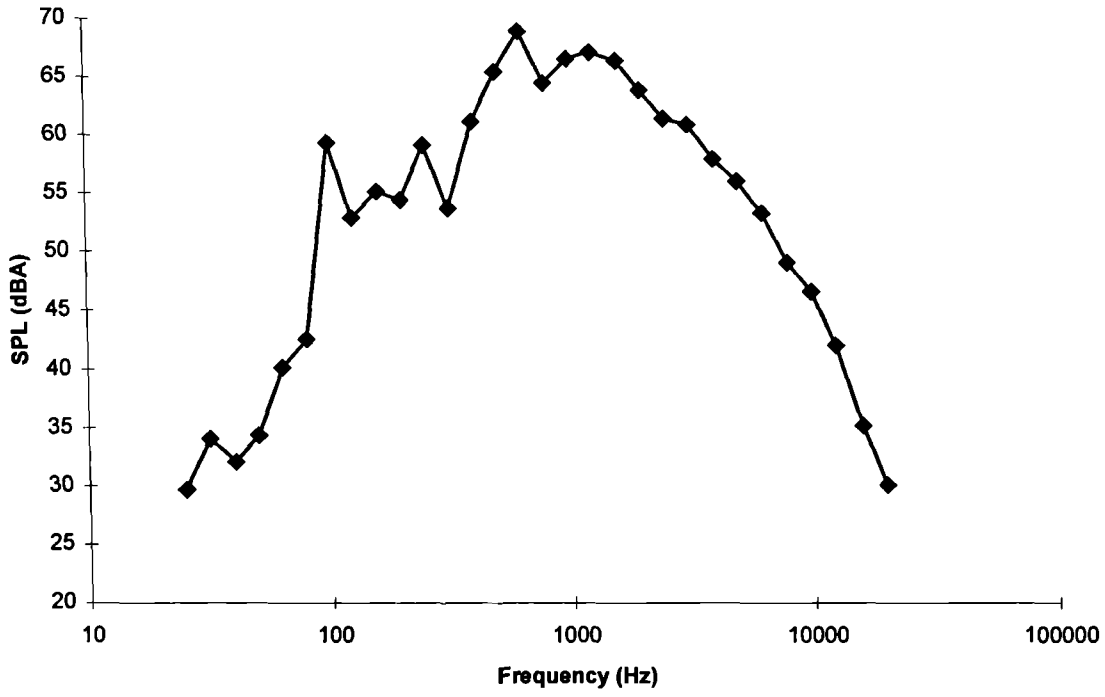


Figure A2.1 Frequency spectrum of the noise emitted by a 35 t RD dump truck being loaded by hydraulic shovel.

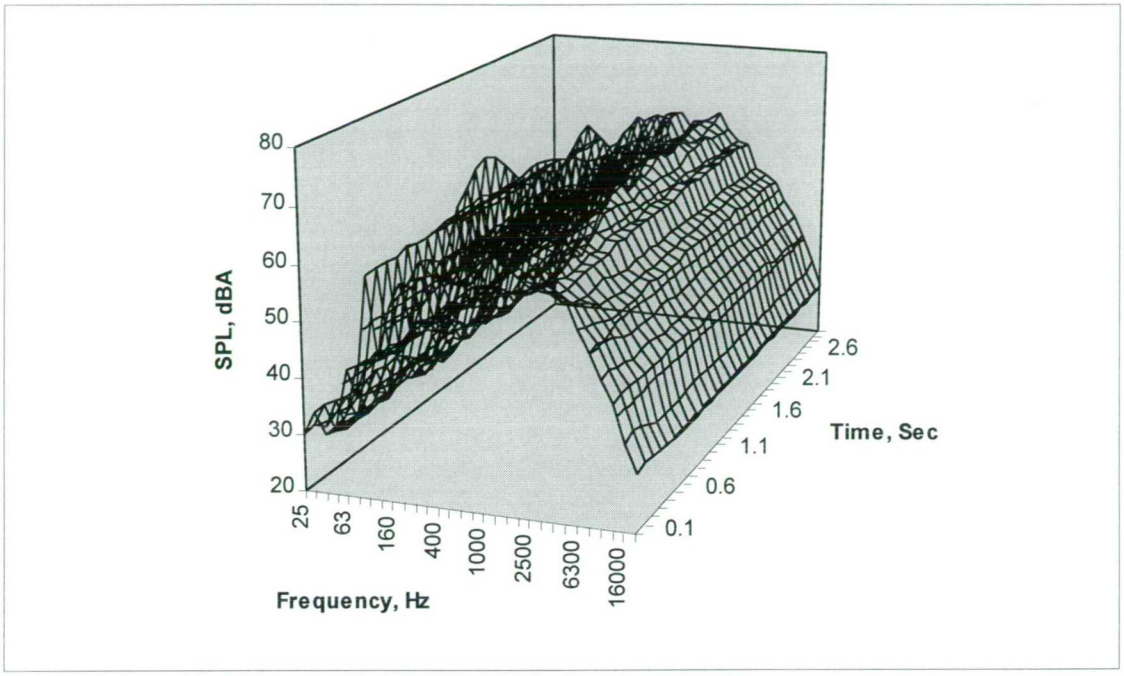


Figure A2.1A Frequency spectrum of the noise emitted by a 35 t RD dump truck being loaded by hydraulic shovel.



Figure A2.2 Frequency spectrum of the noise emitted by a hydraulic shovel during face dressing.

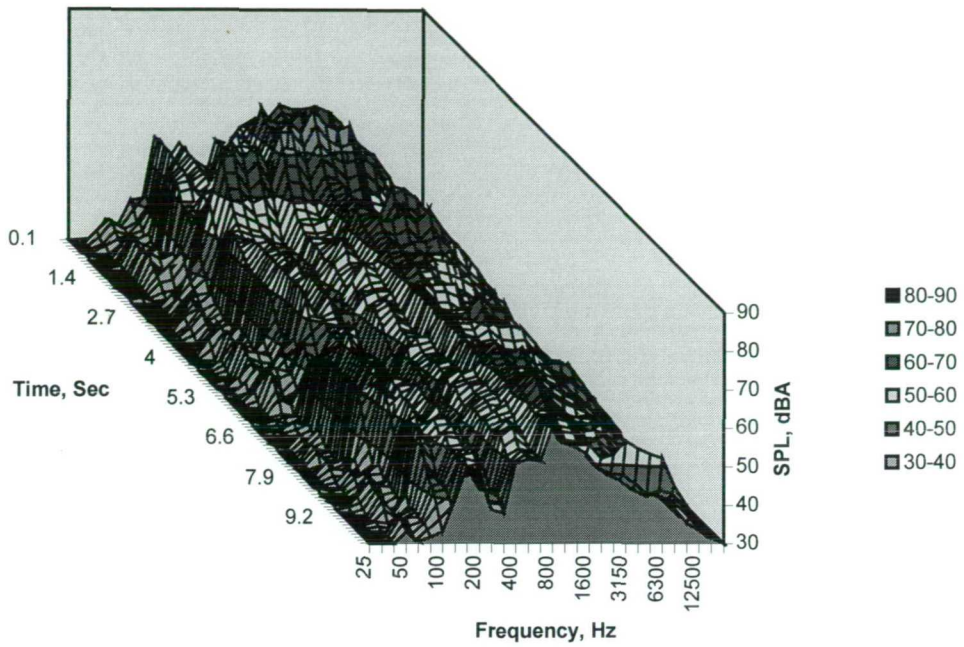


Figure A2.2A Frequency spectrum of the noise emitted by a hydraulic shovel preparing a face while 35 t RD dump truck moving away.

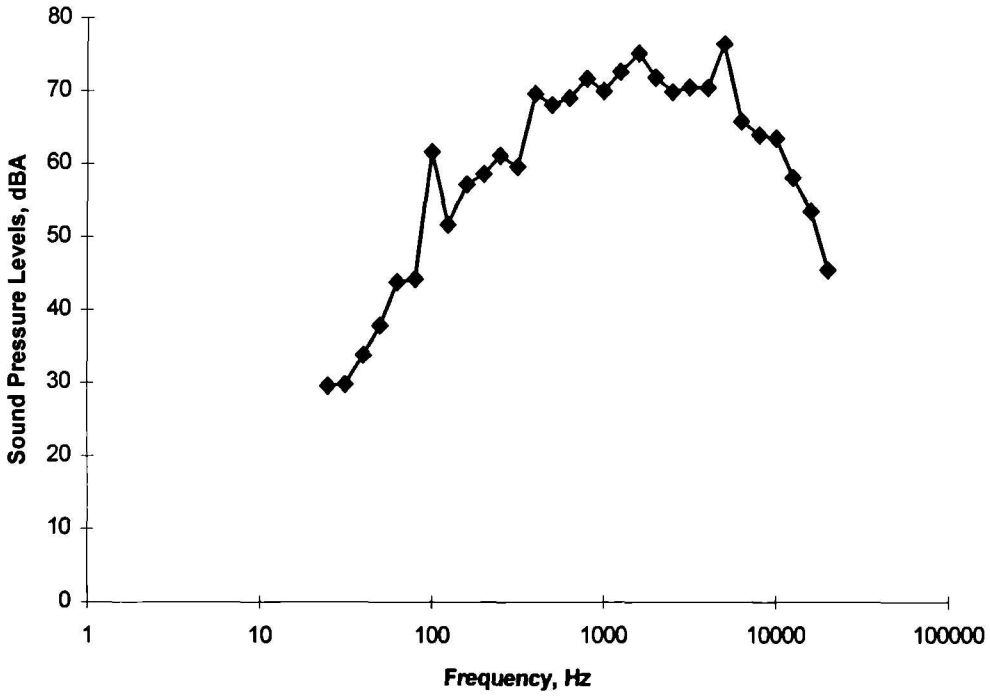


Figure A2.3 Frequency spectrum of the noise emitted by a hydraulic shovel during propelling.

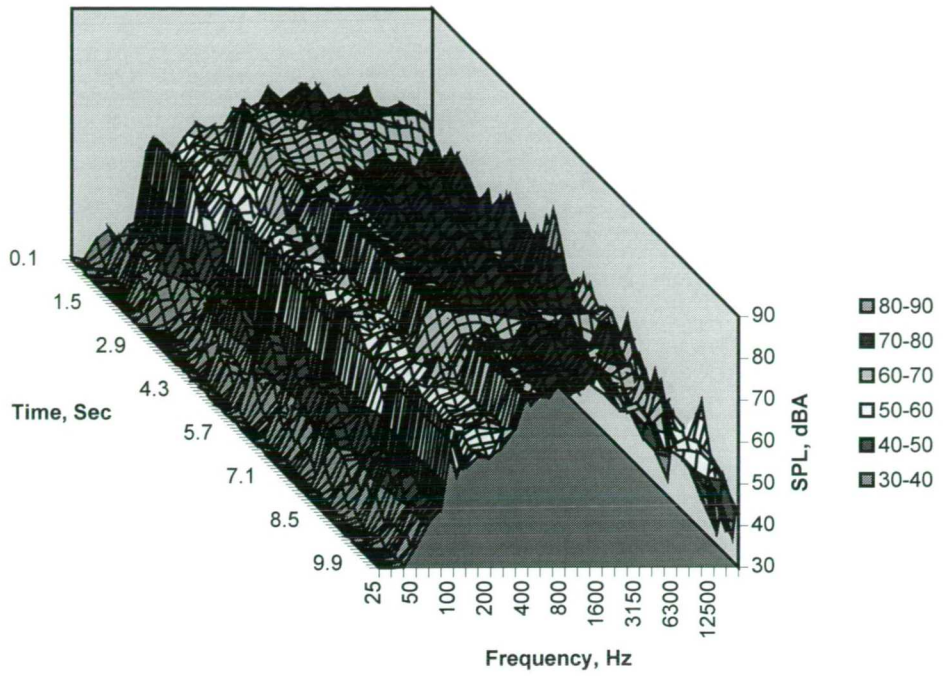


Figure A2.3A Frequency spectrum of the noise emitted by the movement of a hydraulic excavator.

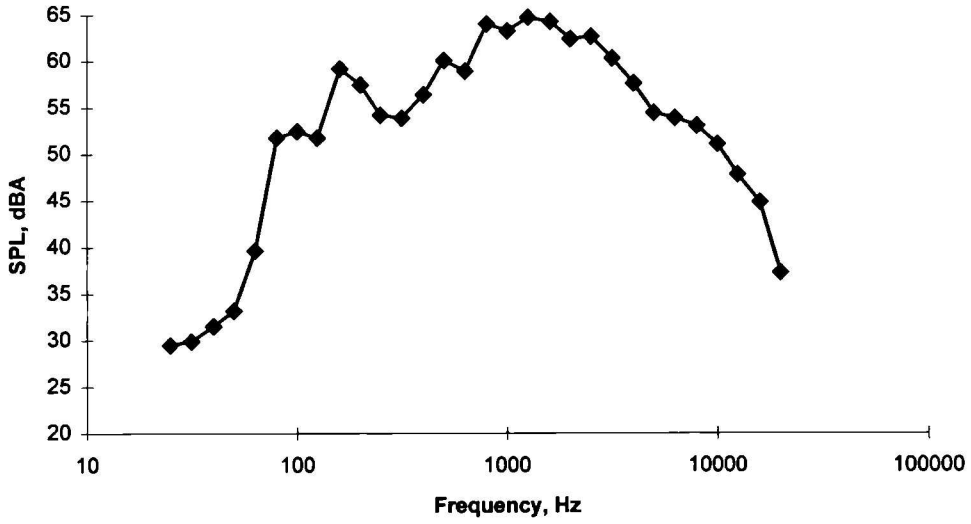


Figure A2.4 Frequency spectrum of the noise emitted by a 35 t RD dump truck down-the-ramp (35 degree).

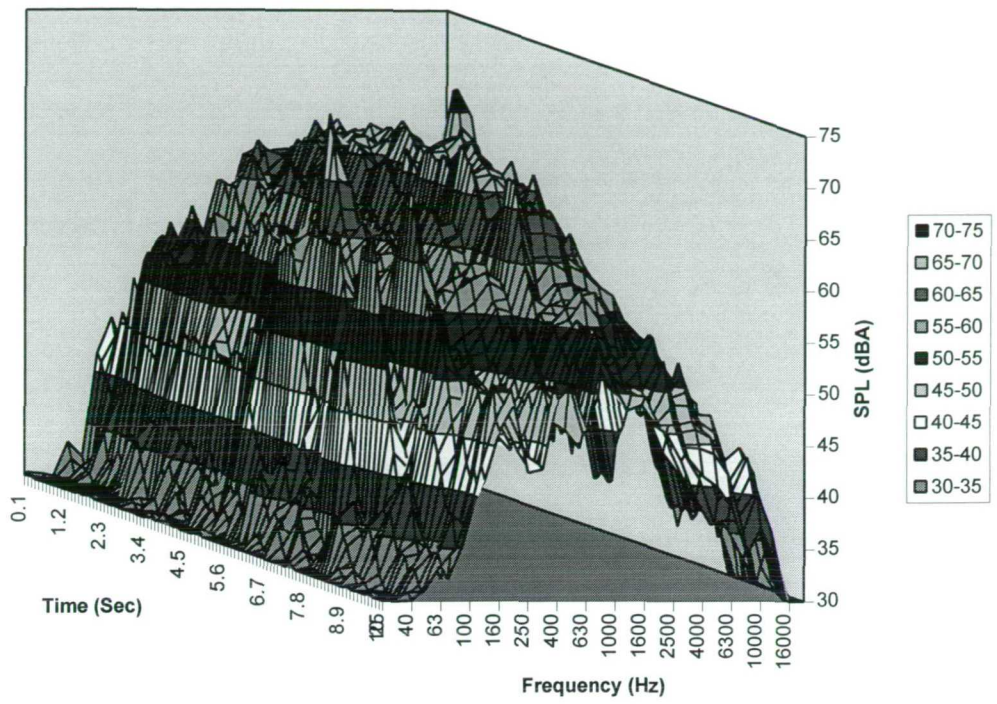


Figure A2.4a Frequency spectrum of the noise emitted by a 35 t RD dump truck down-the-ramp at 35 degree (recorded by Larson Davis RTA 2900).

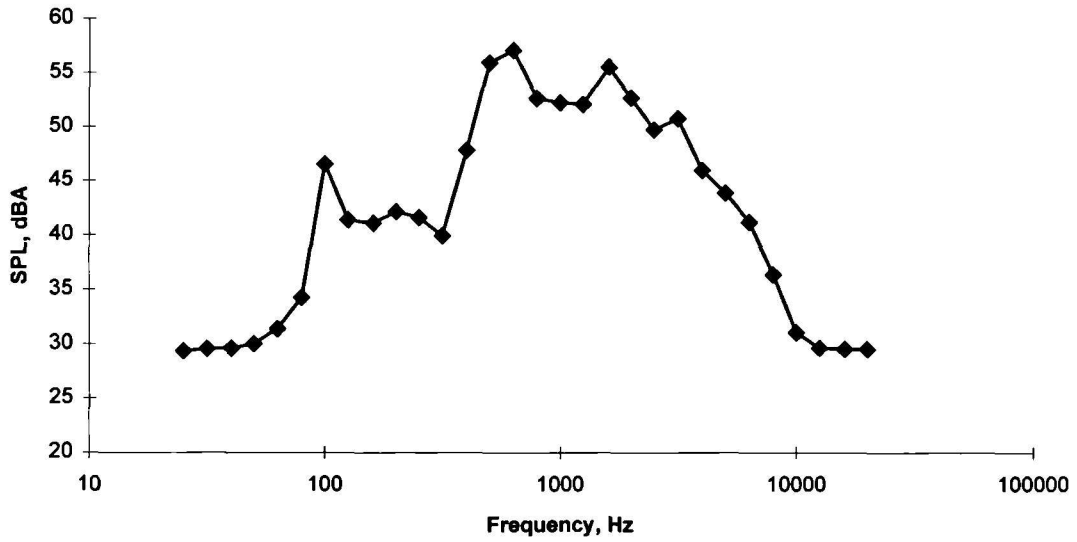


Figure A2.5 Frequency spectrum of the noise emitted by a 35 t RD dump truck on level.

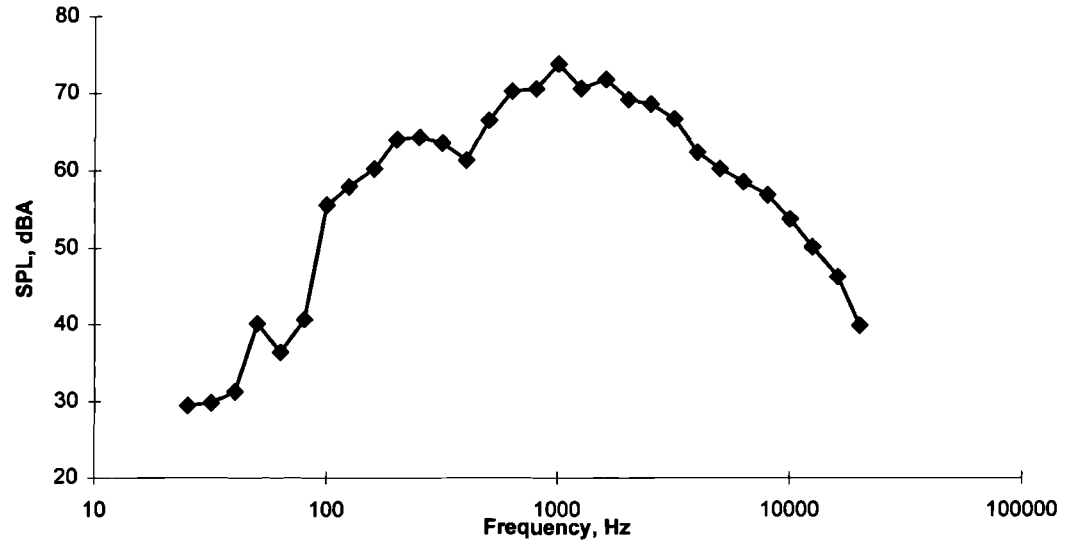


Figure A2.6 Frequency spectrum of the noise emitted by a 35 t RD dump truck on a 35 degree up-ramp.

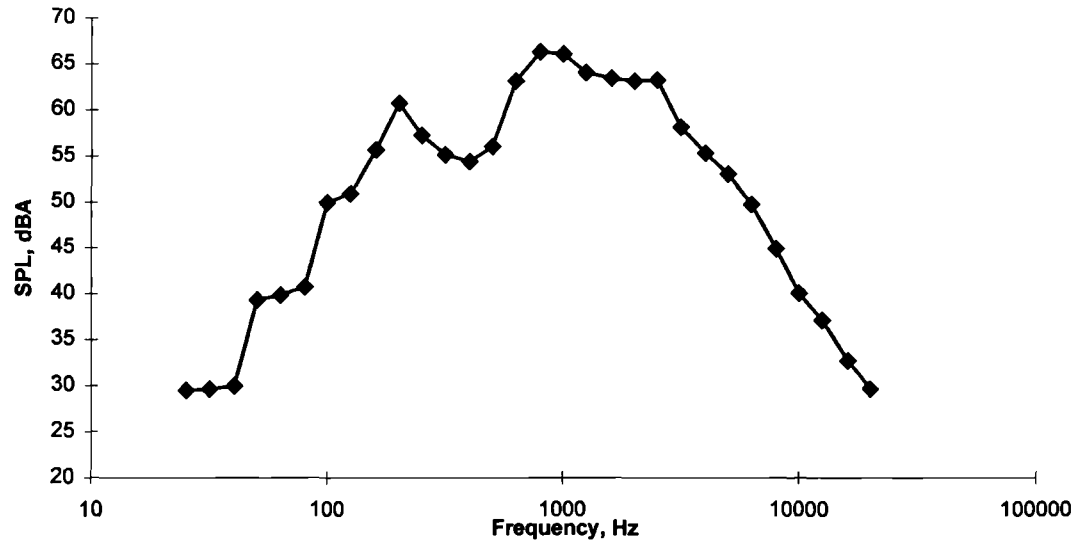


Figure A2.7 Frequency spectrum of the noise emitted by a 35 t RD dump truck on a 35 degree down-ramp.

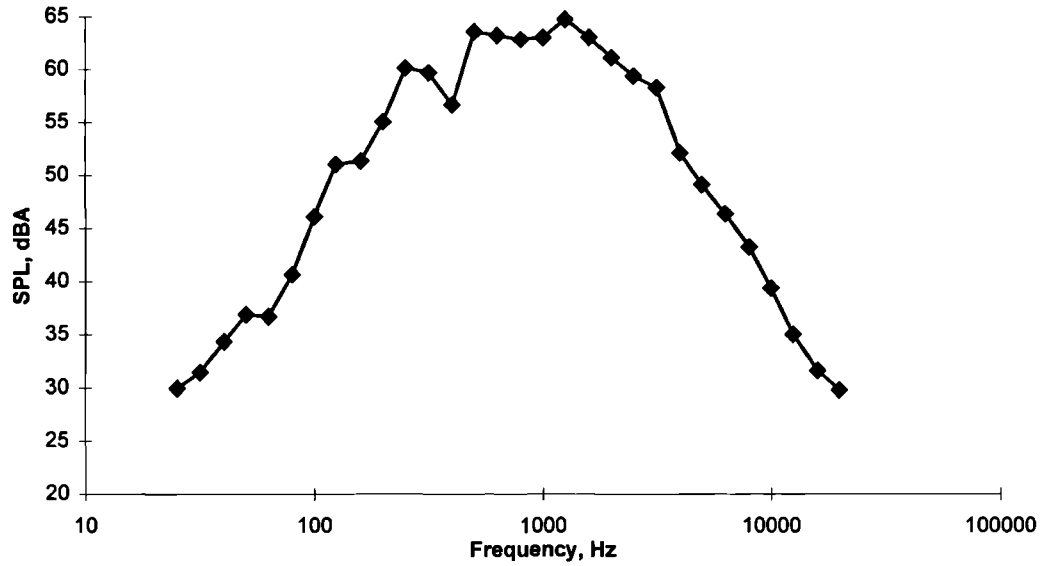


Figure A2.8 Frequency spectrum of the noise emitted by a 35 t RD dump truck near a hydraulic shovel.

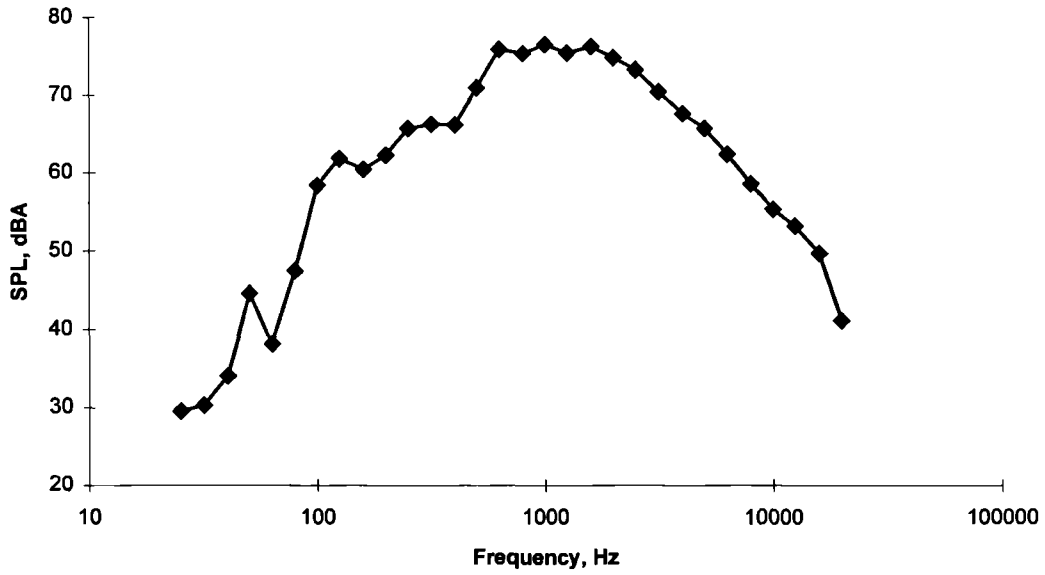


Figure A2.9 Frequency spectrum of the noise emitted by a 35 t RD dump truck on a ramp near the hydraulic shovel.

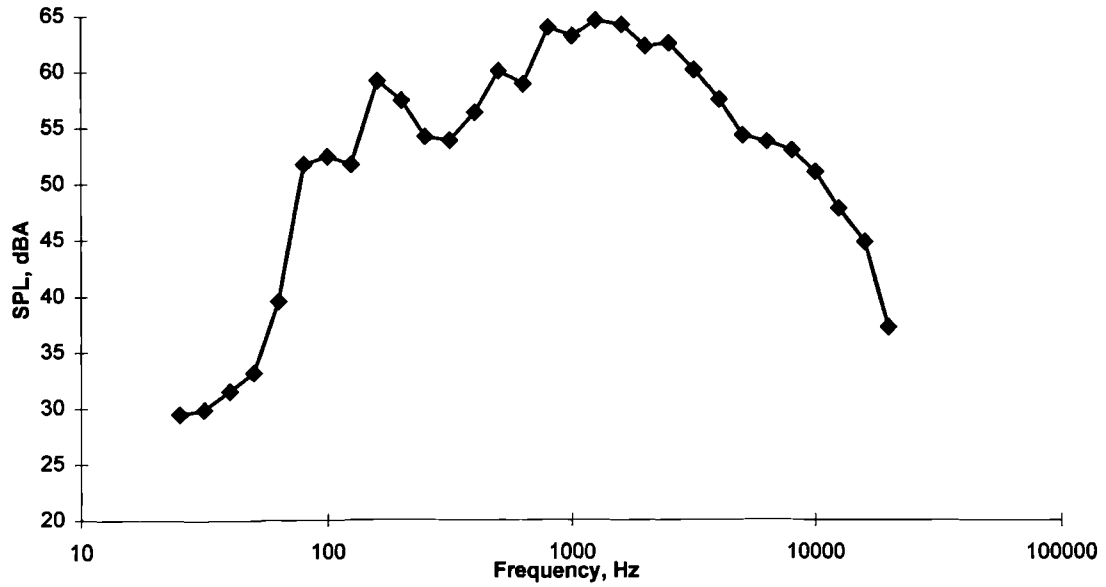


Figure A2.10 Frequency spectrum of noise emitted by 35 t RD dump truck manoeuvring near hydraulic shovel.

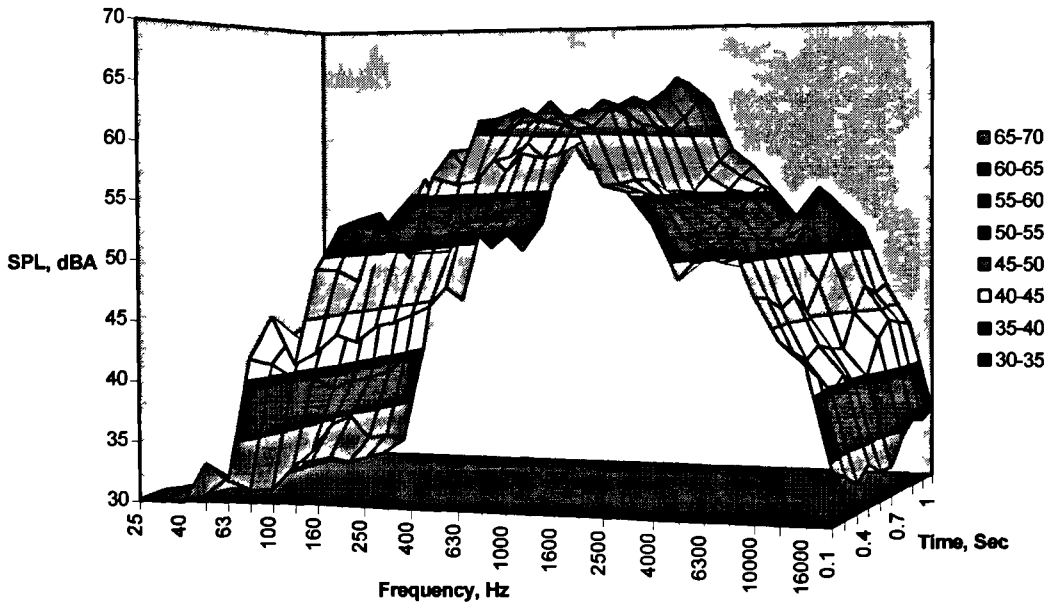


Figure A2.10A Frequency spectrum of the noise emitted by a 35 t RD dump truck manoeuvring near a hydraulic shovel.

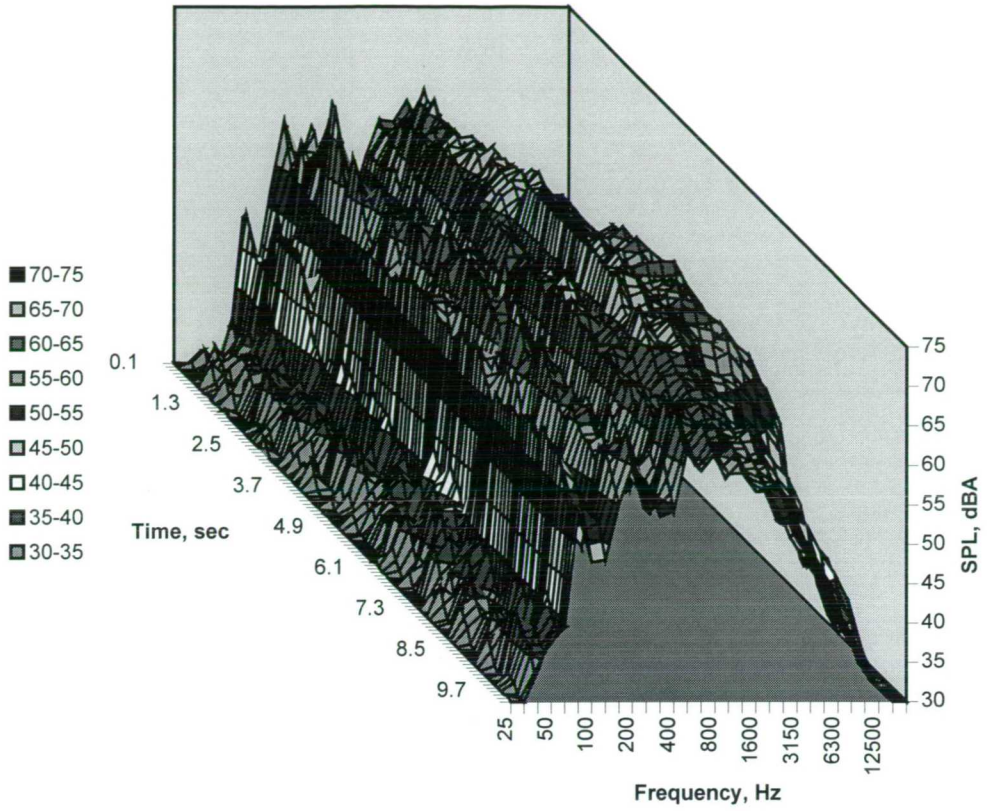


Figure A2.11 Frequency spectrum of the noise emitted by a 35 t RD dump truck during turning on level ground.

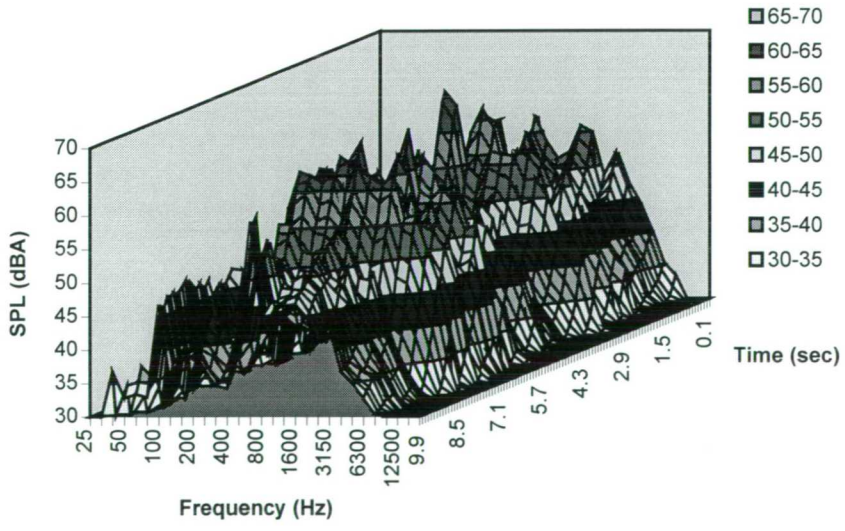


Figure A2.12 Frequency spectrum of the noise emitted by a dump truck travelling with load on the level ground.



Plate A2.1 Shovel-dump truck noise experiments.

APPENDIX 3

Results of Experiments for Excess Attenuation by Ground Absorption

A3 Experiment over grass covered soft soil

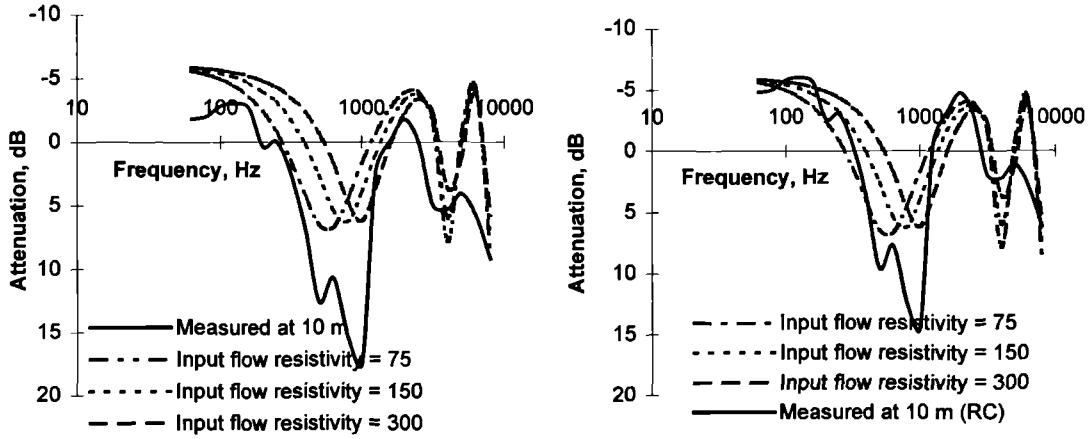
A3.1 Experiment 14-1

Sound pressure levels were measured at distances 1.0 m, 10.0 m, 20.0 m and 40.0 m from the source at 0.375 m. height The heights of the receivers were 1.03 m, 1.14 m, 1.15 m and 1.0 m respectively.

Table A3.1.1 shows the SPL (dB) of recorded at different distances during the experiments. The dBA levels recorded by the instruments have been converted to dB levels. Figure A3.1 shows the plot of the experimental and theoretical excess attenuation for different flow resistivity.

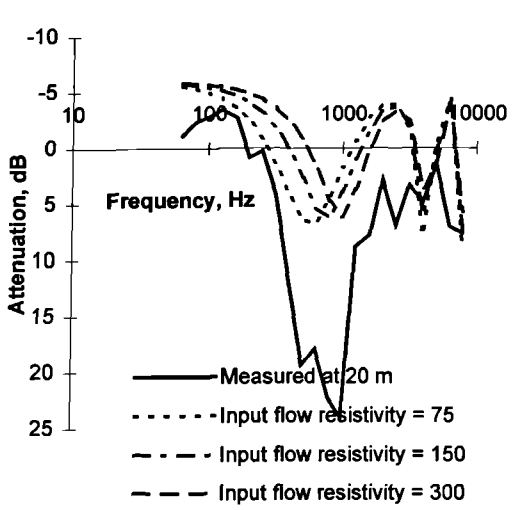
Table A3.1.1 Recorded sound pressure levels for Experiment 14-1.

Frequency (Hz)	SPL (dB) at 1m	SPL (dB) at 10m	SPL (dB) at 20m	SPL (dB) at 40m
63	97.4	77.9	72.5	65.3
80	98.7	79.3	73.7	65.7
100	99.8	80.1	74.2	65.9
125	99.6	80.3	74.8	66.6
160	98.6	79.9	74.1	65.7
200	96.3	76.9	70.5	60.9
250	96.5	77.3	71.1	59.8
315	94.5	74.8	67.2	52.7
400	92.2	70.4	59.3	45.3
500	88.7	64.7	51.9	38.2
630	92.9	66.6	53.4	38.9
800	93.5	61.8	49.0	35.5
1000	90.5	59.8	47.3	35.1
1250	94.1	74.9	62.5	44.2
1600	95.7	77.5	63.5	39.6
2000	99.3	80.8	68.5	45.0
2500	93.2	77.2	64.4	41.9
3150	92.8	72.3	68.0	45.5
4000	94.7	72.0	66.5	38.3
5000	95.5	73.2	69.9	41.8
6300	93.6	71.5	64.3	36.8
8000	90.3	68.1	63.7	33.6

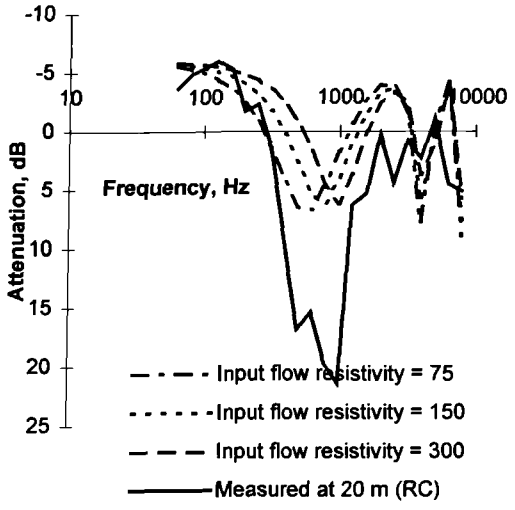


a. At 10 m, without reflection correction. b. At 10 m, reflection corrected.

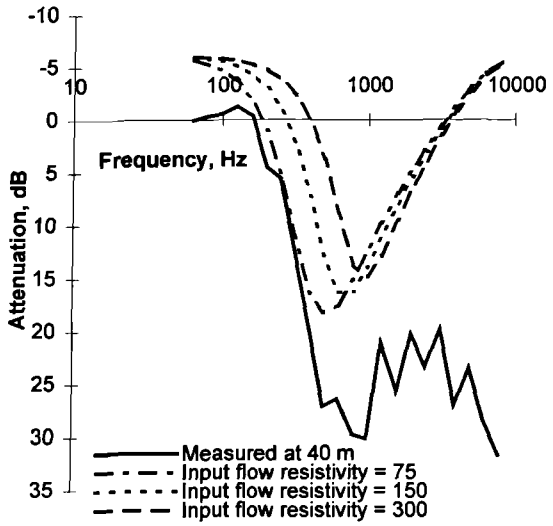
Figure A3.1 Excess attenuation (dB) due to ground absorption over grass covered soft soil.



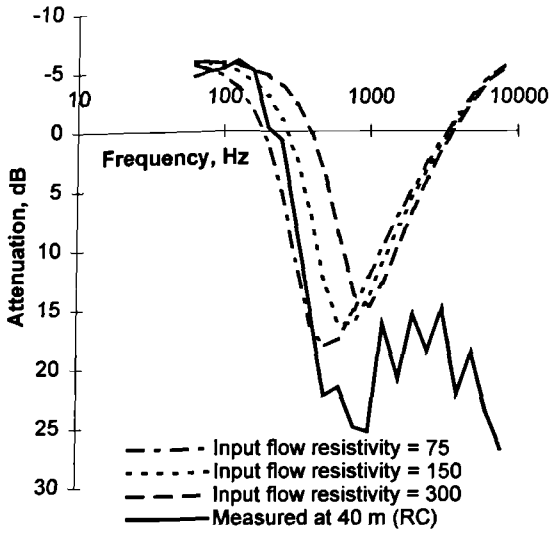
c. At 20 m, without reflection correction.



d. At 20 m, reflection corrected.

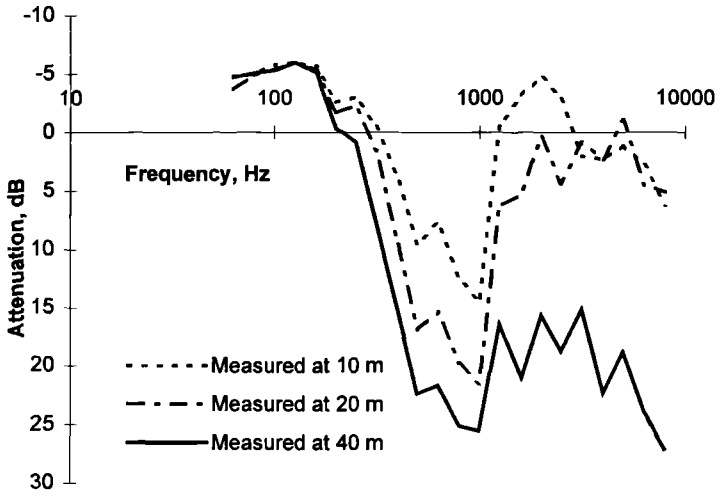


e. At 40 m, without reflection correction.



f. At 40 m, reflection corrected.

Figure A3.1(Contd.) Excess attenuation (dB) due to ground absorption over grass covered soft soil.



g. Different source-receiver distances.

Figure A3.1 (Contd.) Excess attenuation (dB) due to ground absorption over grass covered soft soil.

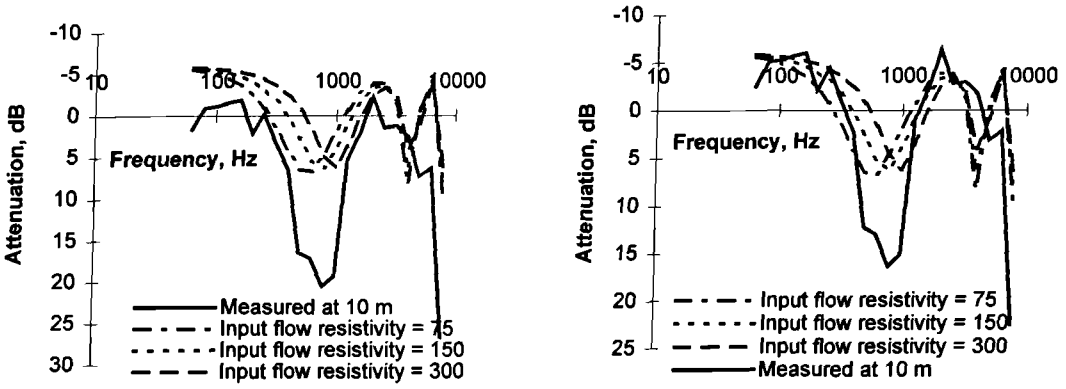
Table A3.2.1 Recorded sound pressure levels for Experiment 14-2.

Frequency (Hz)	SPL (dB) at 1m	SPL (dB) at 10m	SPL (dB) at 20m	SPL (dB) at 40m
63.0	96.7	75.0	71.0	65.3
80.0	98.7	77.6	73.4	68.2
100	99.8	77.8	74.3	69.3
125	99.5	78.2	73.9	68.9
160	98.8	78.5	74.3	68.2
200	96.4	74.6	70.6	64.6
250	96.6	76.9	71.2	61.9
315	94.5	73.4	66.8	53.7
400	91.9	70.2	61.3	42.3
500	88.0	60.2	52.8	40.1
630	88.9	59.5	52.2	42.4
800	89.5	56.1	49.0	37.9
1000	89.5	57.3	50.2	40.0
1250	95.4	71.5	64.3	50.5
1600	94.7	74.8	68.5	55.3
2000	96.2	78.9	73.9	63.5
2500	90.5	75.3	69.7	56.1
3150	92.8	75.5	68.6	50.3
4000	92.6	74.2	70.2	54.4
5000	93.0	69.4	72.3	63.7
6300	90.9	70.4	65.6	60.1
8000	89.1	49.9	62.9	55.1

A3.2 Experiment 14-2

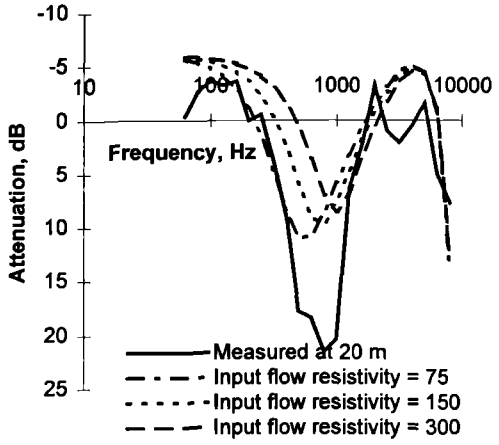
This experiments were also conducted over the same grass covered soft soil. However, the direction of sound propagation was reversed to study the effect of 180^0 change of wind direction. As before, sound pressure levels were measured at 1.0 m, 10.0 m, 20.0 m and 40.0 m from the source of 0.375 m height. The heights of the receivers were 1.03 m, 1.15 m, 1.17 m and 1.03 m respectively. Table A3.2.1 shows the results.

FigureA3.2 shows the plot of the experimental excess attenuation along with the theoretical excess attenuation for different flow resistivities. Figure A3.2a illustrates the excess attenuation over grass covered soft soil under reversal of wind directions.

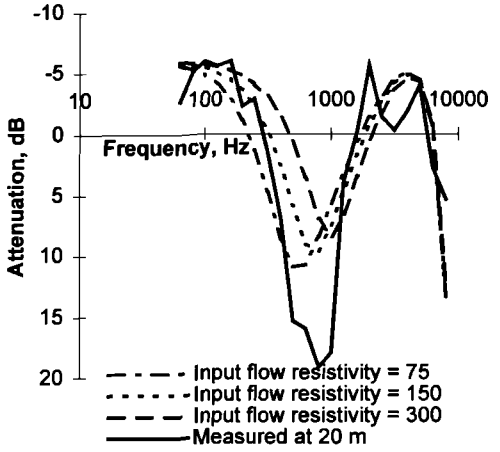


a. At 10 m, without reflection correction. b. At 10 m, with reflection correction.

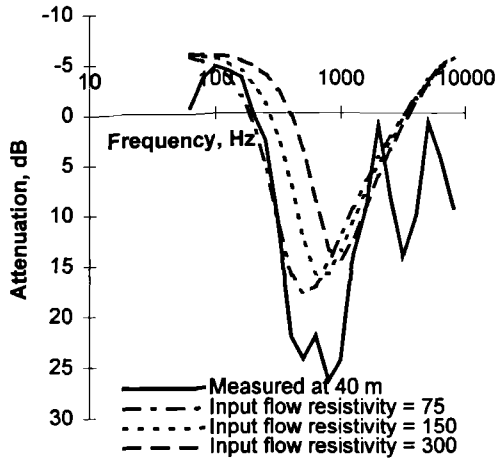
Figure A3.2 Measured and theoretical excess attenuation (dB) over grass covered soft soil under the wind direction 180^0 to that of Experiment 14.1.



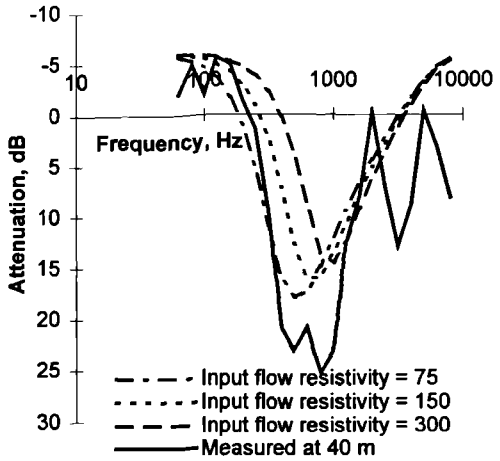
c. At 20 m, without reflection correction.



d. At 20 m, with reflection correction.

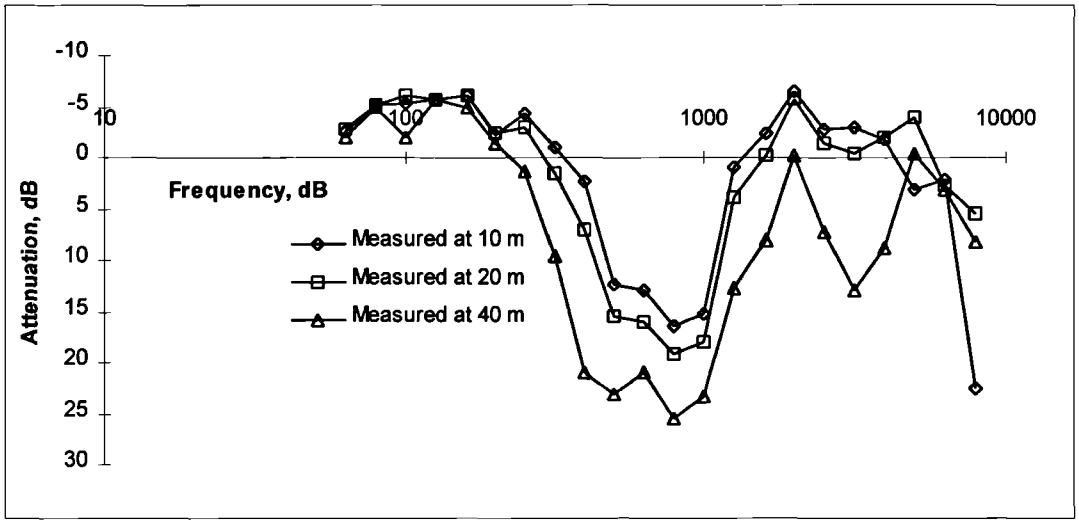


e. At 40 m, without reflection correction.



f. At 40 m, with reflection correction.

Figure A3.2(Contd.) Measured and theoretical excess attenuation (dB) over grass covered soft soil under the wind direction 180^0 to that of Experiment 14.1.



g. Measured excess attenuation at different distances

Figure A3.2(Contd.) Measured and theoretical excess attenuation (dB) over grass covered soft soil under the wind direction 180^0 to that of Experiment 14.1.

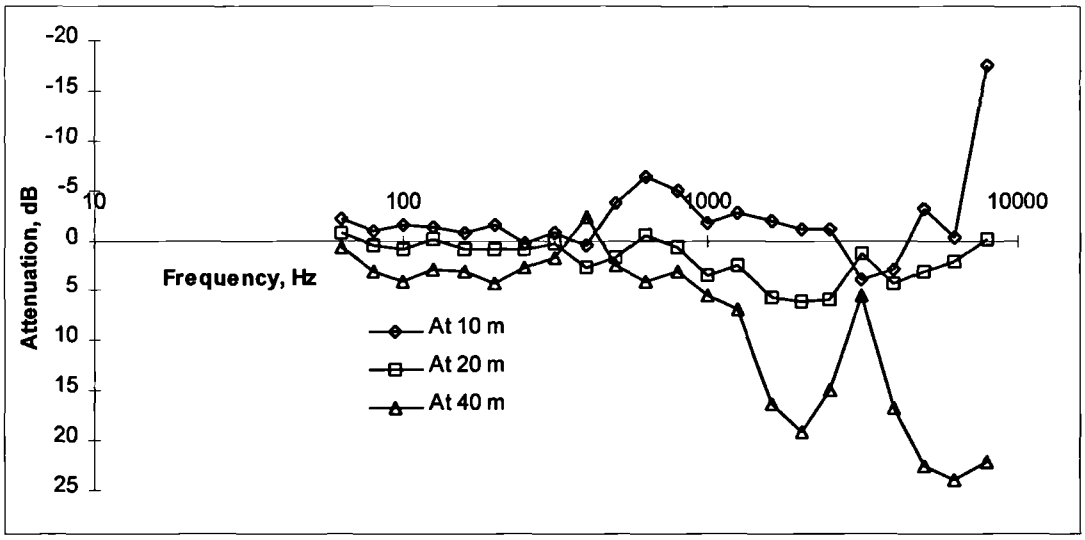


Figure A3.2a Change of excess attenuation (dB) due to reversal of the wind direction.

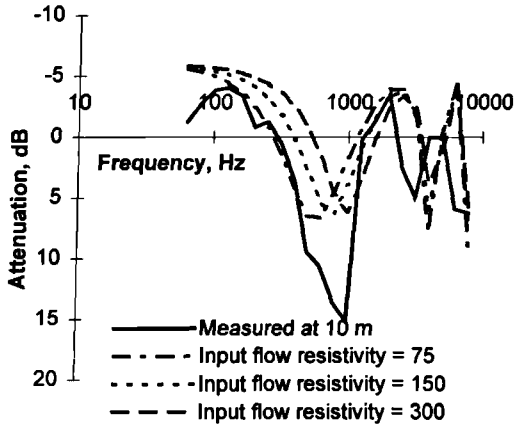
A3.3 Experiment 14-3

This experiment was also carried out over the grass covered soft soil. However, in this case the alignment of the speaker and the microphone was at 135^0 to the line of the experiments 14-1. The best fitted curve shows a flow resistivity of 150 $raylm^{-1}$ in this case. This observation needs to be further analysed to study the effect of the wind direction and speed on the effective flow resistivity of the soil for the purpose of calculating the excess attenuation due to ground absorption.

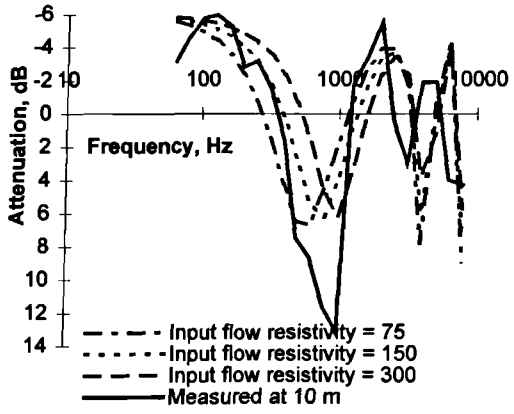
Table A3.3.1 shows the SPL (dB) recorded at different distances during the experiments. The dBA levels recorded by the instruments were converted to dB. Figure A3.3 shows the plots of the measured and the calculated excess attenuation for different flow resistivities.

Table A3.3.1 Recorded sound pressure levels for Experiment 14-3.

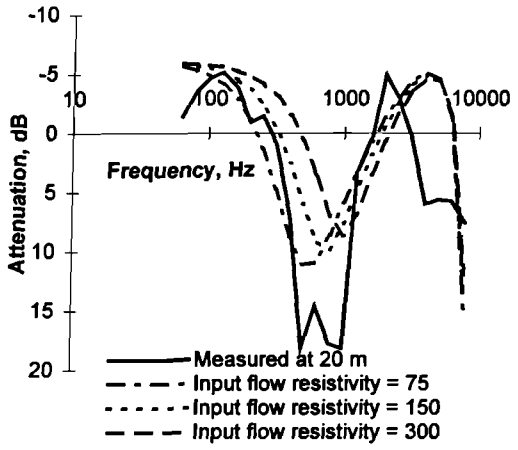
Frequency (Hz)	SPL (dB) at 1m	SPL (dB) at 10m	SPL (dB) at 20m	SPL (dB) at 40m
63	97.6	78.8	73.0	65.9
80	99.4	80.3	75.1	67.6
100	100.6	81.4	76.2	68.9
125	100.3	81.6	76.7	68.8
160	98.9	80.9	75.4	66.7
200	96.6	78.4	72.5	61.9
250	97.0	78.8	73.0	61.4
315	95.6	77.1	70.6	53.3
400	91.7	74.0	64.5	45.7
500	89.2	68.1	53.3	41.4
630	93.4	66.9	56.9	43.8
800	93.3	63.9	53.7	41.5
1000	90.9	62.4	53.3	42.3
1250	95.1	77.3	68.2	56.1
1600	97.0	79.1	71.2	56.5
2000	100.0	81.1	76.5	61.7
2500	95.8	75.1	74.5	64.0
3150	92.0	72.6	71.1	65.5
4000	95.3	77.5	65.5	64.4
5000	96.2	77.5	65.9	66.0
6300	92.6	71.6	65.8	56.8
8000	91.0	71.3	63.9	55.2



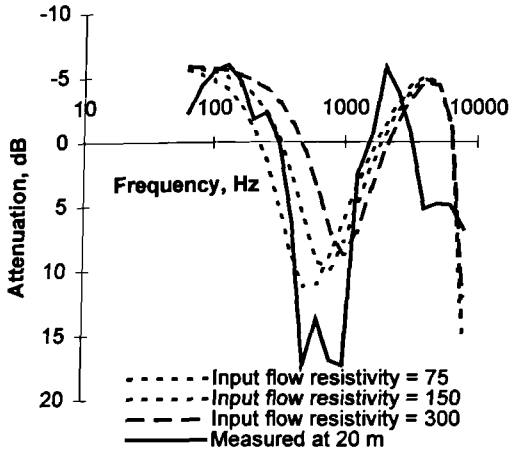
a. At 10 m, without reflection correction.



b. At 10 m, with reflection correction.

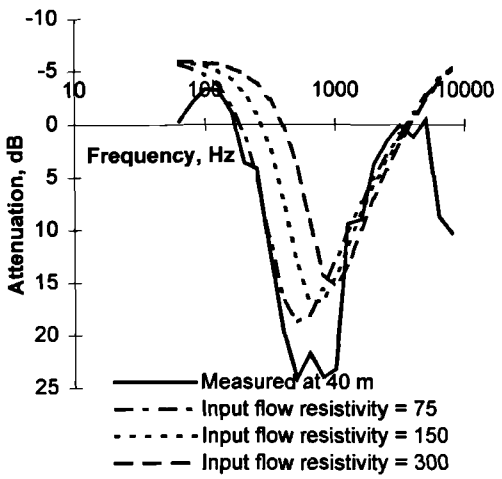


c. At 20 m, without reflection correction.

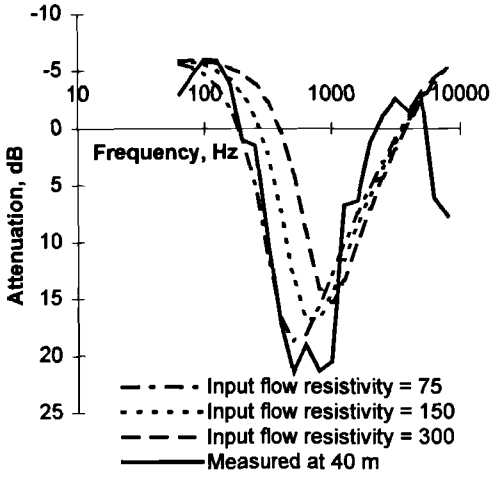


d. At 20 m, with reflection correction.

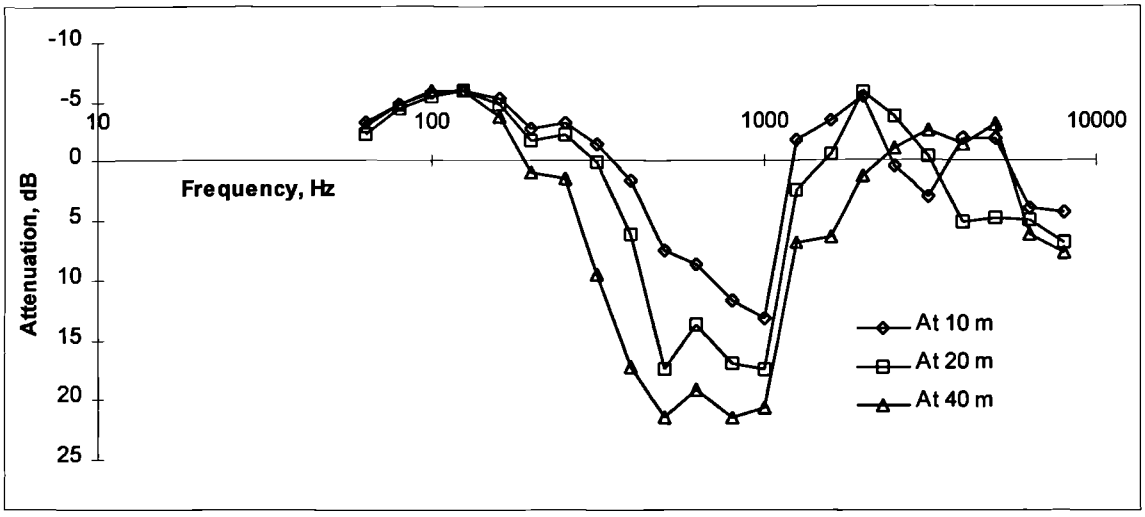
Figure A3.3 Excess attenuation (dB) over grass covered soft soil along 135^0 to the wind direction



e. At 40 m, without reflection correction.



f. At 40 m, with reflection correction.



g. Measured excess attenuation at different distances

Figure A3.3 (Contd.) Excess attenuation (dB) over grass covered soft soil along 135^0 to the wind direction.

B3 Experiments over Settled Quick Sand

B3.1 Experiment 14-4

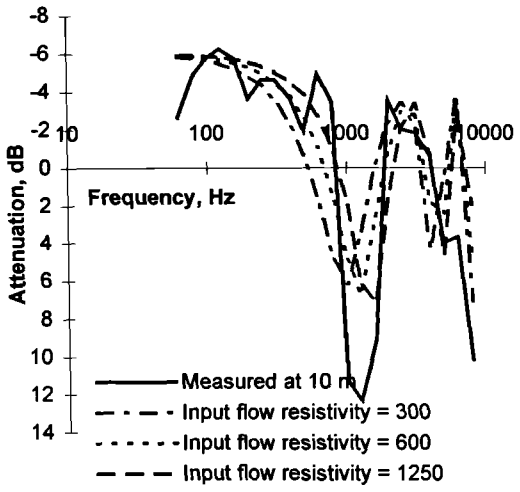
The second set of experiments during this phase of the study were carried out over settled quicksand. These experiments were conducted for four different situations. The relative angular displacement of the direction of sound propagation was 45^0, 90^0 and 180^0. Measurements of sound pressure levels were also carried out at longer distances.

However, these long distance measurement could not provide very clear response to study ground absorption because of the influences of external sounds on site.

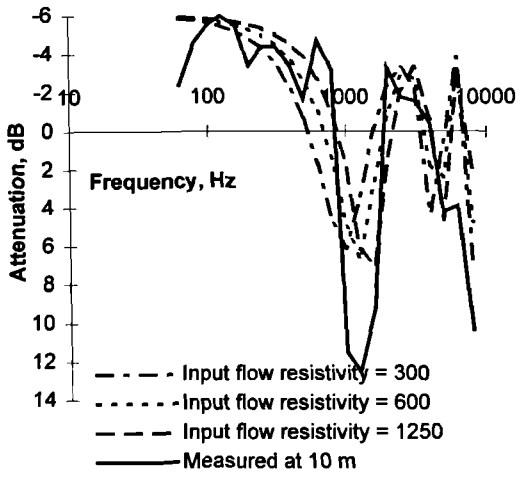
Table B3.1.1 shows the SPL (dB) of recorded at different distances during the experiments. The dBA levels recorded by the instruments have been converted to dB levels. Figure B3.1 show the plot of the experimental and theoretical excess attenuation for different flow resistivity.

Table B3.1.1 Recorded sound pressure levels for Experiment 14-4.

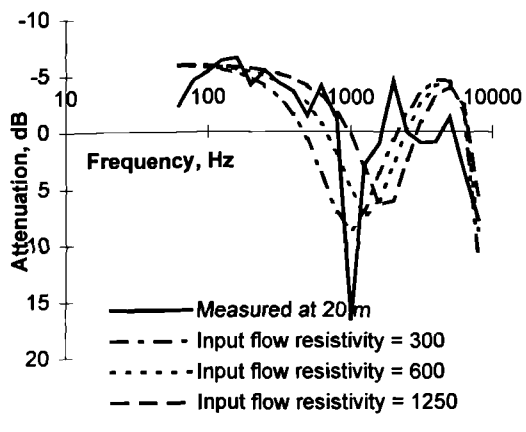
Frequency (Hz)	SPL (dB) at 1m	SPL (dB) at 10m	SPL (dB) at 20m	SPL (dB) at 40m
63	99.4	82.0	75.7501	67.9864
80	101.9	84.2	78.0090	69.8942
100	102.8	85.1	78.7718	71.3828
125	103.0	85.6	79.6897	72.4793
160	102.4	85.1	79.9155	72.4252
200	100.1	83.0	77.5257	70.3271
250	101.1	84.0	78.8353	70.7100
315	99.8	84.0	77.7395	69.0395
400	98.1	83.0	76.9584	68.1071
500	94.7	81.3	74.7902	64.8468
630	94.1	84.3	77.4376	67.0846
800	87.5	82.8	74.4583	62.0576
1000	87.1	68.0	56.5954	45.8029
1250	96.9	67.0	70.4694	58.3995
1600	96.3	70.3	72.3379	57.8356
2000	102.3	82.9	77.8417	60.1242
2500	96.4	81.4	73.2583	59.7446
3150	92.7	81.2	72.3471	55.6704
4000	96.5	80.0	72.4251	53.0874
5000	98.0	75.4	74.6031	56.2542
6300	95.8	75.7	69.9599	50.4366
8000	91.4	69.2	65.5433	42.5585



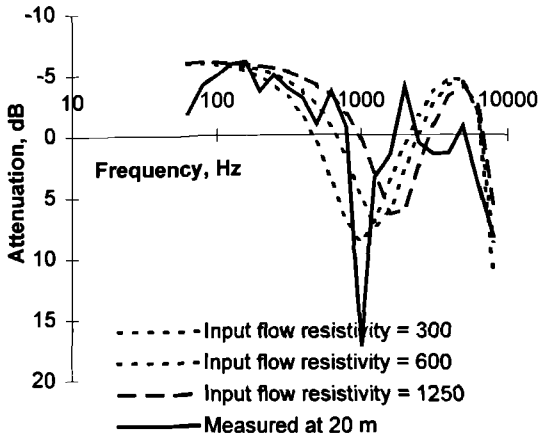
a. At 10 m, without reflection correction.



b. At 10 m, with reflection correction.

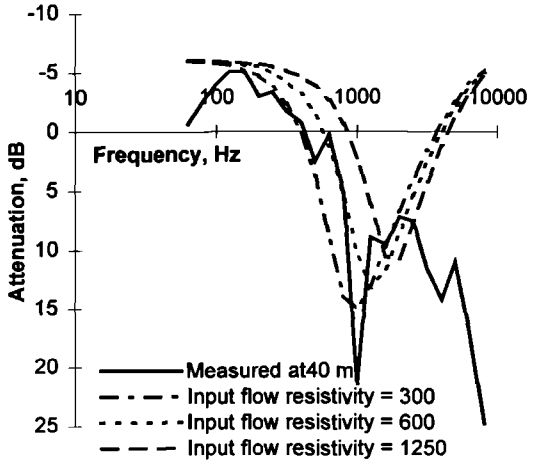


c. At 20 m, without reflection correction.

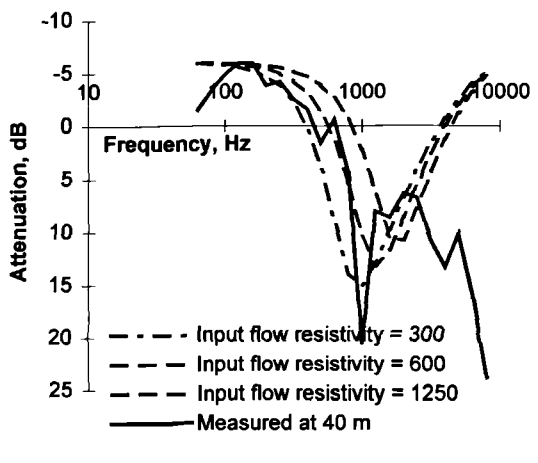


d. At 20 m, with reflection correction.

Figure B3.1 Excess attenuation (dB) over settled quick sand along direction of wind.



e. At 40 m, without reflection correction.



f. At 40 m, with reflection correction.

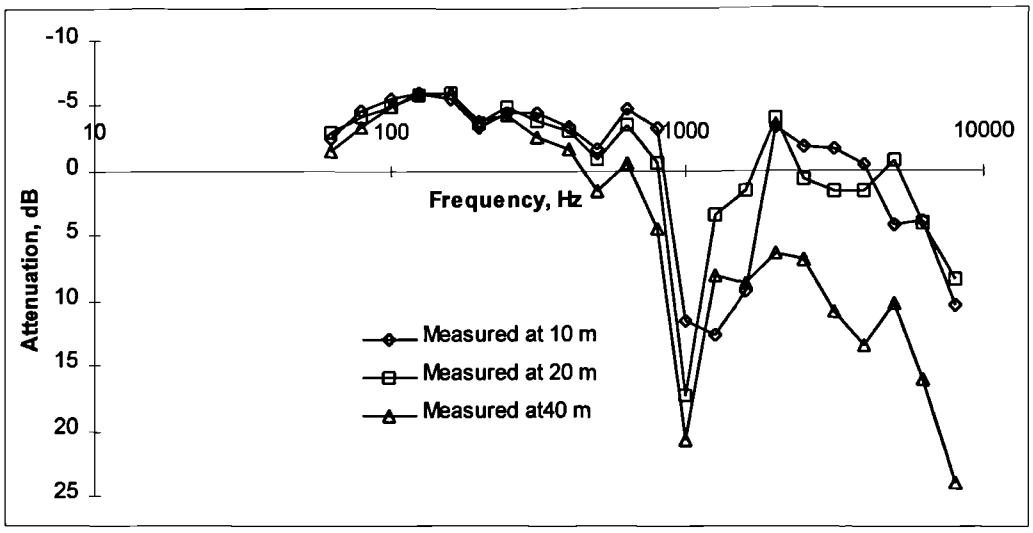


Figure B3.1 (Contd.) Excess attenuation (dB) over settled quick sand along direction of wind.

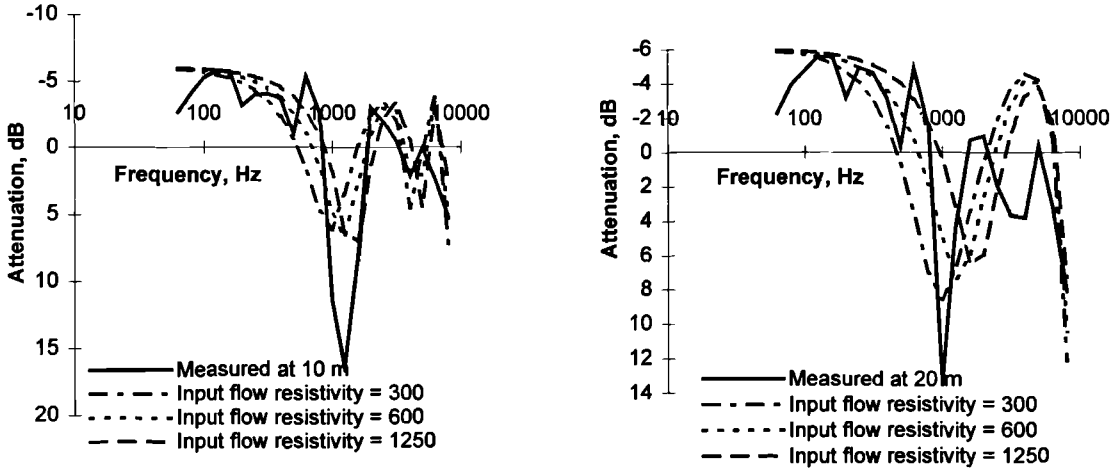
Flow resistivity was found within 300-600 rayls/m. Results will have to be verified with other set of experiments on this ground.

B3.2. Experiment 14-5

This experiment were conducted keeping the direction of sound propagation at 45^0 with respect to that of Experiment 14-4. Table B4.2.1 shows the SPL (dB) of recorded at different distances during the experiments. The dBA levels recorded by the instruments have been converted to dB levels.

Table B3.2.1 Recorded sound pressure levels for Experiment 14-5.

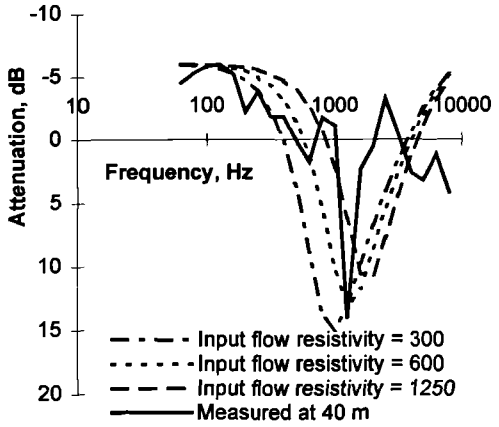
Frequency (Hz)	SPL (dB) at 1m	SPL (dB) at 10m	SPL (dB) at 20m	SPL (dB) at 40m
63	97.7	80.3	73.9691	68.2774
80	99.7	81.8	75.6649	69.0826
100	100.8	82.9	76.4452	69.5934
125	101.0	83.4	77.2588	69.7829
160	100.1	83.4	77.3263	69.0012
200	97.9	80.8	74.8909	65.9733
250	98.8	81.6	76.6424	67.5983
315	98.1	81.7	76.3458	65.5983
400	96.1	81.4	74.8501	65.5806
500	92.4	78.7	72.0191	63.6097
630	90.8	83.0	76.5856	61.9971
800	87.3	80.4	73.2989	65.5495
1000	88.3	66.2	58.0988	64.8204
1250	95.4	61.2	67.3068	49.6474
1600	95.0	69.6	72.4089	61.4387
2000	100.3	80.7	72.6258	63.2639
2500	93.9	79.6	69.7507	66.9889
3150	91.8	78.1	68.0081	64.1616
4000	93.6	75.5	67.8589	61.1443
5000	97.7	77.6	72.0510	60.5740
6300	94.7	75.2	68.5110	62.6132
8000	90.5	72.4	63.5315	59.6407



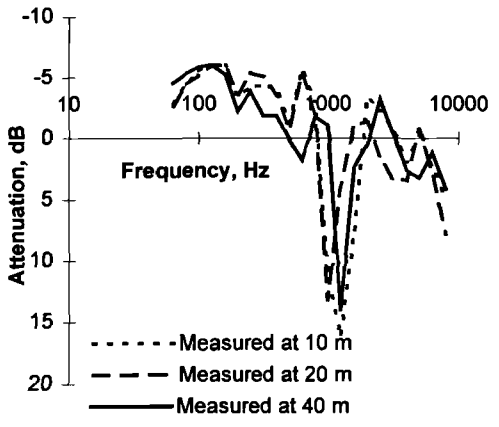
a. At 10 m from the source

b. At 20 m from source

Figure B3.2 Theoretical and measured excess attenuation (dB) over settled quicksand at 45 degree to the wind direction.



c. At 40 m from the source



d. At different distances

Figure B3.2 (Contd.) Theoretical and measured excess attenuation (dB) over settled quicksand at 45 degree to the wind direction.

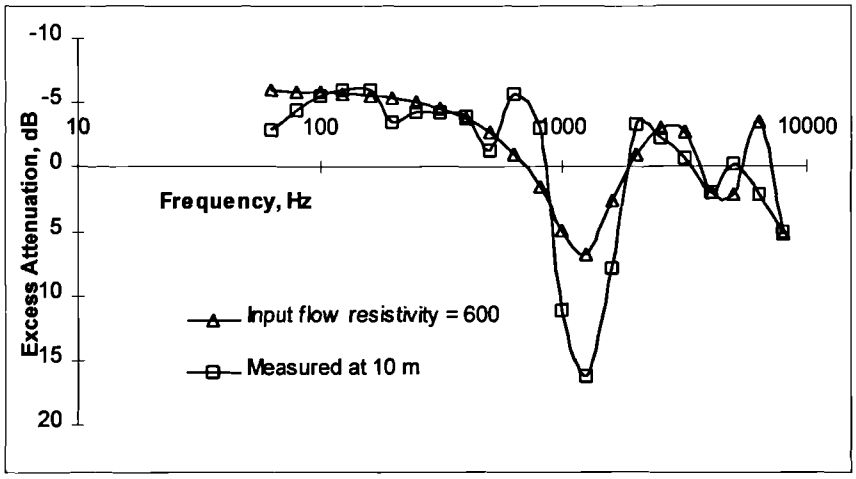


Figure B3.2a Comparison of theoretical and measured excess attenuation (dB).

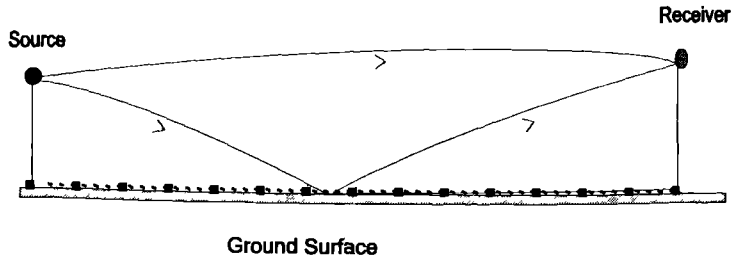


Figure B3.2b Effect of meteorological factors affecting curved ray path.

The possible reason for the above anomaly is that the effects of the wind has not been included in the above theoretical results. Due to wind effects there is a bending of acoustic ray. This will make the effective distance of propagation longer than source-path distance as shown in the Figure B3.2b.

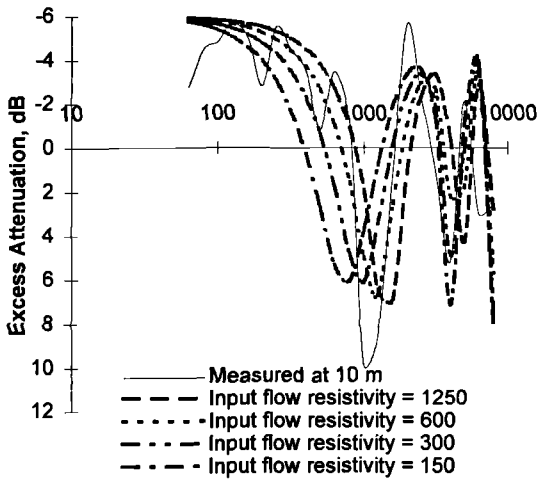
Table C3.1.1 Recorded sound pressure levels for Experiment 13-1.

Frequency (Hz)	SPL (dB) at 1m	SPL (dB) at 10m	SPL (dB) at 20m	SPL (dB) at 40m
63	94.6	77.3	71.4	63.5
80	95.9	79.1	73.0	62.2
100	96.6	79.4	73.2	63.9
125	96.5	80.3	75.3	66.2
160	96.6	79.6	75.2	65.4
200	94.4	77.4	72.1	63.6
250	95.1	80.1	73.3	67.2
315	93.1	79.1	72.6	64.4
400	91.1	78.1	72.4	62.7
500	88.2	75.4	70.2	61.8
630	84.8	78.1	71.9	65.0
800	86.5	75.8	71.5	63.0
1000	88.4	64.7	55.7	47.2
1250	91.6	65.9	58.7	52.0
1600	93.2	73.5	62.6	49.5
2000	96.8	80.2	70.5	59.6
2500	91.7	77.1	70.9	60.7
3150	92.5	73.5	70.2	54.5
4000	92.2	69.4	69.2	62.2
5000	91.5	76.7	71.0	60.6
6300	91.3	71.6	65.0	61.4
8000	88.8	72.0	66.1	50.8

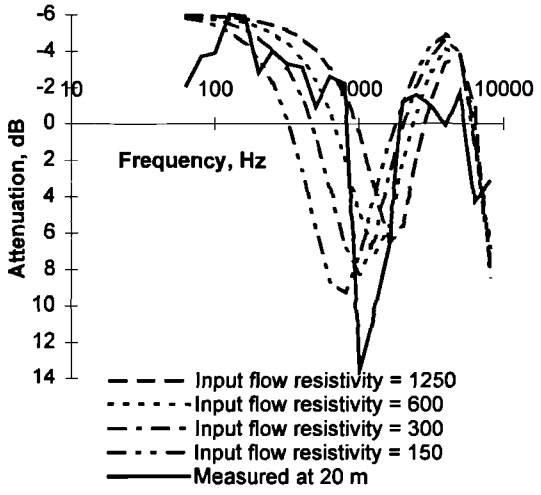
C3 Experiment over Gritty Road Surface

C3.1 Experiment: 13-1

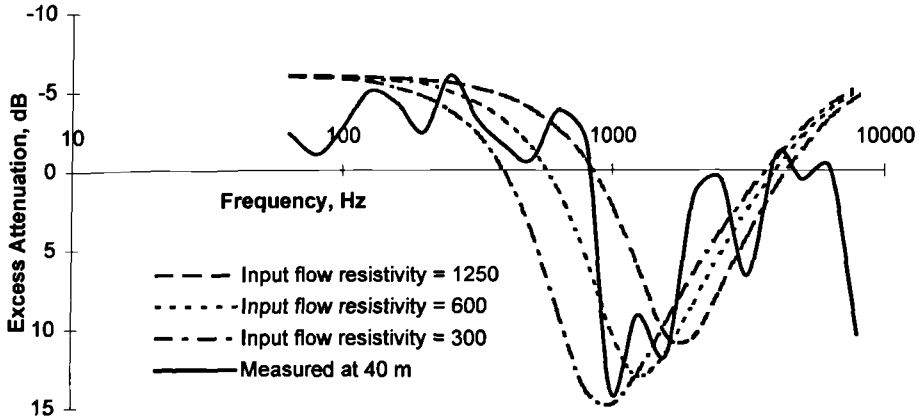
This experiment was conducted over a gritty road surface. The wind direction was at 15^0 degree along the direction of sound propagation. Table C3.1.1 shows the SPL (dB) of recorded at different distances during the experiment. The dBA levels recorded by the instruments have been converted to dB levels. Following figures show the plot of the experimental excess attenuation along with the theoretical excess attenuation for different flow resistivities.



a. At 10 m from the source.



b. At 20 m from the source



c. At 40 m from the source

Figure C3.1 Theoretical and measured excess attenuation over gritty road surface at 15° to the wind direction.

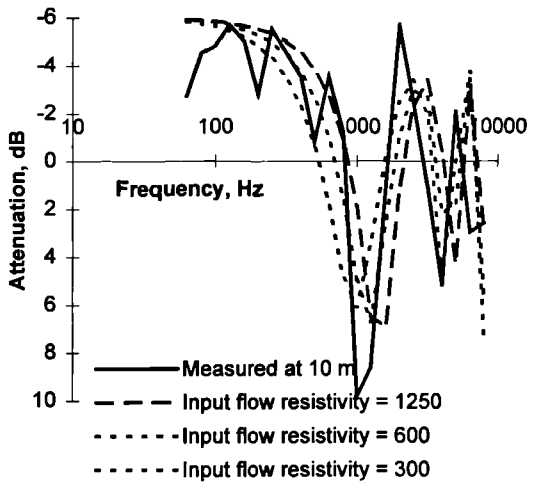
Table C3.2.1 Recorded sound pressure levels for Experiment 13-2.

Frequency (Hz)	SPL (dB) at 1m	SPL (dB) at 10m	SPL (dB) at 20m	SPL (dB) at 40m
63	103.2	84.1	77.5	67.3
80	104.5	85.0	78.7	69.2
100	106.0	86.5	79.7	72.2
125	106.2	86.5	82.0	72.5
160	106.0	85.2	82.0	71.6
200	103.2	83.2	78.2	69.1
250	105.2	85.4	80.2	70.7
315	103.5	85.7	79.9	69.3
400	101.7	84.7	77.0	67.0
500	99.7	80.5	75.2	65.2
630	102.0	84.7	77.4	69.0
800	97.2	81.5	76.2	67.2
1000	90.0	70.0	64.0	54.3
1250	98.5	67.5	72.4	61.7
1600	96.5	75.0	70.5	61.0
2000	105.2	83.5	72.0	64.5
2500	98.7	83.2	72.9	66.0
3150	99.2	82.7	73.5	59.7
4000	99.2	82.5	75.7	58.7
5000	99.5	81.0	80.0	65.2
6300	97.5	80.5	77.5	64.2
8000	104.0	78.0	77.7	59.7

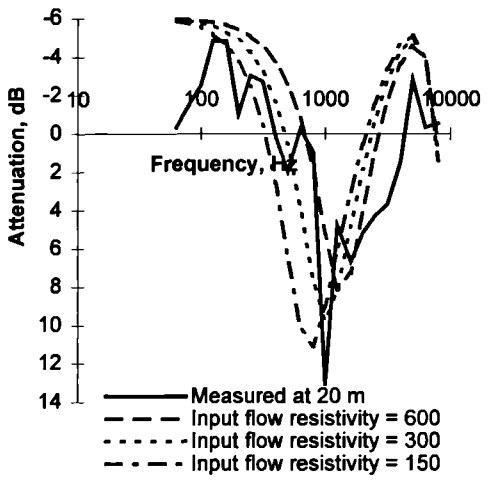
C3.2 Experiment 13-2

This experiment was conducted over a gritty road surface. The wind direction was at 165^0 degree opposite to the direction of sound propagation. Table C3.2.1 shows the SPL (dB) of recorded at different distances during the experiment. The dBA levels recorded by the instruments have been converted to dB levels.

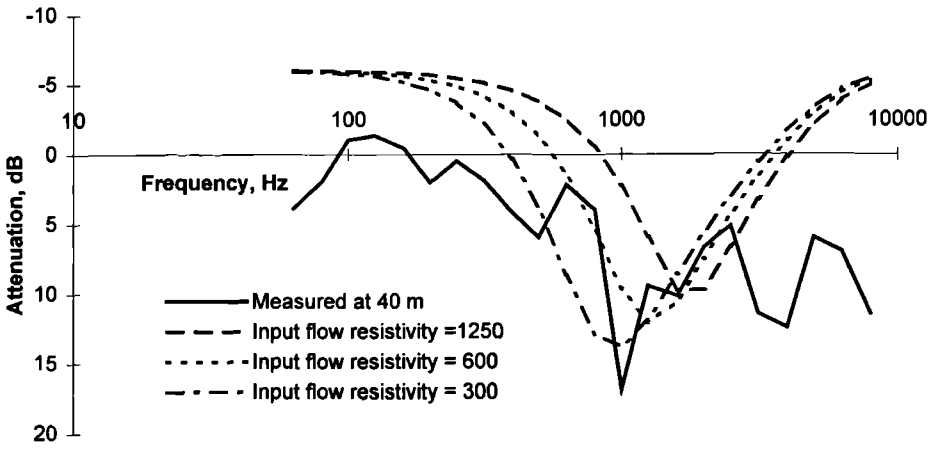
Figure C3.2 show the plot of the experimental excess attenuation along with the theoretical excess attenuation for different flow resistivities.



a. At 10 m from the source.



b. At 20 m from the source



c. At 40 m from the source

Figure C3.2 Theoretical and measured excess attenuation over gritty road surface for Experiment 13.2.